Studies of Physical Properties on the Performance of Novel Recognition Polymers

Thesis

The Open University

Department of Life, Health and Chemical Sciences

Academic Years 2011-2015

Heli A. Brahmbhatt

Studies of Physical Properties on the Performance of Novel Recognition Polymers

Supervisors:

Dr. Nicholas W. Turner

Dr. Maria Velasco-Garcia

Ph.D. Thesis

August 2015

This thesis is submitted for the degree of Doctor of Philosophy.

DATE of SUBMISSION : 19 AUGUST 2015

DATE of AWARD : 13 JUNE 2016

ProQuest LLC.
789 East Eisenhower Parkway
P.O. Box 1346
Ann Arbor, MI 48106 – 1346

"Study the science of art. Study the art of science. Develop your senses-

Learn how to see.

Realise that everything connects to everything else."

-Leonardo Da Vinci

Abstract

Selective interactions occurring between antigen and antibody have been studied intensively for developing bio-sensing platforms, however antibodies suffer from shorter shelf-life and high cost of production. Molecularly Imprinted Polymers (MIPs) on the other hand have drawn huge attention as antibody analogs for their advantages over natural antibodies. Increased research undertaken in this area for over two decades has made it possible to develop MIP nanoparticles that are currently dubbed as the most suitable alternatives to natural antibodies. MIP preparation is cost-effective and also offers flexibility in developing different polymer formats by different methods. However, the resulting MIPs are found to be considerably different due to different experimental variables associated with different methods. This has been one of the biggest challenges in developing MIPs for commercial applications in spite of their excellent recognition performances shown in lab experiments.

To this end, the research undertaken in this project has been executed by performing three case studies where novel recognition polymers have been prepared in different experimental conditions and different formats. Particularly, the study of physical properties of the polymers and their influence on their analyte recognition performance is at the heart of all three case studies performed during this project.

The study presented in Chapter 3 has investigated microwave reactor led thermal polymerisation as a potential alternative method for the preparation of MIP monoliths, whereas the study presented in Chapter 4 has investigated into developing novel polymers as potential recognition materials for ToxiQuant technique which is used for mycotoxin detection. The study presented in Chapter 5 proposes a novel approach for the development of MIP nanoparticles for selective oligonucleotide recognition. The prepared polymers have been analysed for their physical properties (such as, surface area, particle size, zeta potential, cross-linking degree, pore volume, thermal stability) and analyte recognition performance. The obtained results strongly recommend that the experimental parameters used for polymerisations are well reflected in the physical make of the resulting polymers and have further consequences on their analyte recognition performance. Study of the physicochemical properties of the polymers and their underlying causes may help in developing more consistent, predictable and selective recognition polymer materials.

Acknowledgements

I would like to express sincere gratitude to my supervisors Dr. Nicholas Turner and Dr. Maria Velasco-Garcia for their continual guidance and support throughout the project. Working under their supervision has been a great learning experience for me and will fondly remember for helping me improve my skills not only as a researcher but also as a person. I would like to convey thanks to Dr. Alessandro Poma for being an excellent colleague and guiding me greatly through the project. I will remember all the brainstorming sessions we had in the lab every morning.

I would like to thank Toximet Ltd. and the Open University for providing financial support and giving me an opportunity to work on this exciting project. I would like to take this opportunity especially to thank Dr Raymond Coker for showing great enthusiasm and ensuring that all possible help was received throughout the project. I would like to extend my gratitude to Dr Elena Piletska and Dr Joanne Kumire for their help with the chromatographic and porosimetry analysis of ToxiQuant polymers. I also wish to thank Dr. Cameron Alexander for allowing me to visit their labs for carrying out DLS and zeta potential measurements of the polymers developed during this project. I thank Prof. Peter Taylor for allowing me to use their chromatography instrument for analysing caffeine imprinted polymers.

I would like to thank Mrs. Heather Davies and Mr. Gordon Imlach for providing excellent training on electron microscopic techniques and always being around when I needed their help. I wish to thank Dr. Jill Clarke, Dr. Mike Batham and Mrs. Julia Barkans for making sure that all the health and safety measures were in place in the labs throughout the project. I also wish to thank Colin Haynes for his support with logistics. I would also like to thank the staff members and the amazing bunch of fellow PhDs and postdocs of LHCS for making these years a great experience.

Last but not the least; I would thank my lovely family, Ma, Pa, Halak, Vaishvik and Anant for always being there. This wouldn't have been possible without you guys, I owe this to you!

List of Contents

List of figures

List of tables

Abbreviations

AA	Acrylic acid
Ab	Antibody
Abs	Antibodies
AFT	Aflatoxin
AFT B1	Aflatoxin B1
Ag	Antigen
Ags	Antigens
AIBN	Azobisisobutyronitrile/ 2,2'-azobis(2-methylpropionitrile)
AMP	Adenosine monophosphate
BET	Brunauer-Emmett-Teller theory
cAMP	Cyclic adenosine monophosphate
CE	Capillary electrophoresis
CMC	Critical micelle concentration
CPG	Controlled porous glass
CO_2	Carbon dioxide
DCM	Dichloromethane
dA	Deoxyuridine
dC	Deoxycytidine
dG	Deoxyguanine
dU	Deoxyuridine
DMF	Dimethyl formamide
DNA	Deoxyribonucleic acid
DVB	Divinylbenzene
EBPs	Engineered binding proteins
EGDMA	Ethylene glycol dimethacrylate
ELISA	Enzyme linked immune sorbent assay
FAO	Food and nutrition organisation
FTIR	Fourier transfer infra-red spectroscopy
GC	Gas chromatography
HPLC	High performance liquid chromatography
IA	Immuno-affinity
IAC	Immuno-affinity columns
IF	Imprinting factor
IR	Infrared spectroscopy

KDa	Kilo Dalton
KJoule	Kilo Joule
LC	Liquid chromatography
LLE	Liquid-liquid extraction
LOD	Limit of detection
MAA	Methacrylic acid
MeOH	Methanol
MIP(s)	Molecularly imprinted polymer(s)
mM	Milimolar
mmol	Milimoles
Mol %	Mole percentage
MS	Mass spectrometry
MW	Microwave
NaOH	Sodium hydroxide
NMR	Nuclear magnetic resonance spectroscopy
NOBE	N, O- bisacryloyl ethanolamine
NPs	Nanoparticles
O/W	Oil in water
OT	Ochratoxin
OTA	Ochratoxin A
PAAm	Polyacrylamide
PCR	Polymerase chain reaction
PEG	Poly(ethylene glycol)
PLE	Pressurised liquid extraction
Ppb	Parts per billion
PSD	Particle size distribution
PVP	Polyvinylpyrollidone
QCM	Quartz Crystal Microbalance
RNA	Ribonucleic acid
rpm	Rotation per minute
SELEX	Systematic evolution of the ligands by exponential enrichment
SEM	Scanning electron microscope
SFE	Supercritical fluid extraction
SPE	Solid phase extraction
SPE	Solid-phase extraction
SPME	Solid phase micro extraction

TEM	Trasmission Electron Microscope
TLC	Thin layer chromatography
UV	Ultraviolet
W/O	Water in oil
W/v	Weight by volume
Wt %	Weight percentage

Equations

$$\frac{1}{[W\left(\frac{P_0}{P}-1\right)]} = \frac{C-1}{W_m C} * \frac{P}{P_0} + \frac{1}{W_m C} \quad \text{..... (76)}$$

Where, P = partial vapour pressure (Pa) of the adsorbed gas

P_0 = saturated pressure (Pa) of adsorbed gas

W = volume of gas (ml) adsorbed at standard temperature (273 K) and pressure ($1X10^5$ Pa) (STP)

W_m = volume of gas (ml) adsorbed at STP to produce a monolayer on the surface of the sample

C = dimensionless constant related to the enthalpy of adsorption of the gas on the sample surface

Publications

- Accepted peer-reviewed publications
    1. Poma, A., Brahmbhatt, H., Watts, J. K., and Turner, N. W. Nucleoside-Tailored Molecularly Imprinted Polymeric Nanoparticles (MIP NPs) Nucleoside-Tailored Molecularly Imprinted Polymeric Nanoparticles (MIP NPs). *Macromolecules* (2014). **47,** 6322-6330.
    2. Poma, A., Brahmbhatt, H., Pendergraff, H. M., Watts, J. K., and Turner, N. W. Generation of Novel Hybrid Aptamer–Molecularly Imprinted Polymeric Nanoparticles. *Advanced Materials* (2014). **27**, 750–758750-758.
- Publications under revision
    1. Turner, N. W., Brahmbhatt, H., Szabo-Vezse, M., Alessandro, P., Coker, R., and Piletsky, S. Analytical Methods for Determination of Mycotoxins: An Update (2009-2014). *Analytica Chimica Acta* (2015).
- Publications in submission
    1. Brahmbhatt, H. Poma, A. Watts, J. K. Turner, N. W. Improvement of DNA Recognition through Molecular Imprinting: Hybrid Oligomer-Molecularly Imprinted Polymeric Nanoparticles (Oligo-MIPs). *Biomaterials Science* (2015).
- Publications in preparation
    1. Brahmbhatt, H., Cosby, J., Poma, A., and Turner, N. W. Investigation of Microwave Polymerisation as an Alternative Method for the Preparation of Molecularly Imprinted Polymers (2015).

Chapter 1
Introduction to the thesis

This introduction explains the research questions involved in conducting this project and describes the structure of the thesis entitled **"Studies of Physical Properties on the Performance of Novel Recognition Polymers"**.

The project has been designed as a result of the Open University's industrial collaboration with Toximet Ltd. through an OU charter PhD studentship. It has also been a part of an extended research network formed together with other teams of researchers around the UK exploring similar research domains for the development of recognition polymers, based on the principle of molecular imprinting. This is an established technique allowing the preparation of tailor-made polymer materials which are capable of selectively recognising an analyte of interest.

Molecularly imprinted polymers (MIPs) can be prepared in different formats by using different polymerisation methods. This allows recognition of a huge variety of compounds from biomolecules to bacterial cells; and from drug molecules to toxins. At the same time, the use of different methods and different polymerisation conditions often generate polymers with significantly different properties.

Some studies have already identified the importance of studying various experimental conditions of the MIPs since they largely reflect the properties of the resulting MIPs. However, there is a strong need to understand whether the observed properties of the MIPs reflect further in their recognition performance. This is particularly important for developing alternative or newer polymerisation methods for MIP preparation since traditional methods have suffered from batch-to-batch variability in resulting polymers. Moreover, the studies reported so far have mainly investigated traditional polymerisation methods, whereas alternative polymerisation methods may have their own experimental conditions which may impart different effects on the polymer properties and recognition performance.

The collaborative work carried out between the financial sponsors, Toximet and The Open University has led to **three case studies** which have been performed during the course of this PhD studentship. These studies have explored development of polymer materials for the recognition and selective binding of caffeine, aflatoxin and oligonucleotides.

Each study has been presented as a separate chapter in this thesis and each chapter consists of a brief introduction to the study which is supported by a review of literature. This introduction and review is then followed by an experimental section discussing the materials, the chemicals and analytical techniques used for the preparation and analysis of the particular polymers

under study. A results section presents, discusses and summarises the findings obtained from the specific study. An outlook on the potential future work in the area is also discussed in the end. The chapters involving these case studies are briefly described here.

Chapter 3 investigates microwave (MW) polymerisation as an alternative method to prepare MIPs. More importantly, it produces a coherent study which investigates the effects of several underlying experimental parameters on the physical properties and recognition performance of the resulting MW MIPs.

For the first time, a comparative analysis of the MW polymerisation has been reported along with the traditional methods, such as oven and UV polymerisation. The study also marks the first attempt of investigating the effect of different experimental conditions of a MW polymerisation on physical properties and recognition performance of the MIPs.

Chapter 4 involves the study for developing polymers as potential materials to be used in ToxiQuant technology (developed by Toximet Ltd.) for the recognition of aflatoxins. The particular polymer used in this study is based around a previous study carried out by a collaborative project based at Cranfield University by Joanne Kumire. These recognition polymers are not MIPs but have been developed by similar protocols as those used for preparing caffeine imprinted polymers to ensure comparable experimental conditions.

Following the core objective of the thesis, the study attempts to investigate the effect of polymerisation conditions on the physical properties and recognition performance of these polymers. Here, the polymers have been prepared in different formats (monoliths and microparticles) by using different polymerisation methods (MW, thermal, UV) for a comparative study.

Due to the withdrawal of research support from Toximet in later stages of the project, some of the developed microparticles are yet to be analysed for their mycotoxin recognition performance and this is noted in the relevant further work section. However, this study already provides a comprehensive report on the development and analysis of polymer monoliths prepared by MW polymerisation for mycotoxin recognition. The study also provides a comparative outlook on the physicochemical properties of MW polymers presented in Chapter 3 for caffeine recognition, hence has been included in this thesis.

Chapter 5 is based on the development of polymeric nanoparticles (NPs) for the recognition of oligonucleotide sequences. Solid phase nanoparticle synthesis for molecular imprinting has been combined with DNA sequence modification to generate oligonucleotide imprinted MIP NPs. The observed selectivity and specificity of these NPs towards a template oligonucleotide

has been achieved by incorporating a polymerisable complimentary oligonucleotide into the polymer backbone relying on the base pair recognition according to Watson-Crick's DNA model.

In the presented study, a unique modification strategy of the oligonucleotide monomer has been introduced to allow its incorporation into polymer NPs without affecting the size and shape but with improved dispersibility of the resulting OligoMIP NPs. The study incorporates development strategy, physical analysis and template recognition analysis of the prepared OligoMIP NPs.

While this work is not directly linked to those presented in Chapters 3 and 4, the physicochemical analysis and novel development strategies are a unique study which significantly expands on the imprinting field and understanding of the recognition properties of the MIPs.

Around these three core studies, an introduction and supportive discussion is presented. The review of literature presented in **Chapter 2** introduces the technique of molecular imprinting through the concept of selective molecular recognition. It then provides a brief history of the development of the molecular imprinting technique and also briefly discusses different types of molecular imprinting technique. The literature review then also discusses different experimental parameters and polymerisation components involved in molecular imprinting an emphasis is on studying their effect on the physical properties as well as recognition performance of the resulting MIPs. **Chapter 6** consists of general discussion by summarising all the three studies presented and presents final comments and conclusions. Finally a bibliography and appendices, which include published papers, are presented.

Chapter 2

Introductory Literature Review

2.1. Preface

This chapter discusses various aspects of developing polymeric materials by using molecular imprinting technique. The unique strategy of molecular imprinting allows selective recognition of the target analyte at the molecular level. Therefore, in this thesis MIPs have been discussed through the concept of selective molecular recognition. The discussion then extends further describing how the modern molecular imprinting concept has evolved, what its principle is and what different methods are used for imprinting a wide range of target analytes within MIP polymer matrices.

This thesis describes three studies that look at the physical properties of recognition materials that are created in a novel manner. Therefore, this introductory chapter discusses the effects of each polymerisation component (such as initiator, monomers, porogen etc.) on the property of resulting polymers. The discussion continues with the likely effects of various experimental parameters as well (such as, temperature and time) and explains how they are linked to not only the physical make-up but also the template recognition performance of the resulting MIPs. This is followed by the discussion on different MIPs formats, methods of their preparation, their advantages and also the limitations when used as recognition materials. The chapter summarises the literature presented from the perspective of the aim of this study and briefly discusses the future outlook on the development of MIPs for bio-chemical diagnostic applications. Finally a brief description of why this work was performed and where it fits into the larger picture of recognition polymers is also covered.

2.2. The concept of "specific molecular recognition"

Specific interactions occurring between substrates at molecular level are at the heart of complex biochemical reactions. For example, selective interactions between antigens (Ags) and antibodies (Abs) are vital in carrying out immune responses to protect us against pathogens. Such specific recognition is favoured through one's complementing chemistry with its counterpart. An Antibody (Ab) is complimentary to an antigen (Ag) and is generated by the cells in our immune system in response to Ags we are exposed to (such as, bacteria, virus or toxins). Once produced, Abs then selectively interact with the Ags via several non-covalent interactions (hydrogen bonds, van der Waal's force, electrostatic interactions and hydrophobic interactions) followed by a series of cell signalling mechanisms which destroys the Ag and thereby prevents it from harming our cells (1). Likewise, a drug molecule also binds to its receptor present on the target cells via similar selective molecular interactions and produces its therapeutic effect.

This very fundamental principle has been widely explored for the separation and/or recognition of target analytes in techniques such as, ELISA (Enzyme Linked Immuno Sorbent Assay) and immuno-affinity chromatography assays (2,3). In these techniques, Ab complimentary to the target analyte are immobilised on a solid surface (4,5). If analyte of interest is present in the sample (for example, protein biomarkers in a disease condition), its selective interaction with the immobilised Ab takes place which is then transduced further as electrochemical, thermal or optical response (6). As a result of these responses, it can be found out whether or not the analyte is present in a given sample (7). Despite of the sensitivity of these bio-sensing techniques, costs of producing and maintaining Abs is a major concern. Abs are also non-reusable and have a shorter shelf-life due to its sensitivity to temperature, pH and protease enzymes (8).

In this regard, synthesising artificial biomolecules or materials in the laboratories with improved stability, affinity and specificity may help in overcoming existing limitations faced by Abs and other natural bio-macromolecules, such as, nucleic acids. However, it may also be extremely challenging to prepare synthetic materials with equivalent recognition performance to that of its biological counterparts. For example, *in vitro* amplification and isolation of nucleic acid segments for the detection of target molecules is quite elaborate but they are more stable than biological Abs (9).

Such genes are single stranded non-biological oligonucleotide sequences with average molecular weight of 8-12 kDa having 20-100 residues of either DNA or RNA which can be generated for a specific target, such as drugs, proteins and even cells through *in vitro* selection. Once the target selective single gene strand is identified, it is then amplified using PCR (Polymerase Chain Reaction) (10,11). This technique is referred to as SELEX (Systematic Evolution of the Ligands by Exponential Enrichment) and the desired gene sequence has ever since been referred to as an aptamer (9). As aptamers are generated *in vitro* and don't involve activation of an immune system of animals, they can be prepared for the targets that are non-immunogenic where Abs show limited use. Unlike Abs, aptamers can also be used at a wide range of pH and temperature, can be fluorinated, immobilised and regenerated after use which makes them ideal for immunoassay or biosensor applications (9). However, screening process of aptamers by SELEX is very elaborate, expensive and their secondary structures are sensitive to the organic solvents used in bio-sensing applications. More importantly, they are also sensitive towards the nuclease enzymes found in serum and are easily broken down which makes it challenging to use them for *in vivo* applications as well (10). On the other hand, although synthetic polymers can be synthesised to have improved stability than that of Abs or aptamers, traditional polymers alone may struggle to match the selective recognition performance with that of the mentioned biomolecules.

Synthetic materials such as molecularly imprinted polymers (MIPs) can be prepared with more flexibly and with improved stability too (12). Some common differences between Abs and MIPs have been summarised in Table 2.1.

Table 2.1: Summary of the differences between Abs and MIPs, regenerated from (12-14)

Antibodies	MIPs
Produced biologically from animals (mice) or from bacteria (phage)	Direct artificial synthesis
Expensive	Relatively inexpensive
Sensitive to temperature and pH; stored only in lyophilised form	Stable across a vast range of temperature and pH; can be stored easily
Shorter shelf-life	Longer shelf-life
Target has to be macromolecular (12-15KDa)	Target is flexible but works best with lower molecular weight (<1 KDa)
Works precisely even at very low analyte concentrations	Precision depends on how well optimised the polymer recipe is
Has only one or two analyte binding sites per antibody	Has multiple binding sites on one particle
Can be used only in aqueous solvents	Can be used in both organic and aqueous solvents
Needs conjugation prior to analyte detection	Target analytes can be detected directly
Have homogenous binding sites	More chances of having heterogeneous binding sites; could be rectified by careful optimisation of the polymerisation recipe, method and analysis

Section 2.3 discusses various aspects related to the development of the MIPs as selective recognition materials.

2.3. Molecularly imprinted polymers: synthetic antibody analogs

Molecular imprinting has become an established technique for several decades to produce synthetic polymers which are capable of exhibiting selective molecular recognition of the target analyte (12,15,16). Different formats of the MIPs including, monoliths, micro/nanoparticles, membranes etc. have been widely studied for their use as Ab analogs in immunoassays (14,17-19), biosensors (20,21), solid phase extraction (SPE) and chromatographic separations (22,23). Recent studies have also reported the use of MIPs for *in vivo* applications that has opened a completely new dimension for their potential use in various biological and therapeutic fields as well (1).

2.3.1. Historical aspects of molecular imprinting

Although molecular imprinting is a recent approach, similar concepts have been practiced since the early 20th century. The first imprinting like study was reported by Polyakov in 1931 where silica was polymerised in the presence of solvents such as, toluene, benzene and xylene. Silica was then dried and solvent additives were re-introduced subsequently. It was observed that silica bound more selectively to the specific additive it was prepared with compared to other solvent additives (16). Followed by this, some interesting attempts were also made by Pauling and co-workers in 1942 to prepare antibodies by imprinting an Ag into it but their attempts were largely criticised for the differences in their understanding about the Ab structure. However, the method they suggested was quite similar to the concept of imprinting being used today.

Shortly after this in late 1940s, Pauling's student Dickey followed the same concept but this time it was applied for the synthesis of modified silica gels to imprint various dye additives (24). Silica was then polymerised in the presence of methyl orange dye; the dye was then removed and rebound. Upon rebinding the same dye, methyl orange was recognised better than other structural analog additives, such as ethyl orange. This remarkable work was largely appreciated by many scientists and since the term 'imprint' was used as the footprints of the analyte (16,24). In spite of these efforts, it was not until the 1970s when for the first time Wulff (25) and Takagishi (26) actually came up with the modern concept of imprinting a small molecule to form various organic polymers which were then referred to as molecularly imprinted polymers (MIPs) for selective molecular interactions, creating the field as we know it today. Section 2.3.2 discusses the principle of the molecular imprinting technique.

2.3.2. The principle of molecular imprinting

MIPs are prepared by a little modification of the traditional polymerisation method by inclusion of the target (template) in the polymerisation mixture itself. The template is chosen depending on the area of application anywhere from small molecules (such as, pharmaceuticals, toxins or pesticides) to bio-macromolecules (such as, peptides, nucleotides or whole protein) to even microorganisms (23,27,28).

The pre-polymerisation mixture of a MIP consists of functional monomers, cross-linking monomers (cross-linkers), free radical initiator, pore forming solvent (porogen) and the template. Figure 2.1 describes the process of MIP formation.

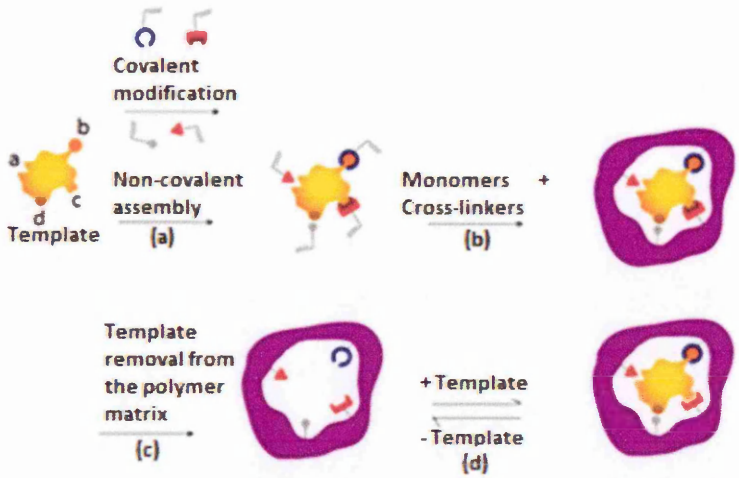

Figure 2.1: The schematic representation of the preparation of molecularly imprinted polymers, (a) monomer-template assemblies formed by covalent or non-covalent (hydrogen bond, electrostatic and hydrophobic) interactions, (b) polymerisation of the monomer-template assemblies in the presence of a cross-linker, (c) removal of the template from the cross-linked polymer matrix by hydrolysis and (d) repetitive template rebinding into the pre-formed cavities within the polymer matrix; adapted from (29).

In a classic free-radical polymerisation experiment, the monomer is chosen on the basis of its ability to interact selectively with the template to form monomer-template complexes by covalent or non-covalent interactions (such as, H-bonding, electrostatic interactions, Vander Waal's interactions and ionic bond formation) between the template and the monomer (as seen in Figure 2.1a). These pre-formed monomer-template complexes along with other components of the pre-polymerisation mixture (such as, initiator, monomers, cross-linkers and porogen) are then either heated or UV irradiated to disintegrate the initiator and to form free radicals. As the polymerisation proceeds, generated free radicals react with the cross-linkers and monomers through their multiple vinyl groups and form highly cross-linked polymer

matrix covalently holding pre-formed monomer-template complexes through the monomers (as seen in Figure 2.1b).

Once the polymerisation is completed, the template is removed from the cross-linked polymer matrix through solvent extraction in a non-covalent imprinting protocol. A polar solvent (such as, methanol) is widely used to remove the template as it would interfere with the non-covalent bond pre-formed between the template and the polymer matrix. Removal of the template is then meant to create a size, shape and functionality driven template binding sites into polymer matrix (30,31) (as seen in Figure 2.1c). Template removal and binding carried out in post polymerisation phase is reversible in changing solvent conditions and is used to study how selectively the formed polymer can recognise the template it has been synthesised against (as shown in Figure 2.1d). Therefore, different physico-chemical characteristics of these binding sites are of great importance in defining the template recognition performance of MIPs. Section 2.3.3 discusses different types of molecular imprinting techniques which are classified by the type of interaction that occurs between the monomer and the template in pre-polymerisation stage.

2.3.3. Types of molecular imprinting

MIPs, as briefly discussed above are mainly classified into four types, (32) which are based on the type of interaction that takes place between the monomers and the template in the pre-polymerisation mixture, such as;

- Covalent imprinting
- Semi covalent imprinting
- Spacer facilitated imprinting
- Non-covalent imprinting

Covalent imprinting is a type of polymer imprinting in which the template interacts to the monomer via covalent linkages (33,34). More importantly, recognition of the template by the resulting polymer also occurs by covalent interactions. Wulff and co-workers reported pioneering research work in this approach where imprinting of carbohydrate derivatives had been achieved covalently in boronic acid-co-polyvinyl based polymers via boronic ester linkages (16,29). Usually, covalent interaction is achieved via condensation reactions of the template's functional groups such as, diols, aldehydes/ketones and amines through formation of ketals/acetals, Schiff's bases and boronate esters (29). Since covalent bonding is much stronger, it assures formation of stable monomer-template assemblies and generates template

selective binding sites. However, such strong interactions between template and polymer may also hinder template removal/binding kinetics from its cross-linked matrix. Therefore, stronger acidic hydrolytic conditions are a must for removing the template once the polymer is formed (29). Aqueous conditions are also preferred during the polymerisation and template rebinding steps in order to avoid any solvent interference into the covalent bond formation; however it limits the choice of the monomer that can be used for covalent imprinting.

Semi-covalent imprinting is a partially modified covalent imprinting technique where the polymerisation is carried out quite similarly to the covalent imprinting using an esterified (hydrolysable) template; however template rebinding to the polymer takes place via non-covalent interactions. It seems to be quite an interesting way of assuring more stable monomer-template assemblies which are formed via strong covalent interactions that can produce more template selective binding sites. At the same time, template rebinding via non-covalent interactions allows for faster template binding/removal kinetics which is very useful for many bio-sensing and immunoassay based applications. Earliest attempts on producing MIPs via semi-covalent imprinting technique were reported by Wulff's research group for the preparation of MIPs selective towards glyceric acid (25). In the reported study, covalent polymerisation was carried out via amide linkage between glyceric acid and boronic acid–co-(vinyl aniline); however upon rebinding, glyceric acid interacted partly via covalent bonding (ester) with boronic acid and non-covalently (through ion pairing) with 4-vinyl aniline (34). Some other earlier studies also reported imprinting of esterified templates in polymer matrix by covalent mechanisms. However, hydrolytic removal of the template generated –COOH or –OH groups at the template rebinding sites for its rebinding to occur via non-covalent interactions (35,36). Despite the flexibility of template binding/removal in this approach, imprinting template derivatives into the polymers can induce inefficient template recognition, cross-reactivity and unpredictable enantio-selectivity too (29).

Sacrificial spacer imprinting is similar technique of preparing imprinted polymers which utilises a spacer between the monomer and the template. The spacer not only helps in binding the template to the monomer but also prevents steric repulsion arising due to hydrophobicity of polyvinyl groups present in the monomers (29). This method was first developed by Whitcombe et al (37). They used vinyl phenyl carbonate derivative of cholesterol as the modified template; yielding cholesteryl [p-(vinyl phenyl) carbonate] and phenyl [p-(vinyl phenyl) carbonate)] monomer-template assemblies upon interacting with p-(vinyl phenyl)

carbonate monomer. These were then cross-linked thermally with EGDMA (ethylene glycol dimethacrylate), as seen in Figure 2.2.

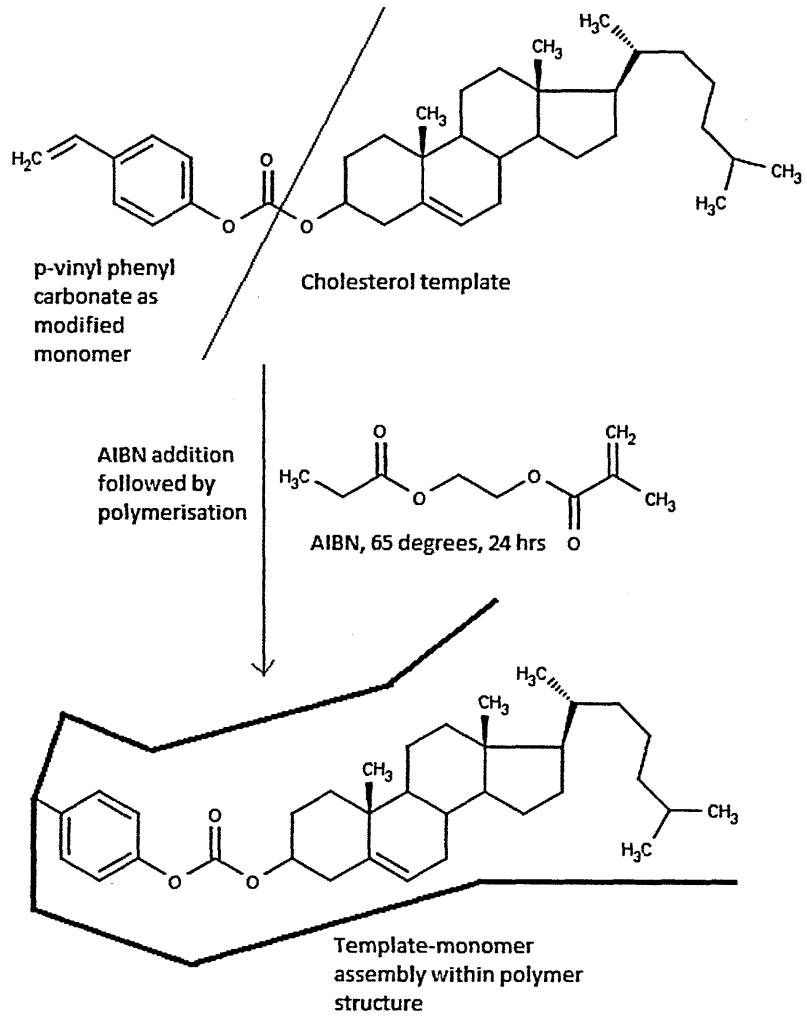

Figure 2.2: Schematics showing cholesterol imprinting using sacrificial spacer in a semi-covalent approach. The monomer (p-vinyl phenol) covalently bound (via ester bond formation) to the template (cholesterol) in the pre-polymerisation mixture. It was then cross-linked via thermal free radical polymerisation at 65 °C for 24 hours using AIBN (azobisisobutyronitrile) as an initiator, as adapted from (37).

The post polymerization removal of cholesterol derivative was facilitated by alkaline hydrolysis, which resulted in the removal of carbonate group as CO_2. This generated phenolic –OH at the binding sites to allow rebinding of cholesterol to occur via hydrogen bonding in a non-polar solvent (as shown in Figure 2.3).

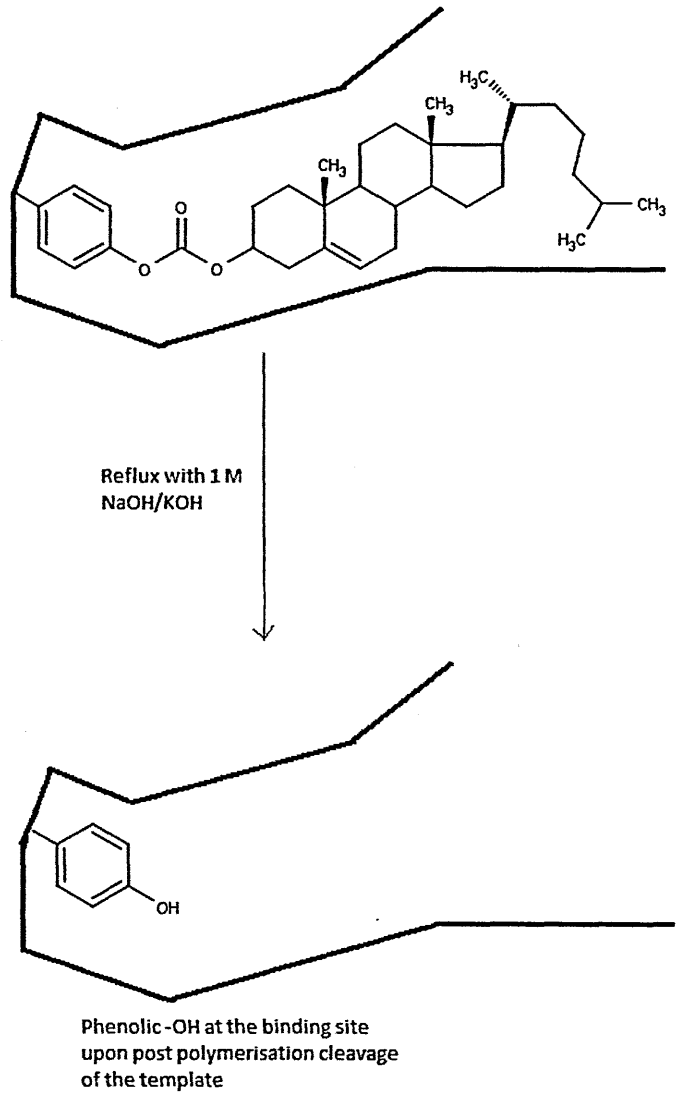

Figure 2.3: Schematics showing cholesterol rebinding site formation upon hydrolysis bearing phenolic –OH; adapted from (37).

Although cholesterol recognition performance of these MIPs may improve by using semi-covalent imprinting approach, introduction of larger functional groups such as -COOR at the binding sites instead of -OH, may not be able to fit relatively bigger templates into the available binding space (34,37). This assures yet again that along with the functionality, the shape and the size fit of a template is essential to obtain improved template recognition performance of the MIPs. Although this may be a very useful technique for carrying out suspension or emulsion based dispersion polymerisations in the presence of water, template rebinding will have to take place in non-polar solvents since it involves non-covalent interactions between the template and the polymer. Therefore, it may also limit the choice of the template that can be used (29).

In this regard, both covalent and semi-covalent imprinting techniques are not as widely preferred as non-covalent imprinting whilst developing MIPs. The following paragraph discusses the non-covalent imprinting approach.

Non covalent imprinting is the simplest (in principle) and the most widely used technique for imprinting templates via non-covalent interactions (such as, hydrogen and ionic bonding, weak electrostatic interactions as well as dipole-dipole or van der Waal's interactions) (8). This type of imprinting was first demonstrated by Mosbach and co-workers (38) when they successfully imprinted amidine moieties by adding sufficient amount of the monomer (carboxylic acid) to obtain stable monomer-template assemblies (binding constant, $\geq 10^3$ M^{-1}) via non-covalent interactions (16). As this technique involves non-covalent bond formation, it can provide faster binding and removal kinetics that is ideal for a lot of bio-sensing and diagnostic applications. It is also devoid of the need for exhaustive organic synthesis that is needed in covalent imprinting which involves preparation of the template derivatives capable of forming covalent bonds with the vinyl monomers. However, non-covalent imprinting tends to produce more heterogeneous binding sites as a higher amount of monomer is generally added to favour the equilibrium towards formation of monomer-template assemblies (36,39). A summary of some most common features of covalent and non-covalent imprinting techniques follows in Table 2.2 (33,36).

Table 2.2: Characteristics of covalent and non-covalent imprinting techniques

Characteristics	Covalent	Non- Covalent
Choice of template molecules	Limited to few template molecules	Widely applicable to almost all template structures
Nature of the interaction	Complex but more specific	Comparatively flexible and non-specific
Polymerization method	Widely suitable for all methods	Not widely suitable for all methods
Solvent suitability	Suitable for imprinting into polar solvents; suitable for the imprinting of biomolecules and dispersion polymerisations	Unsuitable for polar solvents; unsuitable for the imprinting of biomolecules and dispersion polymerisations
Template removal	Difficult and needs severe cleavage conditions	Comparatively easier with simple solvent extraction
Template removal and rebinding	Relatively slow	Relatively quick
Structure of the polymer	More specific and predictable	Less specific and less predictable
Homogeneity of the resulting polymer	Homogenous binding sites	High probability of forming heterogeneous binding sites

The ease and flexibility of the non-covalent imprinting makes it an ideal choice for developing MIPs, however lower yield of high fidelity binding sites also necessitates careful optimisation of its polymerisation protocol.

Unlike covalent imprinting, non-covalent bond formation occurring between the template and the monomer is also hugely affected by the experimental conditions (temperature, time, rate of monomer conversion etc.) used during polymerisation. This is then likely to affect the physical properties (size, shape, spatial distribution of the binding cavities, surface area) and thereby the template recognition performance of the prepared MIPs too. Hence, it is vital to discuss the effects of various experimental parameters on the physico-chemical properties of the resulting MIPs. Through the entire course of this report, non-covalent imprinting will be the method of choice for developing MIPs. The following section discusses different experimental parameters involved with the preparation of non-covalently imprinted polymers.

2.4. Experimental parameters in non-Covalent Imprinting – "polymerisation cookery"

Many studies have already found that different experimental parameters may influence template recognition performance of the resulting MIPs. Piletsky's group has conducted significant amount of research in this area by investigating the effects of experimental parameters (such as, temperature, time, and pressure) and reaction components (such as, the type of initiator, porogen and monomers) on the template recognition performance of MIPs. However, the physical properties of the MIPs have been largely overlooked, although they are directly affected by these experimental parameters and are true determinants of the MIP's recognition performance. The research carried out by this group has shed some light on the effect of experimental parameters on physical properties of MIPs (mainly the surface area); however other parameters (such as, the degree of cross-linking and thermal robustness) need to be further investigated. For example, an optimal cross-linking degree of a MIP matrix is very crucial to obtain desired removal and rebinding kinetics of the template. Extensively cross-linked MIP can hinder the template removal; whereas too little cross-linking may fail in holding template binding sites intact within the MIP matrix which may adversely affect its template recognition performance. Moreover, no study has reported a direct correlation between the experimental parameters of polymerisation and its potential effects on both the physical properties as well as the template recognition performance of the resulting MIPs. With the aid of literature, this section will briefly discuss "polymerisation cookery" and its effects on the properties of the resulting MIPs.

2.4.1. Initiator

Free radial polymerisation is the most convenient method for preparing polymers and initiator is an integral component of its recipe. Upon being exposed to high temperatures or UV irradiation, an initiator produces highly reactive free radicals which drive the process of polymer formation from monomers. Figure 2.4 presents the schematics of free radical formation from azo initiator in a UV initiated free radical polymerisation.

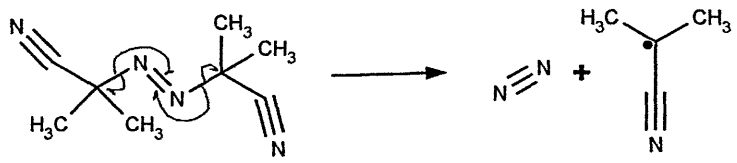

Figure 2.4: Schematics of formation of free radicals from an azo initiator in a typical free radical thermal or UV polymerisation; adapted from (40).

This step of free radical formation from the breakdown of initiator is called the initiation step. The free radicals generated in this way (as shown in Figure 2.4) then rapidly react with the monomer to generate reactive monomer species to grow polymer chain further (40). Figure 2.5 shows reaction that takes place between free radicals and monomers.

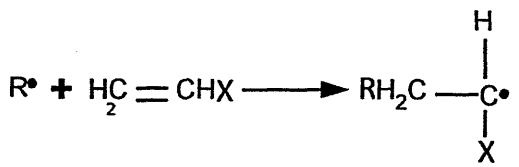

Figure 2.5: Schematics of formation of reactive monomer species through reaction between vinyl monomer and free radicals generated from initiator breakdown (40).

If the reactive monomer species on the growing oligomeric chain react with another molecule of monomer, it leads to elongation of the polymeric chain. However, not all the reactive monomer species participate into polymer chain elongation because sometimes instead of reacting with unsaturated monomer or cross-linker molecules, two reactive monomer species fuse with each other resulting into termination of chain elongation. Figure 2.6 shows schematics of chain propagation through reaction between vinyl monomer and reactive oligomer species.

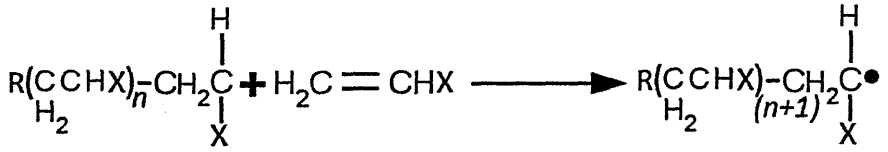

Figure 2.6: Schematics of polymer chain propagation through reaction between unsaturated monomer and reactive oligomer species.

As polymerisation proceeds, more and more unsaturated monomers are acted upon by the reactive oligomeric nuclei and polymer elongates. Polymer chain extends with time but once all the unsaturated monomers are consumed, reactions between already formed radicals and that of radical and oligomeric nuclei lead to formation of non-reactive species. This means that the polymer chain can no longer extend resulting into termination of polymerisation. Figure 2.7 and 2.8 show schematics of polymer chain termination resulting into formation of saturated and unsaturated products respectively.

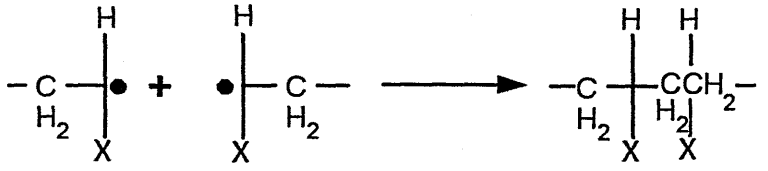

Figure 2.7: Schematics of polymer chain termination resulting into saturated end product (40).

As shown in Figure 2.7, when two radicals fuse together with the formation of hydrogen bonds, it usually forms a saturated end product in the termination step. On the other hand, if the radicals react with each other disproportionately, they may generate different product as shown in Figure 2.8.

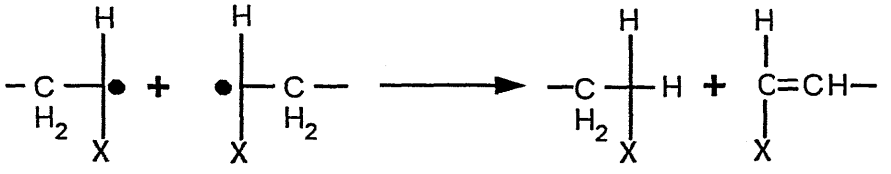

Figure 2.8: Schematics of polymer chain termination resulting into unsaturated end product (40).

Although initiation, propagation and termination are the three main steps of a free radical polymerisation, other reactions may also occur depending on what other ingredients are being used (mainly porogen) in the pre-polymerisation recipe. Chain transfer is one of such phenomena where the free radical reacts with species other than unsaturated monomers which can transfer the reactive radical nuclei on them and not on the monomers or oligomers. This non-monomeric reactive species can react with monomers later thus producing different polymer products. Figure 2.9 shows schematics of a chain transfer reaction occurring between a radical and porogen (chloroform).

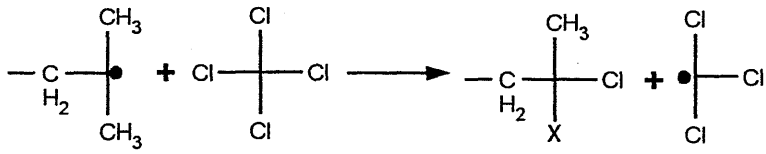

Figure 2.9: Schematics of chain transfer reaction in free radical polymerisation (40).

Since the chain transfer phenomena results into formation of different polymer products and that of different molar mass, this is widely exploited to achieve polymers of desired molar mass and size of the resulting polymer in a free radical polymerisation.

Azo derivatives (R-N=N-R) such as, azobisisobutyronitirile (AIBN) and 2, 2'-azo-bis-(cyclohexylcarbonylnitrile) (ABCH) or peroxide derivatives such as, benzoyl peroxide and lauroyl peroxide are the initiators of choice for MIP recipes due to their solubility in most organic solvents used in MIP preparation, whereas water soluble initiators such as potassium or ammonium persulfate are more popular with biphasic suspension or emulsion polymerisations which are explained further in Sections 2.6.2 and 2.6.3 (16,41,42). Although initiators are the main driving force behind a successful radical polymerisation, they are typically used in very low amounts of about 1 wt % or 1 mol % of the total pre-polymerisation mixture (43). Such polymerisations are thermally initiated by using oven or oil-bath; however microwave reactors have also been investigated lately to prepare AIBN initiated caffeine imprinted polymers. The reported study strongly indicates that thermal polymerisations can be improved by extremely faster polymerisation rates of MW reactor led heating (44). The research into MIP development has increased tremendously in past couple of decades; they still face limited industrial scale production. In this regard, MW polymerisation can be particularly useful for developing MIPs since its controlled and programmable polymerisation can increase the output of MIP production with minimal batch-to-batch variation (44,45).

However, there is an ongoing debate on whether the MW led thermal polymerisation is just a faster heating method or it participates in initiator breakdown by other non-thermal mechanisms such as those observed with the UV irradiation (46). It would be really interesting to study these aspects of MW led thermal polymerisations for the preparation of MIPs. One of the main objectives of the MW project presented in this thesis is to understand whether MW polymerisation can be used as alternate polymerisation method for the development of MIPs (as mentioned earlier in Chapter 1). These research questions are further explored in a comprehensive study presented in Chapter 3 which discusses development of MIPs by MW polymerisations.

Apart from the breakdown mechanism of the initiator, its amounts may also influence the properties of the resulting MIPs. From the porosimetry analysis of prepared MIPs, a study has found that increasing the amount of initiator from 1 wt % to 5 wt % in the pre-polymerisation mixture improves the surface area of the resulting MIPs (40). This has been justified with the hypothesis that higher amount of the initiator generates a higher number of free radical nuclei. However, the fixed volume of the monomer mixture means that the increase in free radicals may compensate for smaller inter-nuclei spaces resulting in smaller pores which ultimately produce larger surface area. In this regard, MIPs having larger surface area would be expected to show higher template recognition performance. However, it has also been found that the MIPs prepared with higher amount of the initiator shows inferior recognition performance in spite of having larger surface area. This is quite an interesting observation which suggests that since the higher amount of initiator generates larger number of free radicals and thereby form highly cross-linked or rigid MIP, it may hinder template binding and removal kinetics from its matrix (40). It is also established that the formation of stable monomer-template assemblies in the pre-polymerisation mixture is equally crucial in producing template selective binding sites within the resulting polymer matrix. An increase in the amount of the initiator may elevate polymerisation temperature which may further increase the kinetic energy of the polymerisation mixture and destabilise the monomer-template assemblies at the same time. As a result, it is likely to form heterogeneous binding sites which give inferior template recognition performance of the resulting MIPs.

2.4.2. Monomers

Monomers are generally used in excess in comparison to the template (template: monomer ≥1:4) to favour formation of sufficient number of monomer-template assemblies in a conventional non-covalent imprinting (43). Structurally, MIPs are co-polymers which consist of at least two different kinds of monomers, functional monomers and cross-linking monomers. Functional monomers bear suitable functionality to be able to interact non-covalently to the template and integrate covalently (via vinyl groups) to the cross-linking monomers, also referred to as cross-linkers (47). Figure 2.10 presents few examples of commonly used monomers for the preparation of non-covalently imprinted polymers.

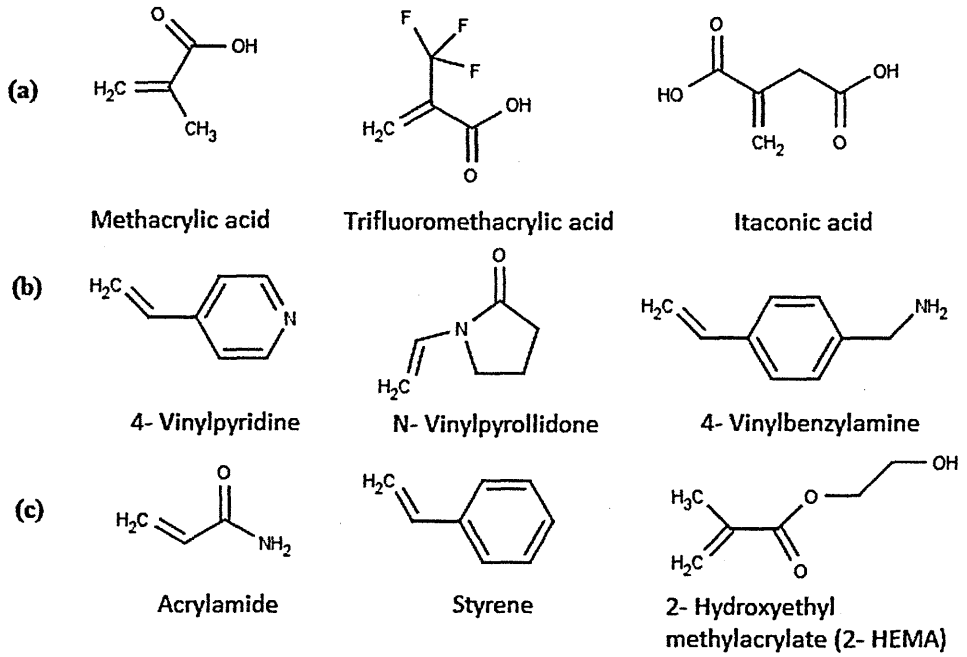

Figure 2.10: Commonly used monomers for non-covalent imprinting, (a) acidic, (b) basic and (c) neutral; adapted from (39,43).

Acrylate derivatives (such as, methacrylic acid) and vinyl derivatives (such as, styrene) are the most widely used monomers. Where methacrylic acid (MAA) participates in forming H-bond with the template; vinyl derivatives interact mainly via hydrophobic interactions (as seen in Figure 2.10). The interactions occurring between a monomer and a template are highly important in a non-covalent pre-polymerisation system. To this end, the energy associated with the monomer-template complex formation is crucial which is influenced by unfavourable factors, such as, the enthalpic energy lost in overcoming unwanted bond rotation and conformation of the monomer-template assembly as well as undesired hydrophobic, ionic, electrostatic or van der Waal's interactions between the template-template and monomer-monomer in the presence of porogen (48).

Hence, thermodynamic calculations of the pre-polymerisation mixture have been of a great concern whilst optimising a MIP recipe to ensure formation of enough stable monomer-template assemblies in order to generate template selective binding sites. These factors are usually determined by NMR titrations of different monomer and template ratios where a shift of the key NMR peaks is indicative of non-covalent bond formation between the species of the pre-polymerisation mixture (16). Some other methods, such as, FTIR and UV spectroscopy have also been used for calculating monomer-template association constants that indicate the strength of non-covalent interactions between the monomer-template moieties at equilibrium

(39,49,50). In addition to this, a slightly different approach has also been reported where the use of a combinatorial library of MIPs is prepared by using different monomer-template ratios, called 'mini-MIPs'. The prepared polymers are then screened using liquid chromatography (LC) based template rebinding assays (50). However, the described methods are extremely tedious and expensive.

On the other hand, computational simulations are much simpler and quicker where the monomer with the least entropic values or the highest binding constant for the template is chosen to maximise stable monomer-template assemblies. The first computational program for the MIP preparation has been developed by Piletsky's research group (50,51). The research has found that the pre-polymerisation recipes optimised by computational approach not only comply with that of traditional methods (such as, NMR titrations and UV spectrophotometry) but also show the highest template recognition in chromatographic separation (52,53). As a result, computational approach has often been used for optimising the pre-polymerisation recipes in developing non-covalent MIPs lately (54-56). For the preparation of caffeine imprinted polymer monoliths reported in Chapter 3, computationally optimised recipe has been adopted from the previously reported studies (44,53). Likewise, computationally optimised pre-polymerisation recipe has also been used for the development of the polymers for mycotoxin recognition, presented in Chapter 4 of this thesis (57).

The other type of monomers used in the development of cross-linked co-polymers is cross-linking monomers or as often referred to as the cross-linkers. Since MIPs are extensively cross-linked co-polymers, they usually contain very high amounts of the cross-linking monomers. An increase in the amount of the cross-linker is linked with increase in the surface area of the resulting MIP (58,59).

Since the surface area of the MIPs is often further linked with its template recognition performance, the type and ratio of the functional monomer to the cross-linking monomer are very crucial in determining the cross-linking degree and thereby template recognition performance of the resulting MIPs. Optimisation of the monomer-template-cross-linker ratio is very elaborate. In an attempt to minimise these optimisation steps, a study has reported the preparation of OMNiMIPs where MIPs can be prepared with a single cross-linking monomer, such as, NOBE (N, O- bisacryloyl ethanolamine). In the reported study, a comparative chromatographic analysis of OMNiMIPs with a traditional co-polymer (MAA-EGDMA) has been carried out which suggests that OMNiMIPs show better enantiomeric separation of a range of

amino acid templates (60). However, the approach has not been widely used as the choice of template and cross-linker becomes very limited.

More commonly used cross-linkers for non-covalent imprinting, such as, divinylbenzene (DVB) and ethylene glycol dimethacrylate (EGDMA) have two vinyl groups which provide two points of reaction through covalent bonding, as shown in Figure 2.11 below.

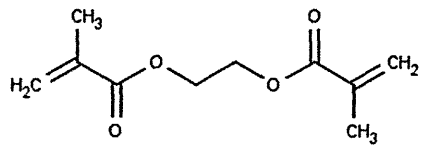

Ethylene glycol dimethacrylate

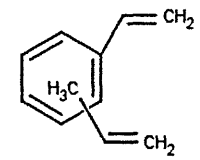

Divinylbenzene

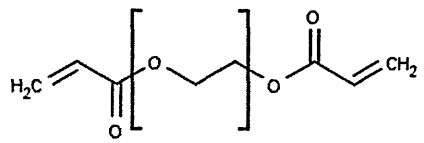

Poly(ethylene glycol) diacrylate

Figure 2.11: Commonly used cross-linkers for the preparation of non-covalently imprinted polymers (43).

MIP preparation in water is challenging as most cross-linkers are hydrophobic in nature. However, poly(ethylene glycol) diacrylate has been reported to be effective for imprinting biomolecules and environmental templates compared to more traditional hydrophobic cross-linkers, such as, EGDMA. Not only in providing the ease of preparation, such MIPs can also be used for the template recognition studies in water based samples due to their reduced hydrophobicity (61). There has also been a growing interest in using multiple vinyl groups bearing cross-linkers as well since they can anchor the monomer-template assemblies from multiple points and produce highly selective template rebinding cavities within the MIP matrix. Figure 2.12 shows the structures of more recently used cross-linkers.

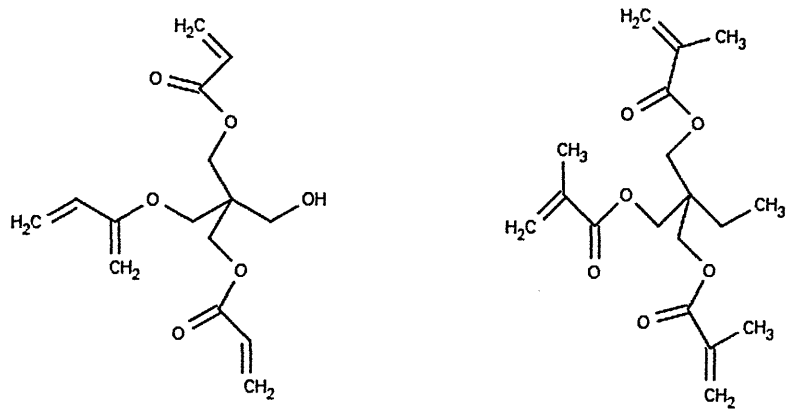

Figure 2.12: Some newer cross-linkers for the preparation of non-covalently imprinted polymers; (a) Pentaerythritol triacrylate (PETRA) and (b) Trimethylolpropane trimethacrylate (TRIM).

The structures of the cross-linkers shown in Figure 2.12 have multiple vinyl groups, for example, PETRA has four vinyl groups; whereas TRIM has three vinyl groups which provide them multiple points of interactions with the functional monomers to form a firmly cross-linked network of polymer. It has been reported that the cross-linkers with multiple vinyl groups are found to be superior in providing better resolution of the racemates in chromatographic analysis (62). However, such cross-linkers also contain carbonyl or hydroxyl groups which provide them ability to interact with the monomer-template assemblies through different non-covalent mechanisms as well. This means that although the cross-linked polymer network is firm enough to hold the binding cavities in place, it may be flexible at the same time due to its non-covalent interactions which may sometimes lead to heterogeneity of the binding cavities formed within its matrix.

To improve recognition of the template, additional special monomers can also be integrated in the pre-polymerisation recipe to aid in the recognition of the template. An example of this has been recently shown by Turner's group where a nucleoside has been used as an 'additional' monomer in preparing MIP NPs. The chemical modifications obtained on a nucleoside (such as, phosphoramidites as well as nitrogen base modifications) allow it to be covalently integrated as a special monomer along with the other functional monomers into cross-linked MIP NPs. It has been found that the chemical modification obtained on the nitrogen base (5-carboxymethylvinyl modification) of a nucleoside (uracil) is electron withdrawing and can covalently integrate itself into the polymer backbone. Incorporation of the nucleoside monomer obtained in this way has also reflected into improved recognition of its complimentary nucleoside template (adenine) in template rebinding experiments (63).

Similar modifications have also been obtained on aptamer sequences by chemically modifying it from multiple nitrogen bases alongside their chain end phosphoramidite modifications. Modifications obtained in this way allows the aptamer to integrate covalently into the polymer backbone from multiple points, at the same time also allowing it to interact with its complimentary base pairs through non-covalent interactions (hydrogen bonding). It has also been found that the template recognition of the polymer NPs having integrated an aptamer by suggested strategy (modifications from multiple points) is improved in comparison to the polymer NPs having incorporated the same aptamer through just one (chain end phosphoramidite) chemical modification (64). This suggests that other functional/cross-linking monomers can be modified similarly to help in their incorporation into the polymer from multiple points and thereby improve the template recognition performance of the resulting MIPs. This approach has been discussed further in Chapter 5 where chemically modified oligonucleotides have been incorporated into the MIP matrix to develop OligoMIP NPs for the selective recognition of an oligonucleotide template.

2.4.3. Porogen

The polymerisation solvent not only serves to bring all the pre-polymerisation components in a single phase but is also responsible for providing morphology and porosity to the resultant MIP. Hence, it is also commonly referred to as the porogen. Porogen for the MIP synthesis should dissolve all the pre-polymerisation ingredients but at the same time shouldn't have detrimental effects on the monomer-template interactions. In this regard, the porogens used for non-covalent imprinting are usually polar aprotic solvents (acetonitrile, dimethyl formamide etc.) or non-polar aprotic solvents (toluene, chloroform, dioxane etc.) that do not interfere with the hydrogen bond formation between the template and the monomer (61). If the monomer and the template can undergo other non-covalent interaction except hydrogen bond, a polar solvent is preferred. Ionic bonding and dipole-dipole interactions between the template and the monomer are more dominant in the presence of polar solvents (29).

Porogen intrudes into the inter-nuclei spaces of a growing polymeric chain and then finally separates from the grown polymer phase imparting certain porous characteristics, which are also dependant on temperature and other factors.

Pores observed in these polymer microparticles vary from 2 nm to 50 nm. Larger pores of greater than 50 nm are regarded as the macropores; whereas any smaller than 2 nm sized

pores are the micropores and the ones in between the mentioned size range are the mesopores (65).

When a good solvent for the polymer is used as the porogen, necessary insolubility for the phase separation mainly arises from extensive cross-linking. When the dispersed phase contains a good solvent as a porogen (such as toluene for polyvinyl), it can penetrate and swell growing oligomeric globule during polymerisation. As the polymerisation proceeds, the degree of cross-linking intensifies and a moment comes beyond which porogen can no longer intrude inside the growing globule and separates out of the phase. This moment comes in the later stage of polymerisation, after the gelation phase of the resulting polymer. Until this point in the polymerisation, numerous reactive nuclei have generated which have smaller inter-nuclei space between them.

Therefore, a good solvent tends to produce microparticles with micro and mesopores and thereby generates larger surface area. This phenomenon is known as v- induced syneresis. Higher surface area is usually deemed to give better recognition performance too, however sometimes the microparticles with lower surface area may also show improved recognition performance. This is because the surface area of particulate MIP is measured in its dry state whereas the template rebinding is carried out in the presence of porogen. This suggests that although the surface area of the polymer is low in its dry state, the pores may swell in the presence of the porogen at the time of template rebinding. Sometimes, macropores may also be located remotely deep within the particle matrix and not on the surface which may also provide sites for the template recognition (66).

On the other hand, when a non-swelling porogen is used in the dispersed phase (such as n-heptane for polyvinyl or dodecanol for polydimethacrylate), it cannot penetrate much in the growing oligomeric globules. Hence the phase separates early on, before even gelation point which results in a polymer with low pore volumes (67,68). Hence, it is more likely to produce macroporous particles with lower surface area ($\leq 100\ m^2\ g^{-1}$) via χ-induced syneresis (65).

It is noted that the pore size is dependent on other factors as well, such as the polymerisation temperature and the time of reaction. When a polymerisation is carried out at an elevated temperature, there is higher number of growing nuclei which result in smaller inter-nuclei spaces and hence generate smaller pore sizes but addition of a poor solvent causes early phase separation in this polymerisation. Since the number of oligomer nuclei is small with larger

inter-nuclei space at this early stage of the polymerisation, an early phase separation brought upon by the poor solvent then can generate a polymer with larger pores too. Moreover, the pore sizes also reflect directly the available surface area of the resulting polymer. For example, smaller pores will yield larger surface area whereas larger pores will give smaller surface area which determines the template recognition performance of the resulting polymer. Porosity characteristics and surface area is inter-linked and also dependent on other experimental parameters (such as, the length of polymerisation and its temperature). Therefore, these parameters are studied and optimised based on the area of application of the resulting polymer. For example, surface area is a preferred measure of the polymer performance in chromatographic analysis; whereas porosity is preferred in polymers for flow through cells and SPE (Solid Phase Extraction) applications to avoid high back pressures (69).

In Chapters 3 and 4 of this report, polymers have been prepared at varying temperatures for different lengths of time and their porosity characters and surface area have been studied in detail. Furthermore, the studies have also linked these parameters to the recognition performance of the polymers.

2.4.4. Temperature

The polymerisation temperature plays a key role in determining many features of the resultant polymers such as porosity, surface area and pore volume as well.

In a radical polymerisation, free radicals generated upon the activation of an initiator produce reactive nuclei which develop further cross linking as the polymerisation progresses. However when the oligomer chains grow, they separate out from the porogen phase due to limited solubility of the globules followed by the precipitation of the polymer.

When the same polymerisation is carried out at an elevated temperature, it is likely to generate a much larger number of free radical nuclei but since the volume of the monomer mixture is the same, a higher number of the nuclei get accommodated into small volumes resulting in numerous smaller pores in the polymer matrix (69). Not to mention, pore size and its distribution then also affects the available surface area, as discussed earlier in Section 2.4.3.

Polymerisation temperature is crucial in defining physicochemical properties of the polymer. The *in situ* polymerisation temperatures are generally much higher than the set reaction

temperatures. Figure 2.13 shows recorded temperatures of several thermal and UV polymerisations.

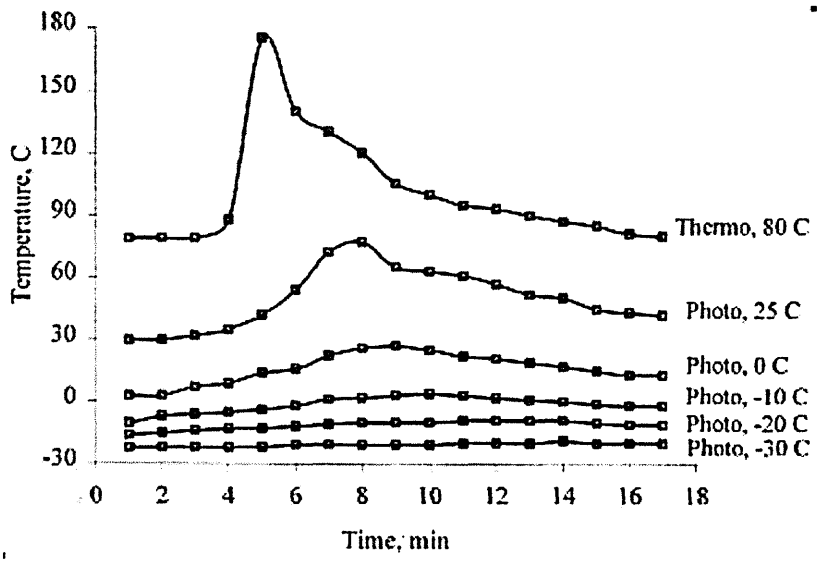

Figure 2.13: Actual polymerisation temperatures recorded with the help of temperature probes during thermal and photo initiated polymerisations; obtained from (70).

The actual temperatures recorded during the UV polymerisations are not too different from their set value, however the polymerisation temperatures almost double or increase even further when it is carried out thermally (as seen in Figure 2.13). It is because the elevated temperatures set in thermal polymerisations increase the kinetic energy of the system due to its exothermic nature and accelerate free radical formation which increases the temperature even further. The rise in temperature may be detrimental to the formation of stable monomer-template assemblies which are crucial to forming template selective binding sites in the resulting MIPs (48).

More importantly, elevated polymerisation temperatures may also denature sensitive templates during polymerisation (such as proteins) which further reflect the compromised template recognition of the resulting MIPs (71).

In this regard, MW reactor led thermal polymerisations may be useful as it maintains the reaction temperatures at a set value. When a reaction reaches the required temperature, no further energy is supplied. Therefore the reaction takes place on its own with its own exothermic energy but with added advantage of faster polymerisation kinetics. This means that the pre-formed monomer-template assemblies are cross-linked at a much faster pace

minimising the chances of their deformation. Once the exothermic phase is complete, it controls the reaction temperature for the set length of time which helps in forming and strengthening the pre-formed cross-links within the MIP matrix (44). Traditional thermal polymerisations carried out using an oven and oil-bath do not contain such thermostatic controls which makes it difficult to upscale such thermal polymerisations since the temperatures can go even up to 300 °C for not more than 50 ml of the polymerisation mixture (70). MW polymerisations may be investigated in this regard to carry out polymerisations with larger volumes of the monomer mixtures.

To understand the effect of temperature beyond just maintaining stable monomer-template complex, its effect on the physical properties of the resulting polymers has also been studied. It has been observed that the polymers initiated at lower temperatures show smaller pore volumes and smaller surface area (as discussed earlier in Section 2.4.2). This may be because the polymerisation rate is slower at lower temperatures. Hence, there are fewer growing nuclei at the time of phase separation. The fewer the nuclei, the greater is the inter-nuclei space which helps it create larger pores and hence less surface area (48,69). This way, lower temperatures may help in creating polymers with smaller surface area but may at the same time generate polymers with more template selective binding cavities due to stable template-monomer assemblies generated during the polymerisation. However, it has been suggested that polymerisations carried out at different temperatures do not show significant difference in their cross linking degree although showing different chromatographic separation efficiencies (72). Not only the polymerisation temperatures but operational temperatures may also affect the template recognition performance of the MIPs. Studies report that the template rebinding performance improves with increasing column temperature regardless of polymer's make up due to improved template binding and removal kinetics (48,70).

In terms of surface properties of the MIP particles, lower polymerisation temperature tends to produce smoother particles with fewer larger pores and smaller surface area; whereas higher temperature produces rough particles with many smaller pores and larger surface area (29,73). However, as already discussed in Section 2.4.3, the effect of the temperature can be changed by using appropriate type of porogen. Although higher polymerisation temperatures generate MIPs with larger surface area, addition of a non-thermodynamically favourable solvent for the polymer can induce early phase separation and increase the pore size and thereby decrease surface area (69).

This implies that the performance of the polymers is greatly influenced not only by the thermodynamics but also the experimental parameters. To this end, Chapters 3 and 4 have investigated the effect of different polymerisation temperatures on the physical properties (such as, pore volume, pore size, surface area and cross-linking degree) as well as recognition performance of the polymers. It also presents a detailed study on the characteristics of the polymers prepared by MW polymerisation in comparison to those prepared by traditional methods (oven and UV polymerisations). Section 2.4.5 discusses the effect of the length of polymerisation on the properties of resulting polymers.

2.4.5. Polymerisation time

Polymerization time is an important experimental parameter affecting the physicochemical property of the polymer however to a lesser extent than temperature or porogen. From the studies reported earlier, it appears that thermal decomposition of an azo initiator is about 10 times slower (when initiated for up to 80 °C) than that of its photodecomposition (approximately 2 hours at 25 °C) (74). In this regard, MW reactors have been investigated for the preparation of thermally initiated caffeine imprinted polymers recently which suggests that MIPs can be prepared in a MW reactor for as little as just 15 minutes (44). It has been reported that thermal half-life of azo initiators is over 1000 minutes when initiated by oven or oil-bath (74); however about 100 times faster initiation could be achieved by MW reactors when initiated thermally (44).

Indeed, this has opened up a new direction for exploring if at all microwaves do have a 'wave effect' just as the UV irradiation in speeding up the initiation and hence the polymerisation process. This has been explored in detail in Chapter 3.

It is a general notion that the degree of cross-linking of the polymer remains fairly similar regardless the length of the polymerisation soon after the polymerisation is initiated, when polymerised by a UV chamber or oven. Figure 2.14 shows the effect of the length of polymerisation on the cross-linking degree of the resulting MIPs.

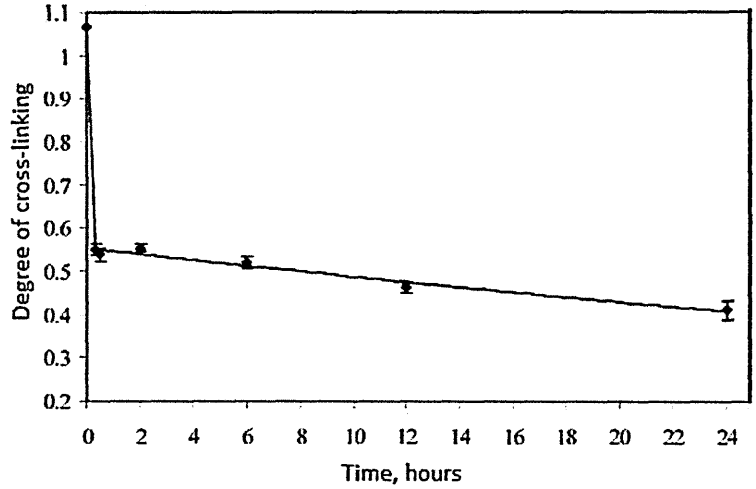

Figure 2.14: Effect of the length of a polymerisation on the cross-linking degree of UV initiated MIPs; adapted from (74).

It has been found that the MIPs prepared for different time durations (from 10 minutes to 24 hours) show much similar cross-linking degree (as seen in Figure 2.14). However, the one polymerised for longer (24 hours) shows improved enantio-separation in chromatographic analysis studies. To understand this further, swelling analysis has also been performed on these MIPs which suggests that despite having a similar degree of cross-linking the MIPs prepared for longer times show lower degree of swelling (74). It appears that improved enantio-selectivity observed with the polymers prepared for long preparation times may arise due to higher rigidity and fidelity of well aligned binding sites created. However, it should not be ruled out that increased rigidity over longer polymerisation times may also retard mass transfer kinetics (70). The studies presented in Chapter 3 and 4 of this thesis will primarily investigate the effect of polymerisation time on the properties of MIPs prepared by MW polymerisation.

In these studies, the MW polymerisations have been carried out from 5 minutes to 60 minutes and its effects on the cross-linking degree, surface area and pore volume of the MW MIPs have been studied. Also to understand whether MW polymerisation can be used as an alternative polymerisation technique to produce MIPs, the observed properties of the MW polymers have also been compared to those polymerised by traditional methods, such as oven and UV polymerisations.

2.5. Formats of non-covalently imprinted polymers

MIPs have been prepared either as particles or membranes. This section will briefly discuss the mentioned formats explaining their advantages and limitations. Polymeric materials are

inherently flexible and can be formed in many ways. This work is based around free-standing materials so a discussion of grafted or surface fixed polymers will not be covered. The discussion on different polymer format is particularly important as one of the objectives of this study is to comparatively analyse monoliths and microparticles prepared by different methods.

Monolith polymers are prepared conventionally as blocks by heating the pre-polymer mixture using an oven or oil-bath or by irradiating UV on it. The formed polymer block is then crushed, ground and sieved in the desired particle size range, typically between 30 µm to 150 µm. However, grinding and sieving involved in monolith preparation is quite tedious and can also lead to the severe loss (>50 %) of irregular particles. In spite of MIPs being extensively cross-linked, vigorous grinding may also lead to the destruction of the binding sites created with the polymer matrix (75). Although monoliths are widely used, their irregular shape may not be ideal for the chromatographic or SPE based applications due to inefficient packing and unpredictable binding or removal kinetics through their matrices. As a result, there is increasing demand for the preparation of spherical microparticles which are devoid of the mentioned limitations. Not to mention, the preparation of microparticles can be easily scaled up as well and does not result into excessive material loss as in case of monolith preparation (70,76).

Transport across the biological membranes is one of the most important phenomena involving highly specific transport via ion channels, receptors and concentration dependent diffusion. Solute transport across non-porous synthetic membrane is usually via diffusion whereas the porous membranes govern it via size exclusion (16).

The solute transport can even be more precise via selective solute exchange based on the shape, size and functionality if the MIP concept is applied on the membranes (77). In comparison to the MIPs monoliths and microparticles, the imprinted membranes have become very popular in continuous mode operations such as flow through filtration cells and biosensors. To this end, Piletsky and Kobayashi have conducted pioneering research work where MIP membranes have been prepared for various applications, such as, electro dialysis and enantio-separation (34,78,79). Most of them are prepared by phase inversion or separation which is achieved by precipitating polymers in presence of non-solvents. Sometimes the porogens are also cooled or evaporated to generate thin *in situ* polymer membranes in either a UV or thermally initiated process between glass plates (34,80,81).

Some characteristics of membranes such as coagulation and strength are very unique. Membranes tend to coagulate in poor solvents and result in lumpy structures which may affect their performance. For a polymer like acrylonitrile, presence of a poor solvent such as water can enhance dipole interactions with it resulting in its coagulation (82,83). Since thermodynamically poor solvent for the polymer results in its early phase separation, it yields higher porosity, larger pores and thereby improve flux of the material through MIP membranes which is sometimes even higher than that of microparticles (84).

Nanoparticle based MIPs is the newest addition to the MIP formats. There has been ever growing interest in developing MIPs on a miniaturised scale to benefit from the nanotechnological advances together combined with the selective recognition through molecular imprinting. Not to mention, MIP NPs are the most suitable alternatives to natural bio-macromolecules (such as antibodies, proteins and aptamers) with comparable molecular recognition property but with improved stability. A number of pioneering studies already have reported successful development of the MIP NPs and have dubbed them as 'plastic antibodies' for their potential *in vitro* and *in vivo* biological applications (64,85-87). MIP based NPs systems have been discussed more in detail in Chapter 5. Since one of the main objectives of this study is also to prepare MIPs by different methods in different formats, Section 2.6 discusses various methods that are routinely used to prepare MIP formulations.

2.6. Polymerisation methods for the preparation of MIPs

MIPs can be prepared in different formats by using different methods. This section will briefly discuss different methods commonly used for the MIP preparation.

2.6.1. Thermal / UV polymerisation

MIP monoliths have been traditionally prepared thermally with the aid of oven or oil bath or by UV irradiation. In comparison to the thermal polymerisation, UV irradiation is faster; however it yields lower surface area in the resulting polymer that may sometimes reflect its inferior template recognition performance of the polymer (as discussed earlier in Section 2.4.4). Therefore, thermal free radical polymerisation is widely preferred for MIP preparation.

Conventionally, ovens, oil baths and heating mantles have been used for thermal polymerisation. It is not only an elaborate method but is also very inefficient in providing homogenous heating throughout the reaction mixture as the heating depends on the conductivity of the reaction vessels and the polymers are likely to be highly non-homogenous.

As discussed earlier in Section 2.4.4, it is very likely that this heterogeneity in the polymer structure may reflect further its physical properties (such as porosity, surface area etc.) and result in its compromised recognition performance eventually. It would be ideal if the polymers can be prepared with homogenous heating at a quicker polymerisation rate. In this regard, the use of microwave (MW) reactors has increased recently with the realisation of its attractive features of good control over experimental parameters and extremely quick heating reactions compared to the conventional heating sources (46). However, the mentioned MW reactors should not be confused with the MW ovens used in the kitchens for heating food. MW reactors are specially designed laboratory equipment that carry out very controlled heating reactions which have been recently explored for the preparation of the MIPs too (44). MW polymerisation has been discussed in detail in Chapter 3 for the preparation of MIPs.

On the other hand, spherical polymer particles are traditionally prepared via different types of dispersion polymerisation techniques, such as suspension, emulsion, precipitation and more recently core-shell polymerisation. From the literature reported so far, it seems that only one study has been conducted for a direct comparison of the recognition performances of the same MIP prepared by different methods (88). Although the reported study has given a good insight into comparative analysis of the polymer's performance, it has not extended investigation into studying physical properties of the MIPs prepared by different methods.

It would be worth mentioning here that the difference in the recognition performance of the polymers simply arise from the difference in their physical properties. To this end, polymer microparticles under the study reported in Chapter 4 have been prepared by suspension, precipitation and core-shell polymerisation for their direct comparison against the monoliths prepared by oven, UV and MW polymerisations.

For the formation of spherical particles, immiscible biphasic systems are necessary which are commonly referred to as dispersions. Dispersion (or solid-liquid) polymerisation techniques are heterogeneous or biphasic in nature as they are composed of two immiscible liquids in which the monomers are dispersed as droplets (referred to as dispersed phase) into another immiscible bulk liquid (referred to as continuous phase). Dispersion polymerisation methods are extensively reviewed in reported studies (41,65,89,90). Section 2.6.2 will discuss suspension polymerisation.

2.6.2. Suspension polymerisation

Suspension polymerisation refers to the formation of spherical polymeric particles in an immiscible solvent system with the help of a droplet stabiliser(s); however the mechanism of polymer formation occurs via free radical polymerisation as observed in case of polymer monoliths. The volume ratio between both immiscible phases is ideally considered to be between 0.1-0.5. In a typical polymerisation set up, the monomer and/or cross-linking monomer is dispersed along with the initiator and porogen (in case of a porous polymer) into an immiscible continuous phase with constant heating and vigorous stirring. Shear force or the turbulent pressure changes generated due to the vigorous stirring then results in formation of monomer droplets into the immiscible continuous phase. Monomer is then acted upon by the initiator to create reactive free radical nuclei when the reaction is heated or exposed to the UV irradiation. These nuclei fuse together and form oligomeric globules. Until this stage, the polymerisation progresses in the dispersed or the droplet phase itself (42,89,91). A typical suspension polymerisation set up has been presented in the following Figure 2.115.

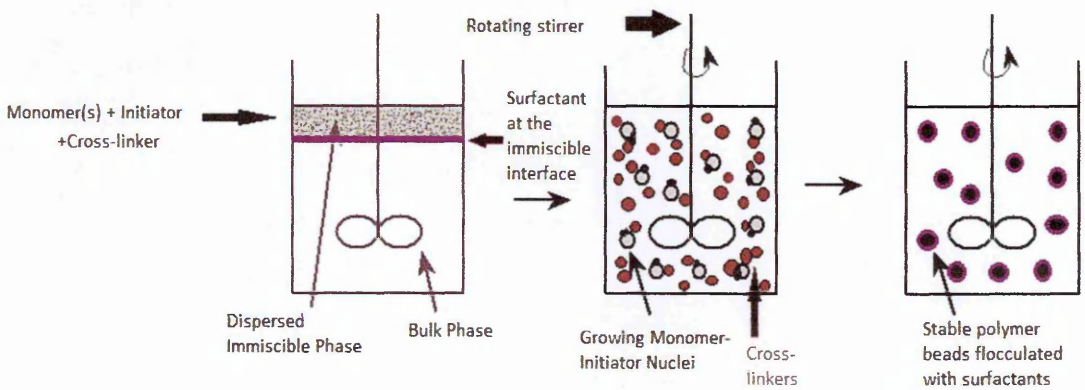

Figure 2.15: A typical instrumental set up used for preparation of polymer microparticles by suspension polymerisation (89).

The phase separation of these growing globules into the immiscible continuous phase is the most essential phase for the bead formation, driven mainly by the insolubility of the resulting polymer in its dispersed monomer phase. It is when insoluble oligomer globules come out of the dispersed phase into continuous phase and form particles. As the particle forms straight from the globule, the globule size is of utmost importance in suspension polymerisation. Hence, the speed of rotation and also the shape of the stirrer as well as the shape of the reactor is crucial in determining the particle size in the suspension polymerisation (65). This means that the particle size is inversely proportional to the speed of rotation. As a rule of thumb, to obtain the particle size of up to 100 µm, rotation speed of 400 rpm to 500 rpm is often used (41). Where the particle size is affected by the speed of rotation, degree of porosity

is affected by the type of porogen and the degree of cross-linking (as discussed earlier in Section 2.4).

The technique of making such polymer beads by O/W suspension is in practice since 1980s; however it is suitable for making mainly covalently imprinted polymers as water being the continuous phase may interfere with other non-covalent interactions (mainly hydrogen bonding and ion pairing) occurring between the template and the monomer in the MIP preparation (32,90). To this end, successful attempts have been made at preparing suspension microparticles of imprinted polymers by using fluorocarbon solvents as the continuous phase instead of water (66,75). However, the issue remains the same with the fluorocarbon solvents that it demands elaborate synthesis of the fluorocarbon monomers and the surfactants, not to mention that their use is limited to only UV initiated polymerisation too.

For a typical O/W non-imprinted suspension polymerisation, the initiator (0.1 – 0.5 wt %) has to be soluble in the dispersed phase along with the monomer hence it is more common to use azo initiators (such as AIBN) or peroxides and last but not least, stabilisers or surfactants which play a crucial role in determining the particle size and size distribution of the resulting polymer. The droplet stabilisers are semi-synthetic or synthetic, hydrophilic, large molecular weighted polymers. Typical examples of oil in water (O/W) suspension polymerisation systems (For example, polyacrylates and polystyrene) include water-soluble polymeric stabilisers such as, polyvinyl pyrollidone (PVP) (89,92-94), poly vinyl alcohol (PVA)(59,95) and cellulose derivatives (96).

Inorganic colloids, such as, $CaCO_3$, $BaSO_4$ and $Al(OH)_3$ are also used as stabilisers (59). Stabilisers do not have a direct surface tension lowering effect but they get adsorbed on surface of the growing oligomeric globule and sterically stabilise the droplets against coalescence (as shown in Figure 2.15). Ideally, O/W suspension polymerisation would not be suitable for a non-covalently imprinted polymerisation system as water could interfere with other non-covalent interactions (mainly H-bond and ionic interactions) occurring between the template and the monomer, however few studies have reported the use of water as the continuous phase as well (97,98). Most of the reported studies have since used perfluorocarbon for the development of non-covalently imprinted polymer microparticles to avoid this limitation (66,99-101).

Water soluble monomers (such as, polyacrylamides) are polymerised via W/O (often referred to as reversed phase) suspension polymerisation with the inclusion of inorganic water soluble initiators in the dispersed phase (102). Here, non-polar surfactants such as polyethylene glycol sorbitan monolaurate, polyoxyethylenesorbitan derivatives (TWEEN) and sorbitan derivatives (SPANS) are used in the hydrocarbon or paraffin oil as the continuous phase (89). The mechanism of particle formation in a W/O suspension polymerisation changes considerably which becomes something similar to emulsion polymerisation which is discussed in the following Section 2.6.3.

2.6.3. Emulsion polymerisation

Emulsion polymerisation is a heterogeneous dispersion polymerisation technique that produces polymers by emulsifying hydrophobic monomer into an aqueous phase by the use of surfactant or an emulsifier. In a typical O/W emulsion polymerisation set up, the surfactant and initiator are in the aqueous continuous phase; whereas the monomeric phase is dispersed as droplets into the continuous phase. The polymerisation initiates in the continuous phase where the initiator dissolves in. This is quite unlike the suspension polymerisation where the initiation starts in the dispersed phase (as just discussed in Section 2.6.2). Before the emulsion polymerisation is discussed further, it would be very important to briefly discuss the surfactants.

Surfactants are natural or synthetic amphiphilic polymeric molecules. Upon being added to an O/W mixture of immiscible liquids, they align at the liquid interface due to the presence of both hydrophilic and hydrophobic segments within them. The hydrophobic end interacts with the growing oligomer nuclei electrostatically or sterically whereas the hydrophilic tail forms hydrogen bond with the hydrophilic continuous phase. This alignment eventually reduces the surface tension between the two immiscible phases more efficiently than just the droplet stabilisers (as discussed in Section 2.6.2). That is the reason why suspension polymerisation can produce particles from few micrometres to 1-2 mm whereas, emulsion polymerisation produces sub-nanometre to only few micrometres sized particles (65,89). Water soluble surfactants are mainly ionic (anionic or cationic), non-ionic and amphoteric types. Ionic surfactants produce amphiphilic ion in an aqueous continuous phase and interacts electrostatically to the dispersed monomer droplets whereas; non-ionic surfactants don't produce ions and hence stabilise monomer droplets sterically.

The mechanism of polymerisation in an emulsion is considerably different to that of a suspension polymerisation. Nucleation starts in the phase where the initiator is dissolved, either in the aqueous continuous phase where water soluble initiator such as potassium peroxydisulfate is dissolved or in the hydrophobic dispersed phase where AIBN is dissolved. The size of the globule doesn't reflect the final particle size in the emulsion polymerisation. It's rather the concentration of the surfactant, the solubility of the monomer and the type of the initiator that are the most crucial parameters (103). In an O/W emulsion polymerisation, if the surfactant is used beyond its critical micelle concentration (CMC) in the presence of an oil soluble initiator (such as, AIBN), the hydrophobic monomer nuclei are most likely to be embedded within intra-micellar hydrophobic cores from the continuous aqueous phase.

As the polymerisation proceeds, the micelles take up more and more of reactive monomer nuclei from the aqueous phase. These monomer swollen micelles outnumber individual monomer nuclei and hence are more likely to dominate the initiation to produce high molecular weight polymers (103,104).

On the other hand, when the surfactants are present in lower concentrations than their CMC, they may not be homogenously and/or completely distributed among the hydrophobic oligomer nuclei. This results into the nuclei bearing unequal electrostatic charges on them which aggregate with other oligomer nuclei in presence of an aqueous phase. Hence, nucleation mainly occurs via coagulation of individual oligomer nuclei resulting into low molecular weight polymers (103). In this way, not only the type of the initiator (hydrophilic or hydrophobic) but also its amount is very important in determining the polymer propagation mechanism and thereby the property of the resulting polymer.

It has been found that the surfactant amounts as high as even 10 % of their CMC cannot overcome the attractive hydrophobic forces between the p(DVB) particles. When this is increased to their CMC, they may be able to encapsulate hydrophobic monomers completely. Hence, the concentration of the surfactant is very crucial in controlling aggregation between the monomers and thereby the final size of the polymer particles too. However, it is sometimes also tricky to remove surfactants from the particle surface in the post-polymerisation stage due to stronger ionic interactions. In this regard, non-ionic surfactants (such as, Triton X-100) do not suffer from this limitation (105,106). Amphoteric surfactants, such as, sodium dodecylsulfate (SDS) are also used for the preparation of imprinted polymer spheres (88,89). In Chapter 4, the optimised pre-polymerisation mixture has been prepared by

suspension polymerisation to prepare microparticles as potential recognition materials for aflatoxin detection in ToxiQuant technique. In the presented study, suspension polymerisation has been carried out under varying polymerisation conditions, such as, different rotation speeds as well as surfactant type and its amount.

2.6.4. Precipitation polymerisation

Precipitation polymerisation is the simplest of all dispersion polymerisation methods and produces fairly homogenous spherical polymer particles from 0.1 μm to 10 μm sizes. It starts as a homogenous dispersion containing monomer, initiator and porogen with gentle stirring but with no surfactant.

Where other methods pose a risk of having surfactants stuck on the particles, precipitation polymerisation is devoid of it making it the method of choice for producing comparatively smaller particles (107). Thermal initiation is the most common way of polymerising materials using this method; however UV initiated polymerisation can be performed too (65).

The principle mechanism of the polymerisation is mainly via precipitation of the monomer nuclei from the continuous phase; whereas growing oligomeric chains remain soluble in the continuous phase. As the polymerisation proceeds, the precipitated nuclei swell with the porogen and take up more and more monomers from the polymerisation medium (89). The reason why this method does not need a stabiliser or a surfactant is due to self-stabilisation tendency of oligomeric chains that remain soluble in the polymerisation medium. They surround growing polymeric nuclei and prevent aggregation of the particles. The solvent used in this method is known as the zero theta solvent (thermodynamically inert solvent) in which the polymer shows its natural random walk without exchanging any chemical energy, acetonitrile is the most commonly used solvent for preparing polymethacrylate and poly(DVB) based microparticles. However, changing the solvents and their mixing ratio may also produce particles with varying porosities. For example, toluene is widely used in varying combinations with acetonitrile for preparing porous poly(DVB) and polymethacrylate particles (65,107,108).

From the reported studies, it has been found that precipitation of MAA-co-DVB in acetonitrile can produce sub-micron sized spheres with considerably larger surface area (500-600 $m^2 g^{-1}$). However, the research also suggests that the optimum polymerisation time for achieving homogenous particle size distribution by precipitation polymerisation is considerably longer 48 hours (107,108). Another drawback of this method is that the pre-polymerisation solution

needs to be highly diluted (2-5 % w/v) and hence the polymerisation kinetics is much slower compared to other dispersion techniques such as suspension polymerisation (65,107,108).
In Chapter 4, precipitation polymerisation has been discussed for the preparation of polymer microparticles for its use in ToxiQuant technique.

2.6.5. Core-shell polymerisation

Core-shell polymerisation is a method for preparing spherical MIP particles in nanometres to sub-micrometre diameter range. It has been more than a decade since the first ever molecularly imprinted core-shell polymers have been reported (109). This technique generally produces much smaller particles ranging from nanometre to few micrometres in diameter. Indeed, their much smaller sizes offer a new dimension to wider research areas and also offer great flexibility in designing the surface of the particle for various applications.

As the name suggests, core-shell particles are prepared in layers either by building from the core to the shell (bottom to top approach) or from the shell to the core (top to bottom approach). The latter is usually carried out by controlled protocols involving mechanical grinding, such as, photolithography; whereas the former is more appropriate for synthetic chemistry based protocols, such as dispersion polymerisations (110). Core-shell polymerisation is an excellent way of enhancing several particulate properties for specialised applications in drug delivery and bio-sensing areas as compared to other "conventional" polymerisations, such as:

- To imprint larger template molecules with more accessible binding sites on the polymer surface and thereby minimise material transfer across a greater depth.
- To use a metallic or fluorescent particle core for various targeted biomedical applications.
- To imprint expensive molecules more efficiently as the shell is only a thin coat of polymer with efficient binding kinetics.
- To prepare micro/nanoparticles with a narrow size range.

Core particles are generally highly cross-linked and prepared by precipitation, suspension emulsion polymerisation methods; however emulsion polymerisation is the common method (111-113). In this method, the core to shell ratio is very crucial in order to achieve the right thickness (no thicker than few nanometres). In this method, the use of porogen is avoided whilst preparing highly cross-linked and non-porous cores in most cases. However, the shell forming step does have porogen in the mixture which influences the porous character of the

shell forming polymer to a greater extent. Although heterogeneous dispersion techniques are not favourable for the preparation of non-covalently imprinted polymers, there have been studies reported where core-shell polymerisation has been successfully used for an aqueous non-covalent imprinting (114).

Perez-Moral and Mayes have contributed extensively in the development of core-shell particles prepared for non-covalent imprinting of the templates. This includes a two-stage emulsion polymerisation approach for preparing fluorescent core-shell particles which suggests that higher amounts of the template (greater than 6 % of the total monomer mixture) may affect the structural arrangement of monomers and hence the solubility of the growing polymer layer. This may also sometime produce particles with smoother surface with smaller surface area (109,114).

The reported findings also suggest that the template recognition efficiency of resulting core-shell particles is slightly worse off in the presence of aqueous media than other polymerisation methods (such as, monolithic bulk polymers), likely due to interference in the non-covalent monomer-template interactions. This has been addressed by preparing MIP microbeads in mineral oil. In this strategy, the pre-polymerisation mixture is dispersed together with non-polar solvents into the continuous phase of mineral oil (115). However, the solubility of vinyl monomers in both the dispersed porogen phase and the oil phase need to be carefully balanced whilst using oil based emulsion protocol. From the recognition performance point of view, combination of styrene/DVB has been found to perform better in comparison to MMA/EGDMA in any rebinding media probably due to its improved hydrophobicity which may help in adhering the shell layer to the core particles (88,116).

Precipitation polymerisation offers more ease and flexibility in developing microparticles as compared to emulsion polymerisation based approach as reported by the mentioned studies. To this end, a precipitation polymerisation based approach has been adapted for developing core-shell particles for the reported study in Chapter 4. This is based on an approach originally reported earlier by Li and Stover where both the core microbeads and the shell layers have been obtained by a two-stage precipitation polymerisation carried out in the single pot (117). Once the core particles are formed, successive layer of the shell polymer is formed by adding varying amounts of the shell monomer mixture to the reaction pot to achieve different shell thickness on the core particles (118). This will be discussed further in detail in Section 4.5.5 of Chapter 4.

2.7. Summary

MIPs and other recognition polymers are highly important entities in drive towards improved molecular recognition needed in a wide range of technologies, be it bio-medical, environmental or security driven areas. However, a significant number of studies focus on the just the performance of the polymer, not the physical reasoning why polymer have certain recognition properties. Sheer flexibility of polymeric materials and its different formats (obtained by different polymerisation techniques) can be seen highlighted in the discussion above, but it is clear that each method will yield materials, that could be the same in chemical composition, but differ significantly in physical structure. The key work of Piletsky and co-workers in his "cookery" series of papers shows that variety will potentially exist even between labs doing the same experiment, depending on the heating method used, or initiator for example.

This thesis seeks to explore some of the properties, both physical and performance related in the design of new polymers. In all three studies presented here, the key descriptor of linking performance with physical properties is considered. In essence, these are studies into structure versus function.

The first of which looks at polymerisation conditions in a MW reactor and seeks to predict performance based on physical properties. The second is a comparative study of a set polymer formed in several different formats. This seeks to offer an understanding of how a polymerisation method affects the resultant polymer. The third discusses the development of a completely novel imprinting method, using DNA as a monomer and an understanding of the physical makeup of these nanoparticulate materials. For each, a specific introduction to the area is given at the beginning of each chapter.

A wide range of analytical techniques have been employed in these studies and these are discussed in detail when first met, explaining how and why they were used.

2.8. Bibliography for Chapter 2

1. Hoshino, Y., Koide, H., Furuya, K., Haberaecker III, W., Lee, S., Kodama, T., Kanazawa, H., Oku, N., Shea, K. J. (2012) The Rational Design of a Synthetic Polymer Nanoparticle that Neutralizes a Toxic Peptide *In Vivo*. *PNAS* **109**, 33-38.
2. Findlay, J. W. A., Smith, W. C., Lee, J. W., Nordblom, G. D., Das, I., DeSilva, B. S., Khan, M. N., Bowsher, R. R. (2000) Validation of Immunoassays for Bioanalysis: A Pharmaceutical Industry Perspective. *Journal of Pharmaceutical and & Biomedical Analysis* **21**, 1249-1273.
3. Ezan, E., Dubois, M., Becher, F. (2009) Bioanalysis of Recombinant Proteins and Antibodies by Mass Spectrometry. *Analyst* **134**, 825-834.
4. Ansell, R. J. Ramstrom, O., Mosbach, K. (1996) Towards Artificial Antibodies Prepared by Molecular Imprinting. *Clinical Chemistry* **42**, 1506-1512.
5. Haupt, K. (2010) Plastic Antibodies. *Nature Biomaterials* **9**, 612-614.
6. Haupt, K., Mosbach, K. (2000) Molecularly Imprinted Polymers and Their Use in Biomimetic Sensors. *Chemical Reviews.* **100**, 2495-2504.
7. Luppa, P. B., Sokoll, L. J., Chan, D. W. (2001) Immunosensors - Principles and Applications to Clinical Chemistry. *Clinica Chimica Acta* **314**, 1-26.
8. Sellergen, B. (1997) Noncovalent Molecular Imprinting: Antibody-like Molecular Recognition in Polymeric Network Materials. *Trends in Analytical Chemistry* **16**, 310-320.
9. Mairal, T., Ozalp, V. C., Sanchez, P. L., Mir, M., Katakis, I., O'Sullivan, C. K. (2008) Aptamers: Molecular Tools for Analytical Applications. *Analytical Bioanalytical Chemistry.* **390**, 989-1007.
10. Brody, E. N., Gold, L. (2000) Aptamers as Therapeutic and Diagnostic Agents. *Reviews in Molecular Biotechnology* **74**, 5-13.
11. Keefe, A. D., Pai, S., Ellington, A. (2010) Aptamers as Therapetics. *Nature Reviews Drug Discovery* **9**, 537-550.
12. Ye, L., Mosbach, K. (2008) Molecular Imprinting: Synthetic Materials as Substitutes for Biological Antibodies and Receptors. *Chemical Materials.* **20**, 859-868.
13. Haupt, K. (2003) Imprinted Polymers: The Next Generation. *Analytical Chemistry* **75**, 376A-383A
14. Lavignac, N., Allender, C. J., Brain, K.R. (2004) Current Status of Molecularly Imprinted Polymers as Alternatives to Antibodies in Sorbent Assays. *Analytica Chimica Acta* **510**, 139-145.

15. Cormack, P. A. G., Mosbach, K. (1999) Molecular Imprinting: Recent Developments and the Road Ahead. *Reactive & Functional Polymers* **41**, 115-124.

16. Alexander, C., Andersson, H., Andersson, L., Ansell, R., Kirsch, N., Nicolls, I., O'Mahony, J., Whitcombe, M. (2006) Molecular Imprinting Science and Technology: A Survey of the Literature for the Years up to and Including 2003. *Wiley Interscience* **19**, 106-180.

17. Ramstrom, O., Mosbach, K. (1996) Artificial Antibodies to Corticosteroids Prepared by Molecular Imprintig. *Chemistry & Biology* **3**, 471-477.

18. Yonamine, Y., Hoshino, Y., Shea, K. J. (2012) ELISA-Mimic Screen for Synthetic Polymer Nanoparticles with High Affinity to Target Proteins. *Biomacromolecules* **13**, 2952-2957.

19. Chianella, I., Guerreiro, A., Moczko, E., Caygill, S., Piletska, E. V., Perez De Vargas Sansalvador, I. M., Whitcombe, M. J., Piletsky, S. A. (2013) Direct Replacement of Antibodies with Molecularly Impritned Polymer Nanoparticles in ELISA - Development of a Novel Assay for Vancomycin. *Analytical Chemistry* **85**, 8462-8468.

20. Haupt, K., Mosbach, K. (2000) Molecularly Imprinted Polymers and Their Use in Biomimetic Sensors. *Chemical Reviews* **100**, 2495-2504.

21. Ye, L., Haupt, K. (2004) Molecularly Imprinted Polymers as Antibody and Receptor Mimics for Assays, Sensors and Drug Delivery. *Analytical Bioanalytical Chemistry* **378**, 1887-1897.

22. Theodoridis, G., Minesiotis, P. (2002) Selective Solid-Phase Extraction for Caffeine Made by Molecular Imprinting. *Journal of Chromatography A* **98**, 163-169.

23. Turner, N. W., Piletska, E. V., Karim, K., Whitcombe, M., Malecha, M., Magan, N., Baggiani, C., Piletsky, S. A. (2004) Effect of the Solvent on Recognition Properties of Molecularly Impritned Polymer Specific for Ochratoxin A. *Biosensors and Bioelectronics* **20**, 1060-1067.

24. Andersson, H., Nicholls, I. (ed) (2003) *A Historic Perspective of the Development of Molecular Imprinting*, Vol. 23, Elsevier, Amsterdam, the Netherlands.

25. Wulff, G., Sarhan, A. (1972) The Use of Polymers with Enzyme-Analogous Structures for the Resolution of Racemates. *Angewandate Chemie International Edition* **11**, 341.

26. Takagishi, T., Klotz, I. M. (1972) Macromolecule-Small Molecule Interactions; Introduction of Additional Binding Sites in Polyethyleneimine by Disulfide Cross-Linkages. *Biopolymers* **11**, 483-491.

27. Pasparakis, G., Alexander, C. (2007) Synthetic Polymers for Capture and Detection of Microorganisms. *Analyst* **132**, 1075-1082.

28. Hoshino, Y., Koide, H., Urakami, T., Kanazawa, H., Kodama, T., Oku, N., Shea, K. J. (2010) Recognition, Neutralization and Clearance of Target Peptides in the

Bloodstream of Living Mice by Molecularly Imprinted Polymer Nanoparticles: A Plastic Antibody. *American Chemical Society* **132**, 6644-6645.

29. Mayes, A. G., Whitcombe, M. J. (2005) Synthetic Strategies for the Generation of Molecularly Imprinted Organic Polymers. *Advanced Drug Delivery Reviews* **57**, 1742-1778.
30. Kiparissides, C. (1996) Polymerisation Reactor Modelling: A Review of Recent Developments and Future Directions. *Chemical Engineering Science* **51**, 1637-1659.
31. Haupt, K., Mosbach, K. (1998) Plastic Antibodies: Developments and Applications. *Tibtech November* **16**, 468-475.
32. Mayes, A. G., Mosbach, K. (1997) Molecularly Imprinted Polymers: Useful Materials for Analytical Chemistry? *Trends in Analytical Chemistry* **16**, 321-332.
33. Komiyama, M., Takeuchi, T., Mukawa, T., Asanuma, H. (2003) *Molecular Imprinting*, WILEY-VCH Verlag GmbH & Co., Weinhei, Federal Republic of Germany.
34. Chen, L., Xu, S., Lee, J. (2011) Recent Advances in Molecular Imprinting Technology: Current Status, Challenges and Highlighted Applications. *Chemical Society Reviews* **40**, 2922-2942.
35. Sellergen, B. (1990) Molecular Recognition in Macroporous Polymers Prepared by a Substrate Analogue Imprinting Strategy. *Journal of Organic Chemisty* **55**, 3383-3386.
36. Whitcombe, M., Vulfson, E. N. (2001) Imprinted Polymers. *Advanced Materials.* **13**, 467-478.
37. Whitcombe, M., Rodriquez, M., Villar, P., Vulfson, E. (1995) A New Method for the Introduction of Recognition Site Functionality into Polymers Prepared by Molecular Imprintig: Syntehsis and Characterization of Polymeric Receptors for Cholesterol. *J. American Chemical Society.* **117**, 7105-7111.
38. Mosbach, K., Andersson, L. I. (1990) Enantiomeric Resolution on Molecularly Imprinted Polymers Prepared with only Non-Covalent and Non-Ionic Interactions. *Journal of Chromatography* **516**, 313-322.
39. Nicholls, I. A., Adboa, K., Andersson, H. S., Ola Andersson, P., Ankarlooa, J., Hedin-Dahlström, J., Jokela, P., Karlsson, J. G., Olofsson, L., Rosengren, J., Shoravi, S., Svenson, J., Wikman, S. (2001) Can We Rationally Design Molecularly Imprinted Polymers? *Analytica Chimica Acta* **435**, 9-18.
40. (a) Mijangos, I., Navarro-Villoslada, F., Guerreiro, A., Piletska, E., Chianella, I., Karim, K., Turner, A., Piletsky, S. (2006) Influence of Initiator and Different Polymerisation Conditions on Performance of Molecularly Imprinted Polymers. *Biosensors and*

Bioelectronics **22**, 381-387. (b) Nicholson, J. W. (2012) The Chemistry of Polymers, 4th Edition. RSC Publishing, 23-27.

41. Arshady, R. (1992) Suspension, Emulsion, and Dispersion Polymerization: A Methodological Survey. *Colloid and Polymer science* **270**, 717-732.
42. Vivaldo-Lima, E., Wood, P. E., Hamielec, A.E. (1997) An Updated Review on Suspension Polymerization. *Industrial Engineering Chemical Research.* **36**, 939-965.
43. Cormack, P. A. G., Elorza, A. Z. (2004) Molecularly Imprinted Polymers: Synthesis and Characterization. *Journal of Chrmatography B* **804**, 173-182.
44. Turner, N. W., Holdsworth, C. I., Donne, S. W., McCluskey, A., Bowyer, M. C. (2010) Microwave Induced MIP Synthesis: Comparative Analysis of Thermal and Microwave Induced Polymerisation of Caffeine Imprinted Polymers. *New Journal of Chemisty* **34**, 686-692.
45. Holtze, C., Antonietti, M., and Tauer, K. (2006) Ultrafast Conversion and Molecular Weight Control Through Temperature Programming in Microwave-induced Miniemulsion Polymerization. *Macromolecules* **39**, 5720-5728.
46. Kempe, K., Becer, C. R., and Schubert, U. S. (2011) Microwave-assisted Polymerizations: Recent Status and Future Perspectives. *Macromolecules* **44**, 5825-5842.
47. Haupt, K. (2001) Molecularly Imprinted Polymers in Analytical Chemisty. *Analyst* **126**, 747-756.
48. Piletsky, S. A., Piletska, E. V., Karim, K., Freebairn, K. W., Legge, C. H., Turner, A. P. F., (2002) Polymer Cookery: Influence of Polymerization Conditions on the Performance of Molecularly Imprinted Polymers. *Macromolecules* **35**, 7499-7504.
49. Andersson, H. S., Karlsson, J. G., Piletsky, S. A., Koch-Schmidt, A. C. Mosbach, K., Nicholls, I. A. (1999) Study of the Nature of Recognition in Molecularly Imprinted Polymers: Influence of Monomer-template Ratio and Sample Load on Retention and Selectivity. *Journal of Chromatography A* **848**, 39-49.
50. Karim, K., Brenton, F., Rouillon, R., Piletska, E. V., Guerreiro, A., Chianella, I., Piletsky, S. A. (2005) How to Find Effective Functional Monomers for Effective Molecularly Imprinted Polymers? . *Advanced Drug Delivery Reviews* **57**, 1795-1808.
51. Nicholls, I. A., Andersson, H. S., Charlton, C., Henschel, H., Karlsson, C. G., Karlsson, J. G., O'Mahony, J., Rosengren, A. M., Rosengresn, K. J., Wikman, S. (2009) Theoritical and Computational Strategies for Rational Molecularly Impritned Polymer Design. *Biosensors and Bioelectronics* **25**, 543-552.

52. Piletsky, S. A., Karim, K., Piletska, E. V., Day, C. J., Freebairn, K. W., Legge, C., Turner, A. P. F. (2001) Recognition of Ephedrine Enantiomers by Molecularly Imprinted Polymers Designed Using a Computational Approach. *Analyst* **126**, 1826-1830.

53. Farrington, K., Magner, E., and Regan, F. (2006) Predicting the Performance of Molecularly Imprinted Polymers: Selective Extraction of Caffeine by Molecularly Imprinted Solid Phase Extraction. *Analytica Chimica Acta* **566**, 60-68.

54. Subrahmanyam, S., Piletsky, S. A., Piletska, E. V., Chen, B., Karim, K., Turner, A. P. F. (2001) 'Bite-and-switch' Approach Using Computationally Designed Molecularly Imprinted Polymers for Sensing of Creatinine. *Biosensors and Bioelectronics* **16**, 631-637.

55. Batra, D., Shea, K. J. (2003) Combinatorial Methods in Molecular Imprinting. *Current Opinion in Chemical Biology* **7**, 434-442.

56. Chianella, I., Karim, K., Piletska, E. V., Preston, C., Piletsky, S. A. (2006) Computational Design and Synthesis of Molecularly Imprinted Polymers with High Binding Capacity for Pharmaceutical Applications-Model Case: Adsorbent for Abacavir. *Analytica Chemica Acta* **559**, 73-78.

57. Piletsky, S. A., Mijangos, I., Guerreiro, A., Piletska, E. V., Chianella, I., Karim, K., and Turner, A. P. F. (2005) Polymer Cookery: Influence of Polymerization Time and Different Initiation Conditions on Performance of Molecularly Imprinted Polymers. *Macromolecules* **38**, 1410-1414.

58. Spivak, D. (2005) Optimization, Evaluation and Characterization of Molecularly Imprinted Polymers. *Advanced Drug Delivery Reviews* **57**, 1779-1794.

59. Benes, M. J., Horak, D., Svec, F. (2005) Methacrylate - Based Chromatographic Media. *Journal of Separation Science* **25**, 1855-1875.

60. Sibrian-Vazquez, M., Spivak, D. A. (2004) Molecular Imprinting Made Easy. *Journal of American Chemical. Society.* **126**, 7827-7833.

61. Kubo, T., Hosoya, K., Tanaka, N., Kaya, K. (2005) Preparation of a Novel Molecularly Imprinted Polymer Using a Water-soluble Crosslinking Agent. *Analytical and Bioanalytical Chemistry* **382**, 1698-1701.

62. Kempe, M. (1996) Antibody-Mimicking Polymers as Chiral Stationary Phases in HPLC. *Analytical Chemistry.* **68**, 1948-1953.

63. Poma, A., Brahmbhatt, H., Watts, J. K., and Turner, N. W. (2014) Nucleoside-Tailored Molecularly Imprinted Polymeric Nanoparticles (MIP NPs). *Macromolecules* **47**, 6322-6330.

64. Poma, A., Brahmbhatt, H., Pendergraff, H. M., Watts, J. K., and Turner, N. W. (2014) Generation of Novel Hybrid Aptamer–Molecularly Imprinted Polymeric Nanoparticles. *Advanced Materials,* **27** 750-758.

65. Gokmen, T. M., Du Perez, F. (2012) Porous Polymer Particles - A Comprenehsive Guide to Synthesis, Characterization, Functionalization and Applications. *Progress in Polymer Science* **37**, 1-46.

66. Ansell, R. J., Mosbach, K. (1997) Molecularly Imprinted Polymers by Suspension Polymerisation in Perfluorocarbon Liquids, with Emphasis on the Influenece of the Porogonic Solvent. *Journal of Chromatography A* **787**, 55-56.

67. Dowding, P. J., and Vincent, B. (2000) Suspension Polymerisation to Form Polymer Beads. *Colloids and Surfaces A: Physicochemical and Engineering Aspects* **161**, 259-269.

68. Viklund, C., Svec, F., Frechet, J. M. J. (1996) Monolithic, "Molded" Porous Materials with High Flow Characteristics for Separations, Catalysis, or Solid Phase Chemistry: Control of Porous Properties During Polymerisation. *Chemical Materials* **8**, 744-750.

69. Spivak, D. (2005) Optimization, Evaluation and Characterization of Molecularly Imprinted Polymers. *Advanced Drug Delivery Reviews* **57**, 1779-1794.

70. Piletska, E. G., Guerreiro, A. R. A., Whitcombe, M., Piletsky, S. A. (2009) Influence of the Polymerization Conditions on the Performance of Molecularly Imprinted Polymers. *Macromolecules* **42**, 4921-4928.

71. O'Shannessy, D. J., Ekberg, B. Mosbach, K. (1989) Molecular Imprinting of Amino Acid Derivatives at Low Temperature Using Photolytic Homolysis of Azobisnitriles. *Analytical Biochemistry* **177**, 144-149.

72. Lin, J. M., Nakagama, T., Uchiyama, K., Hobo, T. (1997) Temperature Effect on Chiral Recognition of Some Amino Acids with Molecularly Imprinted Polymer Filled Capillary Electrochromatography. *Biomedical Chromatography* **11**, 298-302.

73. Hosoya, K., Iwakoshi, Y., Yoshizako, K., Kimata, K., Tanaka, N., Takehira, H., Haginaka, J. (1999) An Unexpected Molecular Imprinting Effect for a Polyaromatic Hydrocarbon, Anthracene, Using Uniform Size Ethylene Dimethacrylate Particles. *Journal of High Resolution Chromatography* **22**, 256-260.

74. Piletsky, S. A., Mijangos, I., Guerreiro, A., Piletska, E. V., Chianella, I., Karim, K., Turner, A. P. F. (2005) Polymer Cookery: Influence of Polymerization Time and Different Initiation Conditions on Performance of Molecularly Imprinted Polymers. *Macromolecules* **38**, 1410-1414.

75. Mayes, A. G., Mosbach, K. (1996) Molecularly Imprinted Polymer Beads: Suspension Polymerization Using a Liquid Perfluorocarbon as the Dispersing Phase. *Analytical Chemistry* **68**, 3769-3774.

76. Turiel, E., Martin-Esteban, A. (2004) Molecularly Imprinted Polymers: Towards Highly Selective Stationary Phases in Liquid Chromatography and Capillary Electrophoresis. *Analytical and Bioanalytical Chemistry* **378**, 1876-1886.

77. Ulbricht, M. (2006) Advanced Functional Polymer Membranes. *Polymer* **47**, 2217-2262.

78. Dzgoev, A., Haupt, K. (1999) Enantioselective Molecularly Imprinted Polymer Membranes. *Chiarality* **11**, 465-469.

79. Piletsky, S. A., Panasyuk, T. L., Piletskaya, E. V., Nicholls, I. A., and Ulbricht, M. (1999) Receptor and Transport Properties of Imprinted Polymer Membranes – A Review. *Journal of Membrane Science* **157**, 263-278.

80. Schneinder, F., Piletsky, S.,Piletska, E., Guerreiro, A., Mathias, U. (2005) Comparison of Thin-Layer and Bulk MIPs Synthesized by Photoinitiated *In Situ* Crosslinking Polymerization from the Same Reaction Mixtures. *Journal of Applied Polymer Science* **98,** 362-372.

81. Takeda, K., and Kobayashi, T. (2006) Hybrid Molecularly Imprinted Membranes for Targeted Bisphenol Derivatives. *Journal of Membrane Science* **275**, 61-69.

82. Wang, H. Y., Kobayashi, T., Fukaya, T., Fujii, N. (1997) Molecular Imprint Membranes Prepared by the Phase Inversion Precipitation Technique: Influence of Coagulation Temperature in the Phase Inversion Process on the Encoding in Polymeric Membranes. *Langmuir* **13**, 5396-5400.

83. Kobayashi, T., Wang, H. Y., Fujii, N. (1998) Molecular Imprint Membranes of Polyacrylonitrile Copolymers With Different Acrylic Acid Segments. *Analytica Chemica Acta* **365**, 81-88.

84. Sergeyeva, T. A., Brovko, O. O., Piletska, E. V., Piletsky, S. A., Goncharova, L. A., Karabanova, L. V., Sergeeva, L. M., El'skaya, A. V. . (2007) Porous Molecularly Imprinted Polymer membranes and Polymeric Particles. *Analytica Chemica Acta* **582**, 311-319.

85. Hoshino, Y., Koide, H., Furuya, K., Haberaecker, W. W., Lee, S. H., Kodama, T., Kanazawa, H., Oku, N., and Shea, K. J. (2012) The rational design of a synthetic polymer nanoparticle that neutralizes a toxic peptide *in vivo*. *Proceedings of the National Academy of Sciences* **109**, 33-38.

86. Hoshino, Y., Koide, H., Urakami, T., Kanazawa, H., Kodama, T., Oku, N., and Shea, K. J. (2010) Recognition, Neutralization, and Clearance of Target Peptides in the

Bloodstream of Living Mice by Molecularly Imprinted Polymer Nanoparticles: A Plastic Antibody. *Journal of the American Chemical Society* **132**, 6644-6645.

87. Poma, A., Turner, A. P. F., and Piletsky, S. A. (2010) Advances in the Manufacture of MIP Nanoparticles. *Trends in Biotechnology* **28**, 629-637.

88. Perez-Moral, N., Mayes, A. G. (2004) Comparative Study of Imprinted Polymer Particles Prepared by Different Polymerisation Methods. *Analytica Chemica Acta* **504**, 15-21.

89. Arshady, R. (1992) Suspension, Emulsion and Dispersion Polymerization: A Methodical Survey. *Colliod Polymer Science* **270**, 717-732.

90. Perez- Moral, N., Mayes A. G. (2001) Novel MIP Formats. *Bioseparation* **10**, 287-299.

91. Dowding, P. J., Vincent, B. (2000) Suspension Polymerisation to Form Polymer Beads. *Colloids and Surfaces A: Physicochemical and Engineering Aspects* **161**, 259-269.

92. Strikovsky, A. G., Kasper, D., Grun, M., Green, B. S., Hradil, J., Wulff, G. (2000) Catalytic Molecularly Imprinted Polymers Using Conventional Bulk Polymerisation or Suspension Polymerisation: Selective Hydrolysis of Diphenyl Carbonate and Diphenyl Carbamate. *J. American Chemical Society* **122**, 6295- 6296.

93. Yang, W. Y., D. Hu, J. Wang, C. Fu, S. (2001) Dispersion Copolymerisation of Styrene and Other Vinyl Monomers in Polar Solvents. *Journal of Polymer Science A: Polymer Chemistry* **39**, 555-561.

94. Strikovsky, A. H., J. Wulff, G. (2003) Catalytically Active, Molecularly Imprinted Polymers in Bead Form. *Reactive & Functional Polymers* **54**, 49-61.

95. Ramirez, J. C., Herrera-Ordonez, J., Gonzalez, V. A. (2006) Kinetic of Styrene Minisuspension Polymerization Using a Mixture PVA - SDS as Stabilizer. *Polymer* **47**, 3336-3343.

96. Zhang, L. C., G. Fu, C. (2003) Synthesis and Characteristic of Tyrosine Imprinted Beads Via Suspension Polymerisation. *Reactive & Functional Polymers* **56**, 167-173.

97. Geng, L., Kou, X., Lei, J., Su, H., Ma, G., and Su, Z. (2012) Preparation, Characterization and Adsorption Performance of Molecularly Imprinted Microspheres for Erythromycin using Suspension Polymerization. *Journal of Chemical Technology and Biotechnology* **87**, 635-642.

98. Flores, A., Cunliffe, D., Whitcombe, M. J., and Vulfson, E. N. (2000) Imprinted polymers prepared by Aqueous Suspension Polymerization. *Journal of applied polymer science* **77**, 1841-1850.

99. Perez- Moral, N., Mayes, A. G. (2006) Direct Rapid Synthesis of MIP Beads in SPE Cartridges. *Biosensors and Bioelectronics* **21**, 1798-1803.

100. Zourob, M., Mohr, S., Mayes, A. G., Macaskill, A., Perez-Moral, N., Fielden, P. R., Goddard, N. J. (2006) A Micro-reactor for Preparing Uniform Molecularly Imprinted Polymer Beads. *Lab Chip* **6**, 296-301.

101. Okubo, M., Minami, H. (1997) Formation Mechanism of Micron-sized Monodispersed Polymer Particles Having a Hollow Structure. *Colloidal Polymer Science* **275**, 992-997.

102. Pang, X., Cheng, G., Li, R., Lu, S., Zhang, Y. (2005) Bovine Serum Albumin- Imprinted Polyacrylamide Gel Beads Prepared Via Inverse-phase Seed Suspension Polymerization. *Analytica Chemica Acta* **550**, 13-17.

103. Karaman, M. E., Meagher, L., Pashley, R. M. (1993) Surface Chemistry of Emulsion Polymerization. *Langmuir* **9**, 1220-1227.

104. Chern, C. S. (2006) Emulsion Polymerization Mechanisms and Kinetics. *Progress in Polymer Science* **31**, 443-486.

105. Sarı, A., Alkan, C., and Karaipekli, A. (2010) Preparation, Characterization and Thermal Properties of PMMA/n-Heptadecane Microcapsules as Novel Solid–liquid MicroPCM for Thermal Energy Storage. *Applied Energy* **87**, 1529-1534.

106. Krajnc, P., Štefanec, D., and Pulko, I. (2005) Acrylic Acid "Reversed" PolyHIPEs. *Macromolecular Rapid Communications* **26**, 1289-1293.

107. Wang, J., Cormack, P. A. G., Sherrington, D. C., Khoshdel, E. (2003) Monodisperse, Molecularly Imprinted Polymer Microspheres Prepared by Precipitation Polymerization for Affinity Separation Applications. *Angewandate Chemie International Edition* **42**, 5336-5338.

108. Sambe, H., Hoshina, K., Moaddel, R., Wainer, I. W., Haginaka, J. (2006) Uniformly - sized, Molecularly Imprinted Polymers for Nicotine by Precipitation Polymerization. *Journal of Chromatography A* **1134**, 88-94.

109. Perez, N., Whitcombe, M. J., Vulfson, E. N. (2001) Surface Imprinting of Cholesterol on Submicrometer Core-Shell Emulsion Particles. *Macromolecules* **34**, 830-836.

110. Ghosh Chaudhuri, R., and Paria, S. (2012) Core/Shell Nanoparticles: Classes, Properties, Synthesis Mechanisms, Characterization, and Applications. *Chemical Reviews* **112**, 2373-2433.

111. Jönsson, J.-E., Karlsson, O. J., Hassander, H., and Törnell, B. (2007) Semi-continuous Emulsion Polymerization of Styrene in the Presence of Poly(methyl methacrylate) Seed Particles. Polymerization Conditions Giving Core–shell Particles. *European Polymer Journal* **43**, 1322-1332.

112. Gao, J., Wang, X., Wei, Y., and Yang, W. (2006) Synthesis and Characterization of a Novel Fluorine-containing Polymer Emulsion with Core/shell Structure. *Journal of Fluorine Chemistry* **127**, 282-286.

113. Pusch, J., and van Herk, A. M. (2005) Emulsion Polymerization of Transparent Core–Shell Latices with a Polydivinylbenzene Styrene and Vinyl Acetate. *Macromolecules* **38**, 6909-6914.

114. Carter, S. R., Rimmer, S. (2002) Molecular Recognition of Caffeine by Shell Molecular Imprinted Core-Shell Polymer Particles in Aqeous Media. *Advanced Materials* **14**, 667-670

115. Kempe, H., and Kempe, M. (2006) Development and Evaluation of Spherical Molecularly Imprinted Polymer Beads. *Analytical chemistry* **78**, 3659-3666.

116. Pérez-Moral, N., and Mayes, A. G. (2007) Molecularly Imprinted Multi-Layer Core-Shell Nanoparticles–A Surface Grafting Approach. *Macromolecular Rapid Communications* **28**, 2170-2175.

117. Barahona, F., Turiel, E., Cormack, P. A. G., and Martín-Esteban, A. (2010) Chromatographic Performance of Molecularly Imprinted Polymers: Core-shell Microspheres by Precipitation Polymerization and Grafted MIP Films via Iniferter-Modified Silica Beads. *Journal of Polymer Science Part A: Polymer Chemistry* **48**, 1058-1066.

118. Li, W. H., and Stöver, H. D. (1998) Porous Monodisperse Poly(divinylbenzene) Microspheres by Precipitation Polymerization. *Journal of Polymer Science Part A: Polymer Chemistry* **36**, 1543-1551.

Chapter 3

Development of Caffeine Imprinted Polymers by Microwave Heating

3.1 Preface

Molecularly imprinted polymers (MIPs) have been studied intensively as recognition materials for various bio-analytical applications for three decades. Traditionally MIP monoliths are obtained by thermal initiation of azo compounds leading to free radical polymerisation. This is commonly performed in an oven or an oil-bath. Despite the ease of preparation, this type of heating results in poor control over the polymerisation kinetics and induces poor batch-to-batch variability and increased heterogeneity in the resultant polymeric materials. A potential alternative is the use of microwave (MW) radiation as an alternative polymer initiation source. Although MW irradiation has been studied significantly for heating chemical reactions and polymerisation; it has received little attention for preparing MIPs. With its controlled conditions and faster reaction speeds, it seems to be a suitable alternative polymerisation technique.

The study presented in this chapter is aimed at understanding the effect of different experimental parameters on the physical and chemical properties of a MIP. To do so, a series of MIPs have been prepared by MW irradiation. The polymerisation conditions including:

- polymerisation heating rate,
- length of polymerisation,
- polymerisation temperature,

These have been altered with an aim to optimise conditions for imprinting using a MW reactor. A series of the NIPs (non-imprinted polymers) have also been prepared for every MIP created as negative controls. In addition to this, both the MIPs and the NIPs have been prepared by traditional oven and UV polymerisations as positive controls for the MW polymers under study. The obtained polymers have been characterised by different analytical techniques to understand their physical properties and template recognition performance.

This study will help towards a better understanding of the MW polymerisation process and the effect of its experimental parameters on the physical and chemical properties of the MIPs. This would also allow us to understand whether MW polymerisation could be used as an alternative polymerisation method for the preparation of MIP monoliths.

3.2 Introduction

MIPs have been studied extensively over the past few decades (1). Previous studies have reported the range of experimental parameters that have considerable effects on the polymer make up and thereby on its performance (2-5).

Ovens have been widely used for carrying out thermal polymerisation reactions. Heating of material in an oven occurs via conduction, which means the heat distribution depends on the thickness and thermal conductivity of the vessel. Moreover, the heat distribution within the material is driven by convection, which is largely affected by its volumes as well (6). The distribution of the heat is not homogenous in all the parts of the oven. The schematic of oven heating is presented in Figure 3.1.

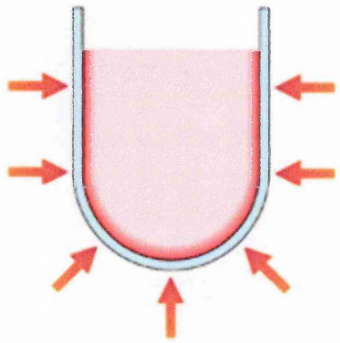

Figure 3.1 : Non-homogenous heating by conventional oven (7). Arrows show the direction of heating. The reaction mixture adjacent to the vessel is over heated (shown in red) whereas the mixture in the middle is much cooler (shown in light pink).

As shown in Figure 3.1, the outside-in heating of conventional ovens or oil baths result in non-homogenous heating profiles of the reaction mixtures. Likewise, when polymerisations are carried out in ovens polymer material on the outside will be heated differently to that in the middle of the reaction vessel. With poor control over the internal polymerisation temperatures, exothermic reactions such as free radical polymerisations can result into excessive internal energy when being held in an oven. This leads to the chain of radical formation, also referred to as auto-acceleration which results into inconsistent and uncontrolled heating. This may have detrimental effects on the make-up of resulting polymers; especially if it is a molecularly imprinted polymer, which ideally relies on some form of set organisation in the structure. In the preparation of the MIPs, elevated energy of the pre-polymerisation mixture can adversely affect formation of stable monomer-template assemblies which are very crucial for the formation of template specific binding sites within the polymers. Not to forget that the make of an oven would be different in the laboratories around the world and will all have different heating profiles (e.g. a fan oven vs. a conventional

oven; different sizes etc.). Different conditions will lead to different chain versus step reactions in a polymerisation which in turn will lead to differences in the internal structure of the resulting polymer.

Hence, traditionally prepared polymers are likely to have non-homogenous make-up in their internal structure as well as their macromolecular structure such as, porosity and surface area. This can eventually affect their template recognition performance. Thermal polymerisations have also been carried out by using oil-bath or sand-baths alongside oven. The materials used such as oil and sand provide slightly more consistent heating due to their high heat capacities compared to oven heaters (6). However, the heating parameters are not controlled and the length of the polymerisation by using such methods is quite time-consuming. On the other hand, UV polymerisation by lamp or focussed beam is faster compared to its thermal counterparts such as those carried out by an oven or oil-bath. However, studies suggest that UV polymers show lower surface area and lower porosity which can be detrimental to their recognition performance (4).

Ideally, a polymerisation method with a faster, controlled and reproducible polymerisation is the way forward for industrial applications. More importantly, it should result into polymers with comparable physical properties and performance. MW polymerisation clearly has an advantage over other methods in increasing the production output for industrial applications due to its much faster reaction kinetics.

Figure 3.2 shows the timescale of MW polymerisation initiation times in comparison to other methods.

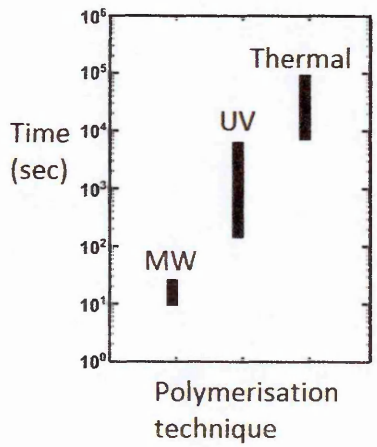

Figure 3.2: Comparison of times taken by different polymerisation initiation techniques; adapted from (8).

MW reactors have proved to be an attractive alternate heating source for carrying out various reactions in synthetic chemistry since late 1970s (9). Their use in the chemistry laboratories

has increased consistently due to their ability to carry out extremely quick and controlled reactions, while still maintaining excellent homogeneity, when compared to the conventional heating sources (10-16).

It is important to understand the principle of MW heating. MW reactors work slightly differently as compared to a conventional oven. Analytical MW reactors emit focussed pulsed microwaves (wavelength 1 millimetre to 1 metre) from an electromagnetic source onto the material. If the subjected material contains polar molecules or charged ions, they re-align themselves in accordance to the changing pulses of the externally applied electromagnetic microwaves.

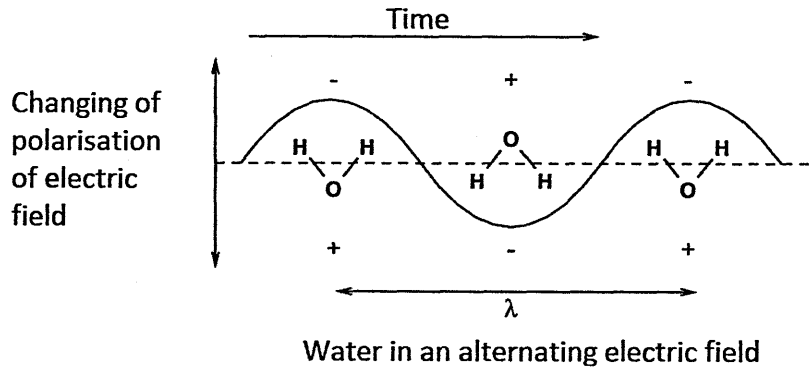

Figure 3.3: Schematics of the realignment of water molecules in a changing electromagnetic field; adapted from (17).

As seen in Figure 3.3, constant re-alignment of the polar molecules such as water generates friction between them and generates heat. In a MW reactor, the material is heated from inside to out unlike the oven or oil-bath heating (7, 18). Hence, MW heating is also termed as the molecular heating or dielectric heating. This means the MWs can heat a material faster without being affected by the conduction or convection unlike the conventional oven heating. Figure 3.4 explains the molecular heating of a reaction vessel inside of a MW reactor.

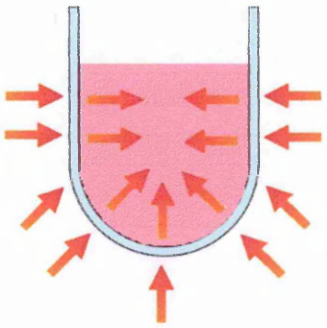

Figure 3.4: Homogenous heating achieved by MW reactor. Arrows show the direction of heating unaffected by the thickness of the vessel wall or depth of solution; overall temperature of the reaction mixture is independent of the thermal conductivity of the vessel. The reaction mixture in the vessel is heated evenly (shown in pink); adapted from (7).

The frequency of the microwaves used in a typical laboratory reactor is 2.45 GHz which is similar to the domestic MW ovens used for cooking (17, 19, 20). The thermal energy is constantly supplied in pulsatile fashion even before the electrons of the reactant molecule relax. This impulsive energy transfer from the microwaves to the material can be as quick as 10^{-9} seconds due to their closed vessel designs. This enhances the kinetic energy of colliding molecules very rapidly and results in considerably faster heating rates (17).

The role of dielectric property of the reactant material is crucial in a MW heating. Although it is favourable to have a polar solvent for MW heating, it is absolutely fine to heat non-polar solvents too. Polar compounds being dissolved in a non-polar solvent could sometimes lead to even higher dielectric heating. This is because the polar molecules can lag even far behind the changing electric field of the microwaves when they are dissolved in a non-polar solvent (21). The type of porogen predominately affects the penetration of microwaves and thereby the heating rate of a polymerisation. As a result of the differential heating patterns, the pore size and the surface area of the polymers are largely affected. The study of the effect of different porogens on the properties of the resulting MIPs can be an interesting area of research as one can produce MIPs with desired physical properties by changing the porogen. Some studies also report that the faster polymerisation kinetics is achieved by faster degradation of the initiator due to localised superheating in a domestic MW heating (22, 23). Localised superheating in domestic MW reactors can lead to inconsistent heating of the material as well. Figure 3.5 explains the drawbacks of using a domestic MW reactor, as those used in kitchen.

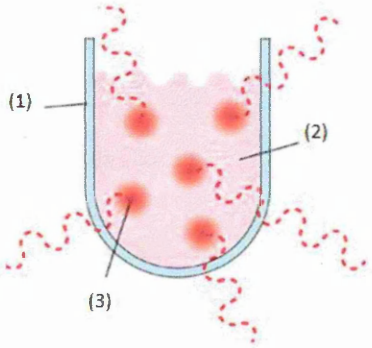

Figure 3.5: Heating reaction in a domestic MW reactor; (1) vessel wall that does not affect the MW heating; (2) reaction mixture that absorbs the MW energy shown by the pink colour and (3) molecular heating by strong MW overcrowding leads to localised superheating as shown by red dots.

Figure 3.5 explains the heating mechanism of domestic MW ovens used for food preparation. Although being quicker in heating substances compared to convection oven, they suffer from non-homogenous distribution of microwaves in the vessel leading to localised superheating in some parts of the food. However, this issue has been addressed with the design of focussed MW reactors. In these reactors, microwaves are transferred in a controlled impulsive form with the aid of specially designed magnetron sources. Such focussed MW reactors produce highly controlled microwaves and are mainly used for laboratory purposes, as illustrated in Figure 3.6.

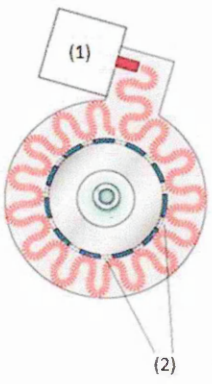

Figure 3.6: Top view of a laboratory MW reactor; (1) Magnetron that generates pulsed microwaves in the channel surrounding the sample cavity and (2) specially designed slits for even radial distribution of microwaves for homogenous heating (7, 19, 20).

Apart from their homogenous heating patterns, MW reactors are also safer to use while handling large polymerisation mixture volumes. Large volumes in traditional oven heating technique pose a risk of explosion due to the exothermic nature of the reaction (5), whereas

the closed and pressure controlled vessel design of laboratory MW reactors ensures safer reactions at higher temperatures (18). Existing commercial MW reactors can take reaction volume of up to 100 litres which may be useful for the easy scale-up of the reaction too. In addition to its much controlled, faster and consistent heating, a MW reactor also comes with additional features for controlled cooling, stirring and condensing to adapt to the nature of the reaction (17, 24). Ever since the MW reactors have been used for heating, it has been debatable if they possess potential non-thermal effects in addition to dielectric heating (18, 25). However, the vast majority of the studies have reported that the heating achieved in MW reactors is solely due to the molecular heating and not due to "non-thermal" effects of microwaves (6, 15).

The presented study focuses on developing MW MIPs prepared by thermal free radical polymerisation. Before MW reactors are discussed further, it would important to understand the nature of a free radical polymerisation. It starts by the breakdown of an initiator and liberation of free radicals. The more the radicals formed, the higher the kinetic energy is liberated which leads to quick onsets of more radical formation throughout the reaction mixture. This positive feedback of radical formation mechanism is referred to as auto acceleration which continues until all the initiator decomposes. The radicals formed from the initiator breakdown leads to dimerization and polymerisation of the monomers present into the reaction mixture (as discussed in the introduction Section 2.4.1). Highly elevated kinetic energy during the polymerisation increases its temperature beyond the set value. This is referred to as Norrish-Trumsdorff effect (11, 26, 27). When the polymerisation is carried out in a MW reactor, it becomes difficult to say whether the decomposition of the initiator is due to the elevated temperature of MW heating or the effect of MW irradiation itself as it is often achieved with the UV irradiation. The best way to assess this would be by carrying out the polymerisation at low temperatures using a MW reactor. To do so, the temperature range should be chosen well below the decomposition temperature of the initiator being used.

It has been established that faster and controlled heating is offered by MW reactors, that allows to run even solvent free reactions to produce much cleaner products than that of conventional heating (6, 14, 16, 28). Also the molecular weights of these MW polymers are similar to that of the oven polymers when prepared in comparable conditions (29). The MW reactors currently available are also within cost reach of most laboartories (~£10 -£20 thousand) (14th August, 2015). Thus, MW reactors could be useful alternative source for carrying out faster, reproducible, controlled, economic and scalable thermal free radical polymerisations of MIPs. By carefully optimising experimental conditions and reaction

components, MW reactors could prepare polymers with desired properties in imprinted materials (13).

The properties of a MW reactor, compared against a traditional thermal heating method are summarised in the Table 3.1.

Table 3.1: Summary of the comparison between MW and conventional heating parameters; adapted from (14)

Experimental parameter	MW heating	Conventional heating
Heating rate	Can be controlled; can be set as needed	Approximately set. Uncontrolled; slow
Reaction temperature	Can be controlled	Non-homogenous heating; under or over heating
Reproducibility	High	Low
Yield	High	Low
Reaction time	Short	Long
Homogeneity of heating	Homogenous; no wall-effect observed	Non-homogenous; wall-effect observed

Thanks to the virtues of MW reactors, their use has continued to rise in past two decades for carrying out polymerisations (11, 25, 29, 30). Figure 3.7 shows the timeline of the total number of articles in scientific journals describing the use of MW reactors for polymerisations.

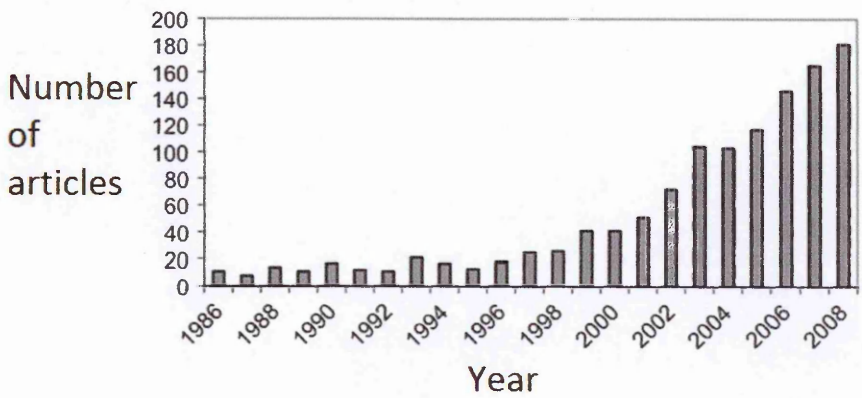

Figure 3.7: Timeline of articles published with MW assisted polymer synthesis; Adapted from (31).

Although MW reactors are used for different types of thermal polymerisations, this work will explore its use to develop free radical MIPs and would be the method of interest for the course of this entire study.

MIPs are tailor-made polymers which have been investigated widely for improved recognition performance compared to other polymeric materials (1, 32, 33). The niche of the MIPs is their ability to selectively identify the target template. This is unlike most other silica or polymeric materials that adsorb the target non-selectively (1, 34). Development of the MIPs by MW polymerisation could help combine the best of both the worlds; the selectivity of the MIPs with scalabality and reproducibility of MW polymerisation.

Numerous studies have reported the use of MW reactor for the development of polymers; however only a handful of them have explored its reaction parameters and their influence on the properties of the resultant polymers. One common finding in most of these studies is that MW reactors significantly enhance the rate of the monomer conversion in comparison to its traditional counterparts (10, 11, 29, 35). This means that MW polymerisation can significantly enhance polymerisation kinetics without affecting the monomer conversion that is usually achieved with traditional methods. Faster polymerisations could be benificial to imprinting as it could ease the scale-up issues for industrial scale preparation of the MIPs. In the presented study, the amount of monomer conversions achieved by short MW polymerisations have been be investigated which will be discussed later in Section 3.4.2 of this chapter.

As discussed earlier in the introduction Section 2.4.1, experimental controls play a crucial role in defining the make-up and performance of the MIPs. Where traditional heating parameters have been studied well in detail, the MW heating has not been investigated thoroughly for the MIP preparation (36). Only a few studies have been reported some two decades ago where MW heating has been found to enhance the polymerisations significantly (10, 11), not to mention this studies have been based on non-imprinted polymers. Both these studies have found that faster MW heating significantly improves polymerisation kinetics. At the same time, different MW heating rates also show considerable differences between their polymerisation kinetics. This suggests that different heating rates could play a crucial role in defining the properties of the polymers, especially that of the MIPs. This is because MIP preparation includes the formation of stable monomer-template assemsblies in the pre-polymerisation mixture before the covalent cross-linking occurs. Such assemblies are formed by comparatively weaker non-covalent interactions, the stability of which may be largely governed by the thermokinetics of the polymerisation (as explained earlier in Section 2.4). Not to mention, the importance of stable monomer-template assemblies in forming template selective binding

sites in the polymer matrix. The lack of such template selective binding sites could also affect the performance of the polymers. Hence, there is a strong need to understand as to how the variables associated with MW and traditional heating can affect the polymerisation process as well as the quality of the MIPs.

The use of MW irradiation has been reported in the MIP literature mainly as a method for the template removal. MW assisted template removal is gaining interest in the areas of MIP preparation as it avoids using large quantities of the solvents unlike soxhlet extraction (34, 37, 38). However, only a handful of studies have explored the real scope of MW assisted MIP preparation (27, 39, 40).

One of the very first attempts were made where MW irradiation was also used at 200 W for five minutes to polymerise α-tocotrienol imprinted polyacrylamide on the surface of the microspheres (41). The polymerisation kinetics achieved with the MW reactor were significantly faster and they also showed improved template recognition. The same group presented another study where the physical properties of the MW MIPs were analysed. From the correlation analysis between the morphology and the performance, it was found that the MW MIPs exhibited rougher surface with higher pore volume and performed better than that of the MW NIPs. MW irradiation showed faster and improved grafting of the acrylamid MIP on the chitosan microbeads. However, this study lacked a direct comparison between the MW heating with the traditional heating (42).

Soon after this, another study was reported where caffeine imprinted MIP monoliths were cured by MW irradiation with 150 W MW power for 15 minutes (27). For the first time, a direct comparison of MW and oven polymerisations was made by comparing the physicochemical properties of the MIPs. This study also highlighted that the performance of the MIPs was greatly influenced by their physical properties, such as, surface area, pore volume, degree of cross-linking and morphology. Although the MW MIPs showed slightly lower template binding performance, their imprinting efficiency was comparatively higher than the oven MIPs. Since the imprinting efficiency of the MIPs is the measure of their selective binding sites, controlled MW polymerisation might result into more stable monomer-template assemblies. MW heating significantly enhanced polymerisation kinetics here as well, in MW polymerisation achieved in just fifteen minutes against 24 hours in the oven.

Another study reported preparation of the MIP magnetic microbeads by precipitation in a MW reactor. The MIPs were characterised for their physical properties and template binding performance. Thermogravimetric analysis of the MIPs ensured considerable stability. The MW MIPs also resulted into more homogenous particle morphology, shape and narrow particle size

distribution in comparison to conventional UV polymerisation. The study was extended to template binding experiments where MIPs showed selectivity and specificity towards the target template. The entire preparation of MW MIP magnetic microbeads took less than an hour compared to 14-24 hours long conventinal polymerisations (30, 43-45).

Another recent study reported the preparation of imprinted polymer fibres in a MW reactor. Here, the MIP monolith fibres were prepared at a high MW power of 800 W for different polymerisation times and the length of the polymerisation was correlated to their template recognition performance, as shown in Figure 3.8.

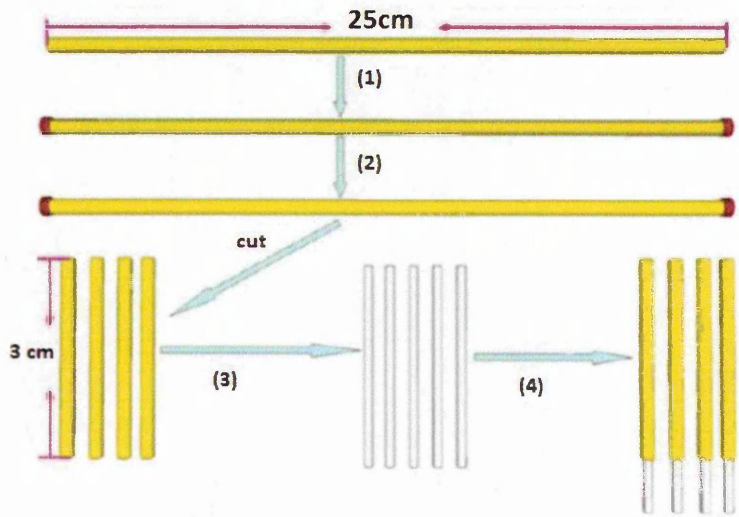

Figure 3.8: Production of MIP fibres by MW polymerisation, adapted from (39). (1) Filling the capillary with the pre-polymerisation mixture; (2) MW polymerisation at 800 W for different times (5 – 35 minutes); (3) Resultant polymer fibres are pushed out to remove the template; (4) Polymer fibres pushed back into the capillary mold.

Polymerisation carried out in a MW reactor was 20 times faster than in water-bath. The recognition performance of the MW MIPs initially increased for up to polymerisation time of eight minutes; however it decreased consistently when the polymerisation times were extended further. Without analysing the MIP fibres for other physical properties, they could not explain as to why the performance of these MIP fibres decreased with the time (39, 46).

A recent study reported comparative analysis of imprinted polymer microparticles prepared by oven and MW irradiation. The MW polymerisation was carried out at 70 °C for 120 minutes, whereas the oven polymerisation was carried out at different temperatures and using different porogens for up to 24 hours. It was found that when the polymerisations were carried out by using the same porogen and other polymerisation components, oven (for 12 hours) and MW irradiation (for 120 minutes) showed comparable recognition performances of the resulting

MIPs (47). This showed that in addition to their quicker polymerisations, MW polymerisations could produce MIPs with comparable properties to that of oven MIPs.

Another recent study reported preparation of MIPs by MW irradiation (40). The study involved the selection of a suitable monomer based on NMR titrations and the optmised MIP recipe was then polymerised for imprinting theophylline in a MW reactor at 60 °C for 15 minutes with 100 W MW power. The oven MIPs on the other hand were left polymerising overnight. Both the set of MIPs were evaluated for physical properties such as, surface area, pore volume and degree of cross-linking. It appeared that both MW and oven MIPs showed comparable degree of cross-linking but the imprinting efficiency was considerably higher in the MW MIPs than the oven MIPs. When both the set of MIPs were compared for their surface area, the oven MIPs showed slightly higher values than that of the MW MIPs. Although this study correlated the physical properties of the MIPs to their recognition performance, it did not explore different experimental parameters and their effects on the properties of resulting MIPs. Experimental parameters related to MW polymerisation (MW power, time and length of polymerisation) especially would be very interesting to study for its possible effect on the properties of the MIPs.

From the discussion on the existing studies, it seems that MW irradiation for the MIP preparation has not been fully investigated; some studies investigated physical properties of the MIPs and the others studied their recognition performance. Unfortunately, there has been no coherent study to incorporate a direct comparison between the traditional and MW polymerisation methods to correlate the physical properties and the performaces of the MIPs.

From the literature review on MW heating, this work proposes that the MIPs polymerised by MW reactor across a wider range of heating rates, temperatures and times could exhibit different physical properties (such as, surface area, pore volume and pore size). This could help in understanding whether the difference into the physical properties reflect further into their performance. In this study, the MIPs polymerised by MW reactor have been directly compared to identical polymer mixtures polymerised by oven and UV irradiation. This is to know whether MW irradiation could be used as an alternate to the traditional methods.

Xanthine derivates such as caffeine and theophylline have been widely studied for the development of MIPs due to their medical importance and ease of forming sufficient non-covalent binding with the conventional monomer mixture (27, 36, 48, 49). In the presented study, caffeine has been chosen as the template to generate polymers with more comparable properties to previously reported ones. The polymerisation recipe in this study consists of co-monomer mixture of MAA-EGDMA with acetonitrile as the porogen. The ratios between the

ingredients have been optimised by NMR, UV titrations and by the computer modelling as described earlier (27, 36). The details on the experimental protocols and analysis of the MIPs are described in the following Section 3.3 of this chapter.

3.3. Materials and methods

This section involves the materials and methods involved in the preparation and analysis of the polymers under study.

3.3.1 Materials

Methacrylic acid (MAA), ethylene glycol dimethacrylate (EGDMA), acetonitrile, 2,2'-azobis(2-methylpropionitrile) (AIBN), caffeine, 2-(dimethylamino) ethyl methacrylate (DEAEM) and 1,1'-azobis(cyclohexanecarbonitrile) were purchased from Sigma-Aldrich (UK). Toulene, methanol (MeOH), glacial acetic acid, divinylbenzene (DVB), dimethylformamide (DMF) were of HPLC grade and were purchased from Fisher Scientific (Loughborough, UK). Double distilled ultrapure water (Millipore, Livingston, UK) was used for analysis. The solid phase extraction (SPE) tubes (Supleco, 1ml) were purchased from Sigma-Aldrich (Gillingham, UK). The Pyrex glass-tubes used for polymerisation were purchased from Discover (Buckingham, UK).

3.3.2. Polymer synthesis

Polymer monoliths were prepared by imprinting caffeine as the template in their matrix. In order to do so, similar protocol was used as reported by (27). 97 mg of caffeine (0.5 mmol) was weighed and dissolved in 2 ml acetonitrile in a 10 ml test-tube. 0.175 ml of MAA (2 mmol) and 1.248 ml EGDMA (6 mmol) were added to the mixture in the test-tube. This was sonicated for 2-3 minutes till all the caffeine dissolved completely. AIBN (15 mg, 0.09 mmol) was then added to the reaction mixture in the test-tube followed by degassing with nitrogen bubbling for about 10 minutes. The test-tube was closed and placed in a 2.45 GHz CEM Discover Benchmate MW reactor (CEM Corp., UK) under different MW powers from 5 W to 300 W at the set temperature of 60 °C for 15 minutes. Specified MW powers heated the polymerisation mixture at different rates to attain the desired temperature (60 °C). When the set polymerisation temperature (60 °C) was attained, the MW system turned off (0 W) and the power was no longer supplied. Hence, any further change in the polymerisation temperature was not due to the supplied MW energy but merely due to the exothermic energy generated as a result of the free radicals created during the polymerisation. Temperature was recorded throughout the polymerisation reaction live on the computer through Synergy™ interface with an aid of *in situ* infra-red temperature probe. Prepared polymeric monolith containing test-tube was removed from the MW reactor and allowed to cool. Monolith was then wet ground using methanol and

sieved to get the particle size range between 45 µm to 63 µm. Desired particle size fraction was collected, dried and subjected to soxhlet extraction in methanol containing 10 % acetic acid for 24 hours in order to remove the template (caffeine). Although MW irradiation is widely used for the template removal in the preparation of the MIPs, soxhlet extraction was used for the template extraction. This is because if the template removal was carried out by MW irradiation followed by a MW assisted polymerisation, it could lead to further polymerisation and false interpretation of the polymer characteristics. This is a commonly found protocol where MW extraction is avoided for the template removal from the MW cured MIPs. Template removal was continued for two more extraction cycles of methanol for 24 hours to clean the polymers completely. MIP extracts were inspected visually under UV light if caffeine was still leaching out of the MIP matrix. Visual inspection under UV lamp ensured that 24 hour long soxhlet extraction cycles with acidified methanol (10 % v/v, 400 mL) followed by methanol (400 mL) was sufficient to remove caffeine completely from the MIP matrix. Polymers were then dried and stored at the room temperature. Figure 3.9 represents the schematics of the polymer preparation protocol used in the presented study.

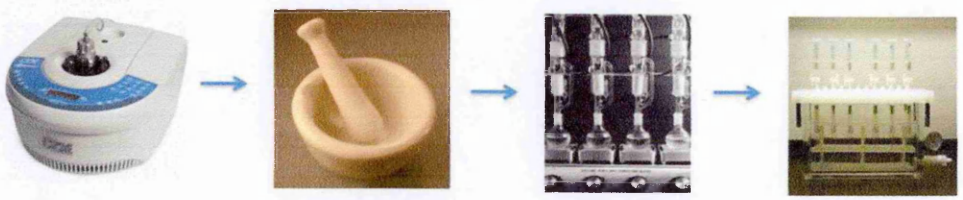

Figure 3.9: Schematics of the polymer monolith preparation; (1) polymerisation using a MW reactor; (2) wet grinding and sieving (45µm - 63 µm); (3) soxhlet extraction (10 volume % acidic methanol) and (4) 100 mg polymer packed in polypropylene SPE cartridges.

A series of the non- imprinted polymers (NIPs) were prepared under identical experimental conditions but with no presence of the template caffeine. Both the MIPs and the NIPs were prepared by the MW reactor by varying its experimental parameters such as, the polymerisation rate, the polymerisation time and the polymerisation temperature. These parameters are summarised in the following tables.

Table 3.2: MW polymers prepared at 60 °C for 15 minutes by varying polymerisation rate

Polymer code	Polymerisation time (minutes)	Polymerisation temperature (°C)	Microwave power (W) used
M30	15	60	5
M15	15	60	50
M10	15	60	150
M34	15	60	300

Polymerisation rate achieved with MW power was optimised to 5 W. The remaining of the polymers was prepared at 60 °C with 5 W MW power by altering the polymerisation temperature. The polymers prepared for different time durations are presented in Table 3.3.

Table 3.3: MW polymers prepared at 60 °C with 5 W powers by varying polymerisation time

Polymer code	Polymerisation time (minutes)	Polymerisation temperature (°C)	Microwave power used (W)
M35	5	60	5
M30	15	60	5
M37	35	60	5
M38	60	60	5

Polymerisation time by MW irradiation was then optimised to 5 minutes. The remaining of the polymers was prepared at 5 W for 5 minutes by altering their polymerisation temperatures. The polymers prepared at different temperatures are presented in Table 3.4.

Table 3.4: MW polymers prepared at 5 W for 5 minutes by varying polymerisation temperature

Polymer code	Polymerisation time (minutes)	Polymerisation temperature (°C)	Microwave power used (W)
M35	5	60	5
M42	5	75	5
M43	5	90	5

Polymerisations were also carried out at 40 °C and 50 °C but they did not polymerise, may be due to non-degradation of the initiator. A series of non-imprinted polymers were also prepared as a control for the each of the MIP listed above.

Likewise, caffeine imprinted and non-imprinted polymers were also prepared by oven and UV polymerisations as a control set of polymers against the MW polymers. Oven polymerisation was carried in identical Pyrex test-tube using a forced air circulation oven (Twin display, Memmert, Germany) at different temperatures (60 °C to 90 °C) for different time durations (from 4 hours to 24 hours). All the oven polymers prepared are summarised in the following tables below.

Table 3.5: Oven polymers prepared at 60 °C by varying polymerisation time

Polymer code	Polymerisation time (hours)	Polymerisation temperature (°C)
O6	4	60
O8	8	60
O10	16	60
O2	24	60

Oven polymerisation time was optimised to 8 hours. The remaining of the oven polymers were prepared for 8 hours by varying temperature.

Table 3.6: Oven polymers prepared for 8 hours by varying polymerisation temperature

Polymer code	Polymerisation time (hours)	Polymerisation temperature (°C)
O8	8	60
O12	8	75
O14	8	90

The UV polymers were prepared by using exactly same polymer recipe using a shortwave (CL-1000, 254 nm) UV cross linker bench top reactor (UVP, CA, USA) with exposure delivery of x100 μJoule cm^2 by varying polymerisation time and temperature as summarised in the following tables. UV polymerisations were carried at 0 °C and 20 °C for different times (from 4 hours to 24 hours).

Table 3.7: UV polymers prepared at 20 °C by varying polymerisation time

Polymer code	Polymerisation time (hours)	Polymerisation temperature (°C)
U4	4	20
U6	8	20
U8	16	20
U2	24	20

Polymerisation time by UV irradiation was optimised to 8 hours to prepare the remaining of the polymers by varying the temperature which are summarised in Table 3.7.

Table 3.8: UV polymers prepared for 8 hours by varying polymerisation temperature

Polymer code	Polymerisation time (hours)	Polymerisation temperature (°C)
U10	8	0
U6	8	20

A series of NIPs were prepared in identical manner for every MIP prepared by all three methods under study (MW, oven and UV), as mentioned earlier. Please note that the reaction volume and the type of reaction vessel (Pyrex test-tube) were kept the same in all three polymerisation methods to avoid inconsistencies among these parameters. MW polymerisation is a fully controlled heating reaction. Hence, it would be important to understand how it functions before the analytical methods are discussed further.

The MW reactor used in these experiments (CEM Benchmate, CEM Corp, UK) can be programmed to carry out heating at a specific power, temperature and time. It is important to understand how it actually carries out a heating reaction with the set experimental parameters.

3.3.3. Polymerisation kinetics

Polymerisation temperatures were recorded per second for the MW polymers via *in-situ* IR temperature probe inserted into the MW reactor (CEM Benchmate, CEM Corp UK). The temperature profiles were reconstructed from the recorded temperatures and were calculated into heating rates (°C minute^{-1}).

3.3.4. Total monomer conversion

Total monomer conversion was calculated for the prepared MW polymers. UV spectrophotometry was used to calculate the total monomer conversion into polymer under different polymerisation conditions. Polymer monoliths obtained from the MW reactor were ground dry with the aid of mortar and pestle for 5 minutes. The powered polymer was filled into the cellulose extraction thimbles and was subjected to soxhlet extraction in analytical grade methanol for 24 hours. Polymer fines were allowed to sediment and aliquots of 2 ml of obtained extracts were taken for each sample. A six-point calibration curve of the monomer mixture (0.095 mM to 2.95 mM) was produced in methanol by the UV spectrophotometric analysis of the mixture at 220 nm in triplicate (see appendix, Figure 1). The methanolic extracts of polymer washes were then analysed for their absorbance by UV spectrophotometry (PerkinElmer LAMBDA Bio+) at λ_{max}=270 nm and monomer amounts in the extracts were calculated from the calibration curve already produced. The amount of the monomers (in mM) leached out in the soxhlet washings was then subtracted from the total amount of the monomers used in the polymerisation to calculate the amount of the monomers converted to the polymer. The monomer conversion amounts were then calculated as the % of the original mixture for all the MIPs prepared through the range of MW powers, temperatures and the lengths of the polymerisation. The total of amount of the monomers converted to polymers was expressed as the % monomer conversion which are listed later in the results Section 3.5.1.

3.3.5. Differential scanning calorimetry

To carry out the analysis, 2.5 mg of polymer sample was placed in the DSC aluminium crucible (40 µl, Mettler Toledo, UK). The pans were then crimped using a crimping device (Mettler Toledo, UK). The pan with the polymer sample was then pin holed and placed in the sensor device along with an empty aluminium pan as the reference. Experimental values were filled into the STARe software (Mettler Toledo, UK). The argon inlet was turned on and set to 80 ml min^{-1} rate (in order to get the Hg pressure reading of 54 mm). The heating cycle (10 - 200°C min^{-1}), the equilibrium phase (200 °C for 3 minutes) and the cooling cycle (200 - 10 °C min^{-1}) were set up in the STARe software. The flow of the argon was maintained at 80 ml min^{-1} throughout the measurement. Analysis of each polymer was carried out in triplicate followed by the calculation of the mean and the standard deviation values of the measured glass transition temperatures (T_g). Different polymer samples were compared against each other for the difference in their T_g values and were plotted as bar graphs as presented in Section 3.5.2 of this chapter.

3.3.6. Thermogravimetric analysis

To carry out the analysis, approximately 5 mg of each polymer was placed in an open DSC aluminium pan. The sample was then heated from 30 °C to 600 °C at the rate of 10 °C minute^{-1} using a Diamond TGA /DTA (Perkin Elmer, MA, USA) and mass loss recorded.

3.3.7. Porosimetry measurements

To carry out the analysis, 20 – 30 mg of sample was first degassed at 110 °C under vacuum for one to two hours to remove any adsorbed solvent. Determinations of specific surface area were performed using an ASAP 2000 instrument (Micrometrics) based on the nitrogen multi-point BET method (maximum experimental error less than 1 %) which aims to investigate the surface area and pore characteristics of a material by physical adsorption of the gases (such as nitrogen and argon) on it. Water permeability measurements were performed in a UF cell (d = 25 mm, model 8050, Amicon Corp.) using different hydrostatic pressures as driving force. The adsorption isotherm of this degassed sample was then measured using nitrogen as the absorbate at a temperature of 77 K (degree kelvin) covering the partial pressure (P/P_0) range of 0.05 to 0.35. Figure 3.10 presents a typical porosimetry plot recorded in the study.

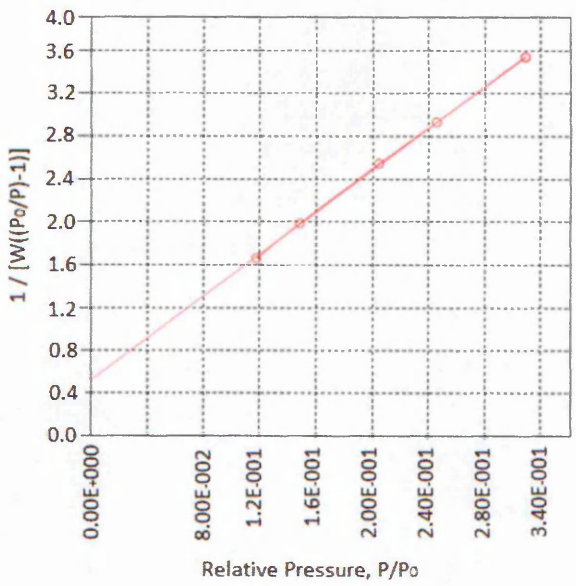

Figure 3.10: A six-point linear BET plot $1/[W (P_0/P)-1]$ vs P/P_0 generated by Quantachrome™ Novawin2.

The specific surface area of each sample was automatically calculated from the slope and the intercept using the linearised BET equation by the Nova1000e from the adsorption data as shown in the Figure 3.13. The calculations could be derived from Equation 3.1 (50).

$$\frac{1}{[W(\frac{P_0}{P}-1)]} = \frac{C-1}{W_m C} * \frac{P}{P_0} + \frac{1}{W_m C} \qquad (3.1)$$

Where, P = partial vapour pressure (Pa) of the adsorbed gas

P_0 = saturated pressure (Pa) of adsorbed gas

W = volume of gas (ml) adsorbed at standard temperature (273 K) and pressure ($1X10^5$ Pa) (STP)

W_m = volume of gas (ml) adsorbed at STP to produce a monolayer on the surface of the sample

C = dimensionless constant related to the enthalpy of adsorption of the gas on the sample surface

The pore size distribution was calculated using a density functional theory (DFT) based approach using Nova 1000e Surface Area (by using Quantachrome™ Novawin2 software) and Pore Size Analyser (Quantachrome, UK). Average surface area, total pore volume and average pore radii were then plotted as bar graphs against the experimental parameter under study (MW power, polymerisation time and polymerisation temperature).

3.3.8. Scanning electron microscopy

Scanning electron microscopy (SEM) was used to analyse polymer samples for their morphology. To carry out the analysis, the ground polymer samples were sprinkled onto the carbon sticker and then coated with gold using POLARON sputter coater at 2.0 kV coating voltage for 2 minutes to give the coating thickness of around 20 - 25 nm. The samples were handled by the specimen holder and viewed under Zeiss Supra 55VP FEG SEM at 250X and 5 KX magnification.

3.3.9. Solid phase extraction

To carry out SPE based analysis, 100 mg of each polymer was packed into 1 ml solid phase extraction cartridges in triplicate (Supelco Ltd, UK). Figure 3.11 shows the schematic describing the steps involved in a typical SPE analysis and explains the method used for the SPE based analysis in the presented study.

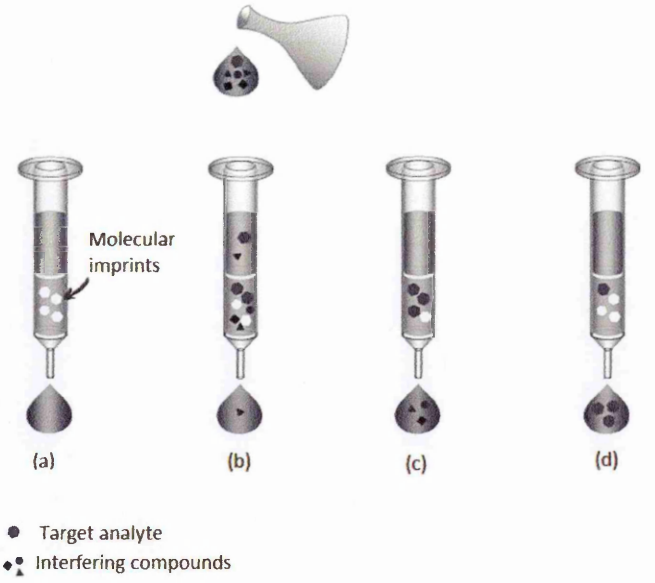

Figure 3.11: Schematic of the operational steps involved in an SPE analysis; (a) conditioning of stationary phase packed into the cartridge, (c) percolation of the template(s) sample through conditioned stationary phase, (c) washing step for the removal of interfering analytes and (d) elution of the target template.

Conditioning: The MIP-SPE cartridges were conditioned by using 1 ml HPLC grade acetonitrile.

Template rebinding / percolation: Rebinding solutions of caffeine (0.05- 3 mM, 1 mL) were prepared using HPLC grade acetonitrile (Chromasolv, Sigma-Aldrich, UK). The solutions were then passed through the cartridges using a Supelco vacuum manifold connected to a vacuum pump. The flow rates were maintained constant to 1 mL minute^{-1} to obtain homogeneity of the binding kinetics.

Washing / removal of interfering components from the MIP: This step was omitted from the SPE protocol used in the study since the rebinding solution only contained caffeine (template) and not a mixture of compounds.

Elution: The template released from the MIP-SPE was collected subjected to further quantification by HPLC (51). In the presented study, caffeine was the only component in the rebinding solution. Therefore, this step was omitted from the protocol. The known amount of caffeine was passed through the MIP-SPE cartridge and the unbound caffeine (collected at the bottom) was subjected to HPLC analysis for further quantification. The amount of caffeine bound selectively to the MIP was calculated by subtracting the amount of template that did not bind to the MIP (or quantified by HPLC) from the total amount of the template that was initially introduced to the MIP-SPE.

For each round of the mentioned protocol, all the cartridges was washed thoroughly with 5x1 mL aliquots of HPLC grade methanol followed by drying with 1 mL HPLC grade acetone to remove previously bound caffeine to the MIPs. Cartridges were then dried under vacuum for about 15 minutes and re-used for another round of rebinding experiments. The reusability of the MIP-SPE cartridges were not analysed for extended period but were re-used for caffeine rebinding experiments for up to 20 times without considerable effect on their template recognition performance.

3.3.10. High performance liquid chromatography

Caffeine rebinding solutions (1 mL) collected through the SPE cartridge was subjected to caffeine quantification by using Agilent 1260 INFINITY LC systems equipped with 60 mm DAD detector cell (λ_{max} 270 nm, noise level 0.6 uAU cm^{-1}). The LC based quantification of 10 µL caffeine extract was carried out using the mobile phase water: acetonitrile (50:50) (30 ± 0.05 °C, 0.1 mL $minute^{-1}$) through reverse stationary phase (ACE Excel 3 Super 18, ID – 150 x 4.6 mm, EXL – 111 – 1546U). Caffeine calibration curve was prepared in the concentration range of 0.05 mM to 3 mM under identical condition (see appendix, Figure 2) and was used for the quantification of the unbound caffeine extracts collected from MIP-SPE. The amount of unbound caffeine was then deducted from the total amount of caffeine introduced to the SPE MIP cartridges, as explained in Section 3.3.9. The amount of bound caffeine was then plotted against the total amount of caffeine introduced as discussed in Section 3.4.6. Caffeine rebinding experiments were also carried out on the parallel set of NIPs and the imprinting factors (IF) were derived as a ratio of ($Bound_{MIP}$/ $Bound_{NIP}$).

Section 3.4 explains the results obtained from various physicochemical analyses of the polymers under study.

3.4. Results and Discussion

The polymers prepared under different experimental conditions were analysed by various physicochemical techniques as described in Section 3.3. This section presents and discusses the findings obtained from this analysis.

3.4.1. Polymerisation Kinetics

Physical properties of the polymers are influenced by their preparation conditions including the rate of heating, heating temperature and even the length of polymerisation. It can been difficult to record such properties while carrying out polymerisations in an oven or oil-bath; however the automated and controlled nature of a MW reactor allows precise record of these parameters.

Before conducting the analysis, it would be important to discuss how a typical heating profile is obtained from a MW reactor whilst carrying out a free radical polymerisation of MIPs. Figure 3.12 illustrates a typical heating profile obtained from MW reactor.

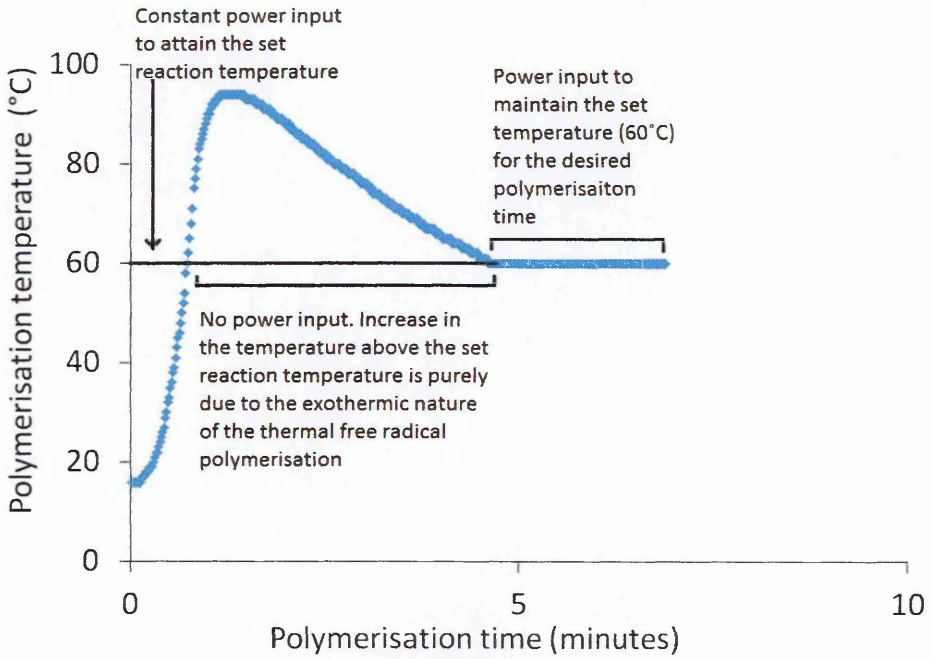

Figure 3.12: Heating profile of a MW reactor for a free radical polymerisation.

As explained in the heating profile in Figure 3.12, the MW irradiation starts heating the reaction mixture at specified power and once the set temperature is attained, it stops inputting any power. This is to let the reaction to be carried out for however long it remains above the set temperature. For a free radical polymerisation, the initiation phase is highly exothermic which in the most cases is much higher than the set polymerisation temperature. The automated MW reactor is designed in such a way that it does not interfere with the initiation process of a polymerisation and its exothermic nature (as shown earlier in Figures 3.3 and 3.4). This makes it comparable to traditionally heated mixtures as it just aids the rate of the initiation by the virtue of the additional power supplied.

When the exothermic initiation phase ends and the chain propagation starts, the temperature decreases gradually. At this stage, the set power is constantly fed to maintain the set temperature for the specified time (as seen in Figure 3.12). It would be important to note here that although the MW irradiator has cooling function; all the polymers prepared in this study have been cooled naturally once the polymerisation is completed. This is to minimise any error in the temperature reading plus to make MW polymers more comparable to the parallel series

of the conventional polymers Following sections explain the physicochemical analytical studies used for the analysis of the prepared polymers.

A record of temperature in particular may help to understand the polymerisation kinetics. In the presented study, polymerisation temperatures were recorded as a function of the polymerisation kinetics as described earlier in Section 3.3.1. Recorded temperatures were plotted as a function of polymerisation time. Out of the three experimental parameters under study (heating rate, time and temperature), two parameters were kept constant at each time whilst the third parameter was varied. The first set of temperature records were of the MW polymers prepared at 60 °C for 15 minutes with varying heating rates by changing MW powers from 5 W to 300 W, as presented in Figure 3.13.

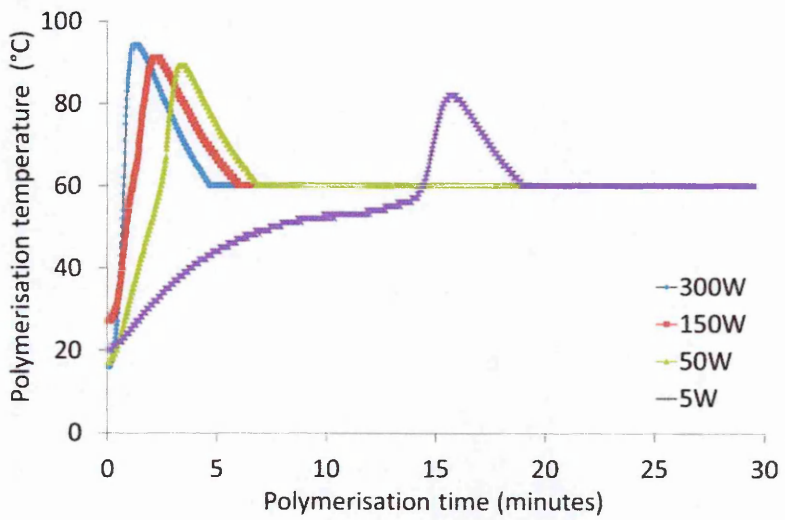

Figure 3.13: Polymerisation temperatures recorded *in situ* by IR probes for MW polymerisations at 60 °C for 15 minutes at variable MW powers; represented by different colours (5 W-purple, 50 W-green, 150 W-red and 300 W-blue).

As seen in Figure 3.13, it was found that the polymerisation kinetics were significantly affected when the polymerisations were carried by varying MW powers. The rate of heating was found to increase by increasing MW power from 5 W to 300 W.

To understand the kinetics further, heating rates (°C minute^{-1}) were calculated by measuring the polymerisation temperature as a function of time from the start of the polymerisation until it reached the set polymerisation temperature (60 °C). This particular heating phase was chosen to study the polymerisation kinetics because different MW powers applied for heating would only affect the heating rate until the temperature reached its set value. Once the desired temperature was attained, MW power would be shutdown to let polymerisation occur with its own kinetics (as described in Figure 3.13). It was found that the slowest heating rates were achieved with the lowest power (5 W) which was 12 °C minute^{-1}. Upon increasing the

MW power to 50 W, 150 W and then 300 W, the heating rates of 25 °C minute^{-1}, 52 °C minute^{-1} and 85 °C minute^{-1} were achieved respectively. This was in agreement with an earlier finding where the heating rates of a MW reactor increased by increasing power used for carrying out polymerisation (15).

In addition to this, an investigation was made to understand whether different heating rates affected the amount of monomer conversion into the polymer. Total monomer conversion and heating rate was then calculated for each polymerisation carried out by varying MW power (as described in Section 3.3.4).

Table 3.9: Heating rate and monomer conversion achieved with different MW powers at 60 °C for 15 minutes

MW power (W)	Heating rate (°C minute^{-1})	Total monomer conversion (%)
5	12	98.57
50	25	99.6
150	52	99.75
300	85	99.98

The heating rates of different polymerisations were found to increase considerably from 4 °C minute^{-1} to 85 °C minute^{-1} when the supplied MW power was increased from 5 W to 300 W (as seen in Table 3.9). However, the % of total monomer conversion increased only a little by 1-2 % from 98 % to 99.9 % when the MW power was raised from 5 W to 300 W. Overall, total monomer conversion in all cases was found to be above 98 % despite using considerably wide range of MW powers. Another interesting observation was that the highest temperature recorded in different polymerisations increased by increasing the MW power used for polymerisation. Figure 3.14 shows the plot of the highest recorded temperature of different MW polymerisations carried out with variable MW powers.

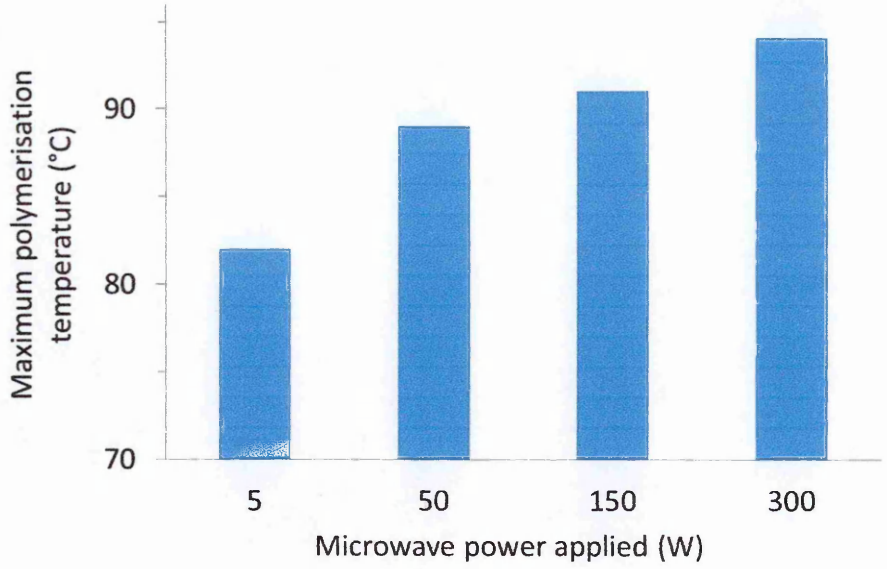

Figure 3.14: *In situ* measurements of the maximum polymerisation temperature recorded by IR probes for MW polymerisations at 60 °C for 15 minutes at variable MW powers.

Following the Norrish-Trumsdorff effect, the temperatures in the performed free radical polymerisations were recorded to be higher than their set temperature of 60 °C (as explained in Section 3.2). The highest temperatures recorded for different polymerisations increased slightly from 82 °C to 94 ° when the MW power was increased from 5 W to 300 W (as seen in Figure 3.14). A previous study stated that the highest recorded temperature would be similar in all polymerisations regardless of the MW power used for their polymerisation (35). It was justified with a hypothesis that the amount of energy fed to heat a material in a MW reactor would remain the same at any power value used. The value of power would rather determine the rate at which the heating would take place, lower power would heat slowly and higher power would heat faster. This finding was supported by other studies with similar hypothesis that as the total amount of energy fed to heat the material was constant at different powers, the reaction temperatures also remained constant (10, 11, 23). On the contrary, the observations made in the presented study indicated that different heating rates (achieved with different MW powers) could slightly affect the polymerisation temperature. The observable difference in the maximum temperatures during this study could be merely a result of broad power range (5 W to 300 W) used for heating which was missing in any earlier study. For example, one study reportedly used narrow power range of 100 W to 200 W (23); whereas others used high MW powers from 200 W to 500 W (10, 11). The heating rates generated from much similar MW powers would likely be similar which might not result into observable difference in the maximum temperature. The presented study on the other hand, investigated MW powers of as low as 5 W to up to 300 W. As postulated, the heating rates attained with

such different powers varied considerably (as seen in Table 3.9). It was reported earlier that the faster heating (achieved with 150 W and 300 W) could in fact accelerate both the rate and the amount of initiator breakdown (35). From these reports, the higher number of reactive initiator radii generated at higher MW powers could increase the thermokinetic energy of the system considerably which might result into higher temperature (as seen in Figure 3.14).

To understand these trends further, polymerisations were also carried out at temperatures from 40 °C to 90 °C, whilst keeping the time (5 minutes) and the power (5 W) constant. Polymerisation temperatures were recorded similarly *in situ* by IR temperature probe. Recorded temperatures were then plotted as a function of time, as seen in Figure 3.15.

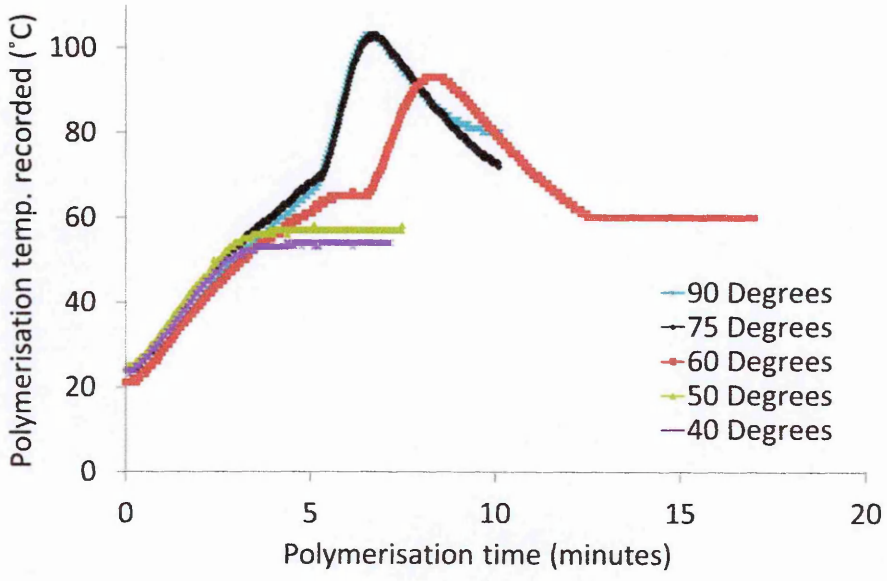

Figure 3.15: Polymerisation tempertaures recorded *in situ* by IR probes recorded for MW polymerisation carried with 5 W for 15 minutes at different set temperatures; represented by different colours (40 °C-purple, 50 °C-green, 60 °C-red, 75 °C-black and 90 °C- blue).

When MW polymerisations were carried at the temperatures of up to 50 °C, neither exothermic behaviour nor a successful polymerisation was observed. For the temperatures of and above 60 °C, the observed exothermic nature of the reaction was indicative of a successful polymerisation (as described earlier in Figure 2.10). In other words, the polymerisation did not take place until the initiator degraded thermally and resulted into reaction temperature higher than that the set value in MW reactor. This also confirmed that the success of a MW polymerisation was solely temperature driven and no other MW effect was observed that could result into a successful polymerisation below the thermal degradation point of the initiator used. This was in agreement with the most other findings that MW irradiation did not

posess any additional non-thermal wave effect such as UV irradiation (29). Not to forgot, this observation was made when AIBN was used as the initiator in this study. For a typical thermal free radical polymerisation, thermal degradation of the initiator would vary depending on its type. Hence, MW polymerisations carried out below 60 °C would need to be investigated further for its possible non-thermal effect by using different types of thermal initiators.

MW power was optimised to 5 W and some more MIPs and their corrosponding NIPs were polymerised for different lengths of time (from 5 minutes to 60 minutes). The rest of the parameters, the temperature and the MW power were kept constant at the values of 60 °C and 5 W respectively. The polymerisation temperature traces were recorded from the MW reactor. Figure 3.16 shows the polymerisation temperature versus the time plot obtained from MW polymerisations carried out for various lengths of time.

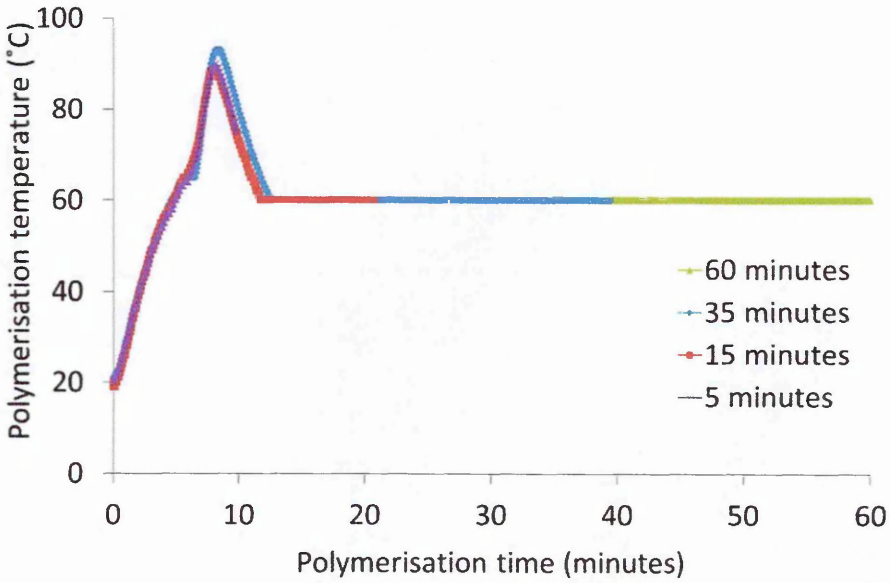

Figure 3.16: Polymerisation tempertaures recorded *in situ* by IR probes when MW polymerisation is carried with 5 W MW power at 60 °C for different time durations; represented by different colours (5 minutes-purple, 15 minutes-red, 35 minutes-blue and 60 minutes-green).

As seen in Figure 3.16, when polymerisation was carried out for different lengths of time, the heating rates were found to be constant between 11 °C minute^{-1} to 13 °C minute^{-1}. This was expected since the more prominent variables associated with polymerisation kinetics such as, the power (5 W) and temperature (60 °C) were kept constant. The total monomer conversions were also caculated for this set of MIPs, as seen in Table 3.10.

Table 3.10: Heating rate and monomer conversion achieved with with 5 W MW power at 60 °C for different polymerisation times

Polymerisation time (minutes)	Heating rate (°C minute^{-1})	Total monomer conversion (%)
5	12	98.35
15	11	98.57
35	12	99.00
60	13	99.81

The UV spectrophotometric analysis of the polymer washes suggested that MW polymerisation carried out for as little as 5 minutes polymerised 98.35 % of the total monomers used in the pre-polymerisation mixture (as seen in Table 3.10). Increase of polymerisation time up to 60 minutes showed a slight increase in the monomer conversion. Having observed considerable monomer conversion in just 5 minutes, the polymerisation time was optimised to 5 minutes alongside already optimised MW power of 5 W. More MW polymerisations were then carried out at different temperatures (60 °C, 75 °C and 90 °C). At this time, the remainder of the parameters such as MW power and polymerisation time were kept constant to 5 W and 5 minutes respectively.

Figure 3.17 shows the polymerisation temperature traces recorded by IR probe for MW polymerisaitons carried out at different temperatures.

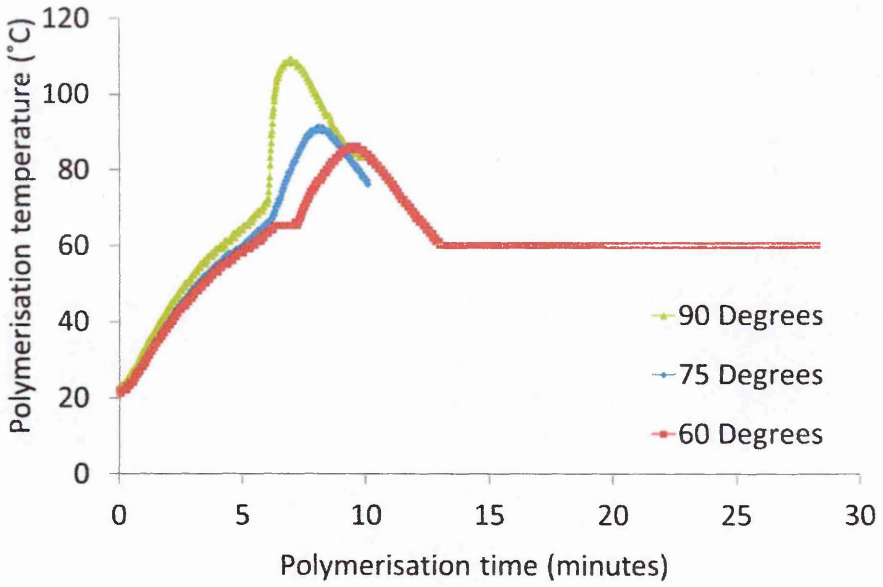

Figure 3.17: Polymerisation tempertaures recorded *in situ* by IR probes for MW polymerisation carried with 5 W MW power for 5 minutes at different temperatures; represented by different colours (60 °C-red, 75 °C-blue and 90 °C-green).

As seen in Figure 3.17, the heating rates of MW polymerisations carried out at different temperatures were quite constant between 11 °C minute^{-1} and 13 °C minute^{-1}. This was expected as the rate of heating (MW power) applied for this set of polymerisations was the same. At the same time, the highest recorded temperatures increased with an increase in their set polymerisation temperature values, as expected. The % monomer conversions for these polymers are summarised in Table 3.11.

Table 3.11: Heating rate and monomer conversion achieved with different polymerisation temperatures with 5 W for 5 minutes

Polymerisation temperature (°C)	Heating rate (°C minute^{-1})	Total monomer conversion (%)
60	12	98.35
75	12	98.81
90	13	98.93

Total monomer conversions increased slightly from about 98.3 % to about 98.9 % when the set polymerisation temperatures were 60 °C and 90 °C respectively (as seen in Table 3.11). This temperature dependent increase in the monomer conversion was in agreement with a previous finding (15).

The oven and UV devices used for polymerisations did not have temperature recording feature. Hence, previously reported studies of oven and UV polymerisation kinetics were considered to compare with the MW polymerisation kinetics presented in this work. An earlier study reported that the % monomer conversion achieved with conventional oven heating could be three times less than that achieved with a MW polymerisation under identical conditions of temperatures and the length of time (35). This might be due to the considerable difference in the heating rates between an oven and a MW polymerisation for a similar time period. Slower heating rates in an oven would more likely result into slower polymerisation kinetics (35).

Another study also established that the higher monomer conversion obtained in a MW polymerisation was subject to the dielectric property of the porogen used (29). UV polymerisations have been quicker compared to oven polymerisations, converting about 70 % of monomers within 5 minutes from the start of the irradiation (52). It would be important to note that the MW polymerisation carried out for similar duration (5 minutes) in the presented study showed even higher monomer conversions of up to 98 % (please refer to Tables 3.9, 3.10 and 3.11). This suggested that given the right porogen, a MW polymerisation could outperform the UV polymerisation in terms of their monomer conversion efficiency. Although the UV polymerisation have been faster than the oven polymerisation, it has suffered from producing polymers with lower surface area than the thermal polymerisations (as disscused in Section 3.2). Hence, a MW polymerisation could offer the best of both traditional polymerisation techniques, producing polymers at a faster rate and with larger surface area too.

An earlier study suggested that the main factors affecting total monomer conversion of the resulting polymer could be the change in the pre- polymerisation recipe, mainly the type of the initiator and the type of porogen used. Obviously, the porogen would affect the heating rate depending on its dipolar character in MW heating but the effect of the type of initiator might need further investigation. However, some studies strongly indicated that the faster heating in a MW reactor could produce radicals faster. The faster chain reaction could thereby produce many more of reactive radii in a MW reactor than in an oil-bath heating for the given length of time. This might explain why kinetics of a MW polymerisation are considerable faster than other heating methods (21, 29).

The total monomer conversion achieved with variable MW powers was found to be comparable to that of the oven heated polymerisations. Importantly, lower MW powers used in this study (5 W and 50 W) have been unexplored for carrying out MW polymerisation in any existing study. The observations drawn from this study showed that for a particular

polymerisation recipe, MW power as low as 5 W successfully converted over 98 % of the total monomers in just 5 minutes when the set polymerisation temperatures were from 60 °C to 90 °C. However the performance of the recognition polymers could vary depending on the type of monomer recipe, especially the type of porogen used. Another important observation made was that the maximum temperature reached in a particular MW polymerisation was subject to the MW power used. On carrying out *in situ* temperature measurements, it was found that temperatures increased with increasing MW power in all polymerisations. The presented study also found that increase in MW power strongly influenced the rate of polymerisation.

All the polymers under study were analysed by several other physical techniques. Section 3.4.2 explains the results obtained from the the dynamic scanning calorimetric analysis.

3.4.2. Differential Scanning Calorimetry (DSC)

Differential scanning calorimetry (DSC) was used to analyse the polymer samples for their cross-linking degree. DSC is a thermal analytical technique widely used for the polymer analysis. The polymer sample is heated at a constant rate in DSC which would lead to the depolymerisation of the polymer. As the depolymerisation is the breaking of the bonds, it would be an endothermic reaction. DSC measures the amount of heat (in calories or kJoule) being taken up by the polymeric sample as a function of time when the polymer is heated at a constant rate. Upon consuming the heat, the polymer transits to the glassy morphology, more commonly referred to as the glass transition temperature (T_g). It is indicative of the degree of the cross-linking of a polymer sample, highly cross-linked polymer taking up more energy to break more bonds in its matrix compared to the ones with comparatively lower degree of cross-linking. Hence, the polymer sample with the higher T_g would be the highly cross-linked polymer and vice-versa. Figure 3.18 shows a typical DSC thermogram obtained by conducting DSC analysis of the polymer.

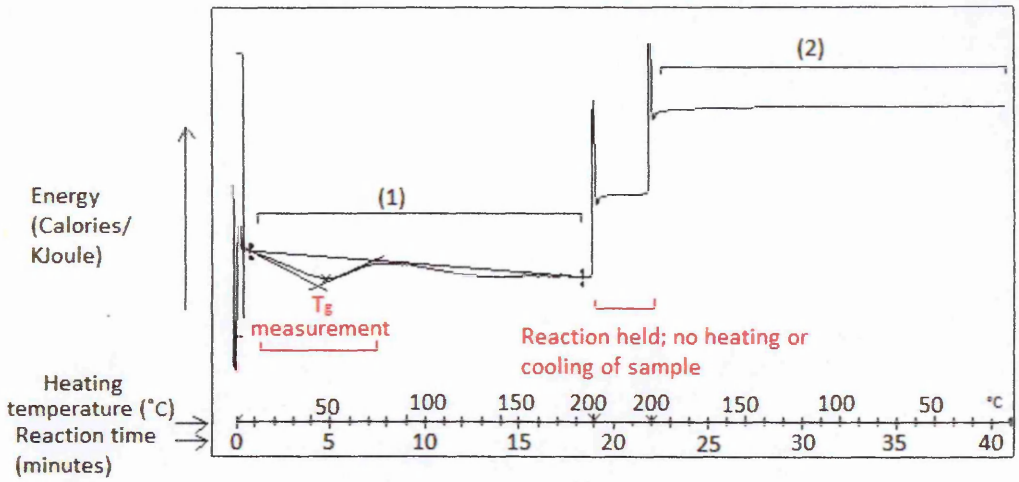

Figure 3.18: A typical DSC thermogram of a cross-linked polymer recorded in the study; (1) heating phase which is endothermic in nature and used for the measurement of T_g; (2) cooling phase.

The reason for understanding this physical property of cross-linking in the context of MIPs, is that the MIPs are structurally cross-linked polymers. Hence, the degree their cross-linking would be crucial in defining their physical properties. Lower cross-linking degree could lead to the deformation of the binding cavities in different experimental conditions whereas a very high degree of cross-linking could hinder the mass transfer kinetics while removing and rebinding the template (5). The optimum degree of cross-linking is also crucial in allowing the template to access all the binding sites within the polymer matrix (48). As the MIPs under study have been prepared in different polymerisation conditions, they would very likely be different in their physical properties incuding their cross-linking degree (2-5). The degree of cross-linking could also help explaining any observed pattern of their differing template rebinding performance. A study suggested that the MIPs with a wide range of T_g would reflect their molecular weights too (27). Hence, the differences in the T_g values of the MIPs could be very helpful in understanding the effect of an experimental parameter on their physical properties.

Figure 3.19 shows the T_g of the MIPs polymerised at 60 °C for 15 minutes by varying MW power from 5 W to 300 W.

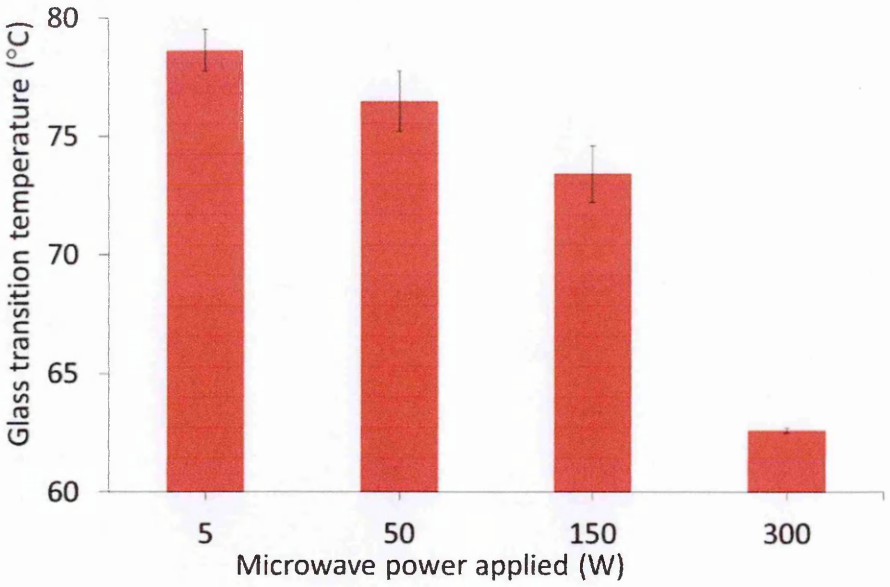

Figure 3.19: Comparison of the T_g of MW MIPs prepared at 60 °C for 15 minutes with different MW powers; standard deviations derived from the triplicate measurements of each polymer sample.

When MW MIPs were analysed by DSC, they showed a MW power (heating rate) dependent T_g (cross-linking degree) values. The T_g values were inversely proportional to the MW powers (heating rates) used for polymerisation. The highest T_g was obtained with the slowest heating rate (5 W) and the lowest T_g was obtained with the fastest heating rate (300 W). To understand this behaviour, it would be important to discuss how the heating rate could affect the length of a MW led heating reaction. In a MW reactor, the set length of a reaction would start counting once the set temperature was attained. For a polymerisation carried out with higher MW powers (with faster heating rates) such as 300 W, the set temperature would be attained more quickly. This means that when two polymerisations were carried out with different powers (heating rates) for similar set time, the one carried out with high MW power (with faster heating) would be shorter in its length compared to the one carried out with low power (slower heating). The hypothesis was that when polymerisation mixture was heated with low power (at a slower rate), it could result into a slightly longer polymerisation reaction. Longer polymerisation would allow enough time for the growing nuclei to form extensive cross-links. Higher MW powers on the other hand could lead to comparatively shorter reactions. Such shorter polymerisation times could stagnate the growing linear chains much faster into polymer matrix before they could create sufficient cross-links. As a result, polymerisations carried out with high powers could show lower degree of cross-linking in comparison to the one carried out with low MW power. When heated in DSC analysis, the MIPs with lower cross-linking degree would need less energy to break those fewer cross-links

in their matrix and would reach its glass transition state (T_g) at comparatively lower temperatures. MW MIPs prepared with low MW powers (with slower heating) on the other hand would consist of higher cross-linking degree which might need high energy to break numerous cross-linking bonds resulting into higher T_g values. The results obtained in these DSC analysis were in agreement with this hypothesis where lower MW powers produced MIPs with higher cross-linking whereas higher MW powers produced MIPs with lower cross-linking (as seen in Figure 3.19). The results obtained from polymerisation kinetics were also in agreement with the hypothesis that higher MW powers heated polymerisation mixtures at faster rates in comparison to low MW powers that heated it at much slower rates (as seen in Figure 3.13 and Table 3.9). No earlier studies have reported correlation of the MW heating power with the cross-linking degree of the polymers as discussed in the presented study. Hence, the findings would need to be further investigated to test the hypothesis over a wider range of MW powers for different polymer matrices.

Another set of MW MIPs were prepared with 5 W power at 60 °C for different lengths of time from 5 minutes to 60 minutes. The results from their DSC analysis were plotted as seen in Figure 3.20.

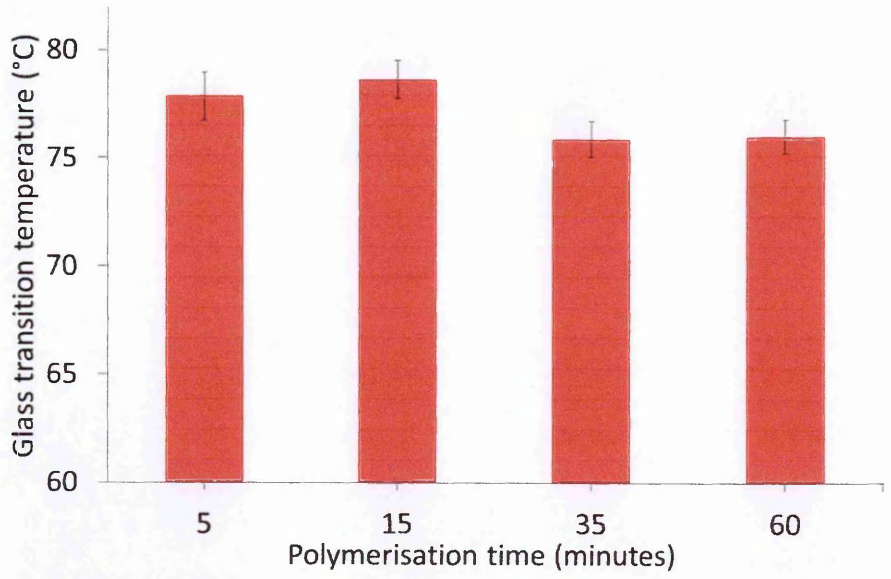

Figure 3.20: Comparison of the T_g of MW MIPs prepared with 5 W at 60 °C for different durations; standard deviations derived from the triplicate measurements of each polymer sample.

The T_g of the MW MIPs prepared for 5 minutes and 15 minutes were found to be 77 °C to 79 °C respectively; however it dropped slightly by 2 °C when the polymerisation time was extended up to 60 minutes. Overall, different polymerisation temperatures did not seem to affect the T_g

of the MW MIPs as considerably as different MW powers (heating rates). Figure 3.21 shows the T_g of MW MIPs polymerised at different temperatures.

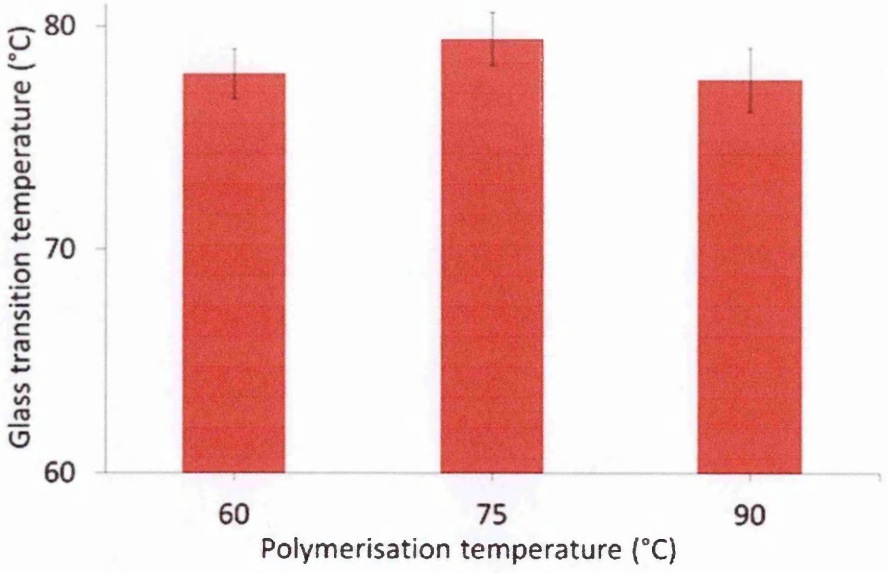

sample.

When the MW MIPs were polymerised at different temperatures, their T_g remained quite consistent between 77 °C to 79 °C. This meant that both the polymerisation time and temperature did not reflect much on the cross-linking degree of the resulting MW MIPs unlike MW power (heating rate). To understand this further, it was important to see whether a similar behaviour was observed in the control set of oven polymerised MIPs as well.

To do so, oven polymerisation was carried out from 1 – 3 hours. Up to this time, the resultant MIPs showed a transparent gel like texture. However, when polymerisation time was extended to 4 hours and beyond, a visual inspection showed MIPs with a solid white monolithic character. Traditionally, oven polymerisations are carried out for 24 hours. Hence, polymerisation time range of 4 hours to 24 hours was chosen to polymerise oven MIPs to prepare control set of polymers in the presented study. The resulting MIPs were analysed by DSC in identical manner and the results were plotted as shown in Figure 3.22.

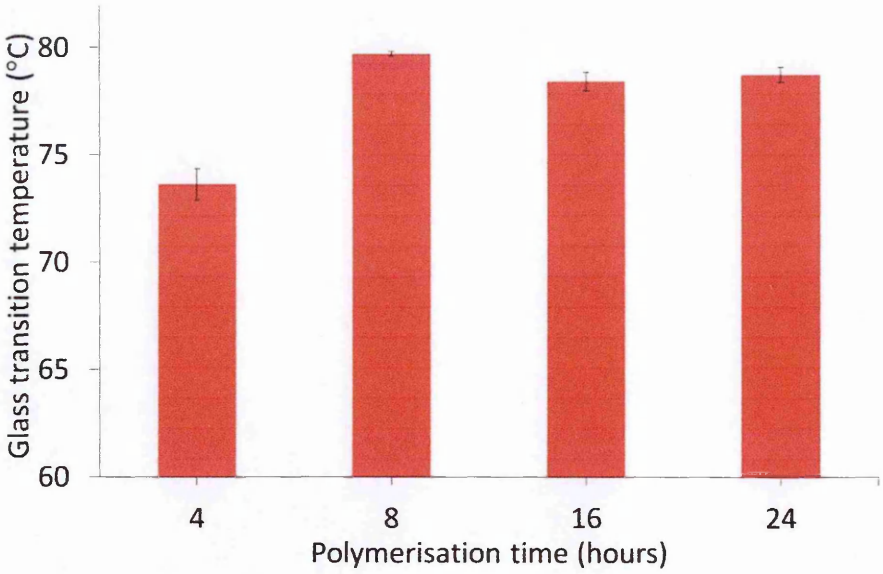

Figure 3.22: Comparison of the T_g of oven MIPs prepared at 60 °C for different time durations; standard deviations derived from the triplicate measurements of each polymer sample.

The T_g of the oven MIPs was found to increase from 73 °C to 79 °C when polymerised for 4 hours and 8 hours respectively. However, upon extending the time further from 8 hours to 16 hours, the T_g dropped slightly by 2 °C and then remained constant for the length of up to 24 hours (as seen in Figure 3.22). The observed trend was much similar to that observed in case of MW MIPs (as seen in Figure 3.20). To see the effect of polymerisation temperature on the T_g of oven MIPs, some more polymerisations were carried out at different temperatures using oven. Please note that the polymerisation time in this case was kept constant to 8 hours. Figure 3.23 presents the DSC analysis of the oven MIPs polymerised at different temperatures.

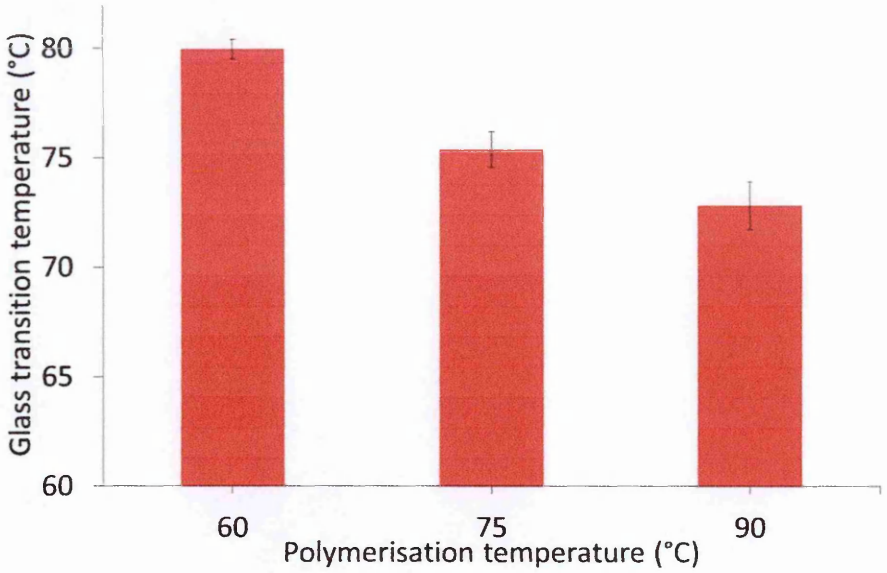

Figure 3.23: Comparison of the T_g of oven MIPs prepared for 8 hours at different temepratures; standard deviations derived from the triplicate measurements of each polymer sample.

When the oven MIPs were prepared at different temperatures, the lowest polymerisation temperature showed the highest T_g of 80 °C which decreased slightly by 2 °C when the polymerisation temperature was increased up to 90 °C. The trend observed was much similar to the T_g (cross-linking degrees) of MW MIPs prepared across similar temperature range (as seen in Figure 3.23). In other words, the cross-linking degree of both the oven and the MW MIPs were comparable when the polymerisations were carried out in similar temperature range, however the effect of different parameters on cross-linking degree was more pronounced in the oven MIPs than the MW MIPs. Not to forget, the MW polymerisation only took five minutes to produce such MIPs compared to the oven which took eight hours.

To understand this further, a secondary control method of UV polymerisation was introduced. The MIPs were prepared in similar manner to that of the oven polymerisation where polymerisation times were chosen from 4 hours to 24 hours at temperatures of 0 °C and 20 °C. Their DSC analysis was performed and the results of the T_g values were plotted in bar graphs as shown in Figure 3.24.

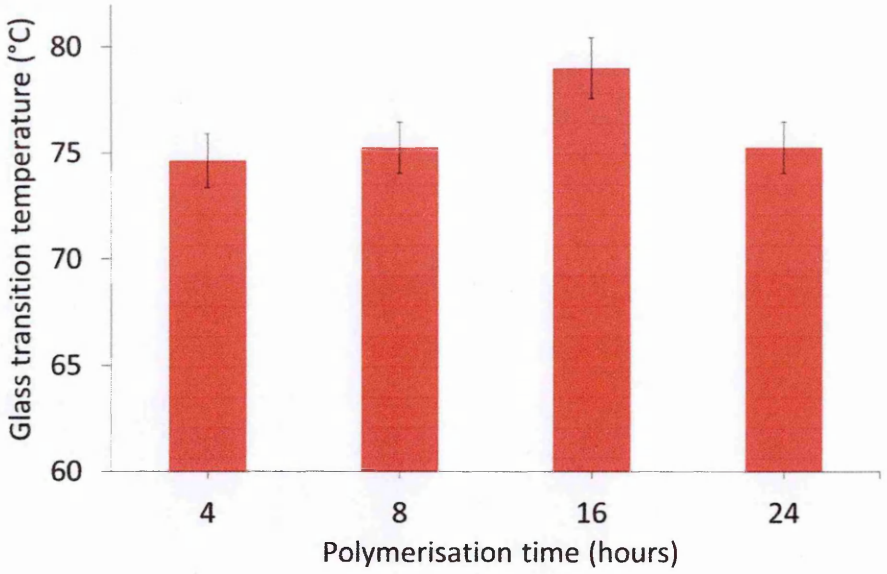

Figure 3.24: Comparison of the T_g of UV MIPs polymerised at 20 °C for different time durations; standard deviations derived from the triplicate measurements of each polymer sample.

When UV MIPs were polymerised at 20 °C from 4 hours to 16 hours, the value of T_g increased from about 75 °C to 79 °C; however the extended polymerisation times of up to 24 hours sucessively decreased the T_g values back to about 75 °C (as seen in Figure 3.24). The trend observed was comparable to those obtained by oven polymerisation where the cross-linking degree of the MIPs increased for up to similar time lengths but extended polymerisation times decreased it (as seen in Figure 3.22). Importantly, the behaviour observed was consistent in all the methods under study (MW, oven and UV). This could be explained by understanding the effect of time on the mechanism of radii formation during a thermal free radical polymerisation. In an active polymerisation, growing radical nuclei present in the polymer mid chain would be less reactive due to steric hinderence. These less reactive radicas would not be easily cross-linked when the polymerisation times are shorter. In contrast, the radicals present at the terminals of a polymer chain would grow much faster and could build cross-links at a faster rate. However, when the polymerisation times are longer, the mid chain radicals would get activated too and participate in forming additional cross-links which might result in higher degree of cross-linking of the polymer (2). This might help in understanding the reported findings that increase in the cross-linking degree was observed when polymerisation time was slightly lengthened (from 4 hours to 16 hours).

Another observation made in these experiments was that the cross-linking degree of the polymers either slightly decreased or remained constant when the polymerisations were carried out for extended durations (24 hours). Probably, the nature of free radical polymerisation could help explain this phenomenon better. This hypothesis was based on a

previous finding that when polymerisation was carried out for longer durations, depolymerisation might start parallel to the bond formation due to highly elevated temperatures. However, this secondary depolymerisation could only occur on few terminal chains whilst the mid chains would continue building cross-links. Polymer chain elongation and cross-linking would still dominate the vicinity of the matrix due to a higer number of reactive nuclei. At the same time, the slight depolymerisation could reduce the overall cross-linking degree to a minute extent (53). This explained that cross-linking degree of the polymers could decrease slightly upon lenghtening polymerisaitons for extended lengths of time.

To understand the effect of temperature on the cross-linking of MIPs, two different UV MIPs were prepared at 0 °C and 20 °C. The polymerisation time was kept constant to 8 hours to make it comparable to the oven polymerisations. The T_g of the resultant MIPs were recorded by DSC and were plotted, as seen in Figure 3.25.

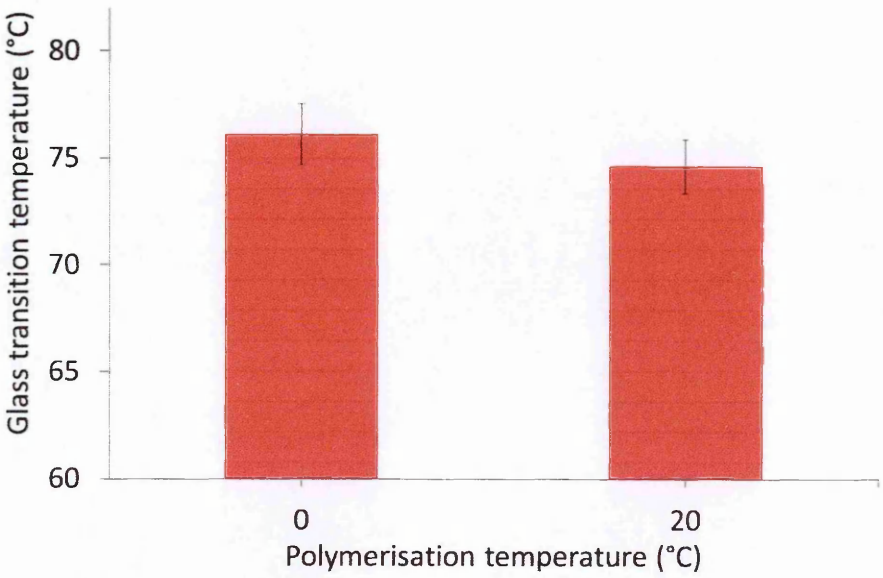

Figure 3.25: Comparison of the T_g of UV MIPs polymerised for 8 hours at different temperatures; standard deviations derived from the triplicate measurements of each polymer sample.

When the UV polymerisation was carried out at 0 °C and 20 °C, the T_g values of the resulting MIPs decreased slightly from about 76 °C to 74 °C. This behaviour of slightly decreasing T_g with increasing polymerisation temperature was comparable to that of oven polymerisation (see Figure 3.25). Similar observation was also reported in another recent study where a comparative analysis of the MW MIPs was presented with oven MIPs (54). Perhaps, the relationship between polymerisation kinetics and temperature could explain this behaviour. Polymerisation carried out at higher temperatures in oven and UV chambers would normally

have higher amount of reactive radii and higher kinetic energy of the pre-polymerisation mixture (55). This meant there could be a very high number of reactive monomer nuclei at higher temperatures at a given time. As a result, numerous nuclei would generate many faster growing oligomeric chains before they could form enough cross-links between them when polymerisations were carried out at comparatively higher temperatures. Lower polymerisaiton temperatures on the other hand would show slower polymerisation kinetics which could result into slightly higher cross-linking degree into resulting MIPs. However, inconsistent heatings carried out in oven and UV could lead to wider differences in the T_g values of the resulting MIPs than that of a controlled MW polymerisation. A MW reactor would heat the reaction at a set heating rate regardless of other experimental parameters. In the presented study, the MW MIPs prepared at different temperatures were heated by using the same MW power (5 W). Consistent MW power would be more likely to heat all the polymerisation mixtures at the same rate which might show much similar cross-linking degree in the resulting MW MIPs (as seen in Figure 3.19). MW power was found to be the most dominant parameter to reflect into cross-linking degree of the MIPs.

In summary, few useful obversations were made when the MIPs prepared by different methods under different polymerisation conditions were analysed by DSC. The MW power used for polymerisation showed considerable effects on the cross-linking degree of the MW MIPs. Cross-linking of the traditional oven and UV MIPs increased as the polymerisation time was increased (from 4 hours to 16 hours); however extended polymerisation times (up to 24 hours) slightly reduced the cross-linking degree. MW MIPs showed similar trend in cross-linking degree when polymerised from 5 minutes to 60 minutes. The reduction in the cross-linking might be persistent for even longer polymerisation times which could eventually affect the spatial distribution of the binding cavities in the MIP matrix. Hence, the common practice of polymerising MIPs for 24 hours or even longer need to be reinvestigated as it might lead to a compromised template rcognition performance.

Polymerisation temperatures seemed to have an inverse relation to the cross-linking degree of the oven and UV MIPs; however the MW MIPs showed a little effect of the temperature on their cross-linking which might be due to controlled heating of a MW reactor than incosistent heating of oven and UV chambers. In general, the cross-linking of the MIPs polymerised by different methods (MW, oven and UV) under different experimental conditions showed comparable cross-linking degree. It would be important to mention here that the cross-linking achieved in MW MIPs in just five minutes was much similar to that of oven or UV MIPs polymerised for eight hours.

The polymers were also assessed by Thermogravimetric analysis (TGA) as described earlier in Section 3.3.6. The following method of TGA analysis could be useful in understanding the robustness of the polymers.

3.4.3. Thermogravimetric Analysis (TGA)

TGA is a thermo analytical technique which is used to study robustness of a material. Here, the polymer sample is heated from 20 °C to 600 °C at a constant rate. The analysis measures the thermal and conformational transitions in a polymer sample usually for up to 200 °C. Upon heating further, it degrades the polymer and the loss of the polymer weight is determined as a function of time.

MIPs are structurally cross-linked polymers. TGA analysis could be a useful study to understand the effect of MIP cross-linking degree on their thermal stability or robustness. The DSC analysis in the presented study suggested that the MIPs showed different degrees of cross-linking depending on the experimental parameters used for their polymerisation. When polymers with different cross-linking degree were heated, the MIP with higher cross-linking degree degraded straight away in comparison to the one that was less cross-linked. This might be because when heated, a less cross-linked (flexible) polymer would more likely undergo regio or stereo selective rotations of their cross-linking bonds. Such bond rotations could take away a lot of total thermal energy applied to heat them. As a result, the actual breakdown of the polymer would be delayed until excess of energy was applied. Hence, this could result into flexible (less cross-linked) polymers surviving higher temperatures or showing higher thermal robustness. Highly cross-linked polymers on the other hand would show lower thermal stability because the polymer would be rigid enough to not undergo bond rotations and all the energy applied would be utilised in the breakdown of the polymer. Correlation of TGA thermograms of the MIPs with their DSC thermograms would be of particular interest in this study in order to to study whether polymer cross-linking degree could affect thermal rigidity of the MIPs.

It is vital to understand how the TGA thermograms would be interpreted in the presented study. Figure 3.26 represeants a typical TGA thermogram of a cross-linked polymer. It is usually the plot of % polymer weight loss upon heating versus the temperature (°C).

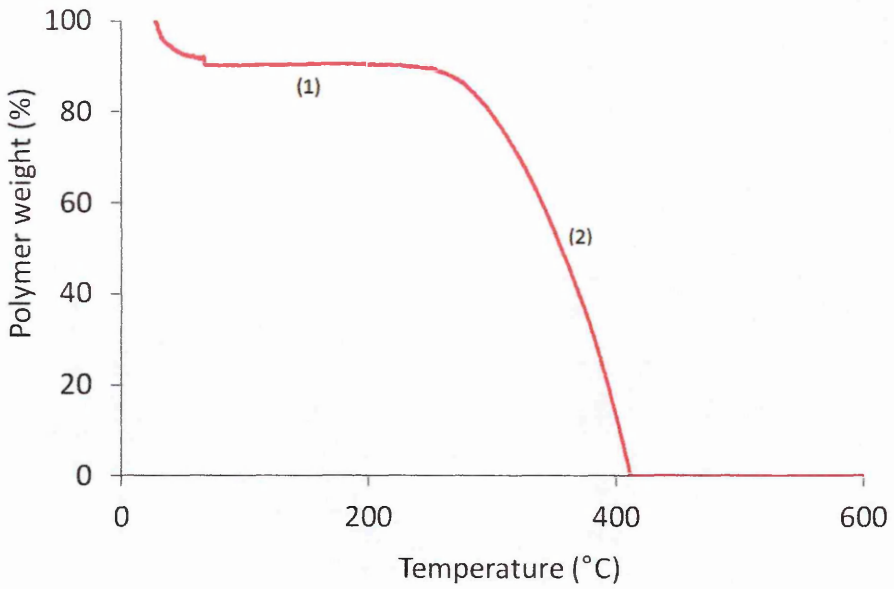

Figure 3.26: A typical TGA thermogram of a cross-linked polymer recorded; (1) the phase with some polymer weight loss and (2) the phase with the steep polymer weight loss.

A typical TGA thermogram shows the polymer weight loss as a function of the temperature. For up to the temperature of 200 °C, polymers do not tend to show a major weight loss however this region could be indicative of some structural changes occuring in the polymer. The structural changes may refer to the glass transition phase and hence this phase could be useful as a comparison to their DSC thermogram profiles (indicated as phase 1 in Figure 3.26). Most polymer samples when heated above 200 °C, show a steep weight loss however some polymers are rigid enough not to be burnt off completely even at the elevated temperatures of as high as 600 °C. Hence, this phase could be a good measure of the robustness of the polymer (indicated as phase 2 in Figure 3.26). Whilst interpreting the TGA profiles of these polymers, both the phase 1 and phase 2 were studied for a better understanding of both their cross-linking degree as well as their robustness.

To carry out analysis, the polymer weight loss from the TGA thermograms have been plotted as a function of the temperature. In a typical TGA profile of % polymer weight versus temperature, the polymer weight loss patterns have been investigated in two temperature ranges, from 20 °C to 200 °C and from 200 °C to 600 °C (as explained earlier in Section 3.3.6). The heating profiles of up to 200 °C would be indicative of polymer cross-linking patterns (as tested in DSC analysis) whereas the temperatures higher than that could show polymer degradation rates which would be ideal to study their thermal robustness. Figure 3.27 shows the TGA profile of MW MIPs polymerised at 60 °C for 15 minutes by varying MW powers.

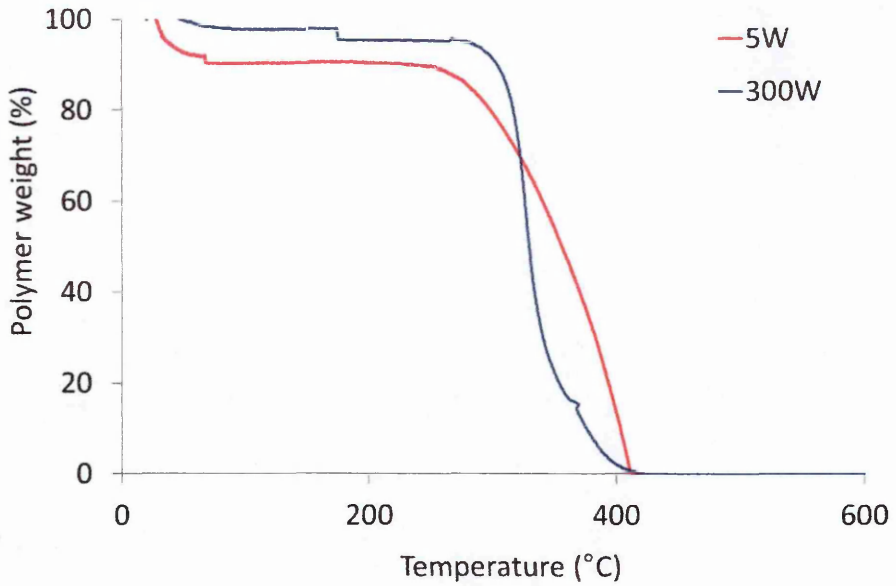

Figure 3.27: Thermogravimetric profiles (expressed as % polymer weight against heating temperature) of MW MIPs polymerised with 5W (red) and 300W (blue) MW powers.

The MIP polymerised with slower heating (at 5 W) showed about slight weight loss (10 %) when heated from 20 °C to 200 °C (seen in red in Figure 3.27), whereas the MIP polymerised with faster heating (at 300 W) showed a slightly less (5 %) weight loss in the similar temperature range (seen in blue in Figure 3.27). According to the initial hypothesis, the MIP showing higher weight loss in this temperature region should be more cross-linked. To test this hypothesis, TGA thermogram was correlated to the DSC analysis where the MIPs were heated at the same rate (10 °C minute^{-1}) and in a similar temperature range (0 °C to 200 °C). According to the DSC analysis, the MW MIP polymerised with slower heating (5 W) exhibited higher cross-linking degree (as seen in Figure 3.19) which showed higher polymer weight loss in TGA thermogram too (as seen in Figure 3.27). This suggested that more polymer weight loss could be an indicative of higher cross-linking degree. The MIP polymerised with faster heating (300 W) showed less weight loss in TGA and also showed lower cross-linking degree in DSC analysis. This meant that both the TGA and DSC thermograms were in agreement with each other that the MIP produced with faster heating exhibited lower cross-linking degree and their flexible matrix also showed less weight loss when heated in TGA (from 20 °C to 200 °C).

Upon being heated further from 200 °C to 600 °C in TGA analysis, both the MIPs completely degraded by 400 °C (as seen in Figure 3.27) which suggested that the MIPs showed similar thermal stability. Importantly, the rates of degradation of both the MIPs were distinguishable between 300 °C to 400 °C. The MIP with higher cross-linking (polymerised with 5 W) degraded slowly compared as compared to the MIP with lower cross-linking (polymerised with 300 W). This suggested that different cross-linking degrees did not necessary affect the thermal

stability of the MIPs; however it did influence the rate of polymer degradation. The MIP with higher cross-linking degree degraded faster in comparison to the one with lower cross-linking, as postulated in the proposed hypothesis. In general, different MW powers affected the polymerisation rates and cross-linking degree but showed little effect on their thermal stability or robustness.

To understand the effect of polymerisation time on polymer cross-linking and robustness, TGA analysis was carried out in a similar way. Figure 3.28 shows the TGA profile of the MW MIPs polymerised at 60 °C with 5 W MW power for different lengths of time.

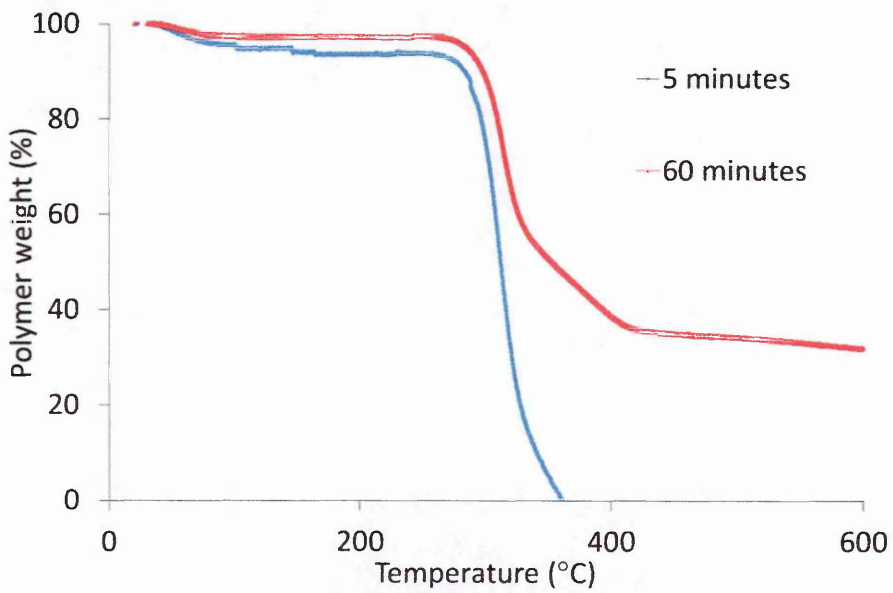

Figure 3.28: Thermogravimetric profiles (expressed as % polymers weight against heating temperature) of MW MIPs polymerised for 5 minutes (blue) and 60 minutes (red).

When MW MIPs polymerised for different lengths of time were subjected to the TGA analysis, the MIP polymerised for 5 minutes showed a little weight loss (8 %) in comparison to the MIP polymerised for 60 minutes which showed negligible weight loss (as seen in Figure 3.28). From the DSC analysis of these MW MIPs, it was found that MW polymerisation times from 5 minutes to 60 minutes produced MIPs with similar cross-linking degree; with shorter polymerisation times showing a little higher cross-linking (as seen in Figure 3.20). When the MIPs were heated above 200 °C, TGA analysis showed that the MW MIP polymerised for 5 minutes degraded completely by 360 °C. On the other hand, the MIP polymerised for 60 minutes showed higher thermal stability as it showed only 60 % weight loss up to 600 °C. This suggested that the longer polymerisation time (60 minutes) produced MIP with higher thermal robustness although the cross-linking degree was much similar for any length of

polymerisation. This supported the hypothesis that the MIPs with higher cross-linking degree would degrade at comparatively lower temperatures than the MIPs with lower cross-linking.

To test the hypothesis on the third paramater, MW MIPs were prepared by varying polymerisation temperature. MW polymerisation was carried out with 5W for 5 minutes at different temperatures from 60 °C to 90 °C. Figure 3.29 shows the TGA thermogram of the prepared MW MIPs.

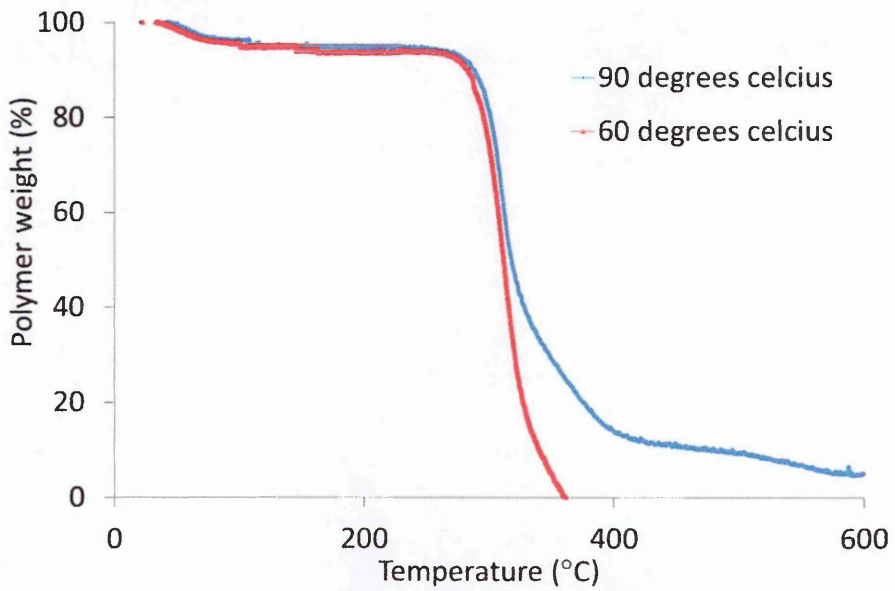

Figure 3.29: Thermogravimetric profiles (expressed as % polymers weight against heating temperature) of MW MIPs polymerised at 60 °C (red) and at 90 °C (blue).

MW MIPs prepared at different temperatures (60 °C and 90 °C) showed much similar thermogravimetric profile when heated up to 200 °C (as seen in Figure 3.30). These MIPs exhibited much similar cross-linking degree which was in agreement with their DSC thermograms (as seen in Figure 3.21). When heated up to 600 °C, the MW MIP polymerised at 90 °C showed higher thermal robustness compared to the MIP polymerised at 60 °C (as seen in Figure 3.30). This suggested that although different polymerisation temperatures of MW MIPs did not necessarily affect their cross-linking degree; higher polymerisation temperature (90 °C) produced slightly more thermally robust MIPs. These observations suggested that TGA could be a useful technique in investigating the thermal stability of cross-linked polymers in addition to DSC.

Some useful observations were drawn from the TGA analysis of the MW MIPs and from its correlation to their DSC analysis performed earlier. TGA and DSC analysis showed similar thermal profiles of MIPs when heated at similar rates in similar temperature range. The results obtained were in agreement with the hypothesis that MIPs with higher cross-linking degree in

DSC showed higher weight loss up to 200 °C due to quicker degradation of cross-linking bonds. On the other hand, the MIPs with lower cross-linking degree showed little weight change up to 200 °C which agreed with the proposed hypothesis that their flexible cross-linking bonds caused their rotation when heated rather than degrade straight away; this made these polymers survive higher temperatures. TGA analysis also suggsted that the cross-linking degree did not necessarily affect the robustness of the MW MIPs. The thermal stability was rather influenced by experimental parameters. Longer MW polymerisations carried out at higher temperatures produced more thermally robust polymers and robustness of the MW MIPs decreased by increasing their heating rates (MW powers used).

To investigate this across other MIP series, the control set of oven MIPs were also analysed to obtain their thermogravimetric profiles. Figure 3.30 shows the TGA analysis of oven MIPs polymerised at 60 °C for different durations (4 hours and 24 hours).

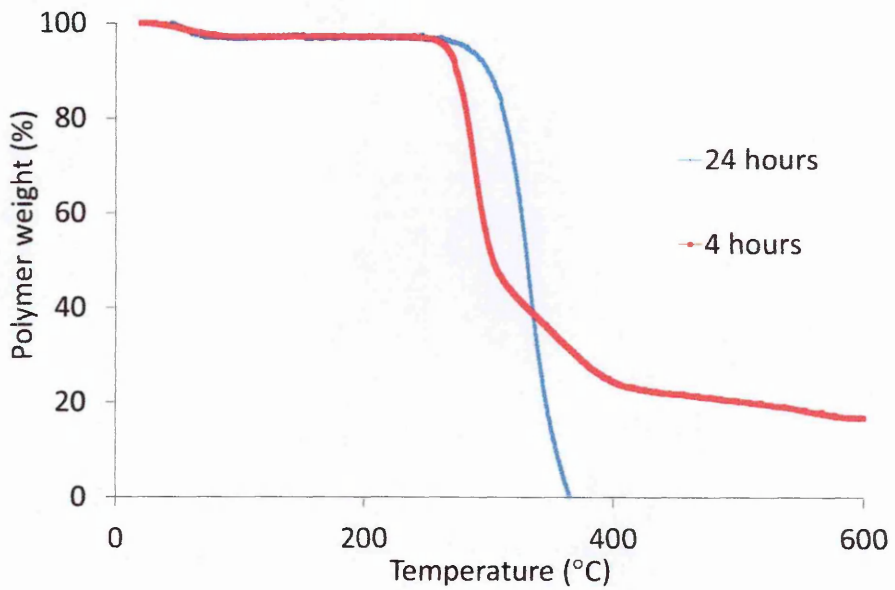

Figure 3.30: Thermogravimetric profiles (expressed as % polymers weight against heating temperature) of oven MIPs polymerised for 4 hours (red) and at 24 hours (blue).

Oven MIPs polymerised for 4 hours and 24 hours both showed a little weight loss during their TGA analysis when heated up to 200 °C (as seen in Figure 3.30). However, when heated further up to 600 °C, the MIP polymerised for 4 hours showed higher thermal stability as it degraded slowly and 20 % of the polymer did not degrade at all. On the other hand, the oven MIP polymerised for 24 hours showed faster degradation and lost total polymer weight below 400 °C (as seen in Figure 3.30). Both the TGA and DSC analysis suggested that although different polymerisation times did not show considerable differences in the cross-linking of MIPs,

shorter durations produced more thermally robust polymers. On the other hand, longer polymerisation times (widely used 24 hours) resulted into MIPs with lower thermal stability.

Figure 3.31 shows TGA profile of the the oven MIPs polymerised for 8 hours at 60 °C and 90 °C.

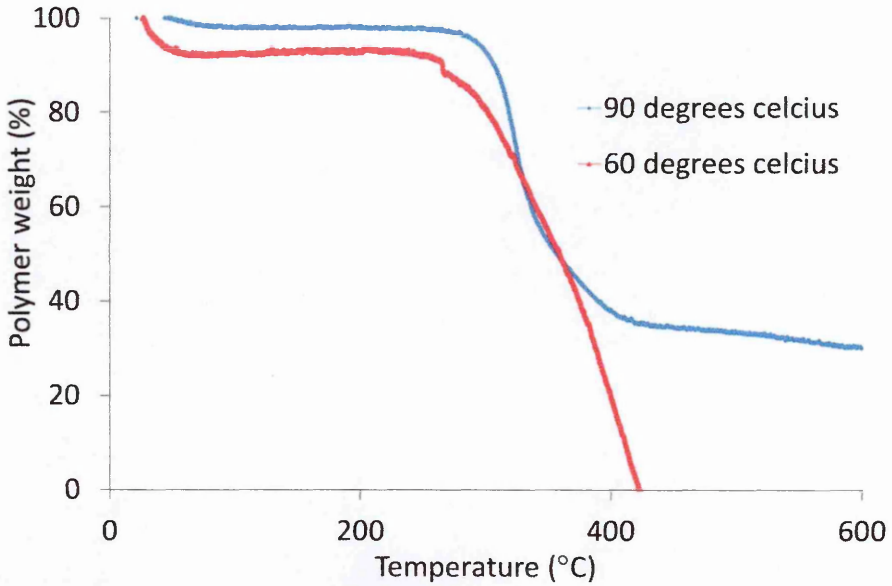

Figure 3.31: Thermogravimetric profiles (expressed as % polymers weight against heating temperature) of oven MIPs polymerised at 60 °C (red) and 90 °C (blue).

When the oven MIPs were heated up to 200 °C, the MIP polymerised at 60 °C showed slightly more weight loss compared to the MIPs polymerised at 90 °C. It could be suggested that the lower polymerisation temperatures produced higher cross-linking in oven MIPs. To test the hypothesis, DSC results were in agreement with the observed trend reaffirmed that the cross-linking degree of the MIPs decreased when their polymerisation temperature was increased from 60 °C to 90 °C (as seen in Figure 3.23).

When heated further, the oven MIP polymerised at 60 °C, degraded completely by 430 °C. On the other hand, the MIP polymerised at 90 °C lost only 60 % of its total weight even at 600 °C. Both the TGA and DSC analysis suggested that increase in polymerisation temperature decreased polymer cross-linking; it also increased the thermal stability. This was in agreement with the proposed hypothesis that thermal stability could be linked to the cross-linking degree of the MIPs where highly crosslinked MIPs would be less thermally stable and vice versa. It was also observed that the shorter oven polymerisations carried at higher temperatures produced MIPs with higher thermal stability similar to the trend observed with MW MIPs.

Control polymers prepared by UV irradiation were subjected to the TGA analysis too. Figure 3.32 shows the TGA analysis of UV MIPs polymerised at 20 °C for 4 hours and 24 hours.

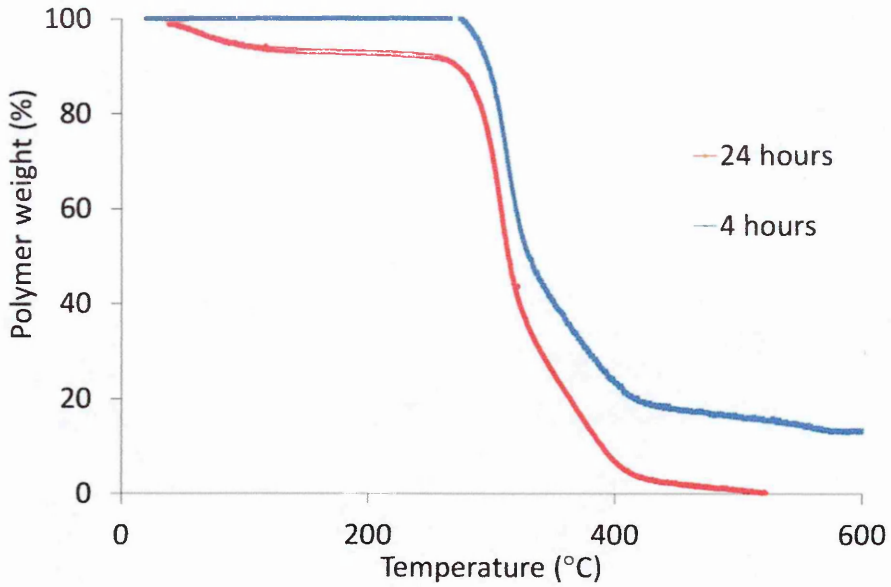

Figure 3.32: Thermogravimetric profiles of UV MIPs expressed as as % polymers weight against heating temperature of UV MIPs polymerised for 4 hours (blue) and 24 hours (red).

In the TGA analysis for up to 200 °C, shorter UV polymerisations (4 hours) produced MIP with slightly more weight loss (10 %) compared to longer polymerisations (24 hours). The higher rigidity observed with longer polymerisation times was in agreement with the findings obtained from TGA analysis of MW MIPs (as seen in Figure 3.28). Some more UV MIPs prepared for 8 hours at variable polymerisation temperatures were also studied by TGA, as seen in Figure 3.33.

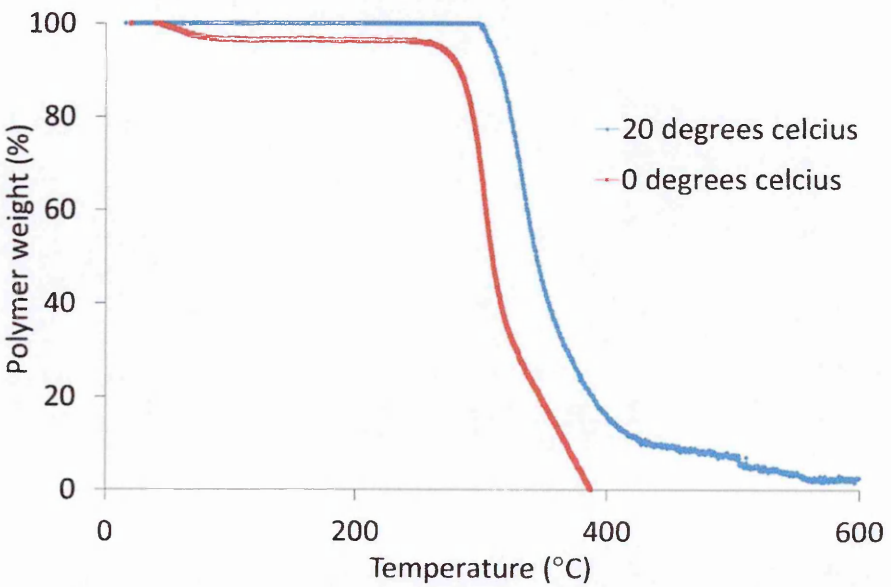

Figure 3.33: Thermogravimetric profiles (expressed as % polymers weight against heating temperature) of UV MIPs polymerised for 0 °C (red) and 20 °C (blue).

The UV MIP polymerised at different temperatures showed little or no weight loss upon being heated up to 200 °C. When heated further, the UV MIP prepared at 20 °C showed more robustness (as seen in Figure 3.33). This was in agreement with other TGA analysis of MW MIPs and oven MIPs where higher polymerisation temperatures seemed to improve the thermal robustness of the MIPs (as seen in Figure 3.29 and Figure 3.31).

There were striking similarities in themograms obtained from DSC and TGA for the MIPs polymerised by different methods under study. The MIPs showing higher cross-links in DSC showed higher weight loss for the temperatures of up to 200 °C in TGA analysis. In other words, highly cross-linked MIPs degraded at a faster rate due to restrictions on their bond rotations as postulated. On the other hand, MIPs with lower cross-linking degree showed little weight loss up to 200 °C, this was in agreement with the proposed hypothesis that polymer with lower cross-linking degree could undergo bond rotations rather than bond breakage.

No direct correlation was observed between the cross-linking degree and thermal stability or robustness of the MIPs. However, thermal stability was strongly influenced by the experimental parameters such as the temperature and the length of polymerisation. In general, longer polymerisations carried out at higher temperatures seemed to produce highly robust MIPs. This finding was supported by earlier study according to which longer polymerisations would be expected to produce highly rigid polymers. This might be because during longer polymerisations, the less active and slow moving midchain radicals could get activated too. This could combine with highly active propogating radicals form extensive cross-linking and could result into higher polymer rigidity (4). However, the presented study also found that extended longer polymerisation time (24 hours in oven polymerisation) rather decreased the thermal rigidity of the resulting polymer. This might be explained by some earlier studies which suggested that when the thermal polymerisation duration was extended, parallel depolymerisation might occur at a minute level which could break some of the cross-links in terminal polymer chains and might affect the thermal stability of the resulting polymer (4, 53). This was also in agreement with another finding that unlike thermal oven polymerisations, longer UV polymerisations were not detrimental to the thermal stability of the resulting polymers. In general, MW polymerisation produced MIPs with comparable rigidity as the oven and UV MIPs. Also longer polymerisations carried out at higher temperatures produced MIPs with improved thermal rigidity.

It was found that gravimetric analysis of the polymers could be very important in understanding the robustness of the polymers (as explained in Section 3.3.6). The performance of the MIPs under study was in agreement with the previous studies that reported similar

gravimetric thermogram of the MIP monoliths (34, 48, 52). Since most of the prepared MIPs were found to be stable for up to 300 °C, they showed comparable thermal stability as already reported by MIP related studies (37).

In addition to the degree of cross-linking and robustness of the cross-linked polymers, it would be important to study the available surface area and the characteristics of the pores formed within the polymer matrix. This might be because the available surface area could eventually affect the template rebinding and thereby the template recognition peroformance of the MIPs. To understand this more in detail, the polymer samples were subjected to the porosimetry analysis to determine surface area, pore volume and the pore size. Section 3.4.4 will discuss some aspects related to porosimetry analysis of the polymers.

3.4.4. Porosity Characteristics

Porosimetry analysis is a routinely used technique for characterising cross-linked porous polymers. In this study, it would be crucial to understand how the changes in the experimental parameters of the polymerisation affected the surface area and other porous characters. Surface area of the MIPs is of great interest since it is deemed to directly affect the template recognition performance of the polymer. In addition to the surface area, the size and volume of the pores could also give useful insight into the polymerisation mechanisms at the molecular level. Such analysis could be very useful in optimising polymerisation conditions although study of surface area and pore volumes are often ignored in MIP related research. Here, a preliminary study of porosity related characters of MW MIPs polymerised in different conditions has been carried out. Results have been correlated with those polymerised thermally by oven. The porosimetry experiments have been carried out offsite in the Piletsky Laboratory at the University of Leicester (UK) as described in the methods Section 3.3.7.

Porosimetry analysis is routinely carried out to study the average surface area and other porosity characters of a porous material where known volume of inert gas (such as, nitrogen or argon) is adsorbed onto it. In the presented study, porosimetry has been used to study the physical properties (such as, surface area, total pore volume and pore diameter) of the prepared polymer samples. Porosimeter and surface area analyser Nova 1000e (Quantachrome, UK) was used for this analysis.

Figure 3.34 shows the surface area of different MW MIPs polymerised at 60 °C for 15 minutes by varying MW powers (heating rates).

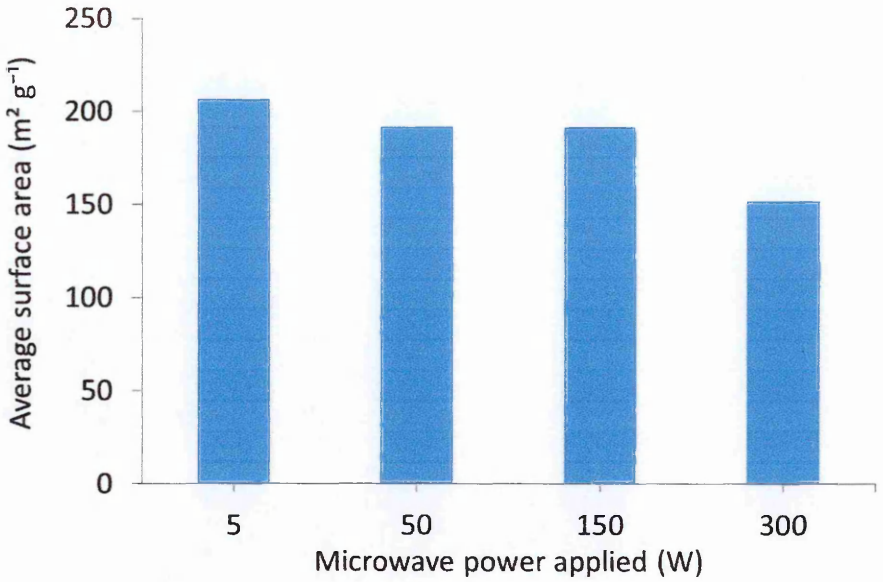

Figure 3.34: Comparison of the average surface area of MW MIPs polymerised with different MW powers.

The surface area of the MW MIPs decreased as their polymerisation rate (MW power) was increased from 5 W to 300W. The lowest rate of polymerisation (5 W) produced the highest surface area of about 206 $m^2 g^{-1}$ which dropped subsequently by 55 units when the MW power was increased from 5 W to 300 W (as seen in Figure 3.34).

There were two striking outcomes from the surface area analysis of the MW MIPs polymerised with different heating rates. First of all, the surface area was inversely related to the heating rate of the MW reactor. Another observation was that MIPs showed higher surface area than the NIPs. To understand this better, these results were correlated to the ones obtained from DSC analysis of these MW MIPs. The correlation suggested that slower MW heating seemed to produce MIPs with higher cross-linking degree and larger surface area (as seen in Figure 3.19 and Figure 3.34). Some earlier studies also reported similar observations and hypothesised that when the degree of cross-linking was higher, the porogen would not be able to intrude enough in the growing polymer matrix which might result in lower porosity. This meant that the total available area would be less occupied by the pores and more available for the binding of the target analyte (2, 4).

Looking into the second finding, the MIPs showed higher surface area (about 151 $m^2 g^{-1}$ to 206 $m^2 g^{-1}$) in comparison to the NIPs (about 121 $m^2 g^{-1}$ to 191 $m^2 g^{-1}$). This was supported by another study which suggested that an increase in the surface area of the MIPs was indicative of the presence of the template rebinding cavities on the surface of the MIPs (27). Larger surface area available in MIPs compared to NIPs assured of presence of surface laden cavities

which might result into improved template recognition performance of the MIPs. There have been no reports in literature on what could lead to this distinguishable behaviour between the MIPs and the NIPs. However, the formation of stable template-monomer assemblies in the pre-polymerisation mixture could be decisive in resulting surface laden template binding cavities in MIPs rather than in NIPs. This might be because once the template-monomer assemblies formed in MIPs formation, further cross-linking could only occur between the monomers and cross-linkers in one direction, that is something which might leave the templates facing outward and polymer formation inward. NIPs on the other hand would have no presence of template which might result into polymer cross-linking more randomly in all directions between the monomers and cross-linkers. However, this hypothesis would need more investigation to support this hypothesis in future studies.

In addition to the surface area, total pore volume and the pore radii of these polymers were also measured as shown in Figure 3.35.

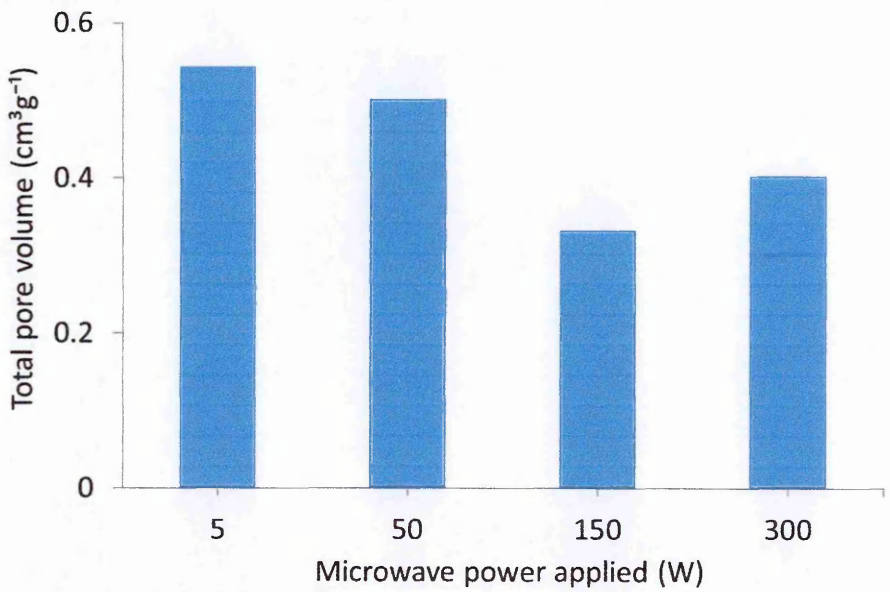

Figure 3.35: Comparison of the total pore volume of MW MIPs polymerised with different MW powers.

The pore volumes of MW MIPs were found to vary depending on the heating rates (MW powers) with which they were polymerised. Total pore volume of the MW MIPs decreased slightly from 0.54 $cm^3 g^{-1}$ to 0.4 $cm^3 g^{-1}$ when the MW power was increased from 5 W to 300 W. This suggested that slower heating rates (lower MW powers) produced MIPs with larger pore volumes. No such sudy has been reported investigating such behaviour of MW heating parameters in the context of morphology of the resulting MW MIPs. But this behaviour could be understood by studying the polymerisation kinetics.

In a traditional heating, the polymerisation kinetics would be very slow. Hence, porogen would get to intrude more and deeper between the growing polymeric chains before extensive cross-links could be formed. As a result, they might show higher pore volumes. In this study, MW polymerisations carried out with slower heating produced MIPs with higher degree of cross-linking and higher pore volumes too. From this, a hypothesis could be proposed that unlike inconsistent oven heating, the constant pulsatile MW heating might enforce the porogen to enter the growing nuclei repeatedly in spite of having sufficient cross-linking. More porogen intrusion facilitated by slower polymerisation rates could then result into higher pore volumes at the same time having higher degree of cross-linking. The results suggested that it might be benificial to use slower MW heating (lower MW powers of up to 50 W) to produce polymers with larger surface area, higher porosity and higher cross-linking all at the same time.

These MW MIPs were also analysed for their average pore sizes. Figure 3.36 shows the comparison of the average pore radii of MW MIPs polymerised by varying MW powers.

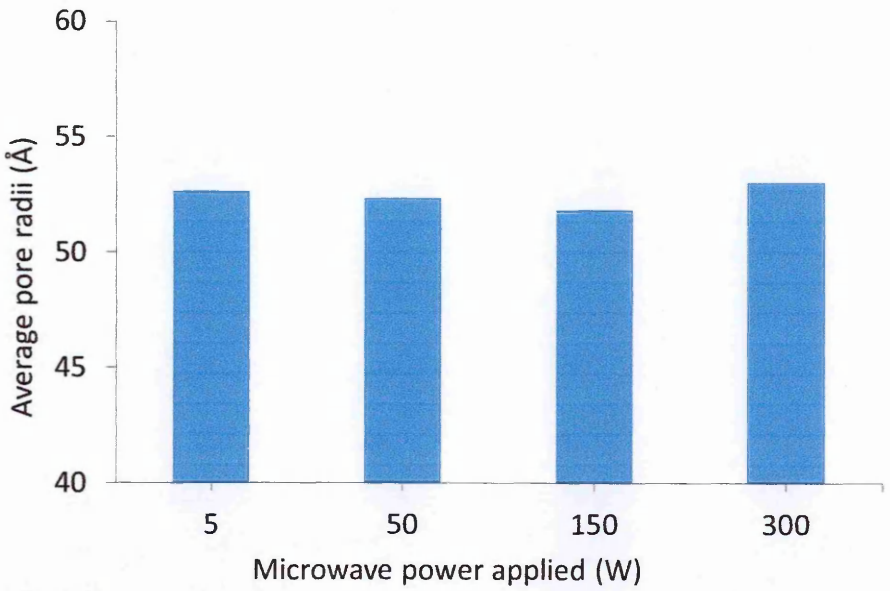

Figure 3.36: Comparison of the average pore radii of MW MIPs polymerised with different MW powers.

The average pore radii of the MW MIPs was found to be much similar (51 Å - 53 Å) throughout the range of MW power (from 5 W to 300 W) used for their polymerisation. In all cases, the radii of the pores did not vary considerably. In other way, much similar radii of the pores also ensured that all the pores created were by the removal of the template which could indicate high selectivity of the polymer towards the template during template rebinding studies. Having similar sized pores in all the MIPs with different surface area and different pore volumes also suggested that the depth and the number of the pores could vary in order to compensate for

the available surface and volume of the polymer matrix. This could be highly dependent on the rate of heating, intrusion pattern of porogen and the degree of cross-linking of the polymer. To understand this further, the porosimetry results were correlated to the DSC results of the same MW MIPs. The correlation suggested that these experimental parameters could indeed greatly affect the cross-linking degree of the polymer as well as the number, size, volume and spatial distribution of pores formed within its matrix.

The correlation of DSC and porosimetry results suggested that in addition to having larger surface area and larger pore volumes, the MW MIPs polymerised with slower heating (lower MW power) showed higher degree of cross-linking too (as discussed in Section 3.4.2). When the polymers were highly cross-linked (during slow heating), pulsatile MW heating could help porogen intrude deeper into the polymer matrix. And the gelation of such polymers would be also delayed due to slower rate of heating. At the same time, higher cross-linking degree in this polymer would most likely result into fewer deeper porogen intrusion in compensating for the limited space due to higher degree of cross-linking and longer available intrusion times. As a result of this, a smaller number of deeper pores could be formed to gain larger pore volume at the same time having larger surface area and higher cross-linking degree. In this way, slower heating with its delayed gelation could end up intruding porogen deeper and might result into smaller number of deeper pores with similar radii within polymer matrix.

On the other hand, faster heating rates produced polymers with lower cross-linking degree (as discussed in Section 3.4.2). This suggested that the porogen had greater area to intrude into the polymer matrix. However, their pore radii were much similar in size. So, faster heating with its quicker gelation could end up intruding porogen to a lesser depth which might result into higher number of shallow pores of the same radii within the polymer matrix. However, this hypothesis would need to be studied in detail with different polymer sets. It has been noted that it has opened up entire new domain to study controlled heating of MW reactors and its predictable effect on the physical properties of the resulting polymers. It might be very useful in optimising polymerisation method with predictable physical properties which has been very challenging with the traditional polymerisation methods.

Along with controlled MW heating rates, it was the time to assess the effect of the length of MW polymerisation on the surface area of resulting MIPs. MIPs prepared with 5 W at 60 °C for different polymerisation time durations were analysed for their surface area, as presented in Figure 3.37.

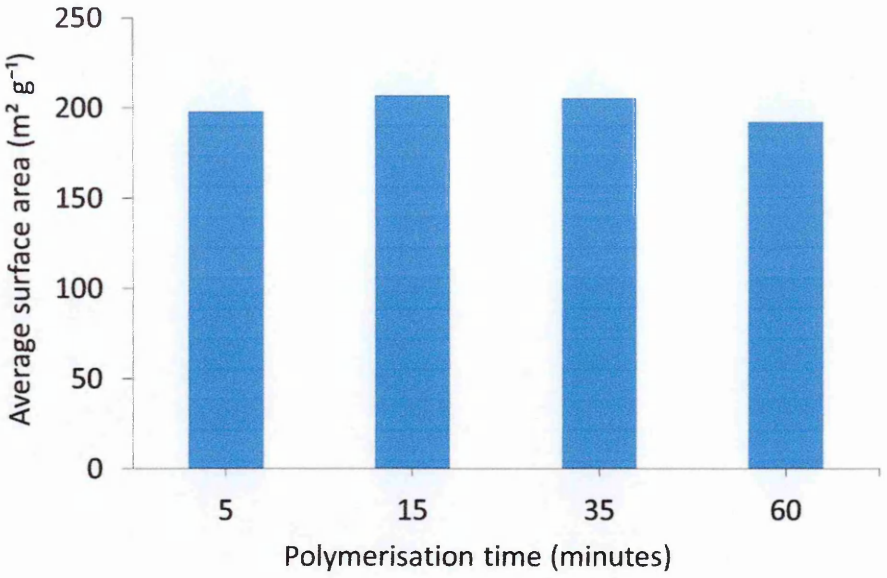

Figure 3.37: Comparison of the average suraface area of the MW MIPs polymerised for different times.

When the MW MIPs were polymerised for different times, their surface area remained consistent between 190 $m^2 g^{-1}$ to 200 $m^2 g^{-1}$ (as seen in Figure 3.37). One observation was drawn from these results was that once the polymer matrix was formed, any extended polymerisation time showed little effect on its surface area. By correlating these observations to the DSC analysis, it was found that the degree of cross-linking of these MIPs hardly changed throught this lenth of time (as described in Section 3.4.2). From these two findings, it could be derived that once enough degree of cross-linking was formed, binding cavities remained intact within the polymer matrix. Hence the surface area remained quite consistent too. It would be important to note here that their heating rate was kept the same so its effect on the pore volume, size and spatial distribution of the pores would less likely to change. However, this would need to be supported by experimental evidence in future studies. A slight decrese in the surface area was observed for the longest polymerisation time (60 minutes). This could arise from the slight depolymerisation effect and slightly lowered degree of cross-linking (as discussed earlier in Sections ection 3.4.2) (5).

The polymerisation time was optmised to 5 minutes and more MW MIPs were polymerised with 5 W at different temperatures. The results obtained were plotted in Figure 3.38.

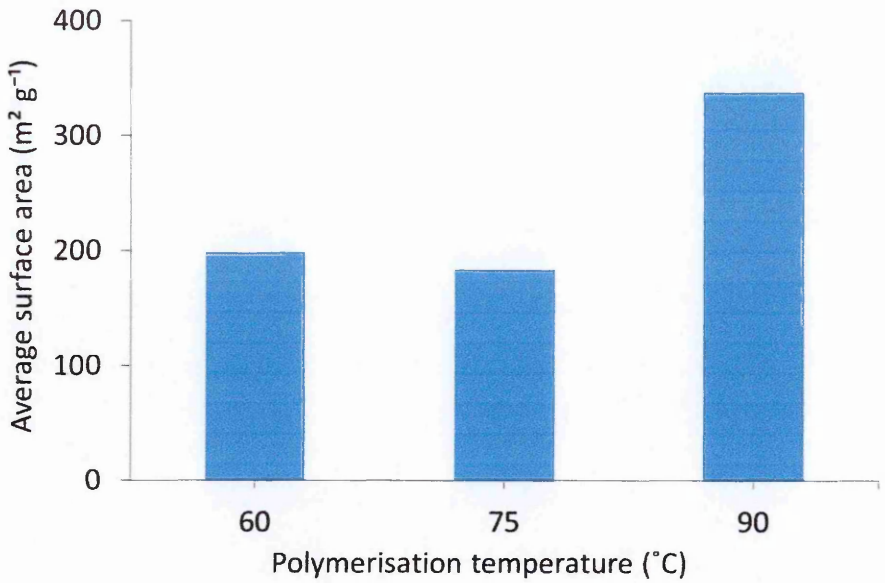

Figure 3.38: Comparison of the surface area of the MW MIPs polymerised at different temperatures.

The MW MIPs polymerised from 60 °C to 75 °C showed much similar surface area of about 200 $m^2 g^{-1}$; however the surface area increased considerably to 340 $m^2 g^{-1}$ when the polymerisation temperature was raised to 90 °C (as seen in Figure 3.38). To understand this further, the obtained results were correlated with that of DSC analysis. It was found that different polymerisation temperatures did not result into any considerable change in the cross-linking degree of the MW MIPs (as seen in Figure 3.23). So the increase in surface area at 90 °C polymerisation could most likely arise from its improved kinetics. From this, it could be hypothesised that elevated temperatures (90 °C) would generate more free radicals from the initiator breakdown; however the length and the rate of polymerisation would be controlled in a MW reactor as the power and the time were set to a fixed value. This meant that at a given time, the polymerisation being carried out at higher temperature would have denser populations of the radicals and would more likely form a compact polymer matrix which might help in improving surface areas. Given that no other studies have been reported earlier on this behaviour of MW polymerisation, it would be interesting to study the pore volume and pore radii of MW MIPs prepared at different temperatures and for different times. It would be helpful in understanding the effect of temperature on pore formation mechanisms of a free radical polymerisation.

The control set of thermal oven MIPs polymerised by varying temperature and time were also analysed for their surface area as summarised in Table 3.12.

Table 3.12: Summary of the comparison of the surface area of the MIPs polymerised thermally by oven at different temperatures and for different lengths of time

Mode of polymerisation	Polymerisation time (hours)	Polymeriastion temperature (°C)	Surface area ($m^2 g^{-1}$)
Oven	24	60	227.62
Oven	8	60	255.73
Oven	8	90	387.74

Surface area of the oven MIPs decreased from 255.73 $m^2 g^{-1}$ to 227.62 $m^2 g^{-1}$ as the polymerisation time was increased from 8 hours to 24 hours, whereas increase in the polymerisation temperature from 60 °C to 90 °C increased the surface area of the oven MIPs from 255.73 $m^2 g^{-1}$ to 387.74 $m^2 g^{-1}$ (as seen in Table 3.12).

Interestingly, the trend observed in the surface area of the oven MIPs was not similar to that of MW MIPs. In MW polymerisations, an increase in the length of the polymerisation did not affect the surface area of the MIPs (see Figure 3.37 and Table 3.12). This suggested that comparatively shorter polymerisation time of up to 60 minutes in a MW reactor did not show any detrimental effect on the surface area of the MIPs, whereas extended polymerisation time of up to 24 hours in an oven reduced the surface area of the MIPs considerably. This reduced surface area could be detrimental to the template binding performance of the MIPs. Hence, the polymerisation time should be carefully optimised whilst preparing MIPs by traditional methods using oven or oil-bath.

Looking into the effect of polymerisation temperature on the surface area of oven MIPs, it was found that the increase in temperature increased the surface area of the MIPs. This trend was similar to that of MW MIPs in the similar polymerisation temperature range (from 60 °C to 90 °C). This increase in surface area at elevated temperatures could arise from improved thermokinetics at elevated polymerisation temperatures, as observed in case of MW MIPs. This however would need further investigation. It was interesting to note that when thermal polymerisations were carried out at similar temperatures, 5 minutes MW polymerisation could produce MIPs with much comparable surface areas to that of oven MIPs which polymerised for 8 hours (see Table 3.12 and Figure 3.37).

The effect of a wider range of temperatures on the surface area of the MW MIPs would be an interesting study to understand whether MW heating continued to generate MIPs with much similar surface area to that of oven heated polymerisations. This could be of a particular

interest in investigating whether thermolabile templates could be imprinted at comparatively lower temperatures using a MW reactor with comparable surface areas to that oven or oil-bath heating. Currently, thermolabile templates and monomers are polymerised faster by UV polymerisation but at the same time it fails to produce the MIPs with the surface area as high as thermal polymerisations (2). Since MW reactors could generate higher surface areas in MIPs with faster polymerisation, it would be worth investigating it further for polymerising materials also at lower temperatures.

Polymer samples were also studied by scanning electron microscopy (SEM) to analyse their morphological characteristics. Section 3.4.5 discusses the results obtained by SEM analysis of the MIPs.

3.4.5. Scanning electron microscopy

MIP monoliths polymerised by different methods were viewed under SEM. Figure 3.39 is a representative electron micrograph of the MIP monoliths.

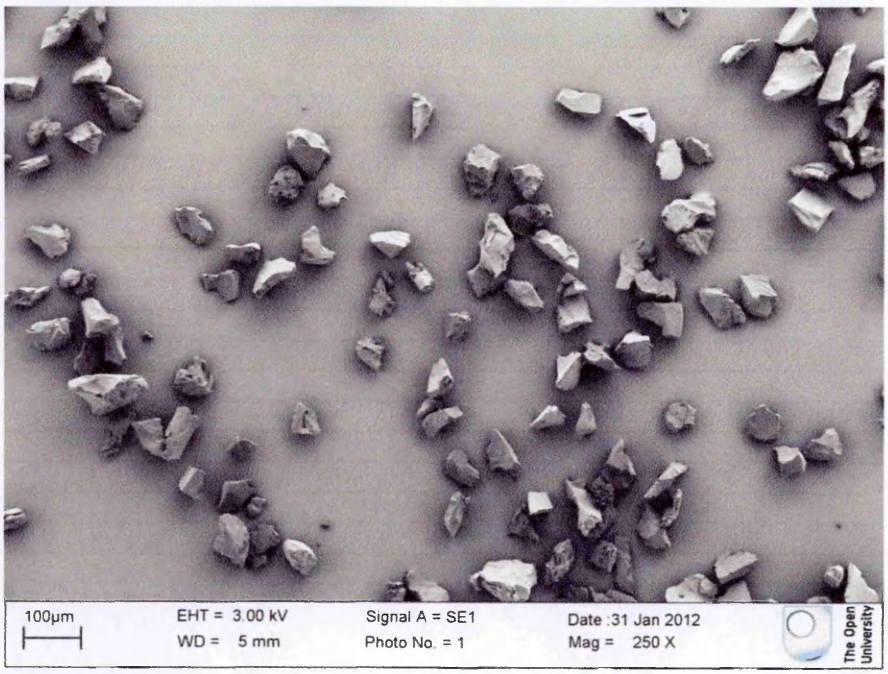

Figure 3.39: A representative scanning electron micrograph of the MIPs monoliths (250 x magnifications).

MIP monoliths polymerised in different experimental conditions were found to be irregular in shape, rough in texture and in the particle size range of 45 µm to 63 µm (as seen in Figure 3.40). The desired particle size was achieved as the monolith particles were passed through the sieves of appropriate aperture size once triturated in a mortar and pestle. Figure 3.40 shows the morphology of MIPs at higher magnification.

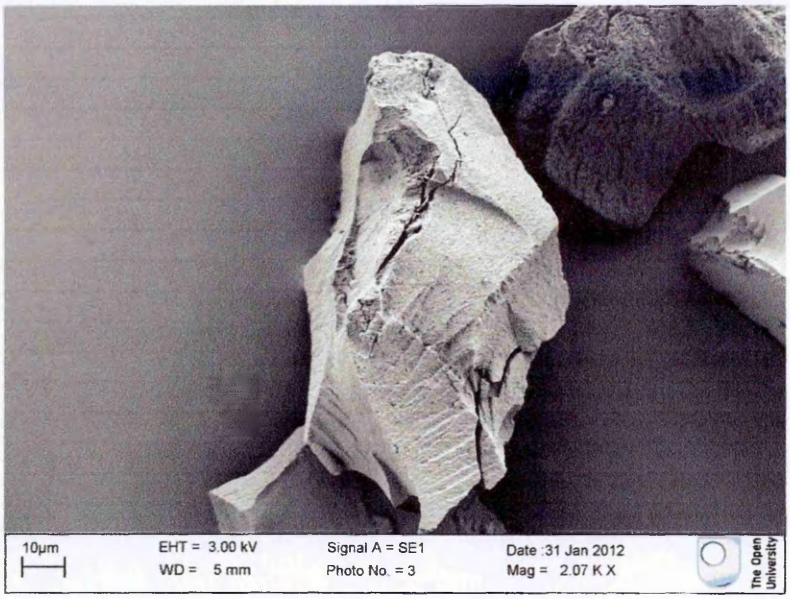

Figure 3.40: A representative scanning electron micrograph of the MIPs monoliths (2000 X magnification).

Figure 3.40 is a magnified image of the MIP monoliths which confirmed its rough texture and irregular shape. The rough texture observed was indicative of the porous character of the polymers, as expected. The size of the pores and their distribution were found to be consistent throughout the particle surface when viewed at this magnification under SEM. In general, the morphology characteristics of the polymers prepared by oven, MW or UV were consistent in SEM analysis.

This brings to the end of physical analysis of the polymers which includes the study of degree of cross-linking, robustness, surface area and morphological characteristics of the obtained MIPs. The next phase of analysis would involve studying template recognition performance of these polymers. To carry out the analysis, the polymers were used as MIP-SPE stationary phases and the templates were introduced to them followed by the quantification of the unbound template (caffeine) by HPLC (as explained earlier in Section 3.3.9). Section 3.4.6 presents the results obtained from the template rebinding analysis.

3.4.6. Template Rebinding Studies

Having analysed the polymers for their physical properties, it was important to test whether the differences observed in their physical characteristics translated into to their template recognition performance. To do so, different caffeine rebinding solutions (0.1 mM to 2 mM) were introduced to the MIP-SPE. The amount of caffeine bound to the MIP was then calculated from HPLC results and plotted against the total amount of caffeine introduced to the polymers in SPE.

Solid phase extraction (SPE) works on the principle of solid-liquid extraction where the adsorbent (stationary phase) is packed in polypropylene cartridges between frits and the sample matrix (mobile phase) is passed through the cartridge with the aid of vacuum or positive pressure. It is a well-established analytical technique for the pre-treatment of the complex mixture of various samples due to its ease of operation, flexibility and simplicity. When MIPs are packed into the SPE cartridges as stationary phases, it is also referred to as MIP-SPE. Figure 3.41 shows the schematic describing the steps involved in a typical SPE analysis and explains the method used for the SPE based analysis in the presented study.

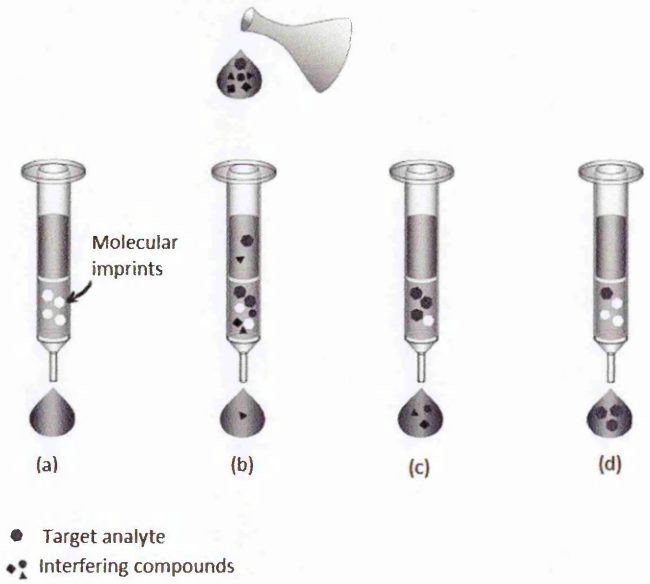

Figure 3.41: Schematic of the operational steps involved in an SPE analysis; (a) conditioning of stationary phase packed into the cartridge, (c) percolation of the template(s) sample through conditioned stationary phase, (c) washing step for the removal of interfering analytes and (d) elution of the target template.

Conditioning: This step is performed by passing a solvent through the cartridge to condition the stationary phase (MIP in this study) packed into them.

Template rebinding / percolation: In a normal phase MIP-SPE protocol, a known amount of the template is introduced to the cartridge once it is conditioned. The template samples are prepared in the same solvent as that used for conditioning. This maximises specific molecular interactions without interfering in the template-MIP binding. The template (due to specific recognition by the MIP) is usually retained whereas other substances (if a mixture of compounds is used) are washed through.

Washing / removal of interfering components from the MIP: This step is aimed at removing any interfering compounds other than the template when a mixture of compounds is

introduced to the MIP-SPE. This step was omitted from the SPE protocol used in the study since the rebinding solution only contained caffeine (template) and not a mixture of compounds.

Elution: It is achieved by passing polar organic solvents through the MIP-SPE that would interfere with the non-covalent bonds between the template and the MIP. The template released from the MIP-SPE is then collected and is subjected to further quantification by chromatographic techniques (mainly, liquid chromatography) (51). In the presented study, caffeine was the only component in the rebinding solution. Therefore, this step was omitted from the protocol. The known amount of caffeine was passed through the MIP-SPE cartridge and the unbound caffeine (collected at the bottom) was subjected to HPLC analysis for further quantification. The amount of caffeine bound selectively to the MIP was calculated by subtracting the amount of template that did not bind to the MIP (or quantified by HPLC) from the total amount of the template that was initially introduced to the MIP-SPE.

The first set of MW polymers were prepared at 60 °C for 15 minutes with different heating rates by means of varying MW powers. The template rebinding performances were measured and analysed as plotted in Figure 3.42.

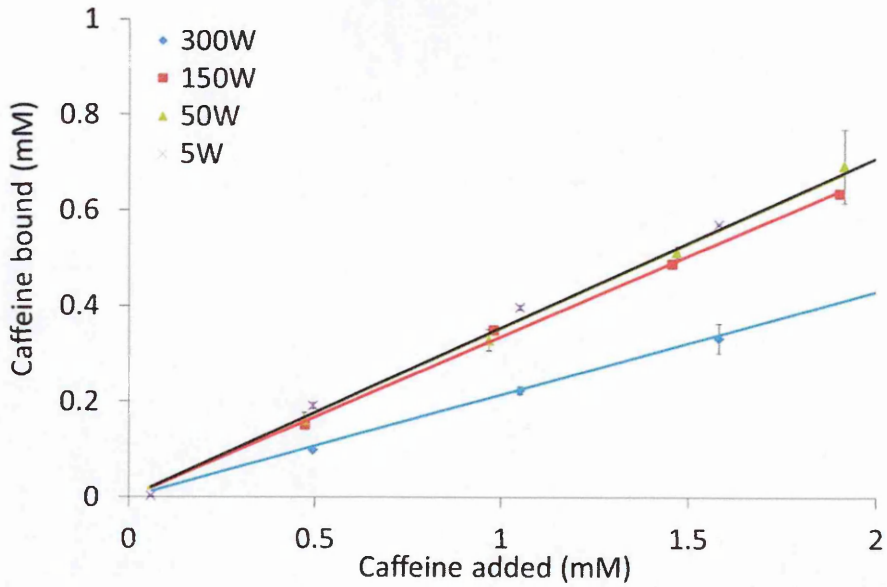

Figure 3.42: Comparison of caffeine rebinding performance of the MW MIPs polymerised with different MW powers; represented by different colours (5 W-black, 50 W-green, 150 W-red and 300 W-blue). standard deviations were derived from the triplicate measurements of each sample.

Caffeine rebinding performance of the MW MIPs was found to be dependent on the MW power used for its preparation. The slower heating (lower MW powers from 5 W to 150 W)

produced MIPs with improved caffeine binding than that of faster heating (higher MW power, 300 W) (as seen in Figure 3.42). Similar caffeine binding measurements were carried out on the parallel set of the NIPs and the imprinting factors (IF) were derived as a ratio of ($Bound_{MIP}$/ $Bound_{NIP}$) as explained earlier in Section 3.3.10. It would be important to note, higher values of IF would be regarded as an indicative of the non-selective template binding of the NIPs than improved imprinting efficiency of the MIPs (27). IF versus concentration of the caffeine solutions were then plotted as shown in Figure 3.43.

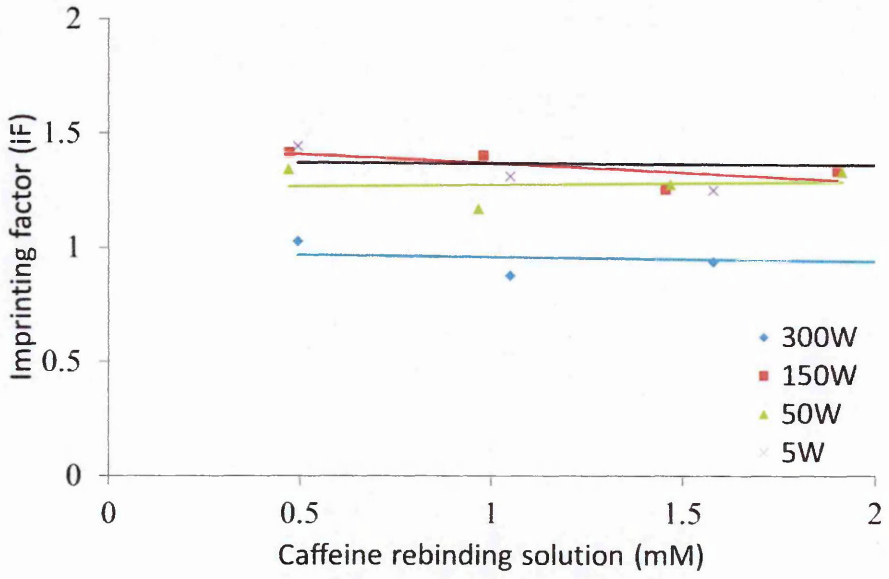

Figure 3.43: Imprinting factors of the MW polymers polymerised with different MW powers; represented by different colours (5 W-black, 50 W-green, 150 W-red and 300 W-blue).

Polymerisations carried out with slower heating (with 5 W to 150 W) produced MIPs with higher IF value of about 1.5, whereas the faster heating rates produced polymers with slightly lower IF values about 1 (as seen in Figure 3.43). In other words, imprinting effect decreased when the polymerisations were carried out with faster heating rates. In general, the highest IF value observed was lower than that reported earlier for similar MW MIPs (27). It was also found that the IF values were quite consistent for all the polymers throughout the concentration range of caffeine explored (0.1 mM to 2 mM). This indicated the presence of equivalent of both the selective and non-selective binding sites present within the MIPs. Rebinding of further lower template concentrations could be useful in preparing Scatchard plot for better understanding of the selectivity of the binding sites; however the use of caffeine concentrations below 0.05 mM in the presented study seemed to be a bit low for the detection limit of the HPLC instrumentation used.

It has been established that the MIPs with larger surface area would give the highest recognition performance due to surface laden binding cavities (4, 27, 43). In agreement with such findings, the MW MIPs prepared with slower heating produced larger surface area which also showed the highest template recognition performance. On the other hand, MW polymerisation with faster heating (300 W) lowered template binding efficiency of the MIPs which also showed lower surface area (as seen in Figure 3.35). In addition, the DSC analysis suggested that the MIPs polymerised with faster MW heating (300 W) showed considerably lower cross-linking degree which might be detrimental to the integrity of the template binding cavities created within its matrix and which might be the reason for their compromised template binding performance (as seen earlier in Figure 3.19).

MW MIPs polymerised with slower heating showed higher IF which suggested that these MIPs consisted of more template selective binding sites than that of the NIPs. DSC Results of these MW MIPs showed higher degree of cross-linking and higher surface area too. This reaffirmed the proposed hypothesis that not only a greater surface surface area but also sufficient degree of cross-links would be crucial in holding the binding cavities intact and thereby show improved template recognition performance. Moreover, formation of stable monomer-template assembly in pre-polymerisation mixture would be crucial in defining template selective binding cavities within the polymer matrix and might reflect into improved recognition performance of the polymers. In fact, the MW MIPs that showed higher cross-linking degree were prepared with slower MW heating (as seen in Figure 3.19). In this regard, lower MW powers (slower heating) might be useful in forming more stable template-monomer assemblies which would be crucial in forming template selective binding cavities. The obtained results were in agreement with the proposed hypothesis that not only the available surface area but the cross-linking degree, total porosity and even heating kinetics of the MIP preparation could play an important role in determining their template binding performance.

MW polymers polymerised at 60 °C with 5 W by varying the length of polymerisation were also analysed for their template binding performances as presented in Figure 3.44.

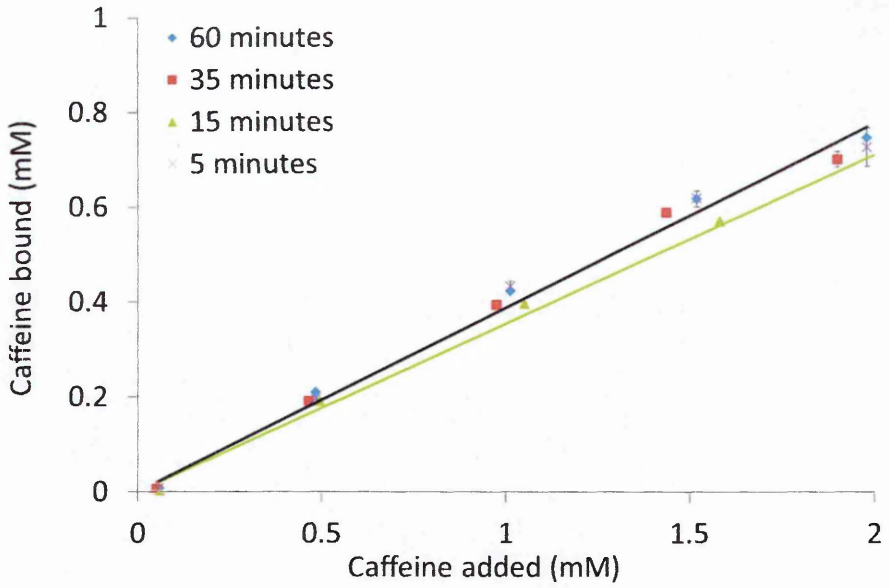

Figure 3.44: Comparison of caffeine rebinding performance of the MW MIPs polymerised for different time durations; represented by different colours (5 minutes-black, 15 minutes-green, 35 minutes-red and 60 minutes-blue). Standard deviations were derived from the triplicate measurements of each sample.

MW MIPs polymerised for different lengths of time (5 minutes to 60 minutes) showed no significant recognition efficiency of the MIPs increased consistently with an increase in caffeine concentration from 0.1 mM to 2 mM. Similar template binding analysis was performed on the corrosponding set of NIPs and derived IF values were plotted as shown in Figure 3.45.

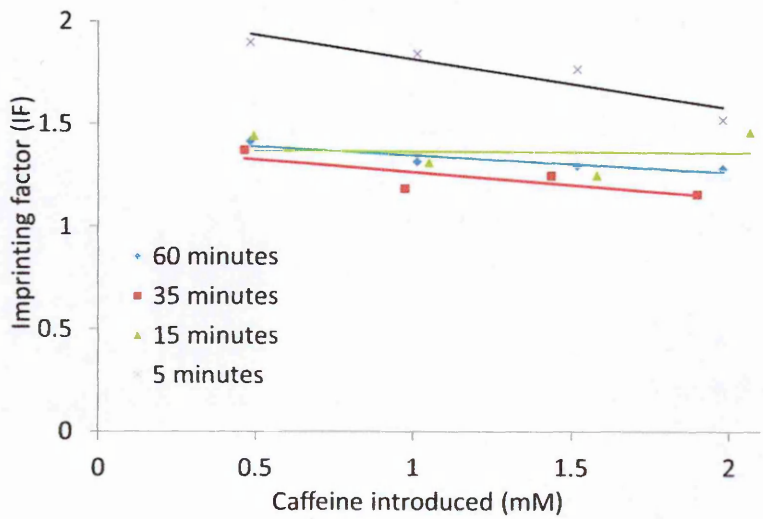

Figure 3.45: Imprinting factors of the MW polymers polymerised for different time durations; represented by different colours (5 minutes-black, 15 minutes-green, 35 minutes-red and 60 minutes-blue).

IF values of the MW polymers prepared for the shortest time (5 minutes) were higher than that prepared for longer times (15 minutes, 35 minutes and 60 minutes). This suggested that the MIPs prepared for longer times (from 15 minutes to 60 minutes) exhibited higher amount of non-selective rebinding than that of the one polymerised just for 5 minutes. Another observation could be drawn from this that the imprinting was achieved better with just 5 minutes than any longer polymerisations. However, the recognition performance of the MIPs polymerised for 5 minutes declined consistently as the template concentration was increased from 0.5 mM to 2 mM (as seen in Figure 3.45). This suggested that the imprinting cavities generated by shorter polymerisations were more selective towards the template. However, they might be fewer in number compared to non-selective cavities which were saturated when higher caffeine concentrations were introduced. On the other hand, the longer polymerisation times (from 15 minutes to 60 minutes) showed consistent IF values between 1.2 to 1.4 throughout the caffeine concentration studied (0.5 mM to 2 mM) which suggested that the non-selective cavities were present in higher numbers in these MIPs which showed non-selective rebinding regardless of the concentration caffeine introduced.

Then, the next set of MW polymers were polymerised at different temperatures and the resulting MIPs were analysed for their template recognition performance. The results obtained were plotted in Figures 3.46 and 3.47.

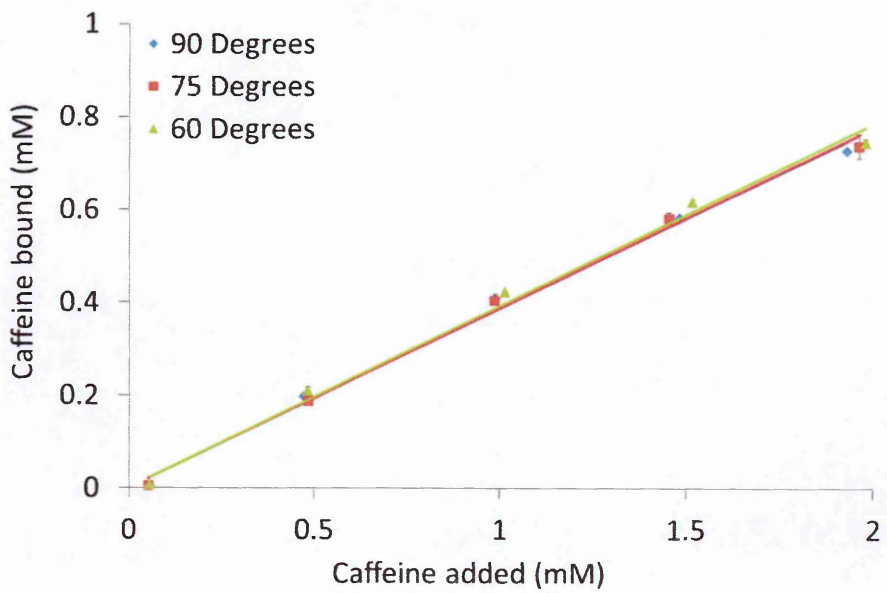

Figure 3.46: Comparison of caffeine rebinding performance of the MW MIPs polymerised at different temperatures; represented by different colours (60 °C-green, 75 °C-red and 90 °C-blue). Standard deviations were derived from the triplicate measurements of each sample.

MW MIPs polymerised at different temperatures showed no considerable difference in their caffeine recognition performance (as seen in Figure 3.46). However, the magnitude of caffeine recognition was directly proportional to its concentration in the range of 0.5 mM to 2 mM. This suggested that different polymerisation temperatures did not necessarily affect the template binding performance of the MIPs. To understand this further, the obtained results were correlated to their physical analysis performed earlier. The correlation suggested that the MIP polymerised at 90 °C exhibited considerably larger surface area however it did not reflect into its improved template recognition performance. This behaviour was slightly different than other MW MIPs where larger surface area largely reflected into improved template recognition performance. This indicated that although higher temperatures could yield larger surface area in the resulting MIP, it might sometimes lead to destabilisation of non-covalently bound template-monomer assemblies due to elevated kinetic energy of the pre-polymerisation mixture. This suggested that although larger surface area were achieved at elevated polymerisation temperatures, lack of template selective binding cavities might be the reason for not necessarily improving the template recognition performance of the resulting MW MIPs.

When the results obtained from DSC analysis were correlated with the template recognition performance of the MW MIPs, it was found that the cross-linking degree of MW MIPs did not vary significantly when they were polymerised at different temperatures (as seen in Figure 3.21). This suggested that unlike the surface area, sufficient cross-linking degree always showed consistent template recognition performance. The IF values of these MW polymers were derived for better understanding of the characteristics of the formed binding cavities. Figure 3.47 shows the IF of MW polymers polymerised at different temperatures.

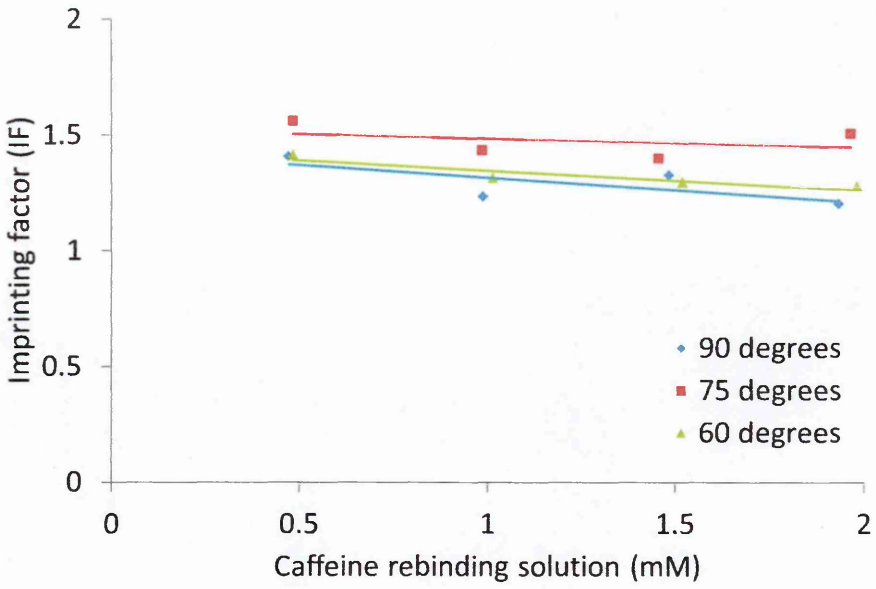

Figure 3.47: Imprinting factors of the MW polymers polymerised at different temperatures represented by different colours (60 °C-green, 75 °C-red and 90 °C-blue).

MW MIPs polymerised at different temperatures showed IF values in a narrow range from 1.4 to 1.5. The IF value improved slightly when the polymerisation temperature was increased from 60 °C to 75 °C; however it declined back to its original value of 1.4 when the polymerisation temperature was increased further up to 90 °C (as seen in Figure 3.47). When the obtained results were correlated with the previously obtained results from DSC and porosimetry analysis, it was found that increase in polymerisaiton temperatures beyond 75 °C did not improve cross-linking degree inspite of generating considerably larger surface area (as seen in Figures 3.21 and 3.38). This was in agreement with the proposed hypothesis that highly elevated polymerisation temperatures could be detrimental in generating newer template selective cavities. This indicated that polymerisation temperatures of above 75 °C might not be suitable for generating MW MIPs with improved template recognition performance inspite of exhibiting considerably larger surface area.

Comparing the recognition performances of different MW MIPs, it was found that elevated temperatures and prolonged times of MW polymerisations either maintained or compromised template recognition performance. MW MIPs polymerised with the lowest power (5 W) for the shortest time (5 minutes) at 60 °C exhibited not only sufficient cross-linking and larger surface area but also exhibited higher template recognition performance.

Template rebinding performance of the control set of oven polymers was carried out in identical manner, as plotted in Figure 3.48.

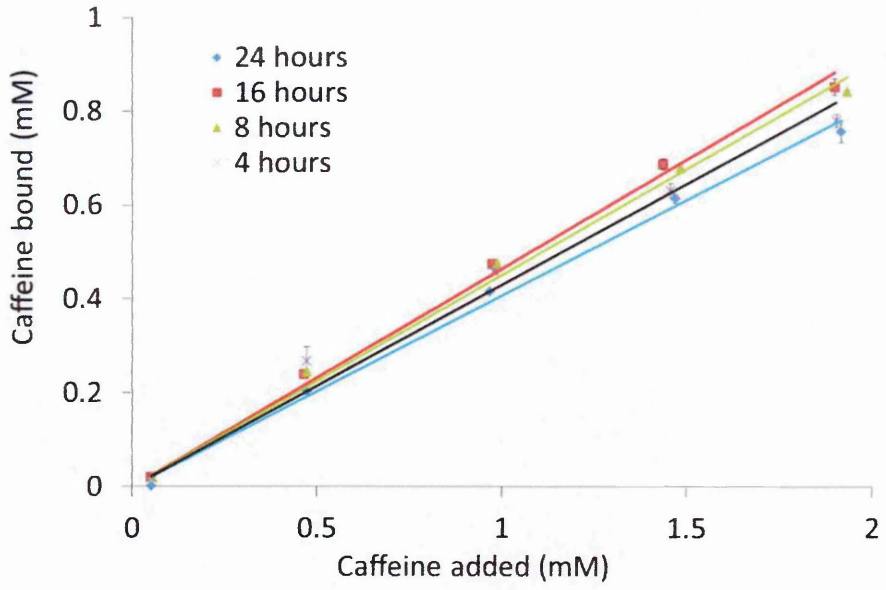

Figure 3.48: Comparison of caffeine rebinding performance of the oven MIPs polymerised for different time durations represented by different colours (4 hours-black, 8 hours-green, 16 hours-red and 24 hours-blue). Standard deviations derived from the triplicate measurements of each sample.

Figure 3.48 showed that the template recognition performance of the oven MIPs improved when their polymerisation time was increased from 4 hours to 16 hours; however the performance dropped slightly when the polymerisations were carried out for extended periods up to 24 hours. The template recognition performance obtained with extended polymerisations (24 hours) was even lower than that achieved with just 4 hours long polymerisations. When this observation was correlated with the findings obtained from DSC and porosimetry analysis, it was found that prolonged oven polymerisation times did slightly decrease the cross-linking degree of oven MIPs as well as adversely affected their surface area which would be likely to degrade their template recognition performance (as seen in Figure 3.21 and Table 3.12). The IF values of these MIPs were also derived as plotted in Figure 3.49.

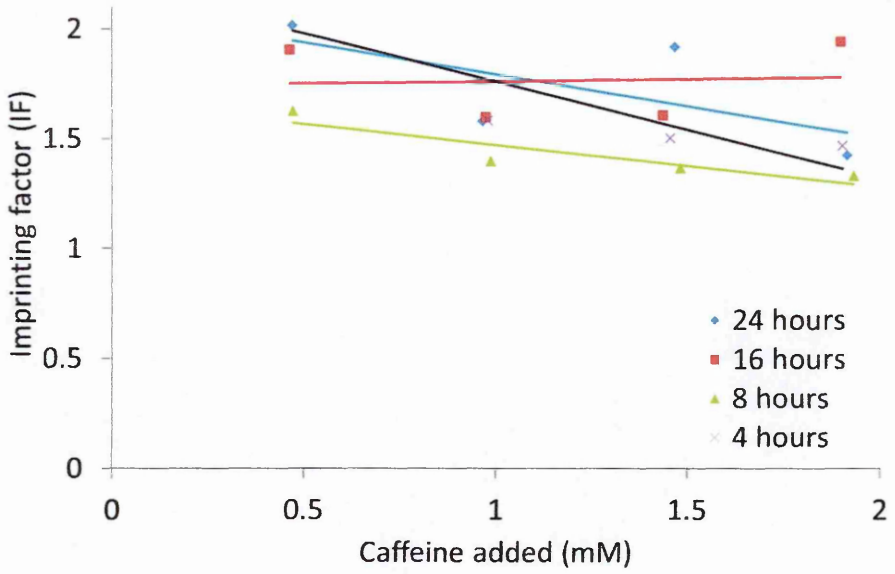

Figure 3.49: Imprinting factors of the oven polymers polymerised for different time durations represented by different colours (4 hours-black, 8 hours-green, 16 hours-red and 24 hours-blue).

When oven polymerisations were carried out from 4 hours to 24 hours, IF values of the resulting polymers were found to be in a broader range of 1.4 to 2. The shortest polymerisation time of 4 hours generated the highest IF which dropped when the polymerisation times were extended up to 16 hour. When the polymerisations were extended even further up to 24 hours, the obtained IF value was similar to what was seen with the 4 hour polymerisation. It was also observed that too short (4 hours) and too long (24 hours) oven polymerisations showed higher imprinting effect which dropped much faster as the template concentrations were increased from 0.5 mM to 2 mM. On the other hand, intermediate polymerisation lengths of 8 hours to 16 hours showed more consistent IF values through the similar concentration of the template. These trends suggested that the shorter polymerisations might produce template selective binding cavities however they might be fewer in number and could saturate when higher concentrations of the template were introduced. Longer polymerisations of up to 16 hours produced polymers with equal amount of the selective and non-selective template rebinding cavities. Surprisingly, even longer polymerisations showed similar imprinting effect as a 4 hour polymerisation which suggested that the inconsistent heating and uncontrolled polymerisation kinetics in oven might have led to parallel depolymerisation as postulated. This was also reaffirmed by the reduction in the cross-linking degree and the reduction in the surface area of these polymers when the polymerisations were carried out for 24 hours (as seen in Figure 3.22 and Table 3.12). In general, the imprinting effect achieved from oven polymerisation was inconsistent as no clear

trends were observed throughout the length of the polymerisation studied. It would be important to note here that the imprinting effects achieved with the MW MIPs in just 5 minutes were comparable to that of oven MIPs for over 24 hours.

Oven polymerisation was carried out at different temperatures too and rebinding performance of the resultant polymers were plotted as shown in Figure 3.50.

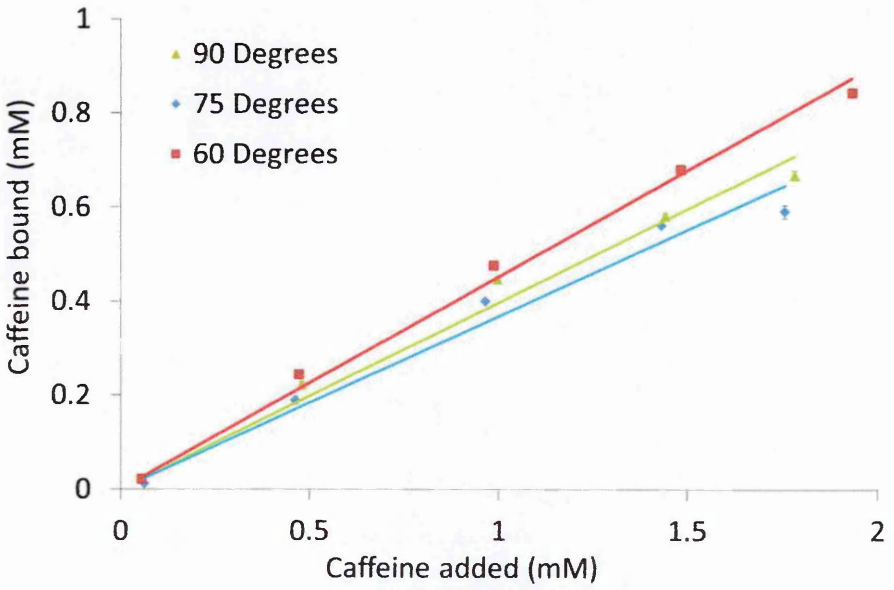

Figure 3.50: Comparison of caffeine rebinding performance of the oven MIPs polymerised at different temperatures represented by different colours (60 °C-red, 75 °C-blue and 90 °C-green). Standard deviations derived from the triplicate measurements of each sample.

The caffeine rebinding performance of the oven MIPs was inversely related to their polymerisation temperature in the range of 60 °C to 90 °C. This implied that the polymerisation temperature of 60 °C produced the oven MIPs with the highest template recognition performance which decreased when the temperature was raised to 90 °C (as seen in Figure 3.50). It was noticable that the reduction in the template recognition at higher polymerisation temperatures was more pronounced in an oven led polymerisation than a MW polymerisation which might be due to inconsistent heating of oven. Similar to the MW MIPs, the surface area of the oven MIPs increased considerably when the polymerisation temperatures were increased from 60 °C to 90 °C. However, improved surface area did not reflect into improved template recognition performance of these MIPs.

To understand this further, the obtained results were correlated with that obtained from DSC analysis which suggested that the increase in the oven polymerisation temperature decreased the cross-linking degree of the MIPs. This reaffirmed the proposed hypothesis that surface area might not necessarily reflect into the template binding perofrmance of the MIPs. An

optimal cross-linking degree also could be crucial in maintaining selective binding sites intact for improved template recognition. It also suggested that the reduced cross-linking degree of the oven MIPs might have led to reduction in their template binding performance although their surface area were highly enlarged (as seen in Figure 3.23 and Table 3.12). This behaviour was very similar to that observed in case of MW MIPs too.

The IF values of these polymers were also calculated and plotted as seen in Figure 3.51.

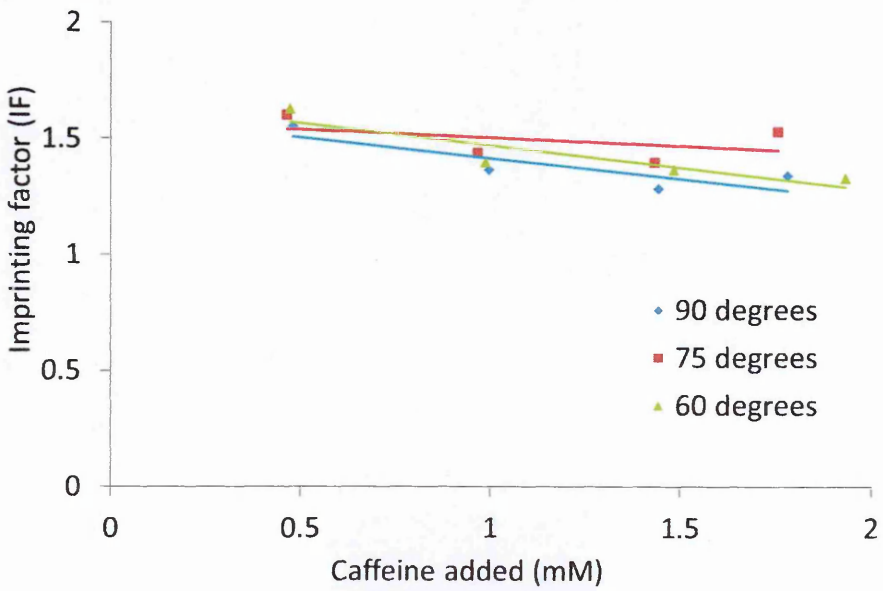

Figure 3.51: Imprinting factors of the oven polymers polymerised at different temperatures represented by different different colours (60 °C-green, 75 °C-red and 90 °C-blue).

The oven MIPs polymerised at different temperatures showed their IF values in a narrow range from 1.4 to 1.5, much similar to that of MW MIPs (as seen in Figures 3.47). The IF value improved slightly when the polymerisation temperature was increased from 60 °C to 75 °C; however when the temperature was increased further to 90 °C, the imprinting effect declined back to its original values (as seen in Figure 3.51). This reaffirmed the proposed hypothesis that imprinted cavities might have increased in the oven MIPs with slight increase in polymerisation temperature but further increase in temperatures could show presence of fewer imprinted cavities. This might be because elevated thermokinetics at higher polymerisation temperatures could lead to destabilisation of the non-covalently bound template-monomer assemblies, crucial in forming template selective binding cavities. This suggested that polymerisation temperatures of above 75 °C could be detrimental in obtaining template selective recognition performance of the oven MIPs inspite of showing larger surface area.

Another set of control polymers prepared by UV irradiation were subjected to template binding analysis in similar way. Figure 3.52 shows the template rebinding performance of the UV polymers prepared for different lengths of time.

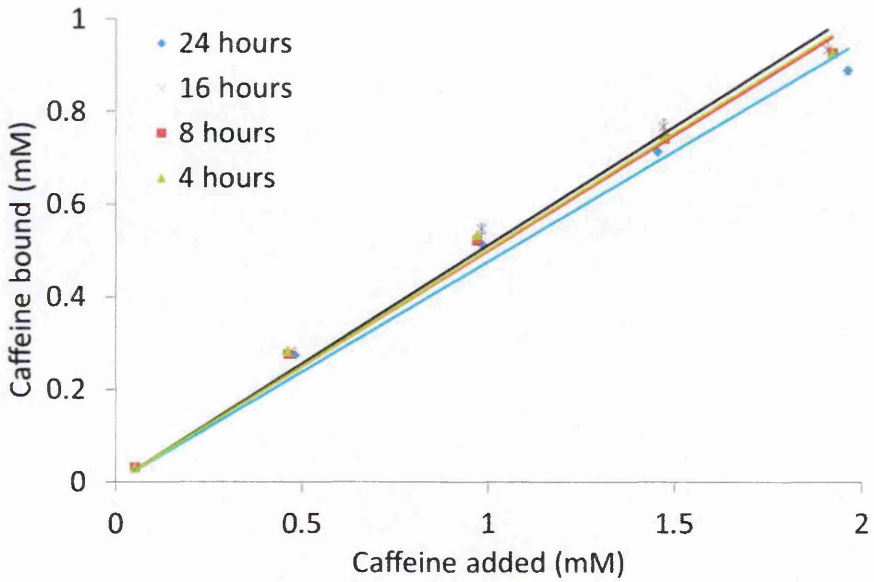

Figure 3.52: Comparison of caffeine rebinding performance of the UV MIPs polymerised for different durations represented by different colours (4 hours-green, 8 hours-red, 16 hours-black and 24 hours-blue). Standard deviations derived from the triplicate measurements of each sample.

The UV MIPs polymerised for different times (from 4 hours to 16 hours) showed much similar template recognition performance; however extended polymerisation times up to 24 hours reduced the template recognition efficiency slightly (as seen in Figure 3.52). The trend observed in the recognition performance of the UV MIPs was similar to that exhibited by MW MIPs (as seen in Figure 3.45) and oven MIPs (as seen in Figure 3.48). These sets of MIPs showed much similar surface area but their cross-linking degree decreased slightly by increasing the length of polymerisation. This suggested that the slight reduction in cross-linking degree observed with longer polymerisations (of up to 24 hours) might be crucial in assuring the integrity of the binding cavities formed. This again reaffirmed the proposed hypothesis that the surface area of the MIPs could not entirely depict their template recognition performance, sufficient degree of cross-linking might be crucial in holding the template binding sites intact for improved template recognition. The IF of these UV MIPs were derived and were plotted as seen in Figure 3.53.

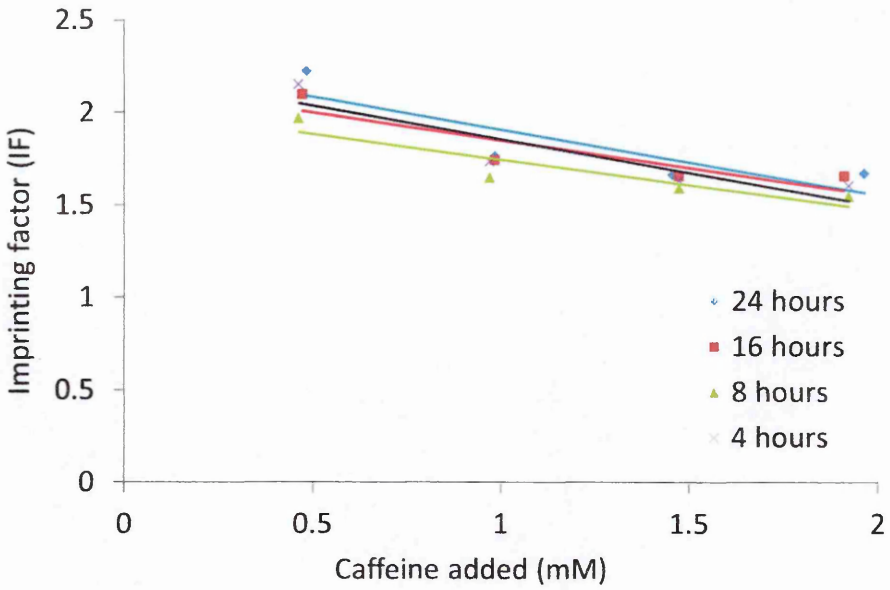

Figure 3.53: Imprinting factors of the UV polymers polymerised for different time durations represented by different colours (4 hours-black, 8 hours-green, 16 hours-red and 24 hours-blue).

IF values of the UV MIPs were found to be between 1.5 to 2.1. No particular trend in IF values was observed here when the polymerisations were carried out for different lengths of time. It could be said that between the control sets of oven and UV polymers, UV polymerisation produced polymers with more consistent imprinting since its imprinting efficiencies were higher than that of MW and oven polymerisations (as seen in Figures 3.45 and 3.48 respectively). This suggested that the binding cavities produced in UV polymers were more selective towards the template. Although UV polymers had been widely reported to produce smaller surface areas as compared to thermal polymers, it did not seem to deteriorate their template recognition performance in the presented study. It was not possible to measure the surface area of UV MIPs to test the hypothesis further during the course of the study; however it would be interesting to study whether the surface area of the UV polymers correlated to their template recognition performance. UV polymers were also polymerised at different temperatures and their template binding efficiencies were analysed as seen in Figure 3.54.

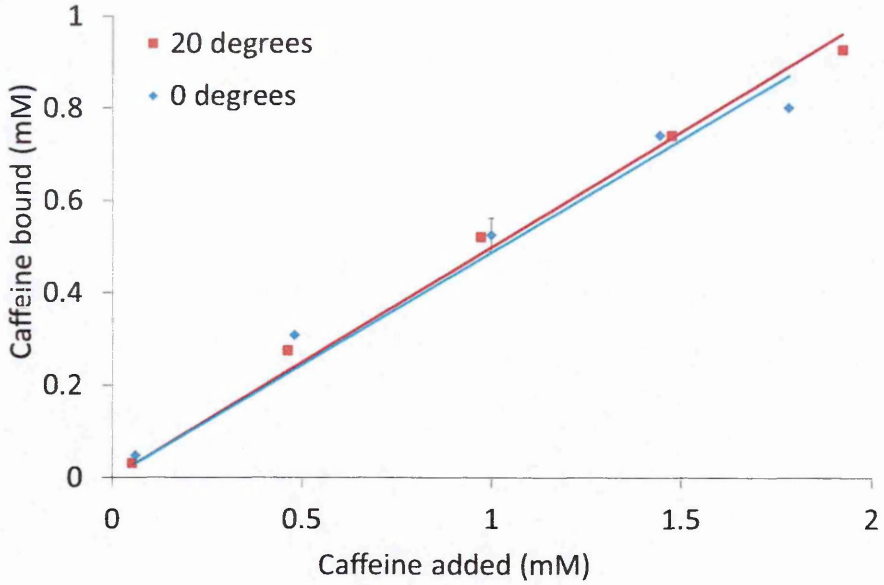

Figure 3.54: Comparison of caffeine rebinding performance of the UV MIPs polymerised at different temperatures represented by different colours (0 °C-blue and 20 °C-red). Standard deviations derived from the triplicate measurements of each sample.

Polymerisation temperature did not seem to affect template recognition performance of the UV MIPs. The amount of caffeine bound to the prepared UV MIPs was quite similar to that of the oven MIPs prepared at 60 °C but slightly higher than that of the MW MIPs (as seen in Figures 3.47 and 3.50). Unlike the thermally produced MIPs in oven and MW reactors, UV polymers did not show any reduction in their template recognition performance when the polymerisations were carried out at 0 °C and 20 °C. The temperatures of UV polymerisation were quite low as such than that used for thermal polymerisations (60 °C to 90 °C). This suggested that thermokinetics of a polymerisation system could influence other crucial parameters such as the integrity of the template-monomer assembly and the overall cross-linking degree of the polymer which could reflect directly onto their template recognition performance. IF values were also calculated for the UV MIPs prepared at different temperatures which are plotted in Figure 3.55.

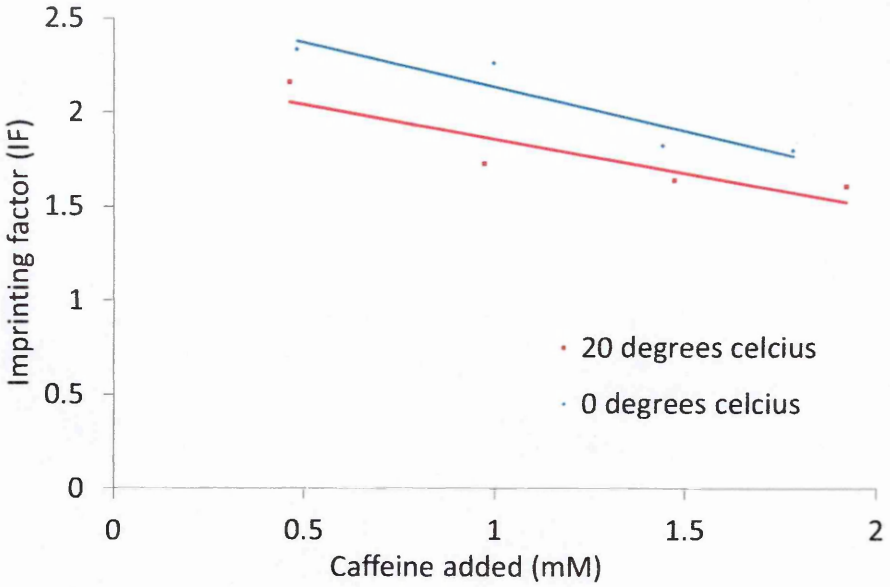

Figure 3.55: Imprinting factors of the UV polymers polymerised for different time durations represented by different colours (0 °C-blue and 20 °C-red).

Although showing similar template rebinding performances, the UV polymers showed considerable differences in their imprinting efficiency for the polymerisations carried out at 0 °C and 20 °C. The UV polymers polymerised at 0 °C showed less non-selective binding than the one polymerised at 20 °C (as seen in the Figure 3.55). The imprinting efficiency of the UV MIP (0 °C) however decreased steeply as the concentration of caffiene was increased from 0.5 mM to 2 mM. This suggested that although freezing polymerisation temperatures created template selctive binding cavities in the UV MIPs, they might be fewer in number as they saturated at lower template concentrations. In comparison to MW and oven polymerisations, UV polymers prepared in all conditions showed improved imprinting efficiency. However, their template recognition performance was much similar to other methods although they are thought to have smaller surface areas. This reaffirmed the proposed hypothesis that the degree of cross-linking and the polymerisation kinetics could be crucial in determining selective template recognition performance of the polymers than just their surface area.

A summary of the results have also been tabulated as seen in Tables 3.13, 3.14 and 3.15.

Table 3.13: Summary of the relationship between various experimental parameters and the physicochemical properties of the MW polymers

Experimental parameter	Cross-linking and thermal stability	Available surface area for template rebinding	Template recognition performance	Presence of template selective binding sites
Heating rate (obtained by MW powers 5 W to 300 W)	Inverse	Inverse	Inverse	Inverse
Polymerisation time (5-60 minutes)	Cross-linking Inversely affected; rigidity directly affected	Inverse	No clear relationship	Inverse
Polymerisation temperature (60 °C-90 °C)	No effect on the cross-linking; rigidity directly affected	Direct	Direct	Inverse

Table 3.14: Summary of the relationship between various experimental parameters and the physicochemical properties of the oven polymers

Experimental parameter	Cross-linking and thermal stability	Available surface area for template rebinding	Template rebinding performance	Presence of template selective binding sites
Polymerisation time (4 -24 hours)	Cross-linking Inversely affected; thermal stability directly affected	Inverse	No distinct relationship; Inversely affected With extended times	Not affected
Polymerisation temperature (60 °C-90 °C)	Cross-linking Inversely affected; thermal stability directly affected	Direct	Inverse	Inverse

Table 3.15: Summary of relationship between various experimental parameters and physicochemical properties of the UV polymers

Experimental parameter	Cross-linking and thermal stability	Available surface area for template rebinding	Template rebinding performance	Presence of template selective binding sites
Polymerisation time (4 -24 hours)	Cross-linking is inversely affected; thermal stability is directly affected	Not available	No distinct relationship; Inversely affected With extended times	Not affected
Polymerisation temperature (0 °C and 20 °C)	Cross-linking is inversely affected; thermal stability is directly affected	Not available	Inversely affected	Inverse

Section 3.5 presents a brief summary of the results and discussion presented in this chapter.

3.5. Summary

The first objective of this study was to understand the effect of several experimental parameters on the physical and chemical properties of MW MIPs. The differences observed in the physical properties of the MW MIPs were influenced by the experimental conditions used for their preparation, as postulated. The obtained results further suggested that the variation in caffeine binding performance of the MIPs was greatly influenced by their physical properties.

MW polymerisation was investigated as a possible alternative method for the development of MIPs in comparison to traditional methods such as, oven and UV polymerisations. The polymerisation recipe was kept the same in all the methods to make different polymers comparable with one another.

The obtained results suggested that MW polymerisation exhibited extremely fast polymerisation kinetics compared to the traditional methods. Different physical properties and the recognition performance of the polymers produced by MW polymerisation were also comparable to that of the oven and UV polymerisations. MW polymerisation was investigated by varying its experimental parameters, such as polymerisation rate, time and temperature. The controlled heating rates achieved with MW reactor allowed investigating the effect of different heating rates on the physical properties and performance of the polymers which has not been reported in any existing study. The obtained results suggested that controlled heating rates achieved only with the MW reactor were far more influential on the physical properties of the resulting polymers than the temperature and the length of polymerisation. The results also indicated that different rates of heating in MW polymerisation could produce polymers with considerable differences in their cross-linking degree, surface area, thermal stability and even porosity. MW polymerisations carried out for as little as 5 minutes produced monomer conversion of greater than or equal to 98 % which were comparable to the traditional methods.

The considerable differences observed in the physical characters of the prepared MW polymers translated into their recognition performance too. This also implied that programmable controlled heating of MW reactors could be exploited in developing polymers with predictable performance. This could be useful in reducing the time taken in optimising different parameters to achieve desired polymer products. The results obtained strongly recommended that MW polymerisation could be investigated further as a suitable alternative polymerisation technique to develop polymers with added advantages of controlled

polymerisations, faster reactions and reproducibility. In particular, MW polymerisation could be a useful technique in addressing existing challenges in commercialisation of MIPs which include lack of industrial scale production and batch to batch variability.

Another objective of this study was to understand the effect of different experimental parameters on the physical properties of the resulting MIPs. The effect of heating rate in a thermal polymerisation has never been studied. The presented study investigated this for the first time with the virtue of a MW reactor where polymerisations were carried out with wide range of MW heating rates. The obtained results indicated that the slower polymerisation produced the MIPs with higher cross-linking degree and lower thermal stability. These MIPs also showed larger surface area, improved template recognition performance and improved imprinting efficiency too.

Polymerisation time was the second experimental parameter in the presented study which was varied whilst preparing the MIPs and the physical properties and recognition performance of the resulting MIPs were studied in identical manner. The obtained results indicated that different lengths of polymerisation slightly affected physical properties of the MIPs. The presented study reported for the first time that shorter polymerisation times, such as 5 minutes of MW polymerisation and 4-8 hours of oven and UV polymerisations were sufficient to produce MIPs with optimum cross-linking degree, surface area, recognition performance and even imprinting efficiencies. Extended polymerisations either maintained or decreased mentioned characteristics of MIPs. This study has found a need to reinvestigate the extended polymerisation times used in traditional polymerisations, as they did not improve properties of the resulting MIPs.

The third experimental parameter under study was the polymerisation temperature where the effect of different polymerisation temperatures (60 °C to 90 °C) on the properties of the resulting MIPs was studied. Controlled nature of MW reactor maintained heating rates as desired even when polymerisations were carried out at different temperatures. The presented study found that MW polymerisations produced MIPs with much similar cross-linking degrees at different temperatures. The measure of the heating rate at different temperatures was not possible in oven or UV polymerisation due to lack of controlled heating. However, the literature has widely reported increasing heating rates with increase in polymerisation temperatures. This was confirmed by the obtained findings that faster heating rates at elevated temperatures led to decrease in cross-linking degree of the MIPs. No other study has reported this finding which supports the proposed hypothesis that polymerisation kinetics would be faster at elevated temperatures in traditional uncontrolled heating. This would

polymerise materials faster before they could be form enough cross-linking. Higher polymerisation temperature (90 °C) produced higher thermal stability in the MIPs and considerably larger surface area. However, unlike general assumption the presented study established that improved surface area did not necessarily result into improved template recognition performance of the resulting MIPs.

For the first time, this study established that improved recognition performance and formation of template selective binding sites within the MIPs were highly influenced by their cross-linking degree and their polymerisation kinetics than just their surface area. The obtained results strongly supported the proposed hypothesis that the slower polymerisation kinetics was crucial in producing stable monomer-template cavities which produced highly selective template binding cavities. On the other hand, sufficient degree of cross-linking was crucial in maintaining the integrity of selective cavities for template rebinding.

The third objective of this study was to investigate whether different properties (both physical and chemical) affected each other. The obtained results showed striking influence of these properties on one another. For example, heating rates affected the cross-linking degree of the polymers which reflected into their recognition performance. Microscopy analysis of the polymers indicated polymers to be porous in texture, irregular in shape and consistent in their size distribution. The surface area and imprinting efficiency of the MIPs was found to be higher than that of the NIPs which suggested the presence of template selective binding cavities present on the surface of the MIPs. This was also confirmed by improved template recognition performance of the MIPs.

3.6. Future work

Porosity characteristics of all the oven and UV polymers could be investigated further for comparison with the obtained results of the MW polymers. It would be very useful to study lower template concentrations for the recognition performance of the MIPs. This would allow plotting Scatchard diagrams for the template rebinding studies which would give better understanding of the distribution of the template selective binding sites created within the MIPs. More experimental work will need to be performed in exploring the effect of different porogens on the MW heating rates using the same polymerisation recipe.

3.7. Bibliography for Chapter 3

1. Alexander, C., Andersson, H. S., Andersson, L. I., Ansell, R. J., Kirsch, N., Nicholls, I. A., O'Mahony, J., and Whitcombe, M. J. (2006) Molecular Imprinting Science and Technology: A Survey of the Literature for the Years up to and Including 2003, *Journal of Molecular Recognition* **19**, 106-180.

2. Piletsky, S. A., Piletska, E. V., Karim, K., Freebairn, K. W., Legge, C. H., and Turner, A. P. (2002) Polymer Cookery: Influence of Polymerization Conditions on the Performance of Molecularly Imprinted Polymers, *Macromolecules* **35**, 7499-7504.

3. Piletsky, S. A., Guerreiro, A., Piletska, E. V., Chianella, I., Karim, K., and Turner, A. P. (2004) Polymer cookery-2. Influence of Polymerization Pressure and Polymer Swelling on the Performance of Molecularly Imprinted Polymers, *Macromolecules* **37**, 5018-5022.

4. Piletsky, S. A., Mijangos, I., Guerreiro, A., Piletska, E. V., Chianella, I., Karim, K., and Turner, A. P. F. (2005) Polymer Cookery: Influence of Polymerization Time and Different Initiation Conditions on Performance of Molecularly Imprinted Polymers, *Macromolecules* **38**, 1410-1414.

5. Piletska, E. V., Guerreiro, A. R., Whitcombe, M. J., and Piletsky, S. A. (2009) Influence of the Polymerization Conditions on the Performance of Molecularly Imprinted Polymers, *Macromolecules* **42**, 4921-4928.

6. Kappe, C. O. (2008) Microwave Dielectric Heating in Synthetic Organic Chemistry, *Chemical Society Reviews* **37**, 1127-1139.

7. Hayes, B. L. (2004) Recent Advances in Microwave-assisted Synthesis, *Aldrichimica Acta* **37**, 66-77.

8. Visentin, A. F., Dong, T., Poli, J., and Panzer, M. J. (2014) Rapid, Microwave-assisted Thermal Polymerization of Poly(ethylene glycol) Diacrylate-supported Ionogels, *Journal of Materials Chemistry* **A 2**, 7723-7726.

9. Stange, H. Greiner, A. (2007) Microwave Assisted Free Radical Copolymerizations of Styrene and Methyl Methacrylate, *Macromolecular Rapid Communications* **28**, 504-508.

10. Chia, H., Jacob, J., and Boey, F. (1996) The Microwave Radiation Effect on the Polymerization of styrene, *Journal of Polymer Science Part A: Polymer Chemistry* **34**, 2087-2094.

11. Jacob, J., Chia, L., and Boey, F. (1997) Microwave Polymerization of Poly(methyl acrylate): Conversion Studies at Variable Power, *Journal of Applied Polymer Science* **63**, 787-797.

12. Langa, F., de la Cruz, P., de la Hoz, A., Díaz-Ortiz, A., and Díez-Barra, E. (1997) Microwave Irradiation: More Than Just a Method for Accelerating Reactions, *Contemporary Organic Synthesis* **4**, 373-386.

13. Holtze, C., Antonietti, M., and Tauer, K. (2006) Ultrafast Conversion and Molecular Weight Control Through Temperature Programming in Microwave-induced Miniemulsion Polymerization, *Macromolecules* **39**, 5720-5728.

14. Sosnik, A., Gotelli, G., and Abraham, G. A. (2011) Microwave-assisted Polymer Synthesis (MAPS) as a Tool in Biomaterials Science: How New and How Powerful, *Progress in Polymer Science* **36**, 1050-1078.

15. Sugihara, Y., Semsarilar, M., Perrier, S., and Zetterlund, P. B. (2012) Assessment of the Influence of Microwave Irradiation on Conventional and RAFT Radical Polymerization of Styrene, *Polymer Chemistry* **3**, 2801-2806.

16. Kappe, C. O. (2013) How to Measure Reaction Temperature in Microwave-heated Transformations, *Chemical Society Reviews* **42**, 4977-4990.

17. Nüchter, M., Ondruschka, B., Bonrath, W., and Gum, A. (2004) Microwave Assisted Synthesis–A Critical Technology Overview, *Green Chemistry* **6**, 128-141.

18. Kempe, K., Becer, C. R., and Schubert, U. S. (2011) Microwave-assisted Polymerizations: Recent Status and Future Perspectives, *Macromolecules* **44**, 5825-5842.

19. Wiesbrock, F., Hoogenboom, R., and Schubert, U. S. (2004) Microwave-Assisted Polymer Synthesis: State-of-the-Art and Future Perspectives, *Macromolecular Rapid Communications* **25**, 1739-1764.

20. Mallakpour, S., and Rafiee, Z. (2011) New Developments in Polymer Science and Technology Using Combination of Ionic Liquids and Microwave Irradiation, *Progress in Polymer Science* **36**, 1754-1765.

21. Albert, P., Hölderle, M., Mülhaupt, R., and Janda, R. (1996) Thermal and Microwave-Activate Non-aqueous Free-radical Dispersion Polymerization of Methyl Methacrylate in n-Heptane, *Acta Polymerica* **47**, 74-78.

22. Costa, C., Santos, V., Araujo, P., Sayer, C., Santos, A., Dariva, C., and Fortuny, M. (2010) Rapid Decomposition of a Cationic Azo-initiator Under Microwave Irradiation, *Journal of Applied Polymer Science* **118**, 1421-1429.

23. Zhendong, L., Yangcheng, L., Bodong, Y., and Guangsheng, L. (2013) Free Radical Polymerization of Butyl Acrylate in Monodispersed Droplets: Comparison Between Two Heating Strategies, *Journal of Applied Polymer Science* **127**, 628-635.

24. http://www.cem.com; accessed on 18-8-2015.

25. Jovanovic, J., and Adnadjevic, B. (2007) Comparison of the Kinetics of Conventional and Microwave Methyl Methacrylate Polymerization, *Journal of Applied Polymer Science* **104**, 1775-1782.

26. Tulig, T. J., and Tirrell, M. (1981) Molecular Theory of the Trommsdorff Effect, *Macromolecules* **14**, 1501-1511.

27. Turner, N. W., Holdsworth, C. I., Donne, S. W., McCluskey, A., and Bowyer, M. C. (2010) Microwave Induced MIP Synthesis: Comparative Analysis of Thermal and Microwave

Induced Polymerisation of Caffeine Imprinted Polymers, *New Journal of Chemistry* **34**, 686-692.

28. Hoogenboom, R., and Schubert, U. S. (2007) Microwave-assisted Polymer Synthesis: Recent Developments in a Rapidly Expanding Field of Research, *Macromolecular Rapid Communications* **28**, 368-386.
29. Stange, H., and Greiner, A. (2007) Microwave-assisted Free Radical Copolymerizations of Styrene and Methyl Methacrylate, *Macromolecular Rapid Communications* **28**, 504-508.
30. Zhang, Y., Liu, R., Hu, Y., and Li, G. (2009) Microwave Heating in Preparation of Magnetic Molecularly Imprinted Polymer Beads for Trace Triazines Analysis in Complicated Samples, *Analytical Chemistry* **81**, 967-976.
31. PolshettiWar, V., and Verma, R. S. (2010) Microwave-assisted Synthesis of Polymers in Aqueous Media, Royal Society of Chemistry 145-175.
32. Haupt, K. (2010) Biomaterials: plastic antibodies, *Nature Materials* **9**, 612-614.
33. Spivak, D. A., and Shea, K. J. (2012) MIP2010: The Future of Molecular Imprinting, *Journal of Molecular Recognition* **25**, 319-319.
34. Turiel, E., and Martín-Esteban, A. (2009) Molecularly Imprinted Polymers for Solid-phase Microextraction, *Journal of Separation Science* **32**, 3278-3284.
35. Stange, H., Ishaque, M., Niessner, N., Pepers, M., and Greiner, A. (2006) Microwave-Assisted Free Radical Polymerizations and Copolymerizations of Styrene and Methyl Methacrylate, *Macromolecular Rapid Communications* **27**, 156-161.
36. Farrington, K., Magner, E., and Regan, F. (2006) Predicting the Performance of Molecularly Imprinted Polymers: Selective Extraction of Caffeine by Molecularly Imprinted Solid Phase Extraction, *Analytica Chimica Acta* **566**, 60-68.
37. Li, J., Li, S., Wei, X., Tao, H., and Pan, H. (2012) Molecularly Imprinted Electrochemical Luminescence Sensor Based on Signal Amplification for Selective Determination of Trace Gibberellin A3, *Analytical chemistry* **84**, 9951-9955.
38. Lorenzo, R. A., Carro, A. M., Alvarez-Lorenzo, C., and Concheiro, A. (2011) To Remove or Not To Remove? The Challenge of Extracting the Template to Make the Cavities Available in Molecularly Imprinted Polymers (MIPs), *International journal of molecular sciences* **12**, 4327-4347.
39. Xu, S., Zhang, X., Sun, Y., and Yu, D. (2013) Microwave-assisted Preparation of Monolithic Molecularly Imprinted Polymeric Fibers for Solid Phase Microextraction, *Analyst* **138**, 2982-2987.
40. Zayas, H., Holdsworth, C. I., Bowyer, M., and McCluskey, A. (2014) Evaluation of 4-substituted Phenyl Styrenes as Functional Monomers for the Synthesis of

Theophylline-specific Molecularly Imprinted Polymers, *Organic & Biomolecular Chemistry* **12**, 6994-7003.

41. Saifuddin, N., Wong, C., and Yasumira, A. (2009) Rapid Biosynthesis of Silver Nanoparticles Using Culture Supernatant of Bacteria with Microwave Irradiation, *Journal of Chemistry* **6**, 61-70.

42. Saifuddin, N., Nur, Y., and Abdullah, S. (2011) Microwave Enhanced Synthesis of Chitosan-graft-polyacrylamide Molecular Imprinting Polymer for Selective Removal of 17ß-estradiol at Trace Concentration, *Asian Journal of Biochemistry* **6**, 38-54.

43. Zhang, Y., Li, Y., Hu, Y., Li, G., and Chen, Y. (2010) Preparation of Magnetic Indole-3-acetic acid Imprinted Polymer Beads with 4-vinylpyridine and β-cyclodextrin as Binary Monomer via Microwave Heating Initiated Polymerization and Their Application to Trace Analysis of Auxins in Plant Tissues, *Journal of Chromatography* **A 1217**, 7337-7344.

44. Keefe, A. D., Pai, S., and Ellington, A. (2010) Aptamers as Therapeutics, *Nature Reviews Drug Discovery* **9**, 537-550.

45. Sellergren, B. (1997) Noncovalent Molecular Imprinting: Antibody-like Molecular Recognition in Polymeric Network Materials, *Trends in Analytical Chemistry* **16**, 310-320.

46. Poma, A., Brahmbhatt, H., Watts, J. K., and Turner, N. W. (2014) Nucleoside-Tailored Molecularly Imprinted Polymeric Nanoparticles (MIP NPs), *Macromolecules* **47**, 6322-6330.

47. Paci, M., Maramotti, S., Bellesia, E., Formisano, D., Albertazzi, L., Ricchetti, T., Ferrari, G., Annessi, V., Lasagni, D., and Carbonelli, C. (2009) Circulating Plasma DNA as Diagnostic Biomarker in Non-small Cell Lung Cancer, *Lung Cancer* **64**, 92-97.

48. Svenson, J., and Nicholls, I. A. (2001) On the Thermal and Chemical Stability of Molecularly Imprinted Polymers, *Analytica Chimica Acta* **435**, 19-24.

49. Lofton-Day, C., Model, F., DeVos, T., Tetzner, R., Distler, J., Schuster, M., Song, X., Lesche, R., Liebenberg, V., and Ebert, M. (2008) DNA Methylation Biomarkers for Blood-based Colorectal Cancer Ccreening, *Clinical chemistry* **54**, 414-423.

50. Ladavos, A. K., Katsoulidis, A. P., Iosifidis, A., Triantafyllidis, K. S., Pinnavaia, T. J., and Pomonis, P. J. (2012) The BET equation, the Inflection Points of N_2 Adsorption Isotherms and the Estimation of Specific Surface Area of Porous Solids, *Microporous and Mesoporous Materials* **151**, 126-133.

51. Huck, C. W. Bonn, G. K. (2000) Recent Developments in Polymer based Sorbent for Solid Phase Extraction, *Journal of Chromatography A* **885**, 51-72.

52. Djozan, D., and Ebrahimi, B. (2008) Preparation of New Solid-phase Micro Extraction Fiber on the Basis of Atrazine-Molecular Imprinted Polymer: Application for GC and GC/MS Screening of Triazine Herbicides in Water, Rice and Onion, *Analytica Chimica Acta* **616**, 152-159.

53. Azzarri, M., Cortizo, M., and Alessandrini, J. (2003) Effect of the Curing Conditions on the Properties of an Acrylic Denture Base Resin Microwave-polymerised, *Journal of Dentistry* **31**, 463-468.

54. Baeissa, A., Dave, N., Smith, B. D., and Liu, J. (2010) DNA-functionalized Monolithic Hydrogels and Gold Nanoparticles for Colorimetric DNA Detection, *ACS Applied Materials & Interfaces* **2**, 3594-3600.

55. Tierney, S., and Stokke, B. T. (2009) Development of an Oligonucleotide Functionalized Hydrogel Integrated on a High Resolution Interferometric Readout Platform as a Label-free Macromolecule Sensing Device, *Biomacromolecules* **10**, 1619-1626.

Chapter 4
Development of Recognition Polymers for the ToxiQuant Technology

4.1. Preface

This chapter forms one of the case studies undertaken during my PhD research which is based on ToxiQuant, an instrument developed by Toximet (UK) for the detection of mycotoxins from commercial produce samples. The work presented in this chapter is aimed at improving existing performance of ToxiQuant.

In ever growing global food supply chain, the quality of food has been of a persistent concern due to their possible contamination with undesirable chemical and biological hazards. Chemical hazards include pesticides, veterinary residues, naturally occurring toxins (including mycotoxins and algal toxins) and illicit additives; whereas biological hazards may include some bacteria, viruses and related toxins. Different analytical techniques currently being used for the detection of such hazards are elaborate and expensive too. Toximet conducted extensive research on mycotoxins and identified strong need for a simple, rapid and affordable testing tool to address current challenges in detecting mycotoxins from various food samples. Their efforts resulted in the successful launch of ToxiQuant, the first prototype technique which is affordable, robust, fast and highly accurate in detecting multiple mycotoxins in food samples. Selective mycotoxin recognition in ToxiQuant is currently achieved by the virtue of immuno-affinity cartridges. These cartridges are highly selective towards the target toxin and accurate in their performance; however they significantly add to the cost of the equipment. Not to mention, they also suffer from limited shelf-life due to antibodies being an integral part of their packing material. The research work presented here will investigate into the development of polymers as alternative packing materials for ToxiQuant cartridges. Herein, polymers have been prepared for the detection of aflatoxin (AFT) and ochratoxin (OT) using the recipe provided by Toximet. The recipe was developed by a PhD study based at Cranfield University.

Polymers have been prepared by thermal (oven and microwave), UV, suspension, precipitation and core-shell polymerisations to generate polymers in different formats, looking towards scale-up and optimal performance. Since the performance of a polymer is largely dependent on its preparation conditions, this study also investigates into the effects of their preparation conditions (such as, polymerisation type, polymerisation length and polymerisation temperature) on both the physical properties and mycotoxin recognition performance of the resulting polymers. The chapter begins with a brief overview of recent literature, the first section of which discusses the importance of mycotoxin detection, different methods currently being employed in detecting mycotoxins and the scope of using polymers as alternative recognition materials in ToxiQuant. It is then followed by methods used for polymer

preparation and their physico-chemical analysis. Then the final section continues with the discussion of the obtained results and presents a future outlook on the current study.

4.2. Introduction

Toxins are secondary metabolites produced by various microorganisms such as virus, bacteria or fungi for their self-defence or growth; however they could be harmful to other animals and humans. Mycotoxins are such secondary metabolic toxins produced by fungi, termed as moulds. They tend to grow in the crops of many commodities having moisture content of more than 7 % by weight at the time of their harvest. Such commodities includes nuts, cereals, oil, coffee, spices, fruits, cocoa etc. (1). If not until their harvest, the crops may also grow mould during their improper storage or processing.

Among different types of mycotoxins, aflatoxin (AFT) and ochratoxin (OT) are the most prevalent and found in abundance in various foodstuffs. Figure 4.1 shows the chemical structures of most commonly found mycotoxins.

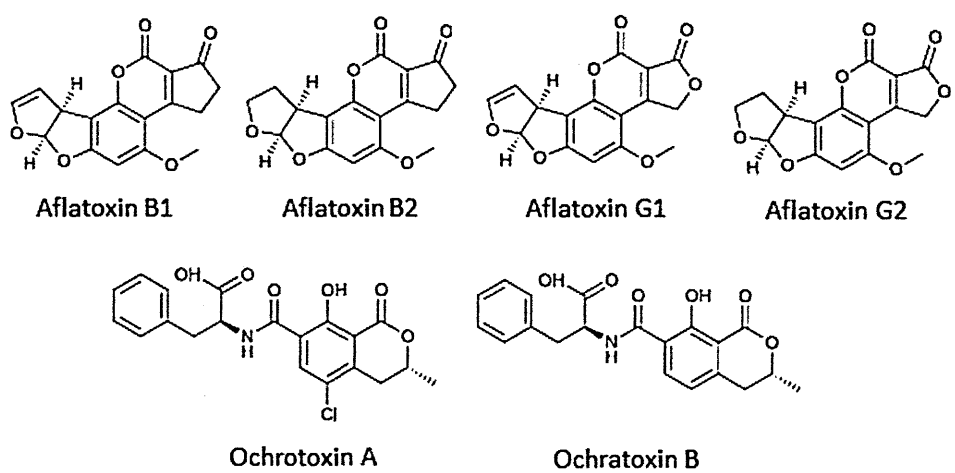

Figure 4.1: Chemical structures of commonly occurring mycotoxins in food samples; adapted from (2-4).

Structurally, AFT are difuranocoumarin derivatives which fluoresce when exposed to UV irradiation. Based on their fluorescence and separation pattern on a chromatographic stationary phase, they are classified into four types, B1, B2, G1 and G2 (2,3). In fact, B and G abbreviations refer to their blue and green fluorescence respectively (5). Indeed, it is the self-fluorescent nature of AFT that makes their detection very convenient and sensitive by simple fluorescent detectors used in conjunction with LC and GC chromatography systems (4).

Among different AFT varieties, AFT B1 is highly abundant and is found to be the most toxic too. Earliest study on bacteria has already established that AFT B1 is converted to harmful epoxide form in the cells by biological enzymes, such as cytochrome P450 (6). Once inside the cells, a strong intercalation between nucleophilic DNA and highly electrophilic AFT epoxide results in impaired DNA transcription and causes genotoxic damage too (7). Studies have further shown that such malfunctioning codon sequences may even mutate the tumour suppression gene and result in cancer (8). Albeit, the severity of AFT related health problems largely depend on their amounts ingested, their processing conditions and the strain of the fungus producing them (9).

Therefore, it is essential to regulate the levels of AFT in the foodstuff and in animal feed. It wasn't until the 1960 when proper laws were laid for their control in food. This came after the widely reported Turkey X disease in England where about 100,000 turkeys died on eating AFT infected groundnuts which were imported in the country (10). Another outbreak of aflatoxicosis in Kenya also led to severe poisoning, this time among its wide population (11). Therefore, the USFDA (United States Food and Drug Administration) and European Union have laid strict guidelines for the permissible limits of AFT, down to ppb (parts per billion) levels (12). In spite of such efforts, FAO (Food and Agriculture Organisation) suggests that about 25 % of the entire globe's crop is still infected with AFT and is likely to spread in global food supply chain unless monitored carefully (13). Table 4.1 shows the AFT allowance in food across the world.

Table 4.1: AFT amounts found in food and its permissible amounts globally; adapted from (13-16).

Area	Total AFT range found in food ($\mu g\ kg^{-1}$)	Maximum AFT limits guided by FAO ($\mu g\ kg^{-1}$)
Africa	10-22	10
Asia/Oceania	5-35	15
Europe	0-12	5
Latin America	0-35	20
North America	15-20	15-20

Another major mycotoxin type commonly found in foods is ochratoxin (OT) which is dihydroisocoumarin derivatives as well, namely OTA and OTB. OT is the most prevalent and is found in a variety of nuts, cereals, wine, rice and spices (4). They are relatively stable and can survive extreme temperatures of cooking or freezing too. This means that once produced, they

do not degrade but deposit in the animal meat fed on a toxin contaminated crop. And from this point, they can enter the human food chain too; moreover they are not even degraded either by cooking or by human digestive enzymes (4). This may result into OT deposition in blood, liver and adipose tissues causing acute kidney, liver dysfunction and even immune depression. In some cases, they can also be teratogenic, mutagenic and carcinogenic by inhibiting participation of phenylalanine in the vital protein synthesis (3,4,10). Since, OT is present in very low concentrations (ppb level); it also becomes quite challenging to detect them. Therefore, most countries across the world have guidelines for the permissible limits of OT in food samples and animal feed (3).

Besides AFT and OT, numerous other types of mycotoxins are produced by about 500 known fungal species. Although toxin production is specific to a certain genotypic fungal strain, sometimes the same mycotoxin is produced by a variety of species depending on the climatic conditions. As a result, different mycotoxins tend to show much diverse range of physicochemical properties and are difficult to be detected by a single analytical technique. Hence, major types of mycotoxins are classified on the basis of their chemical structure, the body organ they target or the source of fungi that produce them.

Since AFTs and OTs are found to be most abundant and toxic, the research presented in this chapter will focus on their detection from nut samples, mainly peanuts (17). Also that the presented research is focused on developing polymers as recognition materials for mycotoxin detection, it would be important to discuss the methods currently being used for the preparation and analysis of mycotoxin containing food samples.

Mycotoxin samples are prepared in three main steps which include sampling, homogenisation of the food material and mycotoxin extraction from this homogenised food matrix. The extracted mycotoxins are then analysed by chromatographic or immunological detection techniques (10). The primary step of mycotoxin extraction from the food matrix is a crucial step, widely regarded as the clean-up step (18). It is carried out by classic extraction techniques, such as, liquid-liquid extraction (LLE), supercritical fluid extraction (SFE) and solid phase extraction (SPE) (3). The optimisation of clean-up step depends on both the type of mycotoxin being extracted as well as the type of food matrix it is extracted from. For example, AFT is highly hydrophobic which demands the use of non-polar solvents such as n-hexane; whereas OT is soluble in methanol and acetone. In general, almost all mycotoxins are largely soluble in polar organic solvents, such as acetonitrile, dichloromethane (DCM), chloroform and methanol (13) and are widely used for toxin extraction from various food matrices.

Sometimes, acidified solvents are also preferred for extracting fatty mycotoxins as they aid in breaking bonds between the toxin and other fatty constituents of food, especially in nuts. Apart from these classic extraction techniques, some newer techniques have also been reported in the literature which includes pressurised liquid extraction (PLE), where mycotoxins are extracted with solvents at elevated temperature (200 °C) and pressure. However, sometimes PLE tends to co-extract interfering compounds from the matrix as well due to higher temperatures (19). Supercritical fluid extraction (SFE) is another newer extraction technique, where highly dense supercritical CO_2 elevates pressure to aid in mycotoxin extraction from the food matrix. However, this extraction technique is highly expensive and the polar nature of most mycotoxins makes it difficult to be penetrated by supercritical CO_2 used.

It is evident from the literature that in spite of some newer extraction techniques, classic liquid-liquid extraction (LLE) and solid phase extraction (SPE) still remain the most widely used methods for mycotoxin clean-up due to their ease of operation and cost-effectives (3,13). In an LLE based mycotoxin extraction, usually higher volumes of solvents are shaken with the powdered food sample to extract mycotoxins. Although alternative use of hollow fibre based LLE is found to perform superior extractions, it is still inconvenient and unsafe compared to SPE due to handling and shaking of large volumes of toxic organic solvents (20). On the other hand, a typical SPE based extraction protocol includes stationary phases which are packed into polypropylene cartridges and mycotoxin containing food samples are passed through them. This provides an affinity based separation of mycotoxins from other interfering food components onto the stationary phase. An optimised SPE protocol is safer, quicker and utilises little volumes of solvents compared to LLE. In addition to this, SPE stationary phases are often reused making it very cost-effective for industrial applications. The stationary phases used in an SPE based mycotoxin clean-up include either whole or combinations of normal phase silica, reverse phase C-8 or C-18, octadecyl chains end capped silanes, charcoal and other ion-exchange polymer derivatives, largely referred to as Mycosep® and Multisep® (21). It has been established that an SPME (solid phase micro extraction) may even surpass the performance of an SPE protocol as it can carry out simultaneous sample clean-up from multiple food matrices (11,22). For an example, a carbon fibre based stationary phase in an SPME clean-up could achieve high throughput by multiple extractions of OT from as many as 96 samples with the LOD (Limit of Detection) down to 0.3 ng mL^{-1} (3). An example of a typical LC chromatogram obtained by SPME clean-up is shown in Figure 4.2.

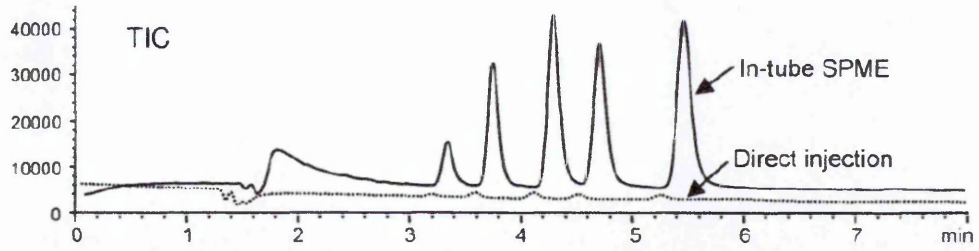

Figure 4.2: Overlay of typical ion chromatograms (TIC) obtained by LC-MS system with and without an SPME clean-up step for the separation of multiple mycotoxins; adapted from (11).

Figure 4.2 shows an LC chromatogram indicating that an SPME based clean-up gives a highly resolved mycotoxin separation in comparison to a poorly resolved chromatogram obtained without an SPME clean-up. With the realisation of numerous advantages offered by SPE over other clean-up techniques, it makes an ideal method for developing simple mycotoxin clean-up protocol. However, the normal or reverse phase stationary materials used in SPE may not be selective for the separation of complex matrices, such as a food matrix containing different mycotoxins.

To resolve this, immuno-affinity columns (IAC) are widely used as stationary phases where monoclonal or polyclonal antibodies are embedded into cartridges. An IAC based clean-up gives cleaner mycotoxin extracts compared to any other clean up method due to higher selectivity and specificity of antibodies towards their targets. At the same time, tremendous specificity of antibody towards its target toxin may make it less favourable for the separation of other toxins or their mixtures. However, AflaOchra™ is an IAC where simultaneous clean-up of both AFT and OT is made possible by using combination of different antibodies (17). Compromised stability and high cost of antibodies still are considered to be major drawbacks of an IAC based sample clean-up. The clean-up cartridge used in ToxiQuant (ToxiTrace®) is also an immuno-affinity based material which suffers from the same limitations. Therefore, the research interest lies in developing alternative materials for mycotoxin clean-up in ToxiQuant technology which will be discussed further in the following sections.

Just before discussing ToxiQuant technology further, it would be important to discuss how mycotoxin quantitation is usually carried out once they are cleaned up from the food matrix. Quantitation of mycotoxins is mainly carried out by chromatography or immunoassay based techniques coupled with various detectors in offline or online mode. These mainly include, thin layer chromatography (TLC), gas chromatography (GC), high performance liquid

chromatography (HPLC) and enzyme linked immuno-sorbent assay (ELISA) (23). TLC is the most basic chromatographic technique where silica gel or C-8 end capped silica grafted to a glass, or metal sheet is commonly used as a stationary phase for the separation and immobilisation of both AFT and OT. The technique is useful particularly for semi-quantitative analysis in conjunction with UV-visible spectrophotometer or fluorimeter for toxin quantitation. Although, it helps screen a broad range of mycotoxins at lower cost, it still demands an efficient sample clean-up of complex mycotoxin containing matrices and lacks automation too. Therefore, TLC is less preferred these days when there are other automated and more accurate chromatographic techniques already available for toxin quantitation. GC is one of the classic chromatography techniques that may be used for mycotoxin quantitation in conjunction with an MS detector for a more precise quantitation than that obtained by TLC (3). But the major drawback is that the most mycotoxin types need derivatisation prior to their separation by GC as they are non-volatile in nature. This is well reflected in the published literature which shows that only about $1/6^{th}$ of the total chromatography based toxin detection studies have been carried out by GC (13). To this end, liquid chromatography is preferred over GC as it does not demand any complex chemical derivatisation prior to mycotoxin separation and quantitation. LC systems are usually combined with Photodiode Array detectors (LC-PDA), Mass Spectrometers (LC-MS) and Fluorescence detectors for toxin quantitation (22-25). Lately, there has been a growing interest in using quadruple MS or MS-MS detectors as well which can quantify multiple mycotoxins in a single-step protocol; however towering costs and complexity of such sophisticated MS detectors has made it less welcomed universally (26-32).

The second major technique used for mycotoxin quantitation is based on immunoassays where the toxin is separated by using antibodies which is then followed by their quantitation with the help of fluorescence detectors (33-35). In fact, currently available ELISA detection kits are faster than HPLC with the equivalent LOD of about 10-20 ng g^{-1} for most food samples (36). However, immunoassays exhibit a much shorter shelf-life due to their sensitivity towards changes in the pH and temperature due to the antibodies used; not to mention they are non-reusable and highly expensive too (20). This limits the use of immunoassay based mycotoxin detection for industrial applications; particularly lower stability of antibodies is a big drawback which restricts its use in different climatic conditions across the globe.

Capillary electrophoresis (CE) is another useful method for separating closely related mycotoxin molecules based on their charge and mass values. These are usually coupled with simple fluorescent detectors avoiding the need for an MS-MS or other complex and expensive

detectors (3). However, CE based mycotoxin separation has not yet been thoroughly investigated and it still poses the issues of high maintenance and expensive instrumentation. Weighing all the odds, HPLC still remains the most widely used method for industrial scale mycotoxin detection with the LOD of about 0.1 ng g^{-1} (13,36). This is well reflected in Figure 4.3 which shows that the frequency of the use of LC based chromatography system is much higher than other analytical techniques for mycotoxin detection.

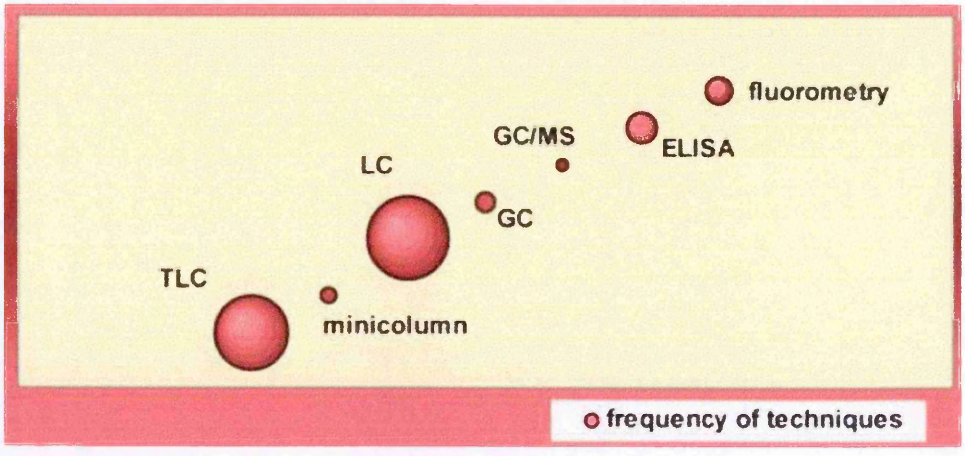

Figure 4.3: Schematic of the frequency of analytical techniques used for mycotoxin analysis for the regulatory purpose; adapted from (14).

There also have been reports of development of faster and novel detection techniques, such as, membrane based or flow through immunoassay (37), lateral flow test strip and membrane selective flow assays (15,38,39). However, these techniques are not yet fully investigated for mycotoxin detection on industrial scale. Not to mention, they already have limitations due to integration of short-lived, expensive and non-reusable antibodies in them. Table 4.2 summarises IA and SPE based mycotoxin detection techniques.

Table 4.2: Summary of IA and SPE based techniques for mycotoxin analysis; regenerated from (15)

	ELISA	Flow through assay	Lateral flow test	Fluorimetric assay with IA clean-up	Fluorimetric assay with SPE clean-up
Type	Quantitative	Semi-quantitative	Semi-quantitative	Quantitative	Quantitative
Limit	2.5 ppb	20 ppb	4-20 ppb	1 ppb	5 ppb
Recovery	~ 94-122 %	N/A	N/A	105-123 %	92-102 %
Time	< 25 min	< 5 min	5 min	< 15 min	< 5 min
Detection	Plate reader	N/A	N/A	Fluorimeter	Fluorimeter

Although newer methods, such as flow through assay and lateral flow tests are quicker, they provide semi quantitative analysis of mycotoxins. This reiterates that HPLC is widely preferred method for mycotoxins detection in spite of its complex and expensive instrumentation. However, it would be important to mention here that the use of HPLC needs scientific expertise and elaborate training on instrumental protocols. This makes it very challenging for a non-scientific personnel to carry out a quicker on-site check of food samples either received or dispatched at various stages of the supply chain. Additionally, HPLC demands high maintenance and large volume of solvents too. In this regard, need for a simple, rapid and inexpensive analytical technique has been addressed by Toximet with ToxiQuant as their first prototype technology (36). Section 4.2.1 discusses the principle and working of ToxiQuant technology.

4.2.1 ToxiQuant

ToxiQuant is the first prototype analytical technique developed by Toximet that can separate and quantify different mycotoxins simultaneously from foods such as nuts. Unlike currently used analytical systems, such as HPLC, ToxiQuant is a portable device that functions with ease and high accuracy without the need for extensive operational training. This means the non-scientific staff dealing with the food supply chain could be easily trained to use it unlike complex operation and extensive training needed for operating HPLC systems. Not to mention, mycotoxin detection in ToxiQuant takes just a couple of minutes in comparison to elaborate procedure and complex instrumentation needed for an HPLC based toxin detection protocol (40).

Mycotoxins are strongly bound to the lipid and other constituents in the food samples which demand their careful extraction from the rest of the food matrix (as discussed earlier in Section 4.2). The protocols used in a ToxiQuant based mycotoxin clean-up or sample preparation are based on SPE, where the filtered extract of a food sample is introduced into the tailor-made SPE cartridge using a typical SPE manifold to extract mycotoxins from other interfering food constituents mainly lipid which are in abundance in nuts. At the end of a clean-up, interfering components are retained on the cartridge whereas mycotoxins pass through. Figure 4.4 shows the schematic describing the clean-up step for the food samples containing mycotoxins.

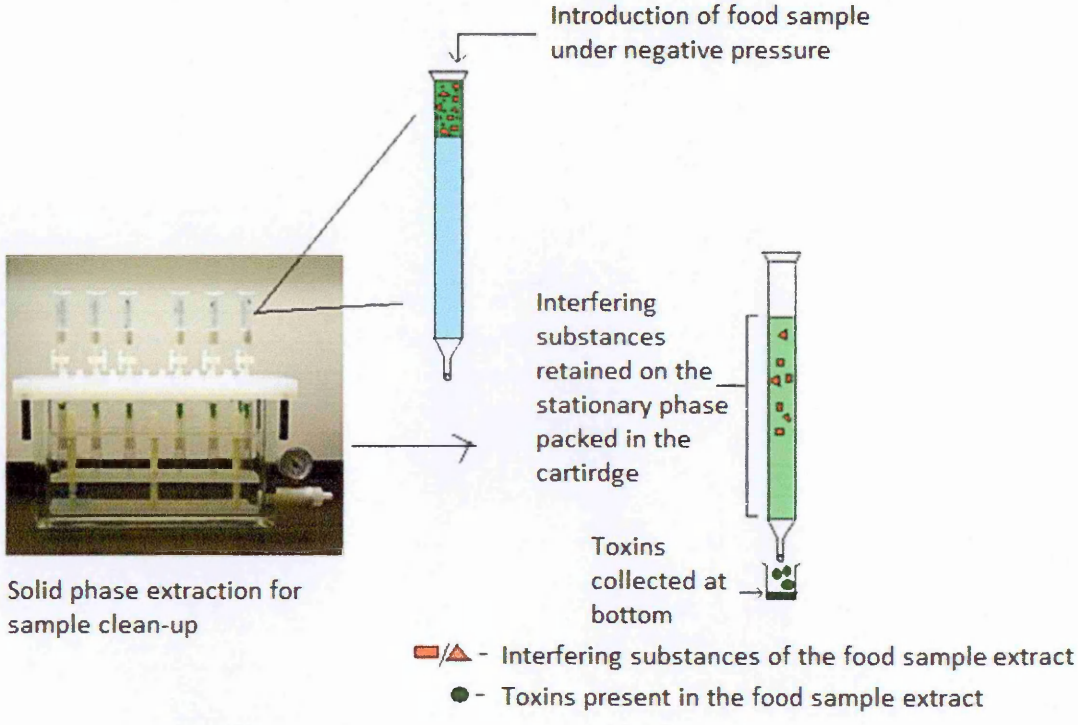

Figure 4.4: Schematics of the mycotoxin clean-up step from the food samples.

Mycotoxins collected from the bottom of the clean-up cartridge are then transferred to another cartridge onto which it is immobilised and then quantified by ToxiQuant. This cartridge is referred to as Toxitrace®. Figure 4.5 shows the schematic describing quantitation of extracted mycotoxins by ToxiQuant.

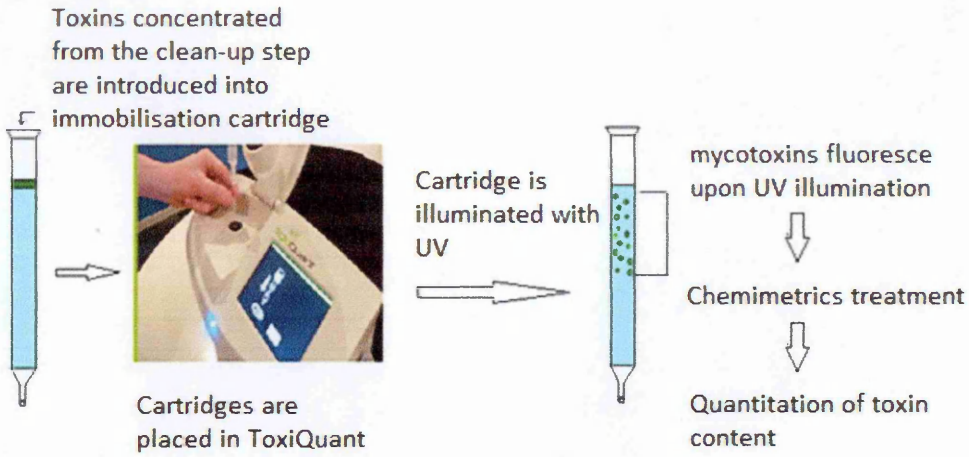

Figure 4.5: Schematics of mycotoxin quantitation step in ToxiQuant technology.

Cartridge containing immobilised mycotoxins sits in the sample holder of ToxiQuant as shown in Figure 4.5. The cartridge is then illuminated with the UV-visible light that makes mycotoxins fluoresce and detected further by built in spectrometer. The resulting spectrogram is then chemometrically treated (40,41). This gives the amount of % of each mycotoxins present in the sample under study. Impressively, the entire process just takes a few minutes in comparison to lengthy sample preparation and analysis carried out in LC based detection systems. ToxiQuant consists of a UV lamp, an SPE cartridge holder, fluorescent detector, some optics, mechanics and software (36). Figure 4.6 shows a summary of the operational steps involved with ToxiQuant technology.

(a) (b) (c)

Figure 4.6: Operational steps of ToxiQuant system, where (a) is the start-up screen displaying cartridge loading into its holder, (b) is the mycotoxin immobilised cartridge being placed into the sample holder and (c) is the toxin count number displayed on the screen as a result of rapid chemometric analysis.

When immobilised mycotoxins are irradiated with the UV light inside ToxiQuant, they tend to show fluorescence. It is important to mention here, that the cartridge holder in ToxiQuant is

specifically designed to allow it to rotate around its axis to move freely which ensures an accurate reading of the total fluorescence from all directions. This unique design of ToxiQuant technology suggests that it can function with a much diverse range of analyte of interest, as long as they show fluorescence upon UV irradiation. In fact, ToxiQuant could be further investigated as a platform technology for the detection of toxins from various other chemical and biological sources, such as, environmental pollutants, pathogens causing food poisoning and even counterfeit drugs. However, the key issue in its further development is the compromised stability of antibodies used which could be addressed by developing stable and cost-effective alternative stationary phases for ToxiTrace® for extraction and immobilisation of the analytes of interest. The following part of the introduction will discuss the limitations of the ToxiQuant cartridges and scopes of further improvement in them.

4.2.2. Scopes of improvement in ToxiQuant

Tailor-made cartridges currently being used in the ToxiQuant are immunoaffinity (IA) types. Here, antibody (Ab) selective for the recognition of a specific mycotxin is covalently immobilised onto a solid stationary phase such as, silica and polysaccharides (agarose) (42). Having immobilised antibodies in them, IA cartridges can be handled only with aqueous solvents. Hence, the choice of clean-up solvents becomes limited to either methanol or acetonitrile (43). Due to higher molecular weight of antibodies, IA cartridges may exhibit poor mycotoxin recognition performance too (44). Moreover, these cartridges suffer from high cost, non-reusability and short shelf-life due to easy denaturation of the antibodies (as discussed earlier in Section 4.1) (45). In this regard, there has been growing interest in developing chemiluminescent biosensors as an alternative to the traditional SPE styled cartridges (46-48); however the fundamental problem of using antibodies as recognition materials in these cartridges make them less stable, tedious to operate and expensive to use. Alternative cartridge packing materials, such as, aptamers are widely investigated as recognition elements that can be used in biosensors as a direct replacement of biological antibodies. Aptamers or antibodies used in this way can also be immobilised onto metal nanoparticles such as, iron oxide and gold which not only immobilise the recognition element (Ab or aptamer) but also enhance the electrochemical signal for the detection of analyte (49-54). Selective interactions between DNA and their target AFT can be implemented in sensors, not to mention that DNA is more stable as compared to antibodies (51,55,56). However, their design and optimisation is much complex, elaborate and expensive. This makes synthetic polymers as the most suitable alternatives to be investigated as SPE stationary phases for the sample clean-up purposes. Unlike biological recognition elements (such as, Ab or aptamer), polymers are very robust, cost

effective and reusable and have been used as stationary phases for SPE, HPLC and other chromatographic techniques for separation, detection and quantitation of a wide range of mycotoxins (4,57,58). More importantly, polymers can be tailor-made for any analyte of interest unlike elaborate selection process of SELEX for aptamers or clonal selection used for antibodies (as discussed earlier in Section 2.2). Most polymers are medium to long chain linear organic materials which are used as reverse phase C8 to C18 stationary phases (30,58-61). However, some highly cross-linked polymers have already shown improved AFT recognition as compared to C8 based SPE stationary phases (62,63). MIPs have also been investigated as SPE stationary phases for mycotoxin analysis (4,54,57,64). Earlier studies conducted by researchers at Toximet and the University of Leicester have found that careful optimisation of pre-polymerisation recipe can generate highly specific cross-linked polymers for mycotoxin clean-up. The research has shown that computational modelling can yield highly specific monomers for the selective recognition of the target analyte equivalent to that of the MIPs. This is particularly useful whilst preparing polymers for mycotoxins since it is devoid of the challenges faced in imprinting bulky mycotoxin molecules and also minimises the possible risk of toxin leaching from its matrix in post-polymerisation stages (36,65).

Although the recipe for preparing clean-up polymers for ToxiQuant technology is established, the investigated polymers are currently in monolithic form. As discussed earlier in Section 2.5, monolithic polymers are irregular in shape which is likely to result into their inconsistent packing inside the cartridge. This may be reflected further into hindered binding and removal kinetics of the target analyte too. Therefore, the aim of the presented study is to develop different polymer formats using the standard recipe provided by Toximet. To this end, polymers have been prepared in both monolithic and microparticulate format since spherical microparticles can improve existing performance of ToxiQuant by the virtue of its improved packing and rebinding kinetics in comparison to monoliths (as described earlier in section 2.5). In this study, monoliths have been prepared by oven, UV and MW polymerisations; whereas the microparticles have been prepared by suspension, precipitation and core-shell polymerisations. Prepared polymers have been packed into SPE cartridges in triplicates and sent to the team of researchers at the University of Leicester and Toximet to test them for their mycotoxin recognition performance. Since different experimental parameters are likely to reflect into the physical make-up and thereby recognition performance of the resulting polymers (as discussed earlier in Chapter 3), the presented study also encompasses investigation into different experimental parameters associated with each polymerisation method and its influence on the physicochemical properties of the resulting polymers. Section 4.3 includes the materials and methods used in the preparation of the polymers.

4.3 Materials and methods

This section contains the materials and methods used in the preparation and analysis of the polymers.

4.3.1. Materials

Diethyleneamine ethylmethacrylate (DEAEM), ethyleneglycol dimethacrylate (EGDMA), divinylbenzene (DVB),2,2'–azobis(isobutyrilnitrile) (AIBN), 1,1'-azobis (cyclohexanecarbonitrile) (AICN), dimethylformamide (DMF), Triton X-100 [4-(1,1,3,3- tetramethylbutyl) phenylpolyethylene glycol], PVP (polyvinylpyrollidone), toluene and chloroform ($CHCl_3$) were purchased from Sigma-Aldrich (UK). Glass beads (75 µm, Supelco), SPE cartridges (Supelco, 1ml polypropylene tubes) and vacuum manifold (Visiprep™, Supelco) were purchased from Supelco (UK). Double-distilled water (Millipore, UK) was obtained from in house distillation unit and used for analysis. All the chemicals and solvents were analytical or HPLC grade and were used without further purification.

4.3.2. Molecular modelling

Molecular modelling for the polymerisation recipe was carried out in collaboration with the researchers at the University of Leicester under the supervision of Dr. Elena Piletska and Dr. Kal Karim. The computational modelling was used to identify the most suitable functional monomer and the cross-linking monomer and their ratio that would produce the cross-linked polymer with the best possible recognition of mycotoxins of interest that is AFT and OT. The system used for modelling was the Centos 5 GNU/Linux. The system was configured with a 3.2 GHz core 2 duo processor, 4 GB memory and a 350 GB fixed drive with software packages SYBL 7.0 (Tripos Inc., St. Louis, Missouri, USA).

4.3.3. Screening of a suitable monomer

The choice of the functional monomer was performed by using LEAPFROG algorithm in the configured computer system as described above. LEAPFROG algorithm allows choosing the most suitable monomer candidate by performing its bond forming energies with the target template. It is carried out by considering about 10,000 iterations for each monomer. LEAPFROG was used to screen the best monomer candidate from the library of about 20 most commonly used monomers. It would do so by assessing every single monomer molecule from the library for its ability to bond with the target mycotoxin in all possible conformations. This is because the monomer would need to make easier but reversible non-covalent bonds (such as hydrogen, dipole-dipole, ionic, electrostatic and hydrophobic and Van-der-Waal interactions)

with the mycotoxin for repeated binding and removal from the resulting polymer matrix. In this regard, the monomer was chosen on the basis of their binding score (Kcal mol^{-1}). Energy minimisation was performed on mycotoxin, where the charges on the each atom of the mycotoxin were calculated and minimised down to the value of 0.01 Kcal mol^{-1} binding score. Form this; it was found that the monomers that could predominately form electrostatic, Van-der-Waal and hydrogen bonds with target mycotoxin would be favoured on the basis of their binding score given by LEAPFROG. Target mycotoxins were then used for the screening of the monomers from the virtual library.

4.3.4. Molecular dynamics

After choosing a combination of monomers, their optimisation was carried out by an earlier protocol (65). Here the monomeric mixture including the functional monomer and the cross-linking monomer are pre-arranged and are saturated in a space in a defined box which is heated at 600 K and cooled slowly to 300 K. The heating and cooling is achieved by minimising the box by the molecular mechanics at the intervals of 100 K. Following this, Energy minimisation was minimised (to the value of 0.05 Kcal mol^{-1}). At the end of the cycle, the total number and the positions of the monomers were examined.

4.3.5. Synthesis of polymer monoliths

Polymer monoliths were synthesised thermally by MW assisted polymerisation. Different ratios of DEAEM (5 wt %, 15 wt % and 20 wt %), DEAEM / DVB (95 wt %, 85 wt % and 80 wt %) and AIBN/AICN (0.5 wt %, 15 mg) were added together in a 10 mL Pyrex test-tube. To the monomeric mixture, DMF (50 wt %, 1.58 mL) was added as the porogen. The pre-polymerisation mixture was degassed by purging N_2 for 15 minutes and the test-tube was then sealed. The tube was placed in the MW reactor (Discover Benchmate, CEM, Matthews, NC, USA) and heated with variable MW powers (from 5 W to 150 W) for 15 minutes at the set temperature of 60 °C. The polymerisation temperature was monitored by an *in situ* infra-red thermometer, which stopped inputting MW irradiation (0 W) when the desired temperature was attained. This was to ensure that the polymerisation was carried out at desired temperature for the fixed length of time 15 minutes. Series of control polymers were also prepared thermally by convection oven at 60 °C for 8 hours and by UV irradiation at 20 °C for 8 hours.

It would be important to mention here that the experimental parameters of MW polymerisation chosen whilst preparing ToxiQuant polymers are based on the earlier findings from the analysis of caffeine MIPs (Chapter 3). For example, earlier study on the caffeine MW

MIPs suggested that quicker heating rates of MW reactor (such as 300 W), longer polymerisations (30 minutes to 60 minutes) and higher temperatures (75 °C- 90 °C) failed to improve surface area, pore volume, cross-linking degree or even template recognition performance of the resulting polymers (as discussed in Chapter 3). Therefore, shorter polymerisation time (15 minutes), lower temperature (60 °C) and lower MW powers (5 W to 150 W) have been chosen to prepare ToxiQuant polymers by MW polymerisation in the presented study. Where the effects of polymerisation time and temperature have been widely investigated earlier, MW powers have not been fully investigated for their potential effects on the recognition properties of the polymers. Hence, this chapter will emphasise on studying the effect of different MW powers on physical properties and recognition performance of the resulting MW ToxiQuant polymers. Since the range of MW powers chosen here is similar to that used for preparing caffeine imprinted MW MIPs, it would allow generating a comparative study from the findings obtained in this study with the earlier findings (Chapter 3).

Once the polymerisation was over, the monoliths were crushed and wet ground in a mortar and pestle using methanol. The ground polymer particles were then passed through 63-125 µm sized sieves to remove fines. The particle size fraction that passed through the 125 µm but retained on the 63 µm sieve was left to dry in a fume cupboard. Dried polymer particles were then transferred into soxhlet extraction thimbles (Fisher, 22×80 mm cellulose thimbles) and extracted in the soxhlet apparatus using methanol for 24 hours allowing over 100 washing cycles (15 minutes per wash cycle). Cleaned polymer particles were then dried and stored in air tight labelled vials.

The polymerisation recipe was optimised by changing the ratio of the monomer to the cross-linker from 5:95 to 15:85 and finally to 20:80. Polymeric monoliths were then prepared by using the optimised polymerisation recipe in different experimental conditions as summarised.

Table 4.3: Summary of different polymer monoliths prepared by MW assisted polymerisation

Polymerisation time (minutes)	Polymerisation temperature (°C)	MW polymerisation power (W)
15	60	5
15	60	10
15	60	20
15	60	50
15	60	100
15	60	150

This optimised polymer recipe was also used to prepare polymer micro particles by other methods.

4.3.6. Synthesis of polymer microparticles: suspension polymerisation

Synthesis of polymer microparticles was carried out by suspension polymerisation. As the monomer phase was hydrophobic in the current polymer recipe, an O/W type of suspension polymerisation protocol was established where hydrophobic monomer phase was dispersed into continuous aqueous phase. In order to achieve homogenous stirring, motorised shaft rotors were used. Extra care was also taken in maintaining reaction temperature by attaching the polymerisation flasks to the condenser with thermometer for constant monitoring of the reaction temperature. The polymerisation flasks were also equipped with the constant supply of N_2 throughout the polymerisation. As explained earlier in Figure 2.10, typical suspension polymerisation set up was used in these experiments too (see Figure 4.7).

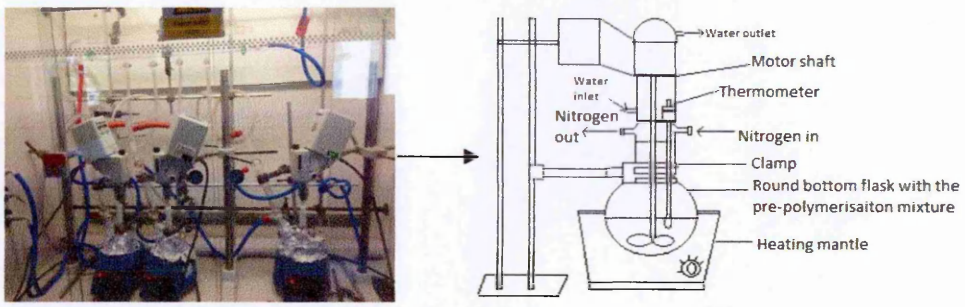

Figure 4.7: Experimental set up for suspension polymerisation reactions.

Other experimental parameters such as, volume of the reaction mixture, ratio between the dispersed and the continuous phases, stirring speed and type and amount of the dispersant were optimised once at a time whilst other parameters were kept constant. The polymerisation temperature and time were kept constant at 90 °C and 8 hours respectively to ensure that the suspension polymers were prepared in comparable conditions to that of oven, MW and UV polymers. For faster optimisation, six parallel 250 mL reaction set ups were run at a given time (as seen in Figure 4.7). Optimal volume ratio of the dispersed phase to the continuous phase was found to be 1:10. In order to optimise the stirring speed, different speeds were tried in the range of 200 rpm to 800 rpm. The speed yielded the highest amount of polymer beads in desired size range (63-125 μm) was chosen for carrying out further experiments. Lower stirring speed for up to 300 rpm resulted in bigger polymer aggregates lumps whereas; speed above 600 rpm resulted into much of the polymer sticking to the wall of

the flask. So, 500 rpm was the chosen speed of rotation for carrying out further polymerisations.

To formulate this O/W suspension, different amounts of the dispersant PVP (0.1 wt % to 1 wt %) were tested as described earlier (66,67). Thereafter, different concentrations of the non-ionic surfactant Triton X-100 (0.5 mM to 20 mM) were also tested to form a flocculent suspension as described earlier (68-70). The selection of the optimal concentration of dispersants was also made on the basis of the total yield of desired particle size range (63 µm-125 µm). It was found that the optimal amounts of PVP and Triton X-100 were 0.5 wt % and 10 mM respectively. The porogen should be miscible with the monomer phase in a suspension polymerisation recipe to intrude into growing monomeric nuclei. Since the porogen from the original recipe (DMF) was miscible with water, toluene was chosen as the suitable porogen for this O/W dispersion system.

Once all the experimental parameters were optimised, the dispersed phase was prepared by combining DEAEM (0.83 mL, 20 wt %, 0.77 g), DVB (3.37 mL, 30 wt %, 3.1 g) and toluene (4.1 mL, 50 wt %, 3.9 g) in a 10 mL Pyrex test-tube. The continuous phase was prepared with 77.9 mL water with the dispersant PVP (0.1 wt %) or triton X-100 (10 mM) dissolved in it. Both the phases were purged separately with N_2 bubbling for 15 minutes. The continuous phase was taken in a 250 mL round bottom flask and placed on the heating mantle pre-heated to 90 °C temperature. The flask with the magnetic bead was stirred at 500 rpm (as shown in Figure 4.7) to allow the dispersant to mix well with the aqueous phase. Whilst the aqueous phase was stirred, the initiator AICN (0.5 wt %, 21 mg) was added to the test-tube containing the monomer phase and mixed well. The dispersed phase was then added drop wise to continuous phase in the flask and the reaction was continued for next 8 hours. Upon completion of the reaction, the polymer micro beads were filtered through a cellulose filter paper (Whattman, grade 1, 15 mm diameter). Polymer micro beads were dried under vacuum and used for further analysis.

4.3.7. Synthesis of polymer microparticles: precipitation and core-shell polymerisation

To prepare microparticles by core-shell polymerisation, poly (DVB) microparticles were first prepared by precipitation polymerisation. To do so, DVB (3.56 mL, 25 mmole) and AIBN (164.21 mg, 1 mmole) were dissolved in 100 mL acetonitrile. The pre-polymerisation mixture was purged with N_2 for 15 minutes and then polymerised at 60 °C for 24 hours with gentle stirring (71). Upon completion of the polymerisation, obtained polymer micro particles were filtered on a cellulose filter paper (Whattman, grade 1, 15 mm diameter). Dried micro particles were analysed for their particle size and used further for shell formation on it.

For the formation of polymer shell, different weight ratios of the core to shell were prepared from 1:2 to 1:4. For example, to prepare the shell with 1:3 (core: shell) weight ratio, a 3 g of the poly (DVB) core microparticles were weighed and 9 g of the shell monomer mixture was prepared. In a typical shell monomeric phase, DEAEM consisted of 20 wt % of the total monomers (1.952ml); whereas DVB accounted for 80 wt % (7.877 mL) of the monomers. Each core-shell polymerisation flask containing different core: shell ratios (1:2, 1:3, 1:4, 1:10 up to 1:40) were put on the heating mantle in acetonitrile and the precipitation polymerisation was carried out for 24 hours at 90 °C temperature. The resulting microparticles were dried under vacuum and used for further analysis.

All the polymer samples were analysed for its physicochemical properties, such as, DSC, TGA, porosimetry and SEM as described earlier in Section 3.3. Polymers were then analysed for their mycotoxin recognition performance by SPE and HPLC. Section 4.4 describes the SPE and HPLC protocols which were used to study recognition performance of the polymers in this study.

4.4. Polymers analysis

The experimental protocols for the physical analysis (DSC, TGA, porosimetry, SEM) were identical to those used for caffeine MIPs (Chapter 3). Please refer to Section 3.3 for further the details. This section explains the experimental protocol used for SPE based analysis. The optimised protocol used for HPLC analysis could not be provided here due to confidentiality.

To carry out analysis, 100 mg of 20 wt % DEAEM/ 80 wt % DVB or EGDMA polymer was packed into 1 mL SPE cartridges (Supelco, catalogue number- 57023) in triplicate. Peanut extract samples were then spiked with varying concentrations of AFTB1 from 1-10 μg mL^{-1}. Measurements were performed before and after SPE to determine the clean-up and aflatoxin recovery values.

- Conditioning: SPE Cartridge was conditioned with 2 x 1-ml aliquots of 60 % methanol and equillibrated with 1 mL of HPLC grade water using a vacuum manifold (Supleco) equipped with vacuum pump;
- Sample addition: 1 ml of undiluted peanut extract (60 % methanol) containing 10 μg mL^{-1} of AFTB1 was filtered through SPE column at the flow rate of 1 mL min^{-1} and the filtrate was collected;
- Washing: Cartridge was washed with 2 x 1-mL aliquots of 5 % methanol and each fraction was collected in separate vials for analysis;
- Fractions from the sample addition and both the washing steps were collected separately in the vial and quantified by HPLC using fluorescence detector for determining **% sample clean-up efficiency** of the polymer;

- Elution: 1 mL of acetonitrile was filtered through SPE cartridge to extract purified immobilised toxin;
- Eluted AFTB1 were quantified using HPLC coupled with fluorescence detector for determining **% sample recovery** from the polymer.

Section 4.5 discusses the results obtained from different analyses performed on the prepared polymers.

4.5. Results and discussion

Different polymer formats prepared by different methods were analysed for their physical properties and mycotoxin recognition performance. This section discusses the results obtained from the analysis of different polymers under study.

4.5.1. Polymerisation kinetics

A record of experimental parameters, temperature in particular may be useful in understanding the kinetics of a polymerisation reaction. Although it is quite difficult to monitor the temperature of an oven polymerisation, it is possible to do so quite easily whilst using a MW reactor (as described earlier in Section 3.3.3). Here, polymers were prepared for ToxiQuant by varying MW powers that was used for heating the pre-polymerisation mixture. The polymerisation temperature was constantly monitored and recorded temperatures were then plotted as a function of polymerisation time (as explained in section 3.3.3). Figure 4.8 describes the heating rates of different MW polymerisations carried out at different MW powers.

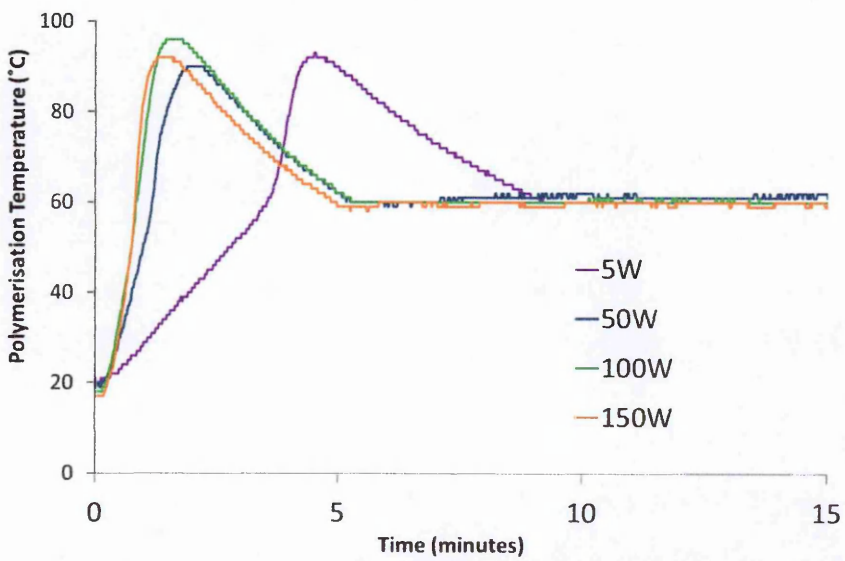

Figure 4.8: Polymerisation tempertaures recorded *in situ* by IR probes when MW assisted polymerisations carried out at 60 °C for 15 minutes with different MW powers.

Before the kinetics could be discussed further, it would be important to reiterate that the amount of energy provided to heat the material in a MW reactor remains the same regardless of the value of MW power used; different power values rather indicate the rate of heating employed by the MW reactor. This way, a lower power would heat the reaction mixture slowly and the higher power would do it at a faster rate (as explained earlier in Chapter 3).

Here, different MW polymerisations shown in Figure 4.8 indicated a power dependent polymerisation kinetics where the heating rate of the thermal polymerisation was found to increase significantly upon increasing the MW power (72). The trend observed here was much similar to what was observed with the MW generated caffine MIPs (as shown earlier in Figure 3.15). From the temperature obtained profiles, the heating rates were also calculated as listed in Table 4.4.

Table 4.4: Heating rate and monomer conversion achieved with different MW powers at 90 °C for 15 minutes.

Microwave power applied (W)	Average heating rates (°C minute^{-1})
5	5
50	25
100	38
150	91

Table 4.4 suggested that when the MW power was increased from 5 W to 150 W, the heating rates increased considerably from 5 °C min^{-1} to 91 °C min^{-1}. The trend observed here was much similar to that observed whilst preparing caffiene MIPs across similar range of MW powers (as described earlier in Section 3.4.1). Notably, the heating rate achieved with 150 W power was significantly higher attaining 91 °C min^{-1} (as seen in Table 4.4). This was much faster than what was observed whilst using 150 W for caffeine MIP preparation (as described earlier in Section 3.4.1). This could be due to the difference in dielectric property of the porogens used in polymerisations, caffeine MIPs and ToxiQuant polymers (please refer to Section 3.2). This is something that is currently under study in our lab and would be of further interest.

Apparently, both acetonitrile and DMF have much similar dielectric constants of 37.5 and 36.7 respectively. Since the porogens have similar dielectric behaviour, the observed difference in the heating rates could also be attributed by the different dielectric properties of the monomer mixtures being used.

To understand the MW polymerisation kinetics better, two different polymerisations were also carried out at 30 °C and 60 °C by using 2 W MW power. The temperature profiles of the polymerisations were recorded by an in-situ IR probe and were plotted as shown in Figure 4.9.

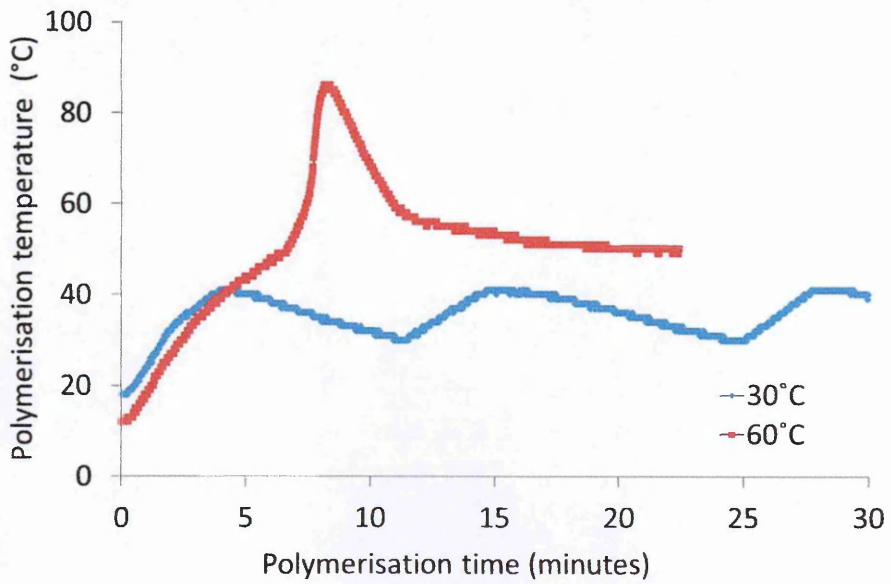

Figure 4.9: Polymerisation tempertaures recorded *in situ* by IR probes when MW assisted polymerisations carried out at 30 °C (blue) and 60 °C (red) by using with 2 W MW power.

When the MW reactor was set to 30 °C, the reaction did not result into successful polymerisation. This was indicated by the absensce of any exothermic bump (as explained earlier in Figure 3.10). On the other hand, a successful polymerisation was observed when the MW reactor was set to 60 °C temperature. As dicussed earlier in Chapter 3, it was expected that a set MW power would heat the reaction mixture at a specific rate to attain the desired temperature. Once the set temperature attained, it would stop inputting any energy and allow the reaction to proceed by its own exothermic energy (please refer to Section 3.4.1). From the analysis of caffeine MW MIPs, it was evident that the polymerisation rates in MW polymerisations were driven by the MW power used for heating the pre-polymerisaiton mixture. In addition to that, lack of a successful polymerisation at 30 °C observed in this study also suggested that the set temperature of a MW reactor was also crucial for a successful polymerisation (as seen in Figure 4.9). This implied that if the polymerisation rate was determined by the value of MW power used, the amount of energy input was determined by

the set reaction temperature. Studies of both the caffeine MIPs and ToxiQuant polymers suggested that the polymerisations carried out below the thermal degradation temperature of an initiator were most likely to be unsuccessful (as seen in Figures 3.17 and 4.9). This was in agreement with the proposed hypothesis that a successful polymerisation in the MW reactor would be possible only due to the molecular heating of the polymerisation mixture without any additional MW effect (as discussed earlier in Section 3.4.1). However, the effect of temperature on thermal MW polymerisations would need further investigation since both the initiators (AIBN and AICN) used in the presented studies (Chapter 3 and 4) were azo initiators. This would necessitate a study of different initiator types across a wider range of temperatures. Several other physical techniques were also used to understand the effect of both the experimental parameters (such as, heating rates of polymerisation) and the reaction components (such as, monomer: cross-linker ratios) on the physicochemical properties of resulting polymers. Section 4.5.2 would discuss the results obtained from the the dynamic scanning calorimetry (DSC) analysis of prepared ToxiQuant MW polymers.

4.5.2. Dynamic scattering calorimetry (DSC)

DSC analysis is routinely used to characterise a cross-linked polymer for its glass transition temperature (T_g) which is an indicative of its cross-linking degree (as discussed earlier in Sections 3.3.5 and 3.4.2). The obtained DSC thermograms of the ToxiQuant polymers were analysed and their T_g were plotted against the MW power used for their preparation. Figure 4.10 presents the degree of cross-linking of MW polymers prepared at 60 °C for 15 minutes.

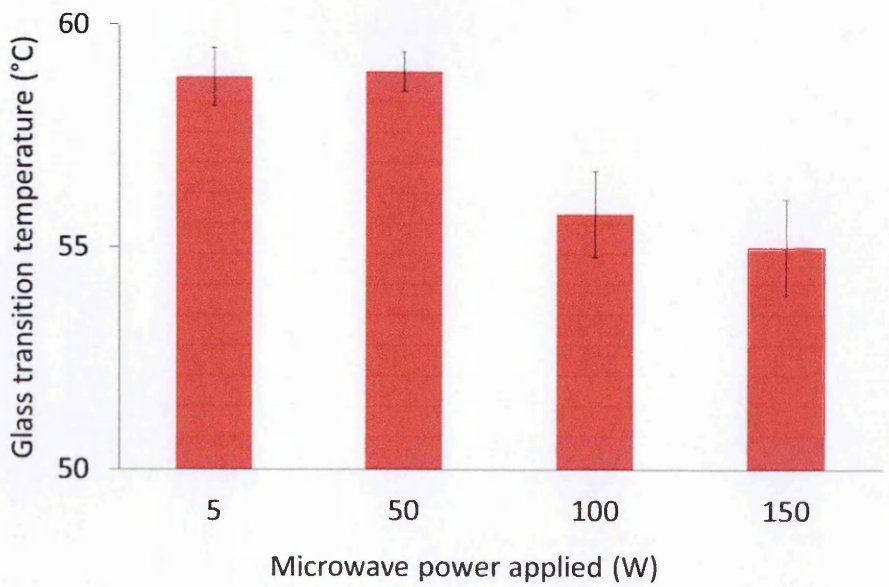

Figure 4.10: Comparison of the T_g of the ToxiQuant polymers (5 wt % DEAEM: 95 wt % EGDMA) prepared by MW reactor at 60 °C for 15 minutes with different MW powers; standard deviations derived from the triplicate measuresments of each polymer sample.

DSC analysis of MW ToxiQuant polymers suggested that the cross-linking degree of these polymers was dependent on the MW power (heating rate) used for their polymerisation. Polymers prepared with 5 W to 50 W powers showed much similar T_g of about 58 °C. However, further increase in the power (from 50 W to 150 W) slightly decreased the T_g values to about 55 °C. Since T_g would represent their cross-linking degrees, it could be implied that their cross-linking degrees slightly decreased as their polymerisation rates (MW powers) were increased from 5 W to 150 W (as seen in Figure 4.10). This suggested that the polymers showed slightly higher cross-linking degree when their polymerisations were carried out with slower MW heating. Likewise, faster heating rates produced polymers with slightly lower cross-linking degree. These observations were in agreement with those obtained from the study of caffeine MW MIPs (as discussed earlier in Sections 3.3.5 and 3.4.2).

The pre-polymerisation recipe was then slightly modified by changing the monomer:cross-linker ratio from (5 wt % DEAEM: 95 wt % EGDMA) to (20 wt % DEAEM: 80 wt % EGDMA). For the ease of undestanding, the ToxiQuant polymers with the formulation of 5 wt % DEAEM: 95 wt % EGDMA would be referred to as 5 wt % DEAEM polymers; whereas the one with 20 wt % DEAEM: 80 wt % EGDMA wpuld be referred to as 20 wt % DEAEM polymers in the presented study. The MW polymers were prepared in identical manner at 60 °C for 15 minutes with different MW powers from 5 W to 150 W. The thermograms obtained from their DSC analysis were then plotted as shown in Figure 4.11.

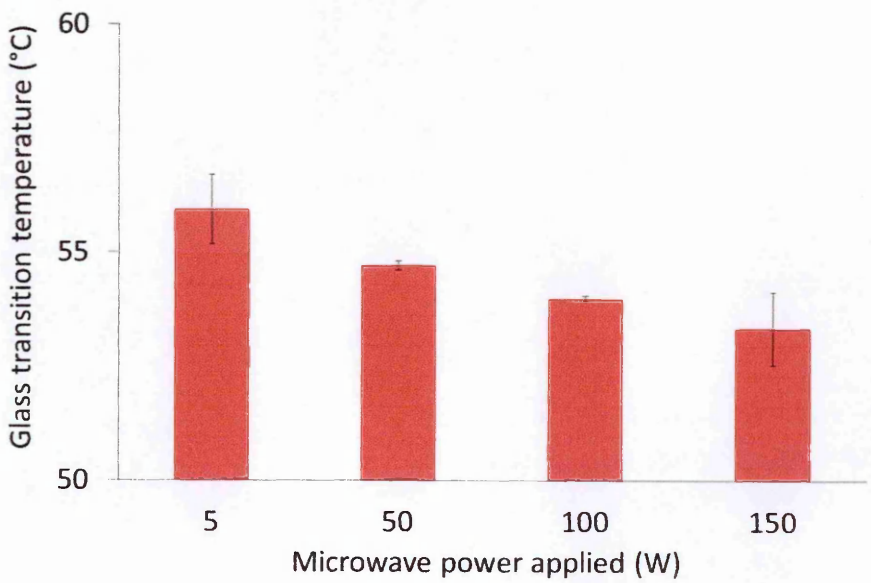

Figure 4.11: Comparison of the T_g of ToxiQuant polymers (20 wt % DEAEM: 80 wt % EGDMA) prepared for different time durations; standard deviations derived from the triplicate measuresments of each polymer sample.

This set of MW ToxiQuant polymers (20 wt % DEAEM) showed a slight decrease in their T_g (cross-linking degree) from 58 °C to 54 °C when their polymerisation rate (MW power) was increased from 5 W to 150 W. Again, the trend observed here in the T_g values of the polymers was much similar to that of the caffeine MW MIPs (as seen in Figure 3.16) and ToxiQuant 5 wt % DEAEM polymers (as seen in Figure 4.11). To understand the effect of relative amounts of monomers on the cross-linking (T_g) of the resulting ToxiQaunt polymers, the results obtained from both the set of pre-monomer mixtures were combined, as plotted in Figure 4.12.

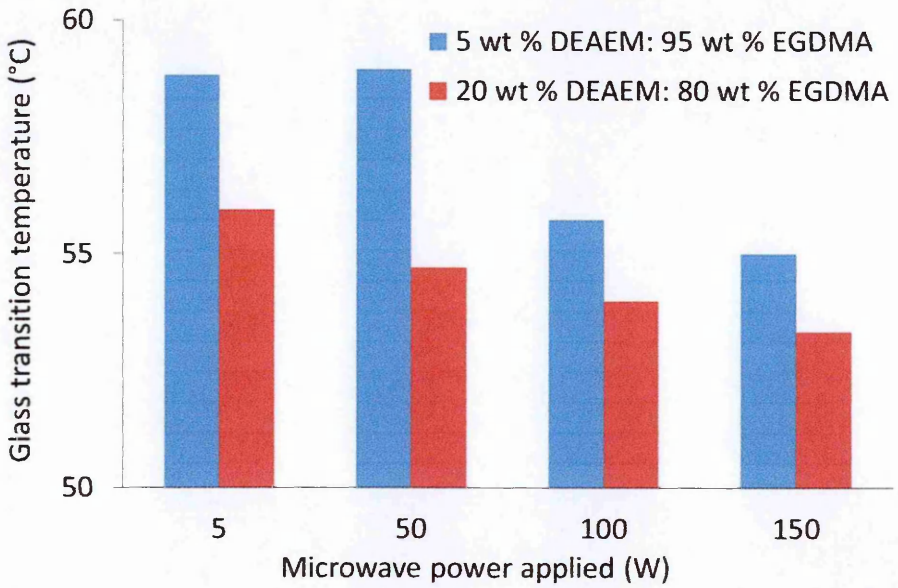

Figure 4.12: Comparative analysis of the cross-linking degree of different ToxiQuant polymers prepared by changing relative amounts of monomers in the pre-polymerisation mixture; blue bars representing the polymer (5 wt % DEAEM: 95 wt % EGDMA); whereas the red bars representing the polymer (20 wt % DEAEM: 80 wt % EGDMA). standard deviations derived from the triplicate measuresments of each polymer sample.

From the correlation, it was also found that the glass transition temperatures (T_g) of the polymers altered upon changing the monomer ratios in the pre-polymerisaiton mixture. The values of T_g and thereby the degree of cross-linking were higher in the polymers with the higher amount of cross-linker (95 wt % EGDMA, shown in blue bars). On the other hand, the polymers with slightly less amount of the cross-linker (80 wt % EGDMA, shown in red bars) showed lowered T_g (as seen in Figure 4.12). This was an expected outcome since the amount of the cross-linker would directly contribute to the cross-linking degree of the resulting polymers.

From the obtained results, it could be concluded that the increase in polymerisation rate (increase in MW power) led to decrease in the T_g (cross-linking degree) of all the MW polymers

(caffeine MIPs as well as ToxiQuant MW polymers) studied so far (as described in Sections 3.3.5 and 4.4.2). Another important observation drawn was that change in the monomer to cross-linker ratios of the pre-polymerisation mixture did slightly affect T_g of the polymers. Increase in the cross-linker amount increased the T_g and thereby cross-linking degree of the polymers, as expected. However, the rate of heating (MW power) used for polymerising the monomer mixture had more pronounced effect on the T_g of the resulting MW polymers. This was in agreement with the proposed hypothesis that a polymerisation carried out with faster heating would comparatively be shorter in its length as faster heating would attain the set MW temperature more quickly (as discussed earlier in Section 3.4.2). This would freeze the growing linear chains much early on before they could create sufficient crosslinking in the polymer matrix. As a result, the formed polymer would likely to be less cross-linked. This further suggested that if such polymers with lower cross-linking degree were heated, their flexible cross-links would undergo regio and stereo selective rotations than breaking down straight away. The loss in energy used up in causing the bond rotation would demand higher energy and higher temperature for breaking the bonds (73). As a result, the polymers with lower cross-linking degree would reach their glass transition state (T_g) at comparatively higher temperatures (as seen in Figure 4.12). In agreement with the hypothesis, ToxiQuant MW polymers prepared with faster heating showed lower degree of cross-linking (lower T_g values); whereas those polymerised with slower heating showed higher cross-linking degree (higher T_g values). All the polymers samples were then also charcterised by TGA to analyse them for their thermal stability or robustness (please see Section 4.5.3).

4.5.3. Thermogravimetric analysis (TGA)

TGA is a thermo analytical technique which is used to study robustness and thermal stability of a polymeric material (as described earlier in Section 3.3.6). In a typical TGA analysis, a polymer sample is heated from 0 °C to 600 °C at a constant rate. As the heating cycle continues, it measures the thermal and conformational transition in polymers for the temperature of up to 200 °C. Upon heating further, the polymer slowly degrades and the loss of the polymer weight is determined as a function of time and/or temperature.

From the obtained results of DSC analysis, it was found that the MW polymers under study showed different degrees of cross-linking depending on the MW power used for their polymerisation. From this, it was hypothesised earlier that when the polymers with different cross-linking degree were heated, the one with higher cross-linking degree would degrade straight away in comparison to other polymer that was less cross-linked (as described earlier in Section 3.4.3).

Since the ToxiQuant polymers are also cross-linked polymers, their cross-linking degree would be crucial in defining their robustness and thermal stability. For example, the polymers with higher degree of cross-linking would be rigid enough to melt straight away when heated in comparison to the one that is less cross-linked. This might be because the less cross-linked polymer would be more flexible to undergo confirmational and rotational change of their cross-linking bonds which would make them survive higher temperatures (as discussed earlier in Sections 3.3.6 and 3.4.3). In this regard, TGA analysis of the polymers could be a useful technique to study such thermal changes occuring in the polymers as they were heated at even higher temperatures (600 °C). For better understanding between cross-linking degree and thermal stability of the polymers, the pbtained TGA thermograms would also be correlated to the obtained DSC profiles.

To carry out TGA analysis, the polymer samples were heated from 0 °C to 600 °C at a constant rate of 10 °C min^{-1} and their weight loss were plotted as a function of the temperature. Figure 4.13 shows the TGA profile of 5 % DEAEM: 95 % EGDMA ToxiQuant MW polymer prepared at 60 °C for 15 minutes by varying MW powers from 5 W and 150 W. The polymer heating profiles in TGA thermograms for up to 200 °C would be indicative of polymer cross-linking patterns (similar to DSC analysis); whereas the temperatures above that would show polymer degradation rates which would be indicative of their thermal robustness (as explained earlier in Section 3.3.6).

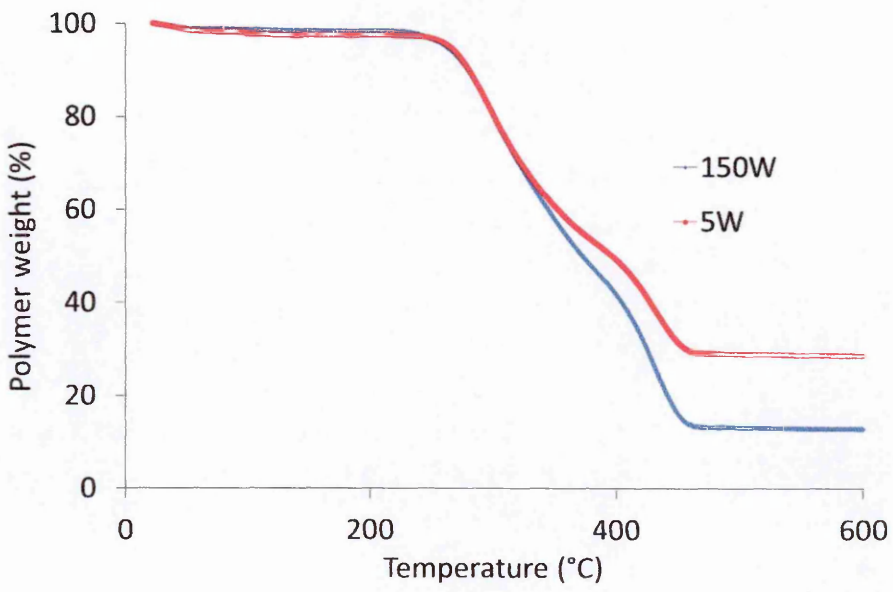

Figure 4.13: Thermogravimetric profiles expressed as % polymer weight against heating temperature of ToxiQuant MW polymers prepared with 5 W (red) and 150 W (blue) MW powers.

Figure 4.13 suggested that the MW polymers prepared with powers from 5 W to 150 W showed a little weight loss (about 2-3 %) when heated for up to 200 °C. On correlating these findings with the DSC results obtained earlier, it was found that their DSC profiles also showed a slight difference in their T_g values (4 °C) when heated in a similar temperature range (as seen in Figure 4.10). After that, when these MW polymers were heated for up to 600 °C, the polymer prepared with 5 W power took longer to degrade; whereas the one polymerised with 150 W degraded at a comparatively faster rate and (as seen in Figure 4.13). In other words, when heated in both DSC and TGA analysis, ToxiQuant polymers did not show any considerable difference in their cross-linking degree. However, slowly polymerised samples showed higher thermal stability in comparison to the one polymerised with a faster MW heating. This observation was exactly similar to that obtained from the TGA analysis of the caffeine MW MIPs when they were polymerised with similar MW powers (please refer to Figure 3.27).

To understand the effect of relative amounts of monomers and cross-linkers on the thermal stability of resulting polymers, a different polymer composition (20 wt % DEAEM: 80 wt % EGDMA) was also analysed by TGA. Figure 4.14 shows the TGA profile of 20 wt % DEAEM: 80 wt % EGDMA ToxiQuant MW polymer.

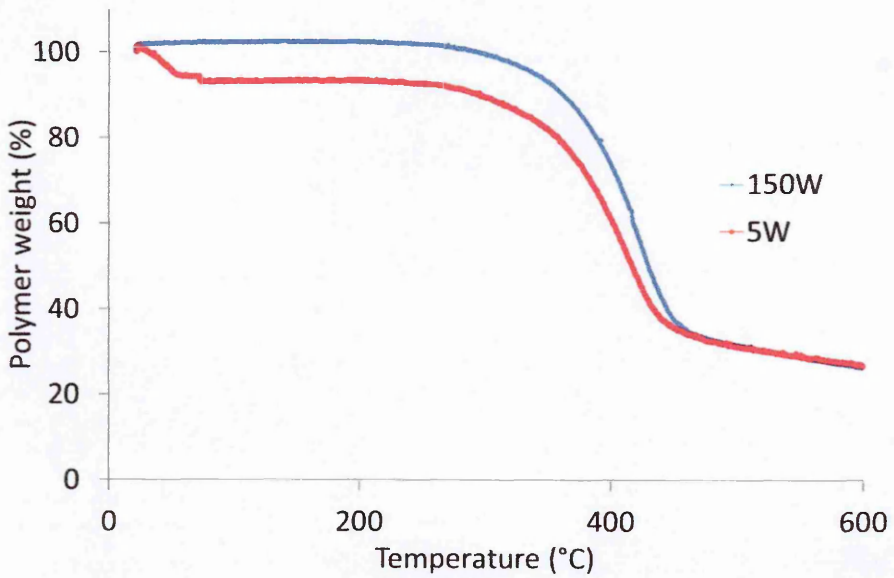

Figure 4.14: Thermogravimetric profiles expressed as % polymer weight against heating temperature of MW ToxiQuant polymers prepared with 5 W (red) and 150 W (blue) MW powers.

Figure 4.14 showed that when 20 wt % DEAEM polymers were heated from 0 °C to 200 °C in TGA analysis, the polymer prepared with slower heating (5 W) showed slightly more weight

loss (about 10 %) compared to the one polymerised with faster heating (150 W). Their DSC analysis suggested that their cross-linking degree decreased slightly when the polymerisation rates were increased. In other words, the polymer prepared with 5 W heating was more cross-linked than that prepared with 150 W (please see Figure 4.11). This observation was in agreement with the hypothesis which suggested that the polymer with higher cross-linking degree would show more weight loss in TGA analysis when heated at moderately high temeratures of up to 200 °C. This might be because highly cross-linked polymer would contain densely cross-linked bonds with little flexibility to undergo regio or stereo selective bond rotations upon applying thermal energy. This would cause cross-linking bonds to breakdown straight away leading to polymer degradation, expressed by their weight loss, for example, the MW polymer prepared with 5 W power exhibited comparatively higher cross-linking degree as it showed more weight loss when heated in TGA analysis (as seen in Figures 4.11 and Figure 4.14).

The obtained results from TGA and DSC analysis were in agreement with the proposed hypothesis that faster thermal polymerisations in a MW reactor produced polymers with lower cross-linking degree and lower glass transition temperatures and lower thermal stability; whereas slower polymerisations produced highly cross-linked polymers that showed higher glass transition temperatures.

Overall, all the polymers prepared with different MW powers (different heating rates) using different monomer compositions did not show complete degradation for up to 600 °C (as seen in Figure 4.13 and 4.14). This suggested that MW polymers showed comparable thermal stability to that of traditional thermal polymers (74-76). Another useful observation was drawn that when the amount of the cross-linking monomer was increased from 80 wt % to 95 wt %, thermal stability of the resulting MW polymers was slightly reduced. The polymer with 5 % DEAEM: 95 % EGDMA showed considerable weight loss from the temperatures above 300 °C. On the other hand, the polymer with 20 % DEAEM: 80 % EGDMA did not show any considerable weight loss even up to 400 °C. This suggested that increasing the cross-linking monomer in the recipe made the resulting polymers more rigid.

The prepared polymers were then also analysed by porosimetry to study the physical properties such as, average surface area, total pore volume and average size of the pores, as discussed in Section 4.5.4.

4.5.4. Porosimetry measurements

These experiments were carried out in Prof. Piletsky's laboratories at the University of Leicester. Porosimetry analysis is a widely used technique for charcterising cross-linked

porous polymers. In this study, it would be vital to understand if the changes in the experimental parameters of a polymerisation could affect the surface area and other porous characters of the resulting polymer. Expecially, the surface area would be crucial in defining the performace of polymers to be used as mycotoxin recognition materals. To carry out the analysis, polymer samples were subjected to porosimetry instrument as described earlier in Section 3.3.7.

Figure 4.15 shows the comparison of average surface area of different ToxiQuant MW polymers prepared by varying MW heating rates (MW powers).

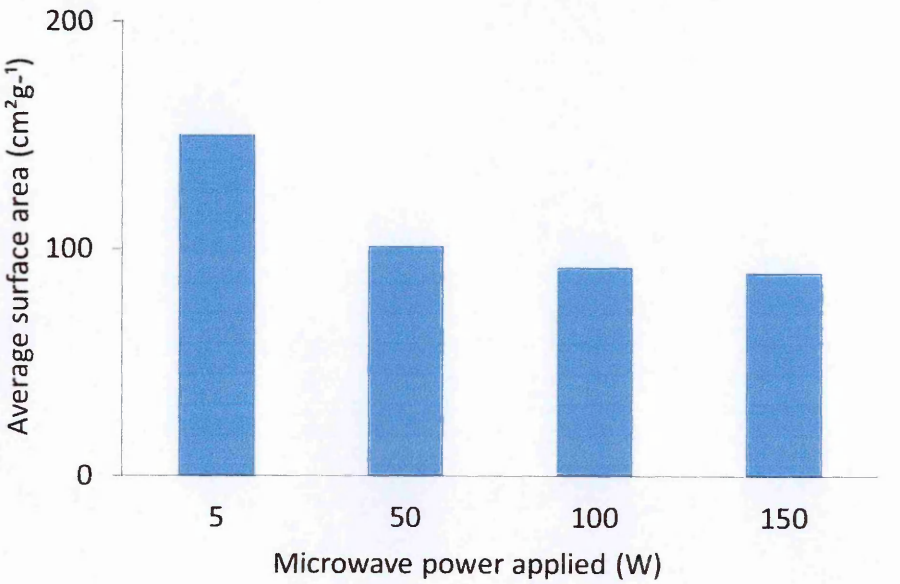

Figure 4.15: Comparison of average surface area of ToxiQuant polymers (5 wt % DEAEM: 95 wt % EGDMA) prepared with different MW powers.

Porosimetry study of ToxiQuant polymers suggested that the average surface area of these polymers were dependent on the rate of MW heating used for their polymerisation. When the MW heating rate was increased from 5 W to 50 W, average surface area of the polymers decreased by about 50 units from 150 $m^2 g^{-1}$ (as seen in Figure 4.15). The average surface area decreased even further by 10 more units ($m^2 g^{-1}$) when the heating rates were increased up to 150 W. The trend seen in surface areas of these polymers were quite similar to that obtained with caffeine MIPs earlier (as seen in Figure 3.34). These results were compared with that obtained from DSC analysis, as plotted in Figure 4.16.

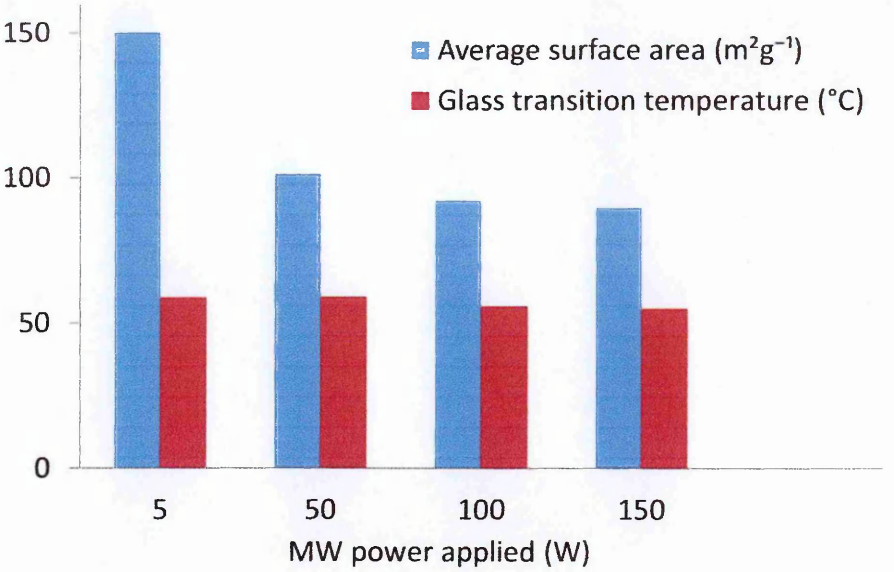

Figure 4.16: Comparative analysis of the cross-linking degree (by the means of glass transition temperature) and average surface area of ToxiQuant polymers (5 wt % DEAEM: 95 wt % EGDMA) prepared with different MW powers.

This correlation suggested that the cross-linking degree of polymers also had direct consequences on the available surface area. MW polymers with higher cross-linking degree (please refer to Figure 4.10) produced larger surface area which was in agreement with the study presented in Chapter 3 that suggested that higher cross-linking degree could leave little space for pore formation within polymer matrix (as observed earlier in Sections 3.4.2 and 4.5.2). To understand this further, total pore volume and average pore radii of these polymers were also measured as shown in Figure 4.17.

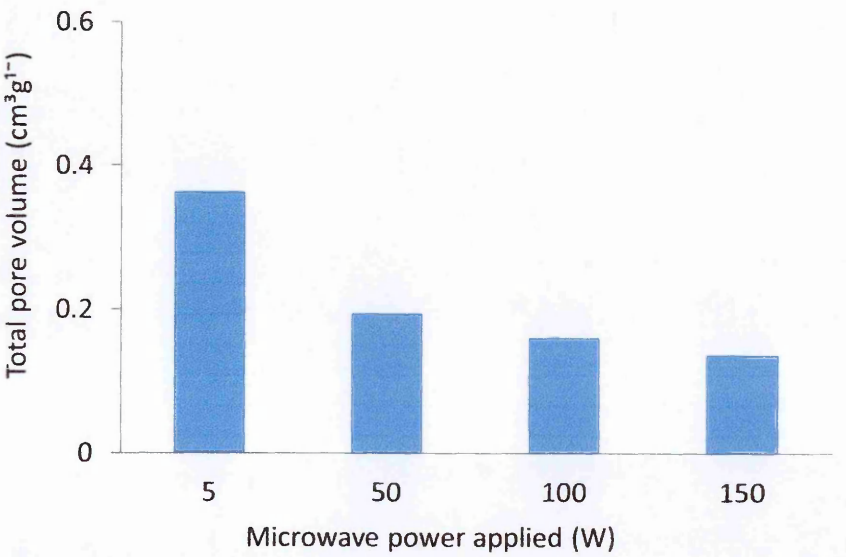

Figure 4.17: Comparison of the total pore volume of MW ToxiQuant polymers (5 wt % DEAEM: 95 wt % EGDMA) prepared with different MW powers.

When the ToxiQuant MW polymers were analysed for their average pore volumes using porosimetry technique, it was found that the pore volumes decreased consistently whilst increasing the heating rate of their polymerisations. Figure 4.17 indicated that the average pore volume of these MW polymers dropped by about a third from 0.36 $m^3 g^{-1}$ when their heating rates were increased from 5 W to 150 W. This meant that the slower MW polymerisations produced larger pore volumes. This behaviour was in agreement with the obtained pore volumes of caffeine MIPs prepared in comparable conditions (as seen in Figure 3.35). Considerably larger pore volumes achieved with slower MW polymerisations reaffirmed the proposed hypothesis that slower polymerisation kinetics combined with pulsatile MW heating could allow sufficient intrusion of the porogen in slowly growing polymeric chains and generate larger pore volumes (as discussed earlier in Section 3.4.4). The same set of MW polymers were then also analysed for their average pore radii to understand its relationship with pore volume and cross-linking degree, as presented in Figure 4.18.

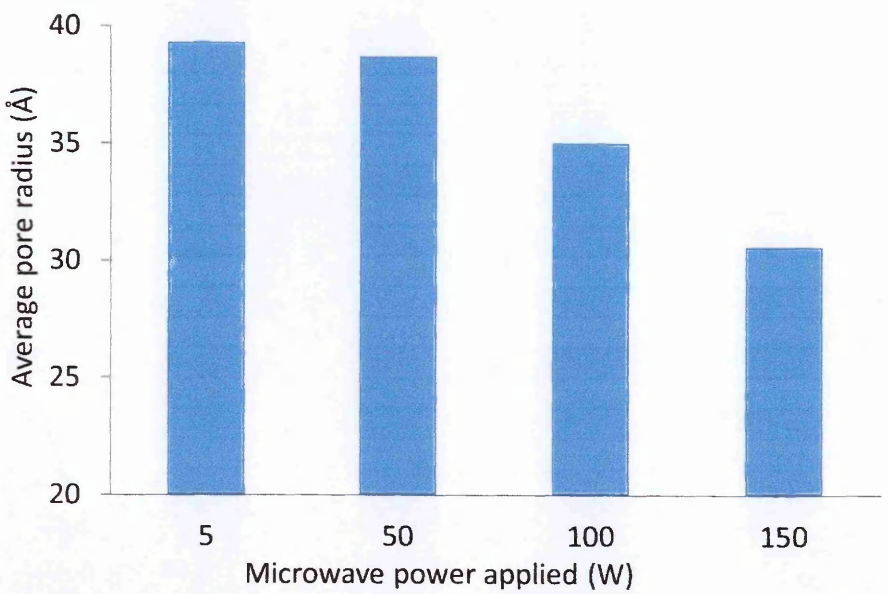

Figure 4.18: Comparison of the avgerage pore radii of ToxiQuant polymers (5 wt % DEAEM: 95 wt % EGDMA) prepared with different MW powers.

Figure 4.18 indicated that average pore radii of ToxiQuant MW polymers was between 30 Å to 40 Å when they were polymerised with MW powers from 5 W to 150 W. It also suggested that the average pore radii consistently decreased when the MW power used for polymerisation was increased. This when combined with their average pore volumes, suggested that faster MW polymerisations produced polymers with smaller pore volume and the pores produced were also smaller in size. This seemed to agree with the proposed hypothesis that the faster polymerisations attained with higher MW powers would barely allow porogen intrusion in the

spaces between fast growing polymeric chains resulting into smaller pores and lower overall pore volume (as discussed earlier in Section 3.4.4).

To understand this further, these results were correlated with those obtained for caffeine MW MIPs. It suggested that caffeine MW MIPs produced pores of the same average size regardless of the MW powers (polymerisation rate) used for their preparation (please refer to Figure 3.36). This could be due to the difference in the recipes of a MIP (caffeine MIPs) and a non-MIP (ToxiQuant polymers). Whilst preparing a MIP, the template would form all the binding cavities formed around its shape and size hence they would remain almost similar regardless of any experimental parameters used (77). On the other hand, a non-MIP recipe would lack the presence of a template. Therefore, polymerisation kinetics along with the cross-linking degree would be far more influential in determining the pore size among growing polymeric chains. This is exactly what was observed when the ToxiQuant polymers were analysed for their pore radii, they were considerably influenced by the MW used for their polymerisation (please refer to Figure 4.18).

This further suggested that the polymerisation kinetics together with the cross-linking degree and porosity characteristics could be crucial in determining the number and spatial distribution of pores within the polymer matrix. Anaysis of these ToxiQuant MW polymers suggested that polymers prepared with slower heating rate showed higher cross-linking degree and larger surface area leaving little volume for pore formation, as observed. At the same time, these polymers also showed larger pores which reflected into their larger pore volumes. This suggested that higher cross-linking degree observed in slowly polymerised matrix might allow it to form fewer pores; however slower polymerisation rate could enhance porogen intrusion which could compensate by forming larger and deeper pores within the matrix of the resulting polymer. Likewise, lower cross-linking observed in quickly polymerised polymers might allow for formation of numerous pores; however faster polymerisation rates might not allow sufficient porogen intrusion which could compensate by forming smaller and shallower pores within the polymer matrix. In other words, faster MW polymerisations could generate polymers with numerous, smaller and shallower pores; whereas slower MW polymerisations could prepare polymers with fewer, larger and deeper pores.

Such properties of the pores would be quite critical in predicting target recognition, especially in binding and removal kinetics of the analyte. Ideally, the pore formation should be surface laden to ensure efficient target binding. Therefore, it would be important to reiterate that larger surface area alone would not be sufficient for improving analyte recognition of the

polymer. The degree of cross-linking should be sufficient enough to hold the cavities intact throughout the template binding and removal stages (as discussed earlier in Section 3.4.6).

Some more ToxiQuant MW polymers were prepared at 60 °C with a different monomer recipe (20 wt % DEAEM: 80 wt % EGDMA) by using similar MW powers from 5 W to 150 W for 15 minutes. They were analysed for average surface, total pore volume and average pore radii in identical manner. Figure 4.19 presents a comparison on the average surface area of different 20 wt % DEAEM ToxiQuant polymers.

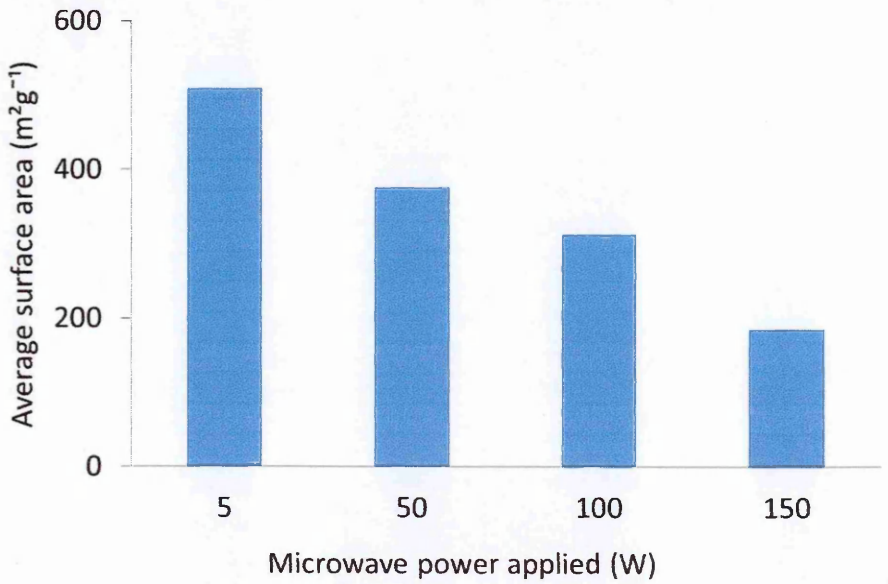

Figure 4.19: Comparison of the avgerage surface area of ToxiQuant polymers (20 wt % DEAEM: 80 wt % DEAEM) prepared at different MW powers.

ToxiQuant MW polymers showed considerably larger surface area of about 500 m^2 g^{-1} when the composition of the pre-polymerisation mixture was changed from 5 wt % DEAM: 95 wt % EGDMA to 20 wt % DEAEM: 80 wt % EGDMA. It also indicated that the average surface of the polymer decreased by more than half of 500 m^2 g^{-1} when the MW power was increased from 5 W to 150 W for polymerisation (as seen in Figure 4.19). This immediately suggested that when the amount of functional monomer (DEAEM) was increased from 5 wt % to 20 wt %, it might have helped in foming more surface laden pockets for analyte binding. When these results were compared to the earlier findings, it suggested that this decreasing trend seen in average surface area of the polymer upon increasing its polymerisation rate (increasing MW power) was consistent in all polymer systems under study regardless of the monomer composition of the polymerisation recipe (as seen earlier in Figures 3.34 and 4.15). This meant that the amount of available surface area was a reflection of the experimental parameters in which the polymers were synthesised; however the amount of the area would vary depending on the

monomer composition. Total pore volumes of these polymers were also obtained by porosimetry and the results were plotted as shown in Figure 4.20.

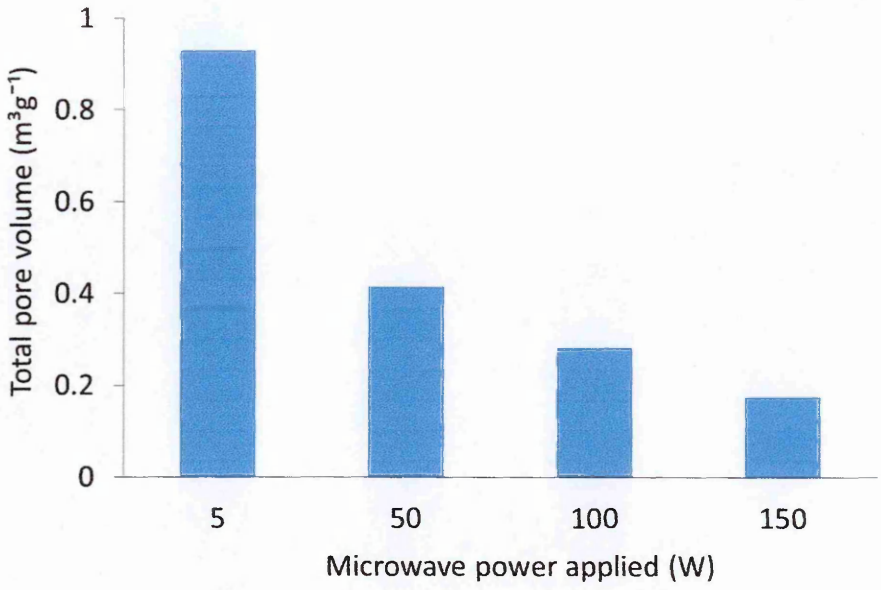

Figure 4.20: Comparison of the total pore volume of MW ToxiQuant polymers (20 wt % DEAEM: 80 wt % EGDMA) prepared at different MW powers.

Total pore volume of this set of ToxiQuant MW polymers nearly trippled by increasing their polymerisation rate in comparison to 5 wt % DEAEM: 95 wt % EGDMA monomer recipe. This suggested that the observed increase in the pore volume at 5 W polymerisation rate might be due to overall decrease in the cross-linking since the amount of the cross-linking monomer in this recipe was decreased from 95 wt % to 80 wt % in this polymer formulation (as seen in Figures 4.17 and 4.20). The obtained results also suggested that the average pore volume of the polymers decreased whilst increasing the MW power from 5 W to 150 W used for their polymerisation (as seen here in Figure 4.20). The observed trend of decreasing pore volume by increasing polymerisation rate (MW power) was found to be consistent regardless of the monomer composition of the polymerisation recipe in both the caffeine MW MIPs and ToxiQuant MW polymers (as seen earlier in Figures 3.35, 4.17 and 4.20). The results obtained for the avergae pore radii were also plotted, as shown in Figure 4.21.

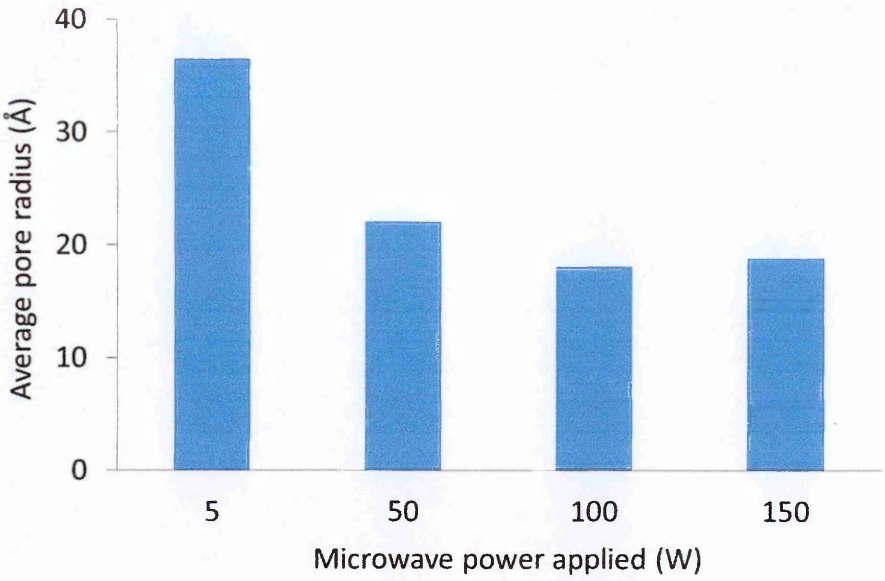

Figure 4.21: Comparison of the avge. pore radii of ToxiQuant polymers (20 wt % DEAEM: 80 % EGDMA) prepared with different MW powers.

As seen in Figure 4.21, average pore radii of ToxiQuant MW polymers was between 20 Å to 40 Å when they were polymerised by varying MW powers from 5 W to 150 W. It also suggested that the average pore radii decreased when the MW power used for polymerisation was increased. Other set of ToxiQuant MW polymers (5 wt % DEAEM: 95 wt % EGDMA) also showed a similar trend in their pore radii, which also decreased in size upon increasing the rate of MW heating (as seen in Figure 4.18). However, the average pore radii in caffeine MIPs remained quite consistent regardless of the rate of MW heating used for their polymerisation (as seen in Figure 3.35). This suggested that consistent size of the pores observed in caffeine MIPs was indicative of a typical pore formation that would occur in the vicinity of the template in case of the MIPs regardless of its experimental conditions. On the other hand, the pore sizes in non MIPs (such as, ToxiQuant MW polymers) would be largely influenced by the heating rates used for their polymerisation.

In summary, the porosity characteristics such as the surface area, pore volume and pore size of ToxiQuant MW polymers consistently decreased as the polymerisation rates were increased (with the virtue of increasing powers from 5 W to 150 W MW) whilst preparing ToxiQuant MW polymers. The obtained results from the analysis of ToxiQuant polymers together with the caffeine MW MIPs established that the rate of heating had direct consequences on cross-linking degree and porosity of the resulting polymers. For example, slower MW polymerisations were found to produce polymers with higher cross-linking degree and also exhibited larger surface area. MW polymers with higher cross-linking also exhibited considerably higher pore volumes. This might be due to the uniqueness of the controlled rate

and pulsatile heating of MW reactor which helped in constant intrusion of the porogen through extensive cross-linking in forming sufficient pores. The study of all the porosity parameters such as, surface area, pore volume and pore radii also suggested that larger pore volumes and larger pore radii in highly cross-linked MW polymers could compensate for having fewer deep pores on the surface of the polymer. Likewise, smaller pore volumes observed in less cross-linked polymers could compensate for a large number of slightly small and shallow pores in the polymer matrices. Since the size, volume and spatial distribution of the pores could be crucial in defining analyte binding and removal from the polymers, these observations would be useful in interpreting the results of recognition performance of these polymers.

In addition to experimental parameters, effects of monomer composition were also studied on the physicochemical properties of the resulting polymers. Upon changing relative amounts of the functional and the cross-linking monomers, no direct effect was observed on the cross-linking degree of the resulting polymers. However, it was also found that the average surface area and total pore volume of these polymers dramatically increased when the monomer composition was changed from 5 wt % DEAEM: 95 wt % EGDMA to 20 wt %: 80 wt % EGDMA (as seen in Figures 4.15, 4.17, 4.19 and 4.20). However, the average pore size was not considerably affected by any change in the polymerisation recipe. This suggested that any change in different polymerisation recipes together with the polymer's cross-linking degree were rather more likely to affect the spatial distribution and the depth of the pores created in its matrix. Since, the correlation between the pore sizes, volumes and their polymerisation components has not been studied much to date, this hypothesis would need further investigation by using different types of monomer mixtures and their relative amounts in co-polymer recipes. Prepared polymer samples were also studied by scanning electron microscopy (SEM) to analyse their morphology which is explained in the following section.

4.5.5. Scanning electron microscopy (SEM)

ToxiQaunt MW monoliths were ground and sieved to get the particle size distribution (PSD) of 63 µm to 125 µm. The segregated size fraction was then viewed under scanning electron microscope (SEM). SEM is a widely used microscopic technique to study the surface characteristics of a wide range of materials. Figure 4.22 is a representative electron micrograph of the ToxiQuant monoliths polymerised with the aid of a MW reactor.

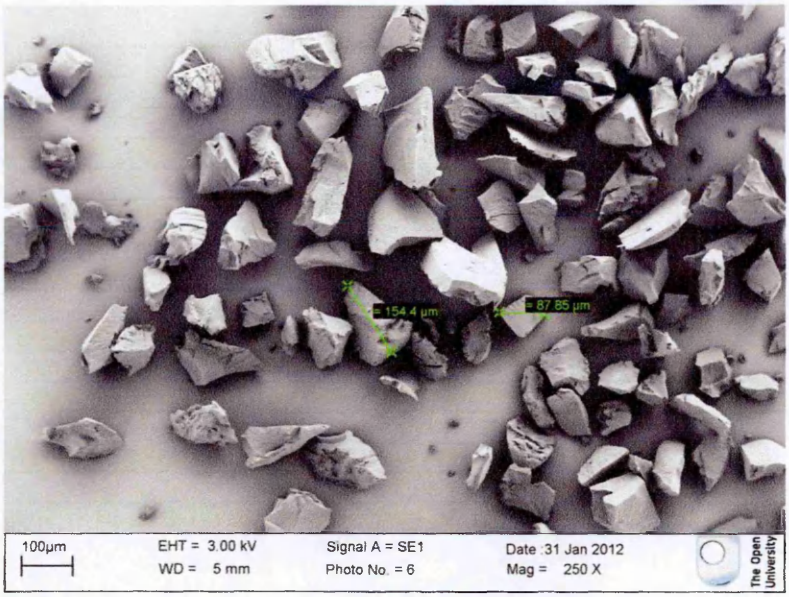

Figure 4.22: A representative scanning electron micrograph of ToxiQuant MW monoliths (250 X magnification).

Polymer monoliths prepred by MW polymerisation were found to be irregular as would be expected. For a precise particle size measurement, the size measurement tool was used as indicated by the green mark drawn along the axis of the particles in Figure 4.22. The sieved fraction of the obtained particle population showed desired PSD which was 63 µm-125 µm. However, there were fewer larger particles still found among the population of the polymer monolith (as seen in Figure 4.22). It would be important to mention here that the irregularity of such monolith particles make it difficult for a strict measurement of their diameters, crucial in defining the quality of a solid phase packing material. Although larger particles would not obstruct the flow pattern of the solvent through the stationary phase columns, they might lead to non-homogenous packing within the columns (78). On the other hand, finer particles below the desired PSD (63 µm-125 µm) would rather be crucial in attaining constant flow rates of the solvents through the columns. In the obtained particle population, fewer fine particles (10 %) were observed (as seen in Figure 4.22) which suggested that the performed soxhlet extraction was sufficient in removing most of the fines from the monoliths. Overall, all MW polymers observed under SEM did not show a smooth texture which was indicative of their porous character; however they needed to be viewed under higher magnifications. Individual pores could not be seen or measured with the resolution power of the SEM since their average pore diameters were microporous (less than 2 nm) in diameter. It would also be important to mention here that no distinct morphological changes were observed by changing the composition of the MW monoliths. The morphology of the polymer particles was also quite consistent when prepared with

different MW heating rates. This was in agreement with the findings when caffeine MW MIPs prepared under different experimental conditions were analysed by SEM (as discussed earlier in Section 3.4.5). Monoliths were further analysed at maginifications, as in Figure 4.23.

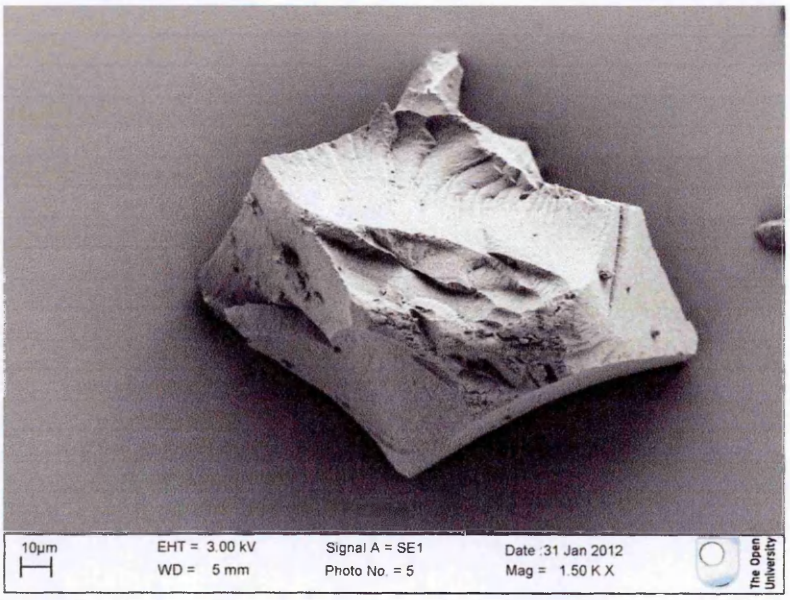

Figure 4.23: A magnified scanning electron micrograph of the ToxiQuant MW polymers (1.5 K X magnification).

When MW monoliths were viewed at higher magnifications, their electon micrographs showed a rough texture on the particle which was indicative of the porous character of MW polymers (as seen in Figure 4.23). It also suggested that the monoliths had a flaky and irregular surface which would be expected as the monoliths were rigourously triturated to attain desired PSD (63 µm-125 µm) from the monolith blocks. As discussed earlier in Section 4.3.7, the same polymer recipe was also used to prepare microparticles by suspension polymerisation. The remaining part of this section would discuss the morphological analysis of the polymer microparticles obtained by suspension polymerisation.

To obtain an optimised suspension polymerisation system, two different dispersants were investigated (as discussed earlier in Section 4.3.7). First of all, PVP was investigated as the dispersant for the formulation of an O/W suspension of the monomer recipe (20 wt % DEAEM: 80 wt % EGDMA). The resulting polymer microparticles were analysed by SEM as shown in Figure 4.24.

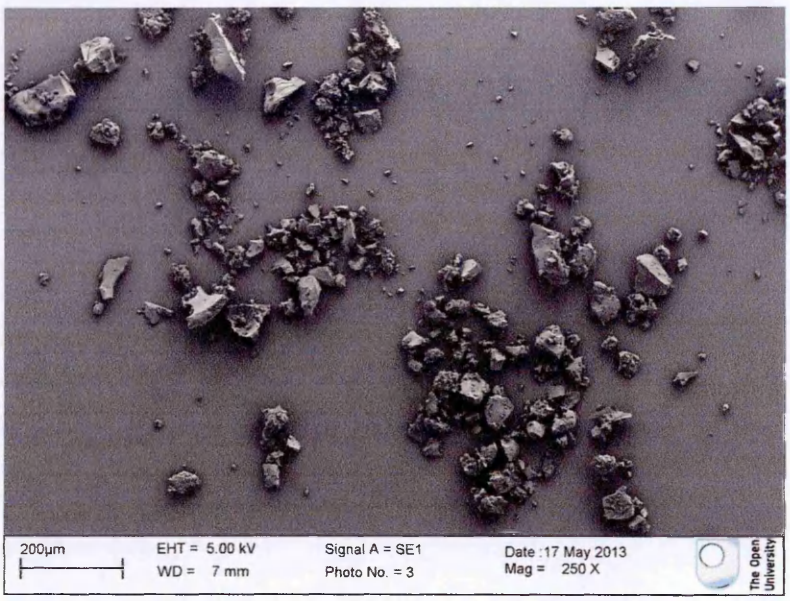

Figure 4.24: A scanning electron micrograph of the ToxiQuant polymer microparticles prepared by suspension polymerisation using PVP (0.1 wt %) as the dispersant (250 X magnification).

The polymer microparticles prepared by suspension polymerisation were found to be within the desired PSD of 63 µm to 125 µm; however they had a broken texture and were irregular in shape with inconsistent when they were viewed under SEM (as seen in Figure 4.24). Then, the amount of PVP was then increased to 1 wt % of the total monomer mixture and resultant polymer microparticles were viewed under SEM as shown in Figure 4.25.

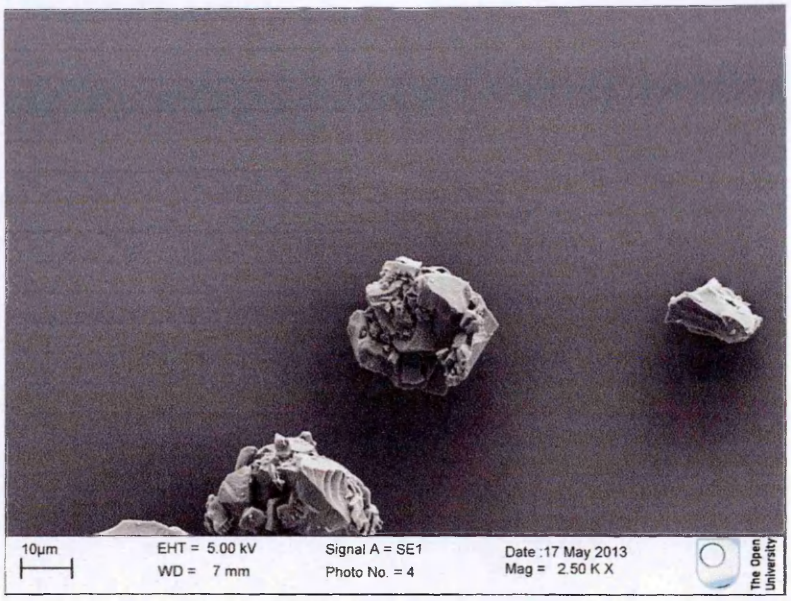

Figure 4.25: A scanning electron micrograph of the ToxiQuant polymer microparticles prepared by suspension polymerisation using PVP (1 wt %) as the dispersant (2.5 K X magnification).

When the amount of PVP was increased to 1 wt % of the total monomer mixture, the resulting polymer microparticles were with slightly spheroid shape. The particles also appered to be flaky and irregular in their texture (as seen in Figure 4.25). However, increasing the dispersant amount led to formation of slightly smaller particles since higher amounts would help in forming smaller monomer droplets (as discussed earlier in Section 2.6.2). The procedure was repeated in triplicate and the resultant particles appeared to be similar as shown in Figure 4.25. As surfactants would help in obtaining homogenous dispersion of the monomeric droplets, they could help in improving the shape, texture and PSD of the resulting polymer microparticles. Therefore, non-ionic water miscible amphiphilic surfactant was considered to be used for the polymer recipe under study. Triton X-100, a non-ionic amphiphilic surfactant was used in different concentrations from 0.1 mM to 20 mM to carry out suspension polymerisation of the ToxiQuant polymer recipe (as explained earlier in Section 4.3.6).

Getting a homogenous spherical bead formulation would be a fine act of balance between the amount of the surfactant and the rotation speed. Therefore, a preliminary screening was carried out where the polymer microparticles produced by using different amount of Triton X-100 underwent sieving to to get the homogenous formulation with a narrow PSD between 63 µm-125 µm. It was found that out of all other concentrations of Triton X-100, 10 mM solution resulted into the highest amount of total microparticles (20 wt %) within the desired size range. Just to note here, that the suspension polymerisation was carried

out at same temperature 60 °C for 8 hours with the stirring speed of 800 rpm. The resultant polymer microparticles were then analysed by SEM as shown in Figure 4.26.

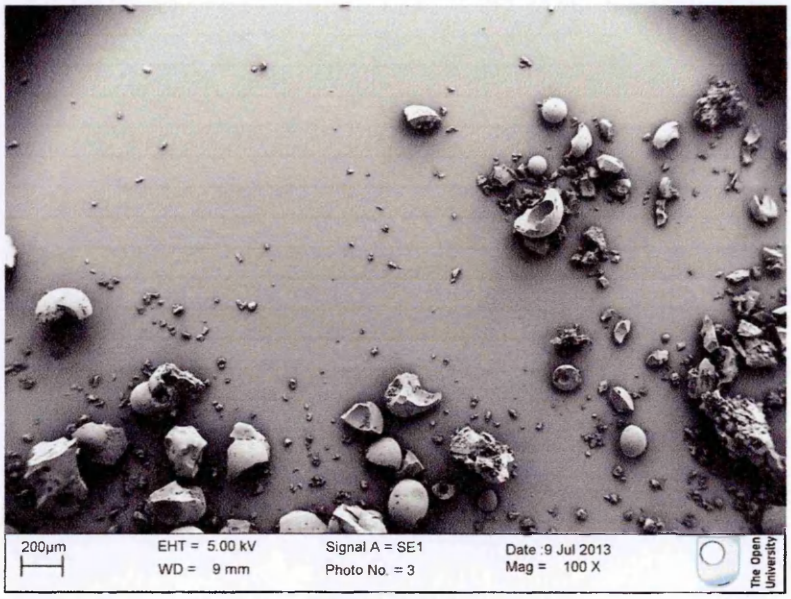

Figure 4.26: A scanning electron micrograph of the ToxiQuant polymer microparticles prepared by suspension polymerisation using Triton X-100 (10 mM) at 800 rpm (100 X magnification).

Polymer microparticles resulted from the suspension polymerisation at 800 rpm with Triton X-100 as a surfactant suggested that the most of the microparticles were either fractured or broken completely (as seen in Figure 4.26). It suggested that the breakage might be caused by a very high rotation speed that was used for carrying out this polymerisation. However, the fewer intact microparticles were spherical and within the desired PSD (63 µm-125 µm). This indicated that the concentration of Triton X-100 might be optimal to obtain the desired PSD; however a higher speed of rotation (800 rpm) might be the reason for producing fractured microparticles. Therefore, the rotation speed was reduced down to 300 rpm and suspension polymerisation was carried out with previously optimised pre-polymerisation recipe. The resultant microparticles were then analysed by SEM as shown in Figure 4.27.

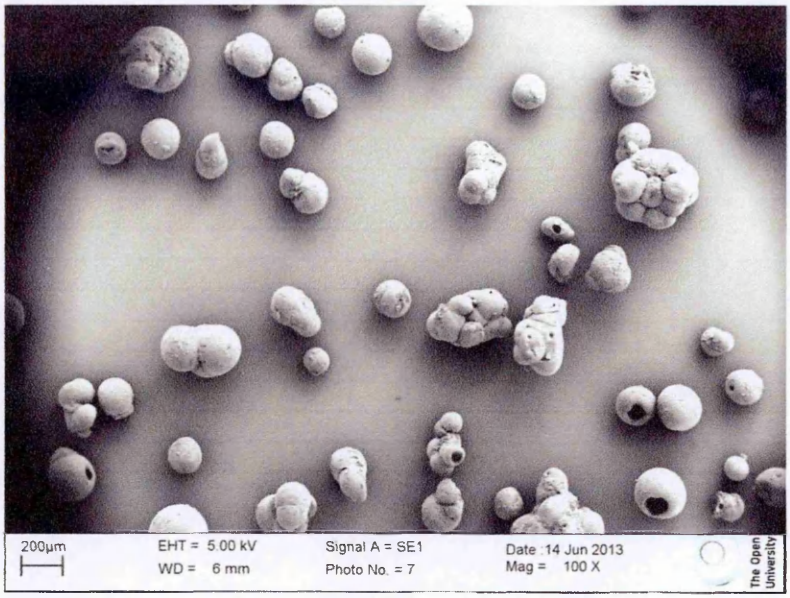

Figure 4.27: A scanning electron micrograph of the ToxiQuant polymer microparticles prepared by suspension polymerisation using Triton X-100 (10 mM) at 300 rpm (100 X magnification).

Figure 4.27 suggested that the slower rotation (300 rpm) certainly helped in preventing the microparticles from breaking as the particles appeared to be more spherical than what was achieved at a very higher rotational speed (as seen in Figures 4.26). However, the microparticles achieved here were largely in form of loosely aggregated individual particles which might be formed due to inadequate stirring (as seen in Figure 4.27). This might be caused due to insufficient dispersion which would coalesce monomer droplets into aggregates. Since the amount of the surfactant was already optimised, the only other factor that could help improve the coalescence was the speed of rotation. Therefore, the stirring speed was increased slightly to 500 rpm whilst keeping all other parameters constant. The polymerisation was carried out and the obtainend microparticles were analysed by SEM as shown in Figure 4.28.

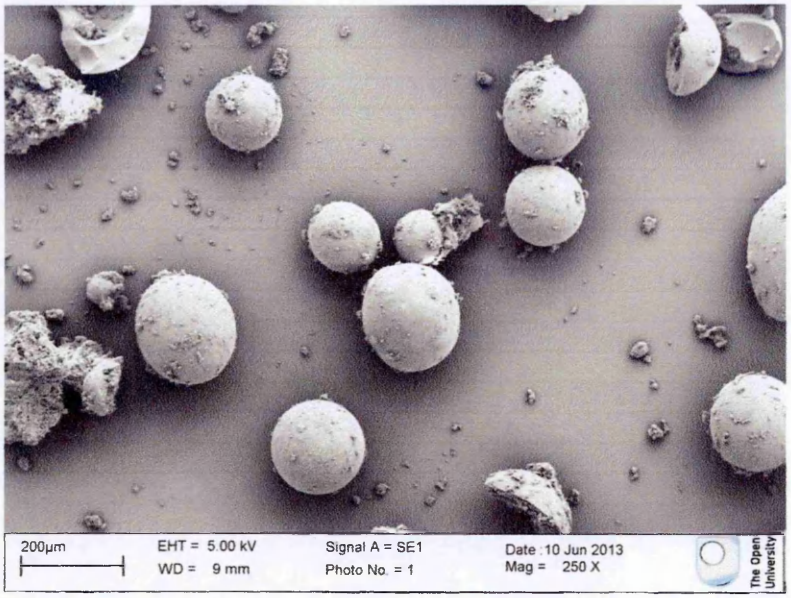

Figure 4.28: A scanning electron micrograph of the ToxiQuant polymer microparticles prepared by suspension polymerisation using Triton X-100 (10 mM) at 500 rpm (250 X magnification).

When the polymerisaiton was carried out with slightly medium speed of rotation (500 rpm), the microparticle formulation was found to be devoid of any loose aggregates previously observed (as seen in Figures 4.27 and 4.28). Importantly, the number of broken or fractured particles was the lowest so far, the fractured particles were also quite fine that they were removed by subsequent sieving through 63 µm-125 µm mesh sizes. Upon sieving the polymer microparticles, it was found that this formulation achieved about 60 wt % of the total polymer microparticles in the desired size range. To study the morphology of the particles further, these samples were analysed by SEM at even higher magnifications as presented in Figure 4.29.

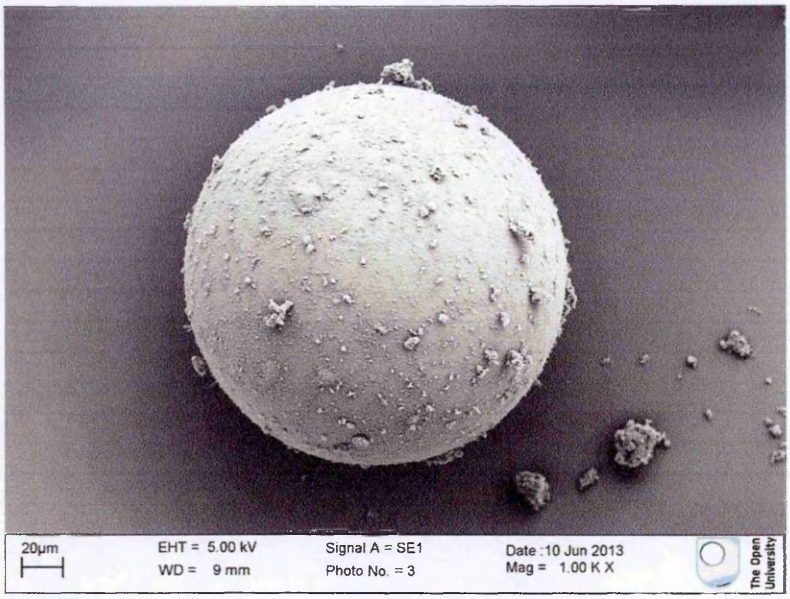

Figure 4.29: A scanning electron micrograph of the ToxiQuant polymer microparticles prepared by suspension polymerisation using Triton X-100 (10 mM) at 500 rpm (1.0 K X magnification).

Polymer microparticles obtained earlier (as seen in Figure 4.28) were viewed at higher magnification and their electron micrograph exhibited uniform rough surface which was indicative of their porous charatcer (as seen in Figure 4.29). The particles had defined spheroid shape as well as desired size (63 µm-125 µm). The amount of other debris was reduced even further once the particles were washed by soxhlet extraction using 10 vol % acidified methanol for 24 hours. This optimised formulation of the microparticles was then packed into SPE cartridges and used further for analyte recognition performance studies.

Polymer microparticles prepared by suspension polymerisation would offer a better alternative than the monoliths. Although suspension polymerisation would produce spheroid shaped particles to give better packing inside the columns than that of the monoliths, suspension polymers is deemed to produce broad particle size distribution (as discussed earlier in Section 2.6.2). However, this could be addressed by few other polymerisation techniques, one of which would be the core-shell polymerisation where a layer of polymer could be formed sorrounding a core spheroid particle. This could generate spheroid core-shell particles with narrow PSD and also could be more efficient in analyte recognition due to improved binding kinetics through a thin layer of the shell polymer (as discussed earlier in Section 2.6.5). In the presented study, preparation of polymer microparticles has been attempted by using core-shell polymerisation whilst using the same monomer recipe as that used earlier in MW and suspension polymerisations.

Precipitation polymerisation is regarded as a popular method for preparing core microparticles due to the ease of polymer preparation. Not to mention, precipitation polymerisation is totally devoid of any troublesome optimisation such as optimisation of the surfactant or vigorous stirring commonly encountred whilst carrying out suspension polymerisation. A stepwise precipitation polymerisation was followed from a previously reported study to obtained precipitation led core-shell polymer microparticles in this study. (71). As the first step in core-shell polymer formation, core poly(DVB) microparticles were prepared by precipitation polymerisation as described earlier in section 4.3.7.

Figure 4.30 presents an SEM image of the core poly(DVB) microparticles resulted from the precipitation polymerisation.

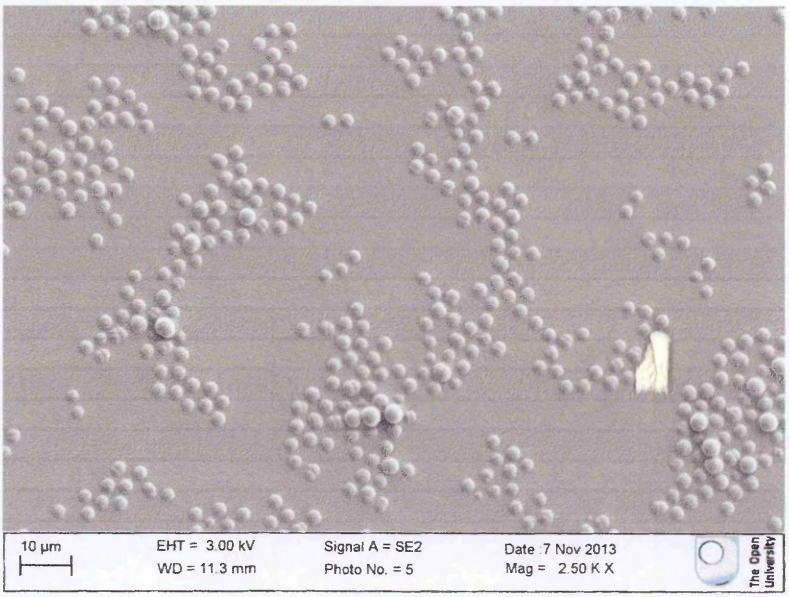

Figure 4.30: A scanning electron micrograph of the ToxiQuant polymer microparticles prepared by precipitation polymerisation (2.5 K X magnification).

Figure 4.30 suggested that the precipitation polymerisation resulted into a homogeneous microparticle formulation of p(DVB) spheroids with a narrow PSD (5 µm-7 µm). The resultant poly(DVB) microparticles were also spherical and but not rough in texture. Unlike, the suspension polymerisaiton, the resultant particles showed a smooth surface texture. This was expected since no porogen was used during the polymerisation. Here, the polymerisation mixture was devoid of the porogen as a smooth surface would be highly desirable for homogenous layering of the subsequent shell formation. The shell was formed by precipitating the ToxiQuant polymer on the surface of the core p(DVB) microparticles. This approach may be considered as the most convenient as the entire core-shell would be formed in a single pot reaction by minimising the loss of material and time.

To carry out the shell formation, different weight ratios of the shell monomers to the core particles (from 1:2 to 1:40) were added in the same reaction pot consisting of the core p(DVB) microparticles. The resultant core-shell particles were then analysed by SEM.

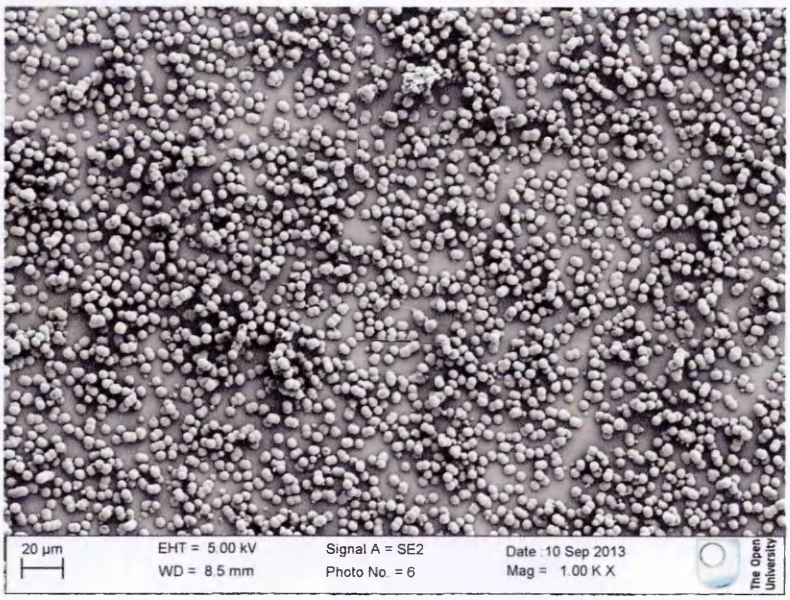

Figure 4.31: A scanning electron micrograph of the ToxiQuant polymer core-shell microparticles (1:10) prepared by precipitation polymerisation (1.0 K X magnification).

The core-shell particles obtained by adding 1:10 weight ratio of the core microparticles to shell monomers appeared as loose aggregates when viewed under an SEM (as seen in Figure 4.31). The average diameter of the particles was still well below 20 µm which was much smaller than the desired PSD of 63 µm-125 µm. This suggested that the ratio of the core to the shell monomers needed to be increased further. As a result, higher amount of the shell monomers were added and precipitated into microparticles, as seen in Figure 4.32.

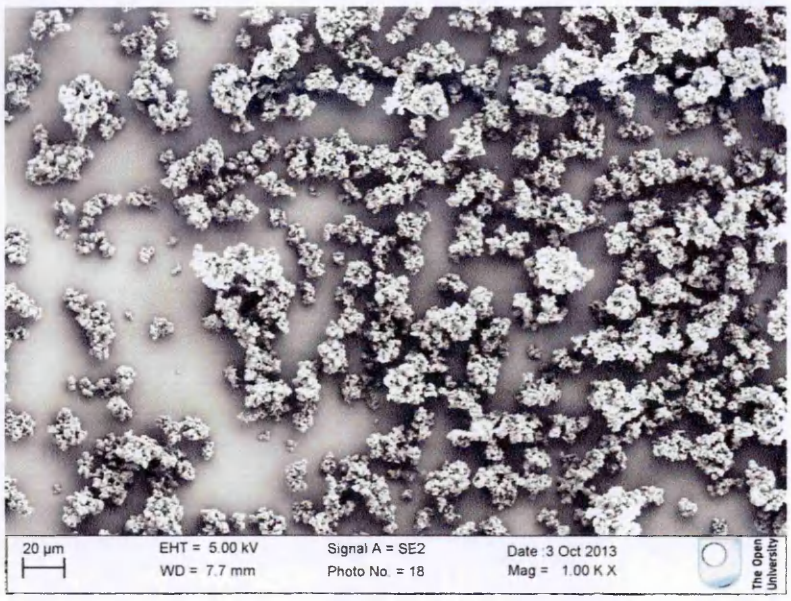

Figure 4.32: A scanning electron micrograph of the ToxiQuant polymer core-shell microparticles (1:20) prepared by precipitation polymerisation (1.0 K X magnification).

When the weight ratio of the core particles: shell monomers was increased to 1:20, the resultant core-shell particles emerged into irregularly shaped polymer aggregates formed by joining small individual particles (as seen in Figure 4.32). Although the particle were irregular in shape, they had increased in size from the core particles. To decide on the shell amounts further, the obtained core-shell particles were sieved through the set of 63 µm-125 µm mesh sizes. It was found that there was still about 50 wt % of the formed particles that passed through the sieves, implying that they were quite small than the desired PSD. As a result, the shell monomer amounts were further increased by 30 times in comparison to the weight of the core p(DVB) microparticles. The resulting core-shell microparticles were then viewed under SEM, as seen in Figure 4.33

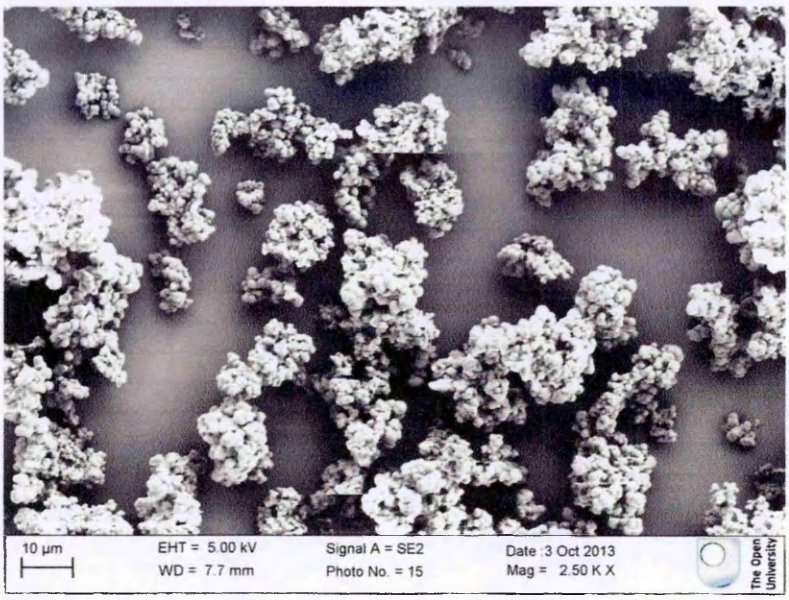

Figure 4.33: A scanning electron micrograph of the ToxiQuant polymer core-shell microparticles (1:30) prepared by precipitation polymerisation (2.5 K X magnification).

The core-shell particles obtained by using 1:30 core particles:shell monomers were found to be loose aggregates of irregular shaped microparticulate clusters (as seen in Figure 4.33). The shell monomer amount was increased further to 40 times by weight compared to the core p(DVB) microparticles and the resulting core-shell particles were analysed by SEM, as seen in Figure 4.34.

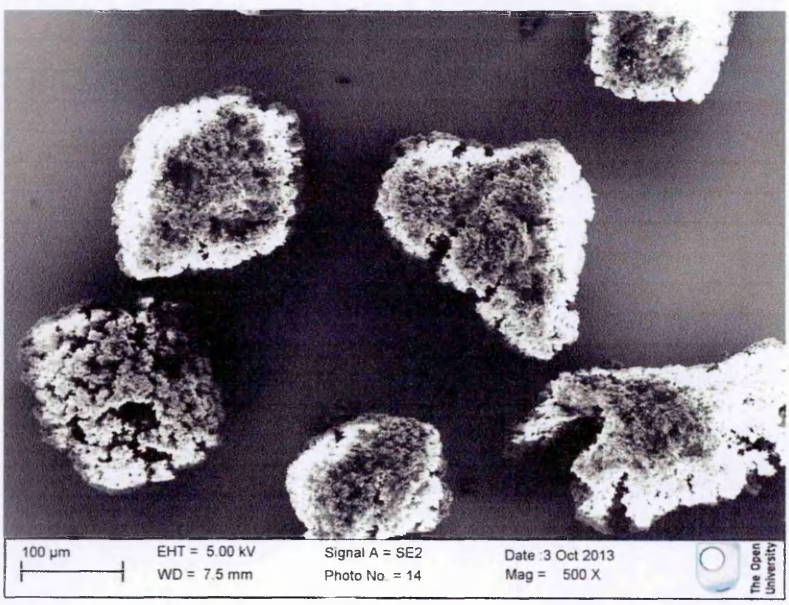

Figure 4.34: A scanning electron micrograph of the ToxiQuant polymer core-shell microparticles (1:40) prepared by precipitation polymerisation (500 X magnification).

The core-shell particles grew considerably large in size when the shell monomer amount was increased further to 40 times by weight as compared to that of core particles. However, the resulting core-shell particles were still in the desired size range between 63 µm to 125 µm (as seen in Figure 4.34). Microparticles were tightly packed and also exhibited rough surfaces indicative of their porous character. Although some particles were spheroid shaped, oval shaped particles were also observed. It was found that the size of the core-shell particles was dependent on the weight ratio between the core particles and the shell monomers and the particle size was found to increase by increasing the amount of the shell monomers. However, the used protocol did not result into homogenously spheroid microparticles containing formulation. The prepared core-shell microparticles were then packed into SPE cartridges in identical manner as other polymer formats to carry out mycotoxin recognition performance studies on them. Once all the polymer formats were prepared as SPE stationary phases for mycotoxin clean up, they were sent to the collaborators at the University of Leicester to carry out further analysis on their mycotoxin recognition performance.

4.5.6. Mycotoxin recognition analysis

Since the polymers under the presented study were to be used in ToxiQuant technology, it was vital to analyse their AFT clean up efficiency from the food matrix and then AFT recovery efficiency from its matrix. From the analysis performed earlier on caffeine MIPs, it was evident that the physical properties of the polymers affected their analyte recognition performance. Therefore, having mycotoxin clean-up and recovery performance of ToxiQuant polymers was expected to reflect their physical characteristics obtained from analysis performed earlier in Section 4.5. For mycotoxin clean-up and recovery on the prepared polymers, they were packed as stationary phases in SPE cartridges in triplicates. Supermarket bought peanuts were crushed and their 15 vol % and 30 vol % methanolic extracts were prepared with having different AFT concentrations spiked in them (as explained in Section 4.4). Prepared extracts were then passed through the SPE cartridges and analysis was plotted in Figure 4.35.

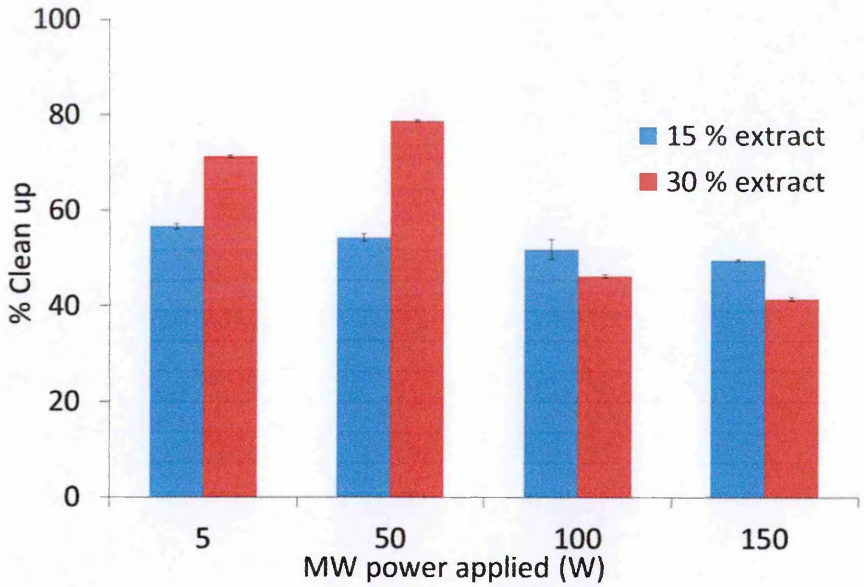

Figure 4.35: AFT clean up efficiencies of the ToxiQaunt MW polymers (5 wt % DEAEM: 95 wt % EGDMA) prepared with different MW powers (5 W to 150 W), blue and red bars representing AFT clean up obtained from 15 vol % and 30 vol % methanolic peanut extracts respectively; standard deviations were derived from the triplicate measurements of each sample.

As seen in Figure 4.35, it was found that the clean up efficiency of the polymers decreased as their polymerisation rates were increased from 5 W to 150 W. Lower MW powers (5 W and 50 W) produced polymers that exhibited significantly higher (more than 20 %) AFT clean up efficiency as compared to those prepared by faster polymerisations (100 W and 150 W). In general, all ToxiQuant MW polymers (prepared by different MW powers) showed minimum 50 % AFT clean up efficiency from 30 % peanut extract (as seen in Figure 4.35).

Clean up efficiency of polymers prepared with slower MW heating (5 W and 50 W) increased by more than 15 % when the concentration of the food matrix was increased from 15 % to 30 %. In general, these two polymers showed higher clean up efficiency for both the concentrations of peanut extract. On the other hand, polymers prepared with faster MW heating (100 W and 150 W) showed higher clean up efficiency from diluted AFT samples (15 % peanut extract) which reduced by about 10 % when AFT was extracted from a more concentrated the peanut matrix (30 %). This suggested that the polymers prepared with faster MW heating saturated upon increasing the concentration of food matrix from 15 % to 30 % (as seen in Figure 4.35).

The monomer recipe was then changed to 20 wt % DEAEM: 80 % EGDAM and was polymerised by using MW heating achieved by varying powers from 5 W to 150 W. The resulting MW

polymers were tested identically for the AFT clean-up efficiencies from 15 % and 30 % peanut extracts and the obtained results were plotted as shown in Figure 4.36.

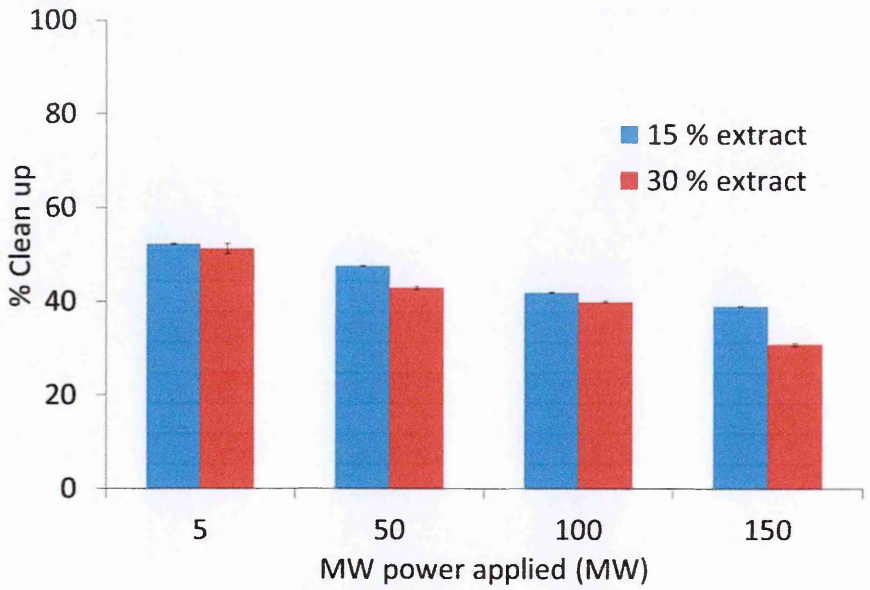

Figure 4.36: AFT clean up efficiencies of the ToxiQaunt MW polymers (20 wt % DEAEM: 80 wt % EGDMA) prepared with different MW powers, blue and red bars representing AFT clean up from 15 vol % and 30 vol % methanolic peanut extracts respectively; standard deviations were derived from the triplicate measurements of each sample.

Clean up efficiencies of the MW polymers were found to slightly decrease when the heating rate (MW power) used for their polymerisation was increased from 5 W to 150 W. MW power of 5 W produced the polymers with the highest AFT clean efficiency (about 53 %) which was gradually decreased by aboout 10 units when the analysis was carried out on quickly heated MW polymers. The clean up efficiency of the ToxiQuant polymers was found to be slightly affected by their monomer composition; it slightly decreased upon changing the monomer:cross-linker composition (from 5:85 to 20:80) (as seen in Figures 4.35 and 4.36). All 20 wt % DEAEM polymers (as seen in Figure 4.36) showed slightly higher clean up efficiency from a diluted samples (15 % peanut extract) which slightly decreased when the food matrix was concentrated (30 % peanut extract).

There were few striking outcomes from the AFT clean up analysis where three different parameters (MW power, monomer composition and concentration of the peanut extract) were found to affect each other as well as reflect onto the clean-up efficiency of the resulting ToxiQuant MW polymers. One of these observations suggested that the clean up efficiencies of the polymers prepared with slower MW heating were influenced by their preparation condition (MW power); slow MW heatings produced polymers that showed higher clean up

efficiencies. Another observation was made that the monomer ratio of 5 wt % DEAEM: 95 wt % EGDMA showed the higher AFT clean-up efficiency than the 20 wt % EGDMA polymers regardless of their preparation conditions (MW powers used).

The obtained results also indicated that the low power (5 W) produced polymers which showed the highest clean-up efficiency regardless of their monomer composition or the concetrations of the sample introduced. However, the clean up efficiency of the polymers decreased when the MW power used for their preparation was increased from 5 W to 150 W. In this way, the clean up efficiency was found to be affected by both the monomer composition of the polymer as well as the heating rate used for the the polymer preparation. Particularly, the monomer composition (5 wt % DEAEM: 95 wt % EGDAM) showed about 20 % higher clean up efficiency from the concentrated peanut extract (30 %).

It was hypothesised that the polymer with higher amount of the functional monomers (20 wt % DEAEM polymers) would selectively bind AFT and not other food components. In other words, these polymers would be expected to show higher AFT clean up efficiency by not binding other components of the food matrix. The proposed hypothesis was tested against the obtained results which suggested that the 20 wt % EGDMA polymers showed slightly lowered AFT clean up efficiency than the 5 wt % EGDMA polymers. This might have arisen due to non-selective binding of some interfering food components alongside AFT which could result into their lowered AFT clean up efficiencies than expected.

To understand these findings better, the results obtained fom the AFT clean up efficiency analysis of the polymers were correlated with those obtained from their DSC and porosimetry analysis and were plotted as shown in Figure 4.37.

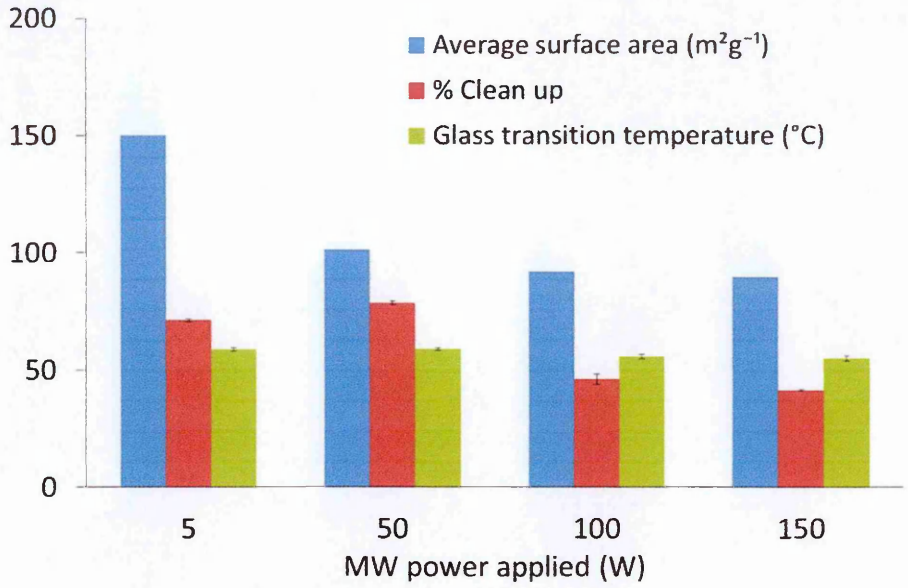

Figure 4.37: Comparative analysis of AFT clean up efficiency from 30 % peanut extract surface area and cross-linking degree of ToxiQuant polymer (5 wt % DEAEM: 95 wt % EGDMA); standard deviations were derived by triplicate measurements.

When MW polymers with the monomer composition (5 wt % DEAEM: 95 % EGDMA) were polymerised with slower heating (5 W and 50 W), they showed considerablly higher AFT clean-up efficiency. It was found that these polymers showed about 80 % AFT clean-up efficiency. However, when the polymerisations were carried out at faster rates (with 100 W and 150 W), the resulting polymers exhibited about 30 % less clean-up efficiency. However, it was quite interesting to note that although the surface area of the polymer (20 wt % DEAEM: 80 wt % EGDMA) was significantly larger, it did not show any significant improvement in its AFT clean-up effieciency (as seen in Figures 4.19 and 4.36). When these observations were correlated with that obtained from other physical analysis performed earlier, it suggested that the lower MW power (5 W) produced the polymers with larger surface area, higher cross-linking degree as well as higher pore volume which indicated that inspite of having larger surface area, higher cross-linking degree could obstruct binding of other food components which might lead to improved AFT clean-up efficiency (as seen in Figures 4.8, 4.10, 4.13, 4.15, 4.17 and 4.35). This pointed at the hypothesis proposed earlier that sometimes having larger surface area might not be an enough pre-requisite for an improved analyte recognition performance, but its degree of cross-linking should also to be taken into consideration (as discussed earlier in Section 3.4.6). Since the cross-linking degree of a polymer would be crucial in holding the binding sites intact whilst conducting analyte binding and removal, it could have larger implications on the performance of the polymer than just its surface area available for analyte binding. Here, the MW ToxiQuant polymers (20 % DEAEM: 80 wt % EGDMA) showed lower

cross-linking degrees which might have resulted into their lower AFT clean-up efficiency inspite of having significantly larger surface area (as seen in Figure 4.11 and 4.19). On the other hand, the polymers (5 wt % DEAEM: 95 wt % EGDMA) exhibited higher cross-linking degree which might have resulted into considerably higher AFT clean up efficiency inspite of having lower surface area.

The following step of the SPE protocol was to recover the previously immobilised AFT from the packed polymer stationary phases. AFT recovery studies were performed in identical manner on different MW ToxiQuant polymers with different monomer compositions and different preparation conditions (MW powers used for their polymerisations) and the obtained results were plotted, as seen in Figures 4.38 and 4.39.

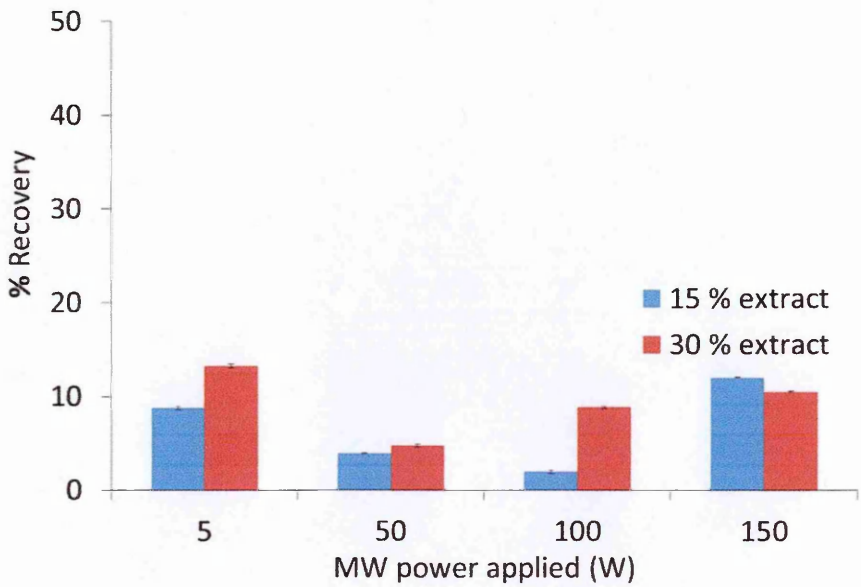

Figure 4.38: Recovery of AFT from the ToxiQaunt MW polymers (5 wt % DEAEM: 95 wt % EGDMA) prepared with different MW powers, blue and red bars representing AFT clean up from 15 vol % and 30 vol % methanolic peanut extracts respectively; standard deviations were derived from the triplicate measurements of each sample.

Figure 4.38 indicated that the recovery of AFT from the MW polymers (5 wt % DEAEM) was considerably low (7 % to 10 %) regardless the concentration of the peanut extract introduced. The polymerisation rate (MW power) used for polymer preparation did not seem to significantly affect the AFT recovery performance of the resulting polymers. This also implied that considerably low recoveries of AFT could arise from strong interactions between the immobilised AFT and the polymer. The study was also performed on different MW ToxiQuant polymers with a different monomer composition (20 wt % DEAEM: 80 wt % EGDMA) that were

prepared using different MW powers (5 W to 150 W). The obtained results were plotted as shown in Figure 4.39.

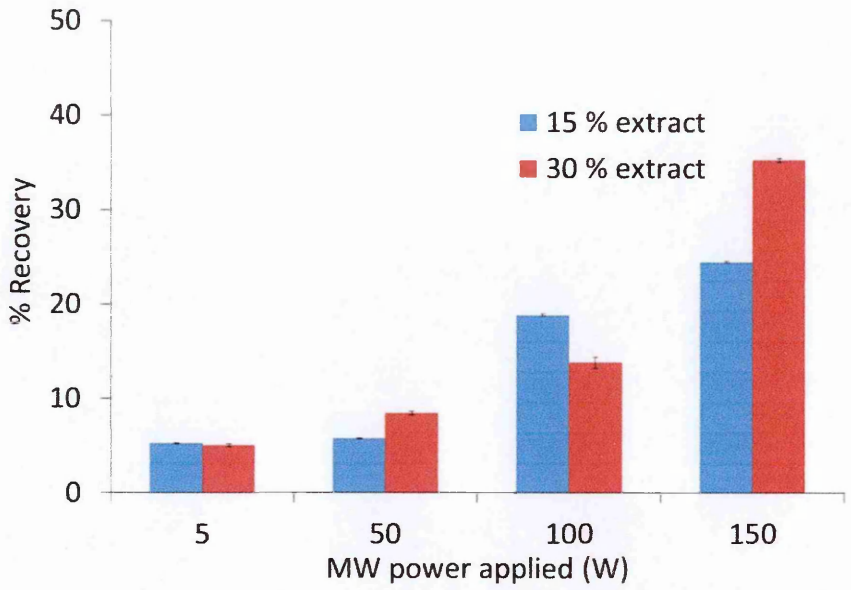

Figure 4.39: Recovery of AFT from the ToxiQaunt MW polymers (20 wt % DEAEM: 80 wt % EGDMA) prepared with different MW powers, Blue and red bars representing AFT clean up from 15 vol % and 30 vol % methanolic peanut matrix extracts respectively; standard deviations were derived from the triplicate measurements of each sample.

AFT recovery efficiency of the MW polymers (20 wt % DEAEM: 80 wt % EGDMA) were found to be dependent on their experimental condition, the rate of MW heating used to cure them. Slower MW heating produced polymers with lower AFT recovery efficiency (5 %); whereas faster MW polymerisations generated polymers with considerably higher AFT recovery efficiency (between 28 % to 48 %) (as seen in Figure 4.39). The obtained results also suggested that the recovery efficiencies of the 20 wt % DEAEM ToxiQuant polymers were considerably higher than 5 wt % DEAEM polymer (please refer to Figure 4.38).

Few striking observations were made from AFT recovery performance analysis of the MW polymers under study. The AFT recoveries obtained by the polymers with higher cross-linker amount (95 wt %) were generally low regardless of different heating rates (MW powers) used for their polymerisations (as seen in Figure 4.38). It was found that inspite of showing the highest AFT clean-up from the food matrix, these polymers showed lower recoveries of immobilised AFT (as seen in Figures 4.38 and 4.39). This implied that these polymers performed better in removing other interfering food compounds from the matrix but could not sufficiently remove bound AFT from their surface.

On the other hand, the ToxiQuant MW polymers with comparatively lower amount of the cross-linker (80 wt %) showed considerably higher AFT recovery efficiencies and they were largely affected by the polymerisation rates (MW powers) used for their preparation. The toxin recovery increased gradually when the polymerisation rates (MW powers) were increased from 5 W to 150 W (as seen in Figure 4.39). To understand this further, the results obtained earlier from their BET anaysis were correlated with these findings since the pore size and the total number of pores would be crucial in defining the AFT removal kinetics from the polymer. Upon correlating the findings, it was found that these polymers exhibited larger pore volumes and larger pore volumes than the formulation with 95 wt % cross-linker (as seen in Figures 4.17 and 4.18). This implied that the large number of bigger pores in polymers (with 20 wt % cross-linker) could be useful in successful removal of previously immobilised AFT in their matrix. However, this finding would need further investigation as the analyte binding and removal efficiency of a polymer would also be partly affected by the SPE protocol in use, such as the type, volume and concentration of the solvents used in sample loading and washing steps.

4.6. Summary

The aim of this study was to prepare cross-linked polymers as alternative recognition materials to be used in ToxiQuant technology for mycotoxin analysis. The presented study discussed the scope of improvement in ToxiQuant technology by replacing antibodies with cross-linked polymers as recognition materials. One of the main objectives of the study was also to prepare cross-linked polymers in different formats by using different methods. To this end, polymers were prepared as monoliths and microparticles by different methods varying their experimental conditions. Similar to Chapter 3, the primary method of preparation was MW polymerisation as an alternative method to generate polymers with faster and automated preparation protocols for industrial applications. As an extension to the study reported on caffeine MW MIPs, here the effect of different MW powers (polymerisation rates) and their possible effects on the physicochemical properties of the resulting polymers were investigated.

The controlled heating rates achieved with MW reactor allowed investigating the effect of different heating rates on the physical properties and performance of the polymers which has not been reported in any existing study. From the results obtained by studying caffeine MW MIPs, the MW powers and other parameters were chosen such that the analysis of both the caffeine MIPs and ToxiQuant MW polymers were comparable. The obtained results suggested that the physical properties of the ToxiQuant MW polymers (such as, cross-linking degree, thermal stability, surface area, pore volumes, pore size and morphology) were considerably

affected by the polymerisation rates (MW powers) used for their preparation. The trends observed in the mentioned properties were in also strong agreement with the results obtained earlier from the study of caffeine MW MIPs in Chapter 3.

Furthermore, the study established that the trend observed in the physical properties of the polymers was extended to their mycotoxin recognition performance too. The pre-polymerisation recipe was changed half-way through as a part of optimisation protocol. This gave an opportunity to also study the effect of the composition of pre-polymerisation mixture on the physicochemical properties of the resulting polymers. The polymers were prepared with different monomer: cross-linker ratios by using similar range of polymerisation rates (MW powers) and analysed for different physicochemical properties. This indicated that the composition of pre-polymerisation mixture was less influential on the physicochemical properties of the polymers than the experimental parameters used for its preparation.

However, this gave some insightful findings which were in agreement with that of the caffeine MW MIPs as well. For example, the performed studies (both caffeine MW MIPs and ToxiQuant MW polymers) collectively found that the change in the composition of the monomer mixture did not affect the size of the pores created in the resulting polymers; the pore sizes were mainly affected by the polymerisation rates (MW powers) used for their preparation. Although the physical properties of the resulting polymers were largely unaffected by the change in its monomer composition, it led to considerable differences in the AFT clean-up and AFT recovery performances of the resulting polymers. In general, the developed polymers could obtain comparable AFT clean-up efficiency; however the obtained AFT recoveries in the subsequent steps were considerably low to that of existing recognition materials used in ToxiQuant.

The study also reported preparation of polymer microparticles by suspension and core-shell polymerisations. Preparation of the suspension microparticles involved the study and optimisation of multiple experimental parameters and reaction components involved in its preparation. Electron microscopy studies indicated that the obtained suspension polymers were spherical, porous and within the desired particle size distribution. Core-shell microparticles were also prepared by a protocol earlier reported and the resulting particles were analysed by electron microscopy. This suggested that the preparation of core-shell polymer microparticles needed further investigation by using other protocols since the resulting polymer particles did not have the desired physical properties.

The results obtained strongly recommended that MW polymerisation could be investigated further as a suitable alternative polymerisation technique to develop non-imprinted or

molecularly imprinted polymers with added advantages of controlled polymerisations, faster reactions and reproducibility.

4.7. Future work

Further investigations would be devoted to understanding more monomer:cross-linker ratios as well as different type of cross-linkers in preparing polymers for ToxiQuant. Alongside developing monoliths by MW polymerisation, other techniques would be explored throroughly in future studies. The team of researchers at Toximet would like to analyse the suspension and core-shell polymers prepared during this study for their AFT and OT clean up and recovery performances. This would give a coherent analysis of all different polymer formats prepared by different methods as reported in this study. During the study, they would also be using ToxiQuant technique alongside HPLC since the ToxiQuant prototype has been successfully launched in the market.

For the development of more ToxiQuant polymers, alternative methods have already been looked at to improve exisiting core-shell format since thin polymer shell in this format could be useful in improving the problems associated with AFT binding and removal kinetics currently being faced in AFT clean up and recovery performance of the polymers. Some preliminary research has already been performed to develop core-shell polymers by using iniferters to address inconsistent shell polymerisation being faced by the current approach based on precipitation polymerisation. It would be investigated further in developing core-shell polymers for ToxiQuant technology.

4.8. Bibliography for Chapter 4

1. Williams, J. H. P., T. D. Jolly, P. E. Stiles, J. K. Jolly, C. M. Aggarawal, D. (2004) Human Aflatoxicosis in Developing Countries: A Review of Toxicology, Exposure, Potential Health Consequences, and Internetions1'2'3. *American Journal of Nutrition* **80**, 1106-1122.
2. Turner, N. B., H. Szabo-Vezse, M. Alessandro, P. Coker, R. Piletsky, S. (2015) Analytical Methods for Determination of Mycotoxins: An Update (2009-2014). *Analytica Chimica Acta*; in submission.
3. Turner, N. W., Subrahmanyam, S., and Piletsky, S. A. (2009) Analytical Methods for Determination of Mycotoxins: A Review. *Analytica Chimica Acta* **632**, 168-180.
4. Ali, W. H., Derrien, D., Alix, F., Pérollier, C., Lépine, O., Bayoudh, S., Chapuis-Hugon, F., and Pichon, V. (2010) Solid-phase Extraction Using Molecularly Imprinted Polymers for Selective Extraction of a Mycotoxin in Cereals. *Journal of Chromatography A* **1217**, 6668-6673.

5. Alcaide-Molina, M., Ruiz-Jiménez, J., Mata-Granados, J. M., and Luque de Castro, M. D. (2009) High Through-put Aflatoxin Determination in Plant Material by Automated Solid-phase Extraction On-line Coupled to Laser-induced Fluorescence Screening and Determination by Liquid Chromatography–triple Quadrupole Mass Spectrometry. *Journal of Chromatography A* **1216**, 1115-1125.

6. Stark, A. A. Essigmann, J. M. Demain, A. L. Skopek, T. R. Wogan, G. N. (1979) Aflatoxin B1 Mutagenesis, DNA Binding and Adduct Formation in Salmonella Typhimurium. *PNAS USA* **76**, 1343-1347.

7. Wang, J.-S., and Groopman, J. D. (1999) DNA Damage by Mycotoxins. *Mutation Research/Fundamental and Molecular Mechanisms of Mutagenesis* **424**, 167-181.

8. Eaton, D. L., Gallagher, E. P. (1994) Mechanism of Aflatoxin Carcinogenesis. *Annual Review of Pharmacology and Toxicology* **34**, 135-172.

9. Yiannikouris, A., Jouany, J. (2002) Mycotoxins in Feeds and Their Fate in Animals: *A Review. Animal Research* **51**, 81-99.

10. Koppen, R. K., M. Siegel, D. Merkel, S. Maul, R. Nehls, I. (2010) Determination of Mycotoxins in Foods: Current State of Analytical Methods and Limitations. *Applied Microbiology and Biotechnology* **86**, 1595-1612.

11. Nonaka, Y., Saito, K., Hanioka, N., Narimatsu, S., and Kataoka, H. (2009) Determination of Aflatoxins in Food Samples by Automated On-line In-tube Solid-phase Microextraction Coupled with Liquid Chromatography–Mass Spectrometry. *Journal of Chromatograhy A* **1216**, 4416-4422.

12. Zheng, M., Richard, J., and Binder, J. (2006) A Review of Rapid Methods for the Analysis of Mycotoxins. *Mycopathologia* **161**, 261-273.

13. Pereira, V. L. F., J. O. Cunha, S. C. (2014) Mycotoxins in Cereals and Related Foodstuffs: A Review on Occurence and Recent Methods of Analysis. *Trends in Food Science & Technology.* **36**, 96-136.

14. Van Egmond, H. P., Schothorst, R. C., and Jonker, M. A. (2007) Regulations Relating to Mycotoxins in Food. *Analytical and Bioanalytical Chemistry* **389**, 147-157.

15. Zheng, M. Z., Richard, J. L., and Binder, J. (2006) A Review of Rapid Methods for the Analysis of Mycotoxins. *Mycopathologia* **161**, 261-273.

16. Desmarchelier, A., Tessiot, S., Bessaire, T., Racault, L., Fiorese, E., Urbani, A., Chan, W.-C., Cheng, P., and Mottier, P. (2014) Combining the Quick, Easy, cheap, Effective, Rugged and Safe Approach and Clean-up by Immunoaffinity Column for the Analysis of 15 Mycotoxins by Isotope Dilution Liquid Chromatography Tandem Mass Spectrometry. *Journal of Chromatography A* **1337**, 75-84.

17. Beltrán, E., Ibáñez, M., Sancho, J. V., Cortés, M. Á., Yusà, V., and Hernández, F. (2011) UHPLC–MS/MS Highly Sensitive Determination of Aflatoxins, the Aflatoxin Metabolite M1 and Ochratoxin A in Baby Food and Milk. *Food Chemistry* **126**, 737-744.

18. Turner, N. W., Subramanyam, S.. Piletsky, S. A. (2009) Ananlytical Methods for Determination of Mycotoxins: A Review. *Analytica Chimica Acta* **632**, 168-180.

19. Carabias-Martínez, R., Rodríguez-Gonzalo, E., Revilla-Ruiz, P., and Hernández-Méndez, J. (2005) Pressurized Liquid Extraction in the Analysis of Food and Biological Samples. *Journal of Chromatography A* **1089**, 1-17

20. Romero-González, R., Frenich, A. G., Vidal, J., and Aguilera-Luiz, M. (2010) Determination of Ochratoxin A and T-2 Toxin in Alcoholic Beverages by Hollow Fiber Liquid Phase Microextraction and Ultra High-pressure Liquid Chromatography Coupled to Tandem Mass Spectrometry. *Talanta* **82**, 171-176.

21. Rahmani, A., Jinap, S., and Soleimany, F. (2009) Qualitative and Quantitative Analysis of Mycotoxins. *Comprehensive Reviews in Food Science and Food Safety* **8**, 202-251.

22. Quinto, M., Spadaccino, G., Palermo, C., and Centonze, D. (2009) Determination of Aflatoxins in Cereal Flours by Solid-phase Microextraction Coupled with Liquid Chromatography and Post-column Photochemical Derivatization-fluorescence Detection. *Journal of Chromatography A* **1216**, 8636-8641.

23. Arroyo-Manzanares, N., Gámiz-Gracia, L., and García-Campaña, A. M. (2012) Determination of Ochratoxin A in Wines by Capillary Liquid Chromatography with Laser Induced Fluorescence Detection using Dispersive Liquid–liquid Microextraction. *Food chemistry* **135**, 368-372.

24. Herzallah, S. M. (2009) Determination of Aflatoxins in Eggs, Milk, Meat and Meat Products Using HPLC Fluorescent and UV Detectors. *Food Chemistry* **114**, 1141-1146.

25. Sheijooni-Fumani, N., Hassan, J., and Yousefi, S. R. (2011) Determination of Aflatoxin B1 in Cereals by Homogeneous Liquid–liquid Extraction Coupled to High Performance Liquid Chromatography-fluorescence Detection. *Journal of Separation Science* **34**, 1333-1337.

26. Romero-Gonzalez, R., Martínez Vidal, J. L., Aguilera-Luiz, M., and Garrido Frenich, A. (2009) Application of Conventional Solid-phase Extraction for Multimycotoxin Analysis in Beers by Ultrahigh-performance Liquid Chromatography–Tandem Mass Spectrometry. *Journal of Agricultural and Food Chemistry* **57**, 9385-9392.

27. Herebian, D., Zühlke, S., Lamshöft, M., and Spiteller, M. (2009) Multi-mycotoxin Analysis in Complex Biological Matrices Using LC-ESI/MS: Experimental Study Using Triple Stage Quadrupole and LTQ-Orbitrap. *Journal of Separation Science* **32**, 939-948.

28. Kokkonen, M. K., and Jestoi, M. N. (2009) A multi-compound LC-MS/MS Method for the Screening of Mycotoxins in Grains. *Food Analytical Methods* **2**, 128-140.

29. Frenich, A. G., Vidal, J. L. M., Romero-González, R., and Aguilera-Luiz, M. d. M. (2009) Simple and High-throughput Method for the Multimycotoxin Analysis in Cereals and Related Foods by Ultra-high Performance Liquid Chromatography/Tandem mass Spectrometry. *Food chemistry* **117**, 705-712.

30. Lattanzio, V. M., Gatta, S. D., Suman, M., and Visconti, A. (2011) Development and In-house Validation of a Robust and Sensitive Solid-phase Extraction Liquid Chromatography/Tandem Mass Spectrometry Method for the Quantitative Determination of Aflatoxins B1, B2, G1, G2, Ochratoxin A, Deoxynivalenol, Zearalenone, T-2 and HT-2 Toxins in Cereal-based foods. *Rapid Communications Mass Spectrometry* **25**, 1869-1880.

31. Van Pamel, E., Verbeken, A., Vlaemynck, G., De Boever, J., and Daeseleire, E. (2011) Ultrahigh-performance Liquid Chromatographic–Tandem Mass Spectrometric Multimycotoxin Method for Quantitating 26 Mycotoxins in Maize Silage. *Journal of agricultural and food chemistry* **59**, 9747-9755.

32. Huang, L., Zheng, N., Zheng, B., Wen, F., Cheng, J., Han, R., Xu, X., Li, S., and Wang, J. (2014) Simultaneous Determination of Aflatoxin M, Ochratoxin A, Zearalenone and α-Zearalenol in Milk by UHPLC–MS/MS. *Food chemistry* **146**, 242-249.

33. Jinap, S., De Rijk, T. C., Arzandeh, S., Kleijnen, H. C. H., Zomer, P., Van der Weg, G., and Mol, J. G. J. (2012) Aflatoxin Determination Using In-line Immunoaffinity Chromatography in Foods. *Food Control* **26**, 42-48.

34. Wang, Y., Ning, B., Peng, Y., Bai, J., Liu, M., Fan, X., Sun, Z., Lv, Z., Zhou, C., and Gao, Z. (2013) Application of Suspension Array for Simultaneous Detection of Four Different Mycotoxins in Corn and Peanut. *Biosensors and Bioelectronics* **41**, 391-396.

35. Speranskaya, E. S., Beloglazova, N. V., Lenain, P., De Saeger, S., Wang, Z., Zhang, S., Hens, Z., Knopp, D., Niessner, R., Potapkin, D. V., and Goryacheva, I. Y. (2014) Polymer-coated Fluorescent CdSe-based Quantum Dots for Application in Immunoassay. *Biosensors and Bioelectronics* **53**, 225-231.

36. Piletska, E., Karim, K., Coker, R., and Piletsky, S. (2010) Development of the Custom Polymeric Materials Specific for Aflatoxin B1 and Ochratoxin A for Application with the ToxiQuant T1 Sensor Tool. Journal of Chromatography A **1217**, 2543-2547.

37. Prieto-Simón, B., Noguer, T., and Campàs, M. (2007) Emerging Biotools for Assessment of Mycotoxins in the Past Decade. *Trends in Analytical Chemistry* **26**, 689-702.

38. Rasch, C., Kumke, M., and Löhmannsröben, H.-G. (2010) Sensing of Mycotoxin Producing Fungi in the Processing of Grains. *Food and bioprocess technology* **3**, 908-916,

39. Anfossi, L., Baggiani, C., Giovannoli, C., D'Arco, G., and Giraudi, G. (2013) Lateral-flow Immunoassays for Mycotoxins and Phycotoxins: A Review. *Analytical and bioanalytical chemistry* **405**, 467-480.

40. www.toximet.com; accessed on 19/8/2015.

41. Piletska, E. K., K. Coker, R. Piletsky, S. (2010) Development of the Custom Polymeric Materials Specific for Aflatoxin B1 and Ochratoxin A for Application with the Toxiquant T1 Sensor Tool. *Journal of Chromatography A* **1217**, 2543-2547.

42. Meulenberg, E. P. (2012) Immunochemical Methods for Ochratoxin A Detection: A Review. *Toxins* **4**, 244-266.

43. Senyuva, H. Z. G., J. (2010) Immunoaffinity Column Clean-up Techniques in Food Analysis: A Review. *Journal of Chromatography B* **878**, 115-132.

44. Vidal, J. C., Duato, P., Bonel, L., and Castillo, J. R. (2012) Molecularly Imprinted On-line Solid-phase Extraction Coupled with Fluorescence Detection for the Determination of Ochratoxin A in Wheat Samples. *Analytical Letters* **45**, 51-62.

45. Khayoon, W. S., Saad, B., Lee, T. P., and Salleh, B. (2012) High Performance Liquid Chromatographic Determination of Aflatoxins in Chilli, Peanut and Rice Using Silica Based Monolithic Column. *Food chemistry* **133**, 489-496.

46. Alonso-Lomillo, M. A., Domínguez-Renedo, O., Ferreira-Gonçalves, L., and Arcos-Martínez, M. J. (2010) Sensitive Enzyme-biosensor Based on Screen-printed Electrodes for Ochratoxin A. *Biosensors and Bioelectronics* **25**, 1333-1337.

47. Bonel, L., Vidal, J. C., Duato, P., and Castillo, J. R. (2010) Ochratoxin A Nanostructured Electrochemical Immunosensors Based on Polyclonal Antibodies and Gold Nanoparticles Coupled to the Antigen. *Analytical Methods* **2**, 335-341.

48. Bazin, I., Andreotti, N., Hassine, A. I. H., De Waard, M., Sabatier, J.-M., and Gonzalez, C. (2013) Peptide Binding to Ochratoxin A Mycotoxin: A New Approach in Conception of Biosensors. *Biosensors and Bioelectronics* **40**, 240-246.

49. De Girolamo, A., McKeague, M., Miller, J. D., DeRosa, M. C., and Visconti, A. (2011) Determination of Ochratoxin A in Wheat After Clean-up Through a DNA Aptamer-based Solid Phase Extraction Column. *Food Chemistry* **127**, 1378-1384.

50. Chen, J., Fang, Z., Liu, J., and Zeng, L. (2012) A Simple and Rapid Biosensor for Ochratoxin A Based on a Structure-switching Signaling Aptamer. *Food Control* **25**, 555-560.

51. Barthelmebs, L., Hayat, A., Limiadi, A. W., Jean-Louis, M., and Noguer, T. (2011) Electrochemical DNA Aptamer-based Biosensor for OTA Detection Using Superparamagnetic Nanoparticles. *Sensors and Actuators B: Chemical* **156**, 932-937.

52. Dinckaya, E., Kınık, Ö., Sezgintürk, M. K., Altuğ, Ç., and Akkoca, A. (2011) Development of an Impedimetric Aflatoxin M1 Biosensor Based on a DNA Probe and Gold Nanoparticles. *Biosensors and Bioelectronics* **26**, 3806-3811.

53. Campàs, M., Garibo, D., and Prieto-Simón, B. (2012) Novel Nanobiotechnological Concepts in Electrochemical Biosensors for the Analysis of Toxins. *Analyst* **137**, 1055-1067.

54. Augusto, F., Hantao, L. W., Mogollon, N. G., and Braga, S. C. (2013) New Materials and Trends in Sorbents for Solid-phase Extraction. *Trends in Analytical Chemistry* **43**, 14-23.

55. Wang, Z., Duan, N., Hun, X., and Wu, S. (2010) Electrochemiluminescent Aptamer Biosensor for the Determination of Ochratoxin A at a Gold-nanoparticles-modified Gold Electrode Using N-(aminobutyl)-N-ethylisoluminol as a Luminescent Label. *Analytical and bioanalytical chemistry* **398**, 2125-2132.

56. Hayat, A., Paniel, N., Rhouati, A., Jean-Loius, M., and Barthelmebs, L. (2012) Recent Advances in Ochratoxin A Producing Fungi Detection Based on PCR Methods and Ochratoxin A Analysis in Food Matrices. *Food Control* **26**, 401-415.

57. Núñez, O., Gallart-Ayala, H., Martins, C. P., and Lucci, P. (2012) New Trends in Fast Liquid Chromatography for Food and Environmental Analysis. *Journal of Chromatography A* **1228**, 298-323.

58. Cao, J., Kong, W., Zhou, S., Yin, L., Wan, L., and Yang, M. (2013) Molecularly Imprinted Polymer-based Solid Phase Clean-up for Analysis of Ochratoxin A in Beer, Red Wine, and Grape Juice. *Journal of Separation Science* **36**, 1291-1297.

59. Capriotti, A. L., Cavaliere, C., Giansanti, P., Gubbiotti, R., Samperi, R., and Laganà, A. (2010) Recent Developments in Matrix Solid-phase Dispersion Extraction. *Journal of Chromatography A* **1217**, 2521-2532.

60. Tessini, C., Mardones, C., von Baer, D., Vega, M., Herlitz, E., Saelzer, R., Silva, J., and Torres, O. (2010) Alternatives for Sample Pre-treatment and HPLC Determination of Ochratoxin A in Red Wine Using Fluorescence Detection. *Analytica chimica acta* **660**, 119-126.

61. Lu, W., Clasquin, M. F., Melamud, E., Amador-Noguez, D., Caudy, A. A., and Rabinowitz, J. D. (2010) Metabolomic Analysis via Reversed-phase Ion-pairing Liquid Chromatography Coupled to a Stand Alone Orbitrap Mass Spectrometer. *Analytical chemistry* **82**, 3212-3221.

62. Liu, X., Li, H., Xu, Z., Peng, J., Zhu, S., and Zhang, H. (2013) Development of Hyperbranched Polymers with Non-covalent Interactions for Extraction and Determination of Aflatoxins in Cereal Samples. *Analytica Chimica Acta* **797**, 40-49.

63. Pascale, M. N. (2009) Detection Methods for Mycotoxins in Cereal Grains and Cereal Products. *Zbornik Matice srpske za prirodne nauke* ***117***, 15-25.

64. Lee, T. P., Saad, B., Khayoon, W. S., and Salleh, B. (2012) Molecularly Imprinted Polymer as Sorbent in Micro-solid Phase Extraction of Ochratoxin A in Coffee, Grape Juice and Urine. *Talanta* **88**, 129-135.

65. Piletska, E. V., Romero-Guerra, M., Chianella, I., Karim, K., Turner, A. P., and Piletsky, S. A. (2005) Towards the Development of Multisensor for Drugs of Abuse Based on Molecular Imprinted Polymers. *Analytica chimica acta* **542**, 111-117.

66. Dowding, P. J., and Vincent, B. (2000) Suspension Polymerisation to Form Polymer Beads. *Colloids and Surfaces A: Physicochemical and Engineering Aspects* **161**, 259-269.

67. Arshady, R. (1992) Suspension, Emulsion, and Dispersion Polymerization: A Methodological Survey. *Colloid and polymer science* **270**, 717-732.

68. Sarı, A., Alkan, C., and Karaipekli, A. (2010) Preparation, Characterization and Thermal Properties of PMMA/n-heptadecane Microcapsules as Novel Solid–liquid MicroPCM for Thermal Energy Storage. *Applied Energy* **87**, 1529-1534.

69. Santra, S., Tapec, R., Theodoropoulou, N., Dobson, J., Hebard, A., and Tan, W. (2001) Synthesis and Characterization of Silica-coated Iron Oxide Nanoparticles in Microemulsion: The Effect of Nonionic Surfactants. *Langmuir* **17**, 2900-2906.

70. Dubinsky, S., Park, J. I., Gourevich, I., Chan, C., Deetz, M., and Kumacheva, E. (2009) Toward Controlling the Surface Morphology of Macroporous Copolymer Particles. *Macromolecules* **42**, 1990-1994.

71. Li, W. H., and Stöver, H. D. (1998) Porous Monodisperse Poly(divinylbenzene) Microspheres by Precipitation Polymerization. *Journal of Polymer Science Part A: Polymer Chemistry* **36**, 1543-1551.

72. Sugihara, Y., Semsarilar, M., Perrier, S., and Zetterlund, P. B. (2012) Assessment of the Influence of Microwave Irradiation on Conventional and RAFT Radical Polymerization of Styrene. *Polymer Chemistry* **3**, 2801-2806.

73. Piletsky, S. A., Piletska, E. V., Karim, K., Freebairn, K. W., Legge, C. H., and Turner, A. P. (2002) Polymer Cookery: Influence of Polymerization Conditions on the Performance of Molecularly Imprinted Polymers. *Macromolecules* **35**, 7499-7504.

74. Svenson, J., and Nicholls, I. A. (2001) On the Thermal and Chemical Stability of Molecularly Imprinted Polymers. *Analytica Chimica Acta* **435**, 19-24.

75. Djozan, D., and Ebrahimi, B. (2008) Preparation of New Solid Phase Micro Extraction Fiber on the Basis of Atrazine-molecular Imprinted Polymer: Application for GC and GC/MS Screening of Triazine Herbicides in Water, Rice and Onion. *Analytica Chimica Acta* **616**, 152-159.

76. Turiel, E., and Martín-Esteban, A. (2009) Molecularly Imprinted Polymers for Solid-phase Microextraction. *Journal of Separation Science* **32**, 3278-3284.

77. Turner, N. W., Holdsworth, C. I., Donne, S. W., McCluskey, A., and Bowyer, M. C. (2010) Microwave Induced MIP Synthesis: Comparative Analysis of Thermal and Microwave Induced Polymerisation of Caffeine Imprinted Polymers. *New Journal of Chemistry* **34**, 686-692.

78. Lai, J., Xie, L., Sun, H., and Chen, F. (2013) Synthesis and Evaluation of Molecularly Imprinted Polymeric Microspheres for Highly Selective Extraction of an Anti-AIDS Drug Emtricitabine. *Analytical & Bioanalytical Chemistry* **405**, 4269-4275.

Chapter 5

Oligonucleotide imprinted polymeric nanoparticles

(OligoMIP NPs)

5.1 Preface

This chapter forms one of the case study undertaken during my PhD research which is based on the development of polymeric materials for the recognition of oligonucleotides. Here, production and characterisation of hybrid oligonucleotide-polymer nanoparticles (OligoMIP NPs) has been introduced by combining the techniques of molecular imprinting and solid phase oligonucleotide synthesis.

The obtained results from the analysis of the prepared OligoMIP NPs suggest that they can selectively recognise the template oligonucleotide, and that the unique strategy of incorporating complementary oligonucleotide strand as "selective monomers" improves their template recognition performance even further without affecting their shape and particle size distribution. Incorporation of oligonucleotides in the polymer matrix achieved in this way is also found to improve the electrochemical stability and dispersibility of the resulting OligoMIP NPs.

Template recognition performance analysis of different OligoMIP NPs suggests that the unique strategy of incorporating oligonucleotides into MIP NPs through their multiple chemical modifications is found to be better than their single point modification. Single chemical modification obtained through the chain ends of the oligonucleotide does not "lock" it in its favourable (template selective) conformation within the polymer backbone which is reflected in its compromised template recognition performance too. The obtained results also indicate that single chemical modification used for incorporating oligonucleotide in the MIP NPs fails to improve template recognition any further than that achieved with PlainMIP NPs (MIP NPs prepared by imprinting the template without the incorporation of oligonucleotide as an additional monomer).

The chapter begins with the literature review discussing the natural base pairing in DNA and their chemical modifications used for the development of bio-sensing platforms. This is followed by discussion on possibility of improving the DNA recognition even further by combining it with the technique of molecular imprinting via proposed strategy of developing OligoMIP NPs. The next section of the chapter gives detailed information on the materials and methods used for the preparation and analysis of the prepared OligoMIP NPs. This is then followed by the discussion of the obtained results with a summary and future outlook on the current work.

5.2 Introduction

Selective molecular interactions are greatly important for several biochemical events occurring within complex biological systems, such as, proteins and nucleic acids (1). As discussed earlier in Section 2.2, the interaction occurring between an antigen and an antibody is a paradigm of such selective interactions. For decades, antibodies have remarkably dominated the research domain in developing various systems for diagnosis, bio-sensing and selective drug delivery applications. However, they suffer from compromised stability, shorter shelf-life and high cost of preparation which has led to growing interest of researchers in developing suitable alternatives (2).

Some of these earlier efforts have resulted in the development of engineered binding proteins (EGB) which consist of selectively bioengineered polypeptide sequences that show comparative recognition performance to that of an antibody. However, the cost of their production is towering as well as the selection process of a suitable polypeptide is laborious. Not to mention, their compromised stability is a major drawback in developing bio sensing platforms (1,3,4).

More recently, aptamers have been widely investigated as alternative affinity tools which are single stranded non-biological oligonucleotide sequences (average molecular weight 8-12 kDa; 20-100 residues of either DNA or RNA). It has already been established that aptamers show selective molecular recognition by forming target specific three-dimensional shapes in biological conditions and can be generated in vitro for a wide range of molecules, such as drugs, proteins and even cells (5). To do so, a large number of combinatorial libraries of short to mid length aptamers are generated *in vitro* followed by their stringent selection for about 5-20 cycles in presence of the target molecule. The most suitable aptamer sequences are chosen at the end of selection cycles and are amplified further by PCR (Polymerase Chain Reaction). This entire process is referred to as SELEX (Systematic Evolution of the Ligands by Exponential enrichment). Whilst preparing RNA aptamers, single oligonucleotide strands are obtained during the transcription (synthesis of RNA from DNA) by using recombinant T7 RNA polymerase enzyme; whereas DNA single strands are simply separated at higher temperature (6-8). In contrast to antibodies, aptamers are generated *in vitro* and do not involve activation of an immune system of animals. Therefore, they can be prepared against the targets that are non-immunogenic as well. Aptamers can also be used at a wide range of pH and temperatures, can be fluorinated, immobilised and regenerated after their use which makes them ideal for immunoassay or biosensor applications in comparison to natural antibodies. Table 5.1 summarises the characteristics of aptamers and antibodies.

Table 5.1: Comparison between natural antibodies and aptamers; regenerated from (9,10).

Antibodies	Aptamers
Produced *in vivo* in animals	Produced by SELEX; produced in vitro and do not require use of animals
Denatures permanently upon their exposure to temperatures of greater than 30 °C	Reusable even after exposing to temperatures of up to 95 °C
Limited only to the targets that produce an immunogenic response	Can be prepared against any target including those that do not produce an immunogenic response
Production often leads to batch to batch variability depending on its host producing them	Smaller in size and can be prepared in laboratory with minimal batch variability
Labelling may result into loss of affinity	Can be labelled without the loss of its affinity towards the target

Since 1980s, the potential to inhibit proteins that cause cancer has been at the forefront in developing anti-cancer treatments. It has been realised that either modification or inhibition of the expression of the gene encoding for such proteins could be vital in developing effective therapeutic and diagnostic platforms for treating life threatening illnesses (11). Some of the earlier studies have already identified genetic biomarkers involved with the pathophysiology and treatment of severe diseases, such as, Alzheimer's and Cancer (12-14). In this regard, nucleosides and oligonucleotides are important class of biomolecules which are not only the building blocks of our genome but also selectively participate in energy distribution in their phosphate forms as well as regulate a wide variety of biological processes as secondary messengers (such as, cAMP- Cyclic Adenosine Monophosphate) in cells (15,16). Like proteins, the ability of DNA and RNA to carry all the information is due to their selective molecular recognition properties, which have drawn researchers' attention in developing DNA-based microarrays as diagnostic platforms (17). Additionally, they are relatively stable as compared to biological antibodies in a wide range of temperature and pH conditions too (3,18-21). However, despite their benefits there is a natural vulnerability of the genetic materials towards enzymatic degradation in biological samples.

5.2.1. The concept of hybrid DNA

Although natural oligonucleotides or aptamers appear to be reasonable alternatives to antibodies, their long term use is debatable as their industrial production is quite laborious and expensive. Not to forget, they are also highly susceptible to the nuclease enzyme when used for analysing biological samples (6). In attempts to resolve this, some studies have reported that suitable chemical modifications of natural DNA can improve their thermal and enzymatic stability (22-25).

Chemical modifications also provide suitable derivatisation for attaching other molecules such as, drugs (26,27), dyes (28) polymers and even nanoparticles for various therapeutic and diagnostic applications (24,29,30). Such chemical modifications are achieved by modifying three key elements present in the structure of the nucleotides which are their nitrogen bases, triose sugars (ribose or deoxyribose) and phosphates as shown in Figure 5.1.

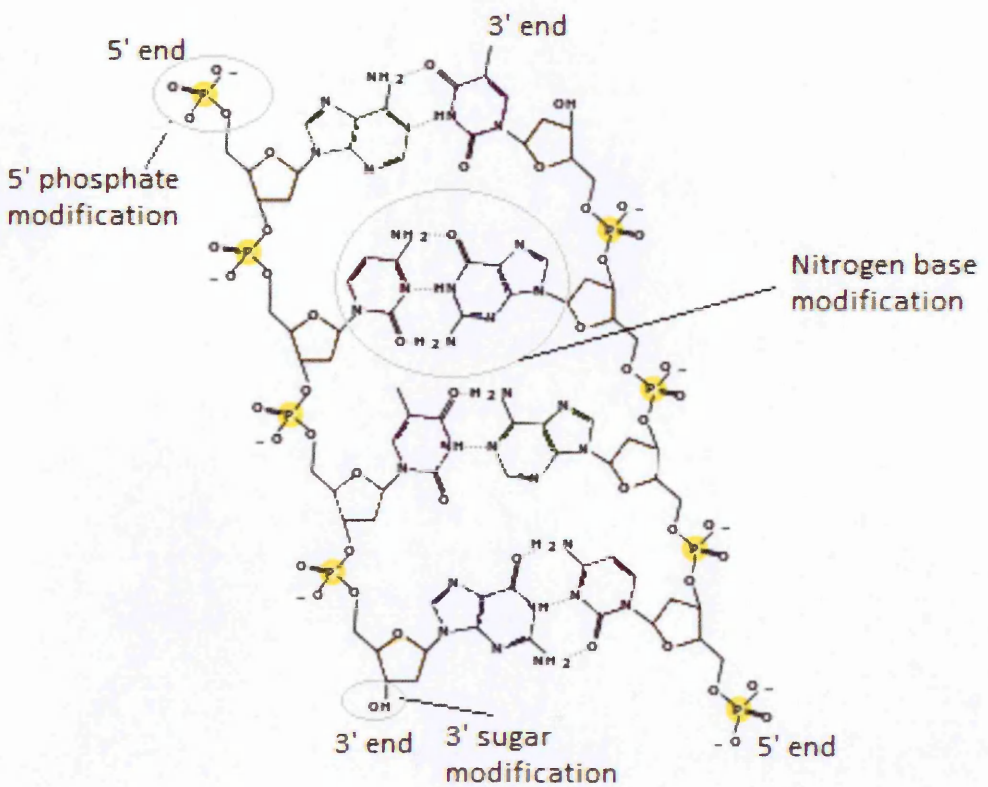

Figure 5.1: Molecular structure of DNA; encircled parts are the sites of chemical modification.

More commonly found oligonucleotide modifications are through its 3' or 5'-phosphates by introducing phosphoramidite derivatives since these are the main sites for nuclease attack and their chemical modifications are also more convenient. Phosphoramidite modified

oligonucleotides are commercially available, such as the Acrydite™ derivatives. This modification in particular is more popular for immobilising the first nucleotide on the solid phase for subsequent addition of other nucleotides whilst preparing a synthetic oligonucleotide sequence using solid phase chemistry. The phosphoramidite derivatives are achieved by esterification of the phosphates of the oligonucleotide chains as shown in Figure 5.2 (31).

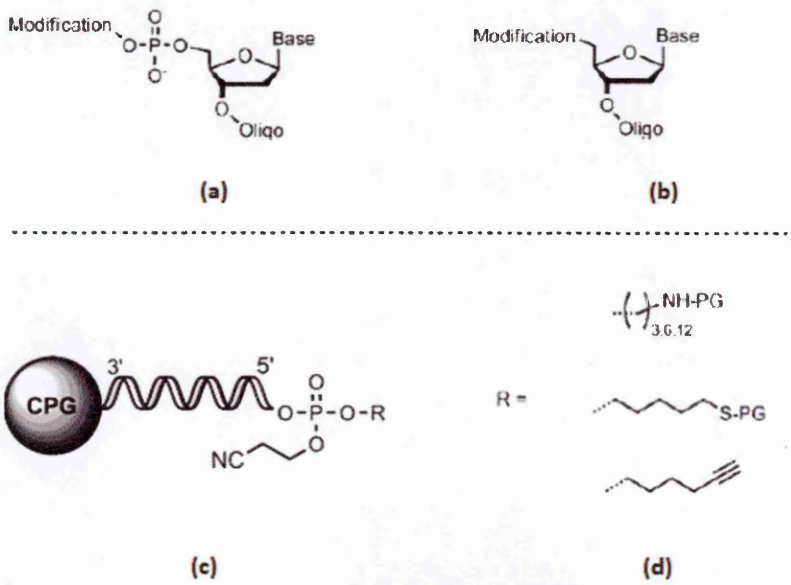

Figure 5.2: Modifications of 5' end of nucleotides in automated solid phase oligonucleotide synthesis; (a) Substitution of 5'- phosphate, (b) complete replacement of 5' phosphate, (c) solid phase DNA synthesis on controlled porous glass beads (CPG) through modified 5' phosphates, (d) examples of some spacers used commercially for the modifications of 3' and 5' phosphates of a nucleotide (R); PG = protecting group used on some spacers during solid phase synthesis; adapted from (24).

Figure 5.2 explains that the immobilisation of nucleotides to CPG can be achieved by modifying the 5' end of the oligonucleotides in two ways; either by 5'-phophorylation carried out with the aid of β-cyanoethyl phosphoramidite or by complete replacement of the 5'- OH of the ribose by introducing -NH_2, -CHO or -COO groups to form amide and ester derivatives of the primer prior to oligonucleotide chain elongation. Synthesis of oligonucleotide sequence can be carried out in the direction of 5' to 3', like that of the biosynthesis of DNA. However, the -OH group on the 3' position of the ribose at the 3' end of nucleotide is less reactive as compared to the 5'- OH group on the 5' end of oligonucleotide sequence. Therefore, laboratory based oligonucleotide synthesis is preferred in 3' to 5' direction for which plenty of 3' phosphoramidite modified DNA sequences are commercially available at economic rate (24).

Among all the modifications, phosphoramidite modifications are the most widely preferred since Acrydite™ modified oligonucleotide sequence can easily co-polymerise with free acrylic acid monomers by forming polyacrylamide. Alternatively, they can also bind to polymer surfaces or stationary phase via different covalent linkages which can be exploited for various biochemical applications.

Another potential site of DNA modification is via modifying the terminal ribose moiety on the 3' end. Such modifications have been mainly studied for the development of anti-sense DNA to treat genetic illnesses, such as muscular dystrophies. Here, the synthesised anti-sense DNA binds to the mRNA synthesised by the disease causing gene and prevents expression of the proteins (32,33). It has also been found that the modification of the 2' position of the ribose or deoxyribose on the 3' end of oligonucleotides increases its binding to the plasma protein and thereby shows improved bioavailability (34). Figure 5.3 explains commonly used base modifications on the 3' end of an oligonucleotide chain.

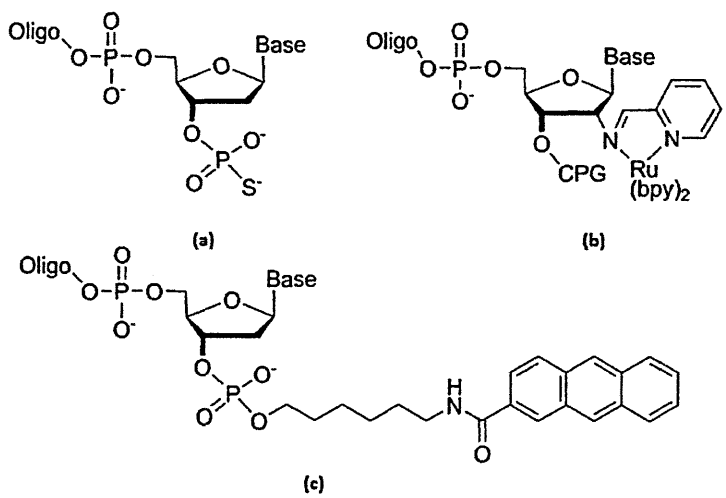

Figure 5.3: Modifications of 3' end nucleotides in automated solid phase oligonucleotide synthesis; (a) monothiophosphate modification, (b) 4'- NH_2 introduction (c) 3'- NH_2 modified DNA; adapted from (24).

Figure 5.3 suggests that the 3' end modifications of the DNA sequences are carried out by introducing thiophosphate or $-NH_2$ groups for immobilising the chain to the –OH functionalised CPG by forming an amide linkage (as seen in Figures 5.3a and 5.3c). Alternatively, 3'-NH_2 modified oligonucleotide strands can be prepared and post functionalised with anthracene after being cleaved from the solid phase in post synthetic stage. However, the simplest way of immobilising the nucleoside or DNA sequence is by functionalization of the solid phase with commercially available -NH_2, -COO and –SH modifiers followed by the addition

of the DNA chain. Chemical modifications of multiple sites is another approach useful for post synthetic functionalization of a pre-formed DNA, for example, introduction of $-NH_2$ derivative on the 4' position of the 3' ribose could be post-functionalised via formation of imine, as shown in Figure 5.3b (35).

Another site for chemical modification of the DNA is via its purine and pyrimidine nitrogen bases. Such chemical modifications are carried out by different means depending on the intended application of the resulting oligonucleotide sequence. Earlier studies have reported that the 2'-OH position of pyrimidine bases is usually substituted with -F and $-NH_2$ groups and resulting modified nitrogen bases are used for the treatment of myasthenia gravis; whereas their 2'-OH and 2'-OCH_3 substitutions have been successful in improving activity of vascular endothelial growth factor for sufficient vasculogenesis in circulatory system (5).

Chemical modification of the nitrogen bases has also been of interest to our research group for its integration into polymers. In recent studies reported by our research group, vinyl and allyl derivatisation of the C-5 deoxyuridine (dU) have been tried; however such modifications have failed to incorporate into the polymers in sufficient amounts. Hydrophobicity added to the DNA chain from such groups may be detrimental to its potential *in vivo* applications too. Bearing this in mind, methyl acrylate substitutions have also been carried out on the C-5 of dU which has improved incorporation (up to 50 %) of dU into polymers under study (36). It would be important to mention that ester substituted nitrogen bases in general are expected to show better incorporation into polymers prepared by free radical polymerisation. This is because its electrophilic property which allows it to form free radicals needed for its incorporation into polymers without affecting its hydrogen bonding with the complimentary nitrogen base.

Chemical modification of the nucleotides also includes complete replacement of the purine and pyrimidine base pairs with the aromatic planar compounds to form a compact stack of fluorescently labelled base pairs. These modifications are ideal for preparing fluorescent DNA markers due to considerable fluorescence quenching in a compact DNA structure (37). Some studies have also reported preparation of size and shape selective base pairing between modified nitrogen bases that can selectively interact via hydrogen, hydrophobic or polar interactions without affecting their natural base pair matching (11,37). Artificial nitrogen bases can also be useful in chelating metals such as copper and iron between two antiparallel DNA strands. Although such an arrangement can change the bonding between the nitrogen bases, it offers a great advantage of stocking metals into the DNA structure which may be useful in the transfer of energy through the molecule like those used in nanowires (24). Modification of the nitrogen bases is also carried out via "click" chemistry which is a single step modification of

bases for their fluorescence labelling and can also be used in conjunction with solid phase synthesis for sequential labelling (38,39). Figure 5.4 explains chemical modifications of the nitrogen bases via click chemistry.

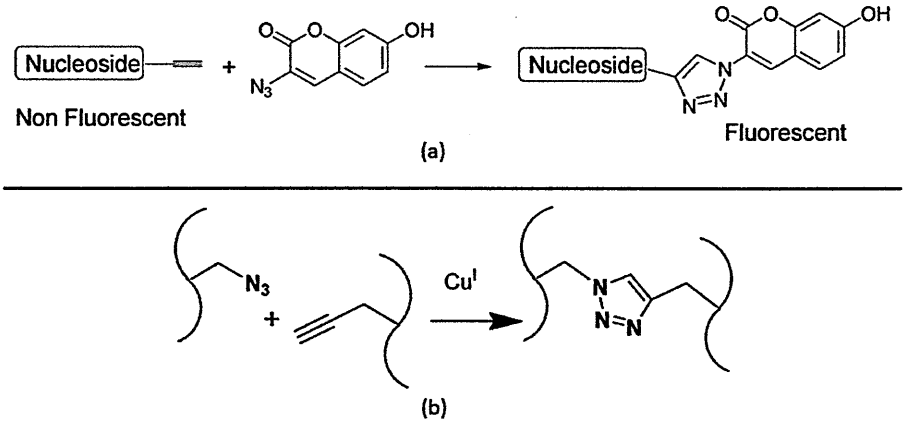

Figure 5.4: Synthesis of triazole oligonucleotide sequences via click chemistry, (a) Click chemistry led fluorescent tagging of a nucleoside, (b) Mechanism of sequential labelling between alkyne and azide containing oligonucleotide chains via formation of triazoles; adapted from (40).

Figure 5.4a shows that an azide or alkyne functionalised nucleosides can be used in a Cu catalysed click reaction. This particular type of click chemistry is a cyclo-addition reaction that results into formation of triazides for fluorescent tagging of the primers. The same reaction can also be carried out between alkyne and azide labelled oligonucleotides for their incorporation into polymers, as shown in Figure 5.4b (40). Although this method is simple, the use of high amounts of metal catalyst such as copper may be toxic for its long term *in vivo* applications. In this regard, modification of nitrogen bases can be carried out by other techniques, such as, MW (microwave) irradiation. Such modifications can be solvent free and are also devoid of any toxic metals as compared to those used in click chemistry. Additionally, these modifications also benefit from extremely quick MW heating producing solvent free products well under five minutes (41).

In agreement to this, one of our recent studies has also pointed out at the usefulness of MW heating for modifying nitrogen bases in comparison to conventional heating. The obtained results suggest that the esterification of nitrogen base can be achieved with the yield of about 45 % in fewer than five minutes with the aid of a MW reactor. The study also reports that although 3' or 5' phosphoramidite modifications are useful for immobilising the nucleoside, they may not be sufficient in holding it intact for its integration into their carriers, such as, a polymer matrix. From the results obtained, it seems that the chemical modifications of the

nitrogen bases along with their phosphoramidite modifications are crucial in improving recognition of its complimentary nucleosides (36). Since the objective of this study is to develop polymer carriers for chemically modified DNA, the following sections of this literature review will discuss different polymers being used for the incorporation of DNA.

5.2.2. DNA- polymer systems

In past few decades, the use solid phase DNA synthesis has achieved tremendous popularity among biologists as it is an automated and incredibly convenient way of preparing and analysing tailor made oligonucleotide sequences as compared to expensive and laborious diagnostic tools generally used, such as, liquid chromatographic techniques (42,43).

However, targeted *in vitro* or *in vivo* delivery of the DNA has always relied on different polymeric and nanoparticular backbones, such as dendrimers, hydrogels and polymer coated gold or iron oxide nanoparticles. These carrier systems are vital for efficient delivery of the gene for desired applications, thanks to their ability to form nanoparticles with stealth characters towards the RES (Reticulo Endothelial System) (22,26-28,42).

To this end, various cationic polymers, such as, PLA [poly(L-lysine)], chitosan, PLGA [(poly(lactide-co-glycolide)] and PEI [poly(ethylene imine)] have been widely used for incorporating DNA for biological applications. Such cationic polymers electrostatically bind with anionic oligonucleotides and condense them into nano-sized vesicles. However, bio-incompatibility of some polymers, such as, PEI could cause cell necrosis and apoptosis upon their internalisation into cells. Not to forget, even biocompatible polymers, such as, chitosan could still be prone to degradation by nuclease in biological samples in loosely aggregated DNA-polymer vesicles. Sometimes, the products from polymer hydrolysis may also generate acidic pH which eventually denatures entrapped DNA before its delivery to the site (44). More advanced polymeric systems such as dendrimers have been investigated for incorporating DNA chains for targeted bio-chemical applications; however their design, optimisation and synthesis are quite laborious and their long term *in vivo* use is cytotoxic.

Poly amino esters have found to be useful in incorporating and transfecting DNA for numerous *in vivo* applications since they are not only cationic and biodegradable but can also be easily modified from the sides with $-NH_2$ functionality to yield significantly improved DNA delivery *in vitro* than that of PEIs (45,46). On the other hand, biodegradable anionic polymers, such as, poly acrylic acid (PAA) and their ester derivatives are also widely used for oligonucleotide incorporation with the aid of a covalent coupling agent, such as EDC (1-ethyl-3-(3-

dimethylaminopropyl carbodiimide) to form an amide linkage between the acids and amino terminated DNA (as shown in Figure 5.5) (31).

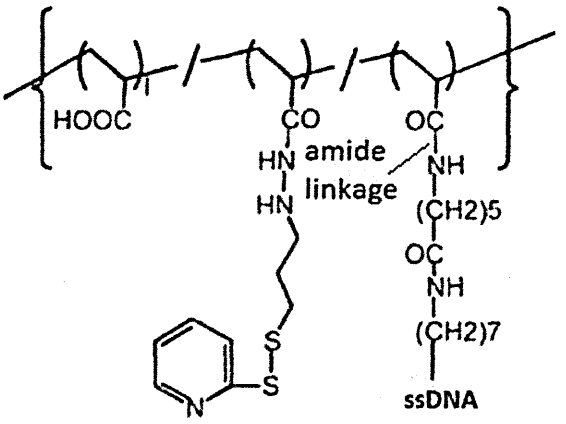

Figure 5.5: DNA conjugated poly acrylic acid through EDC coupling agent; adapted from (47).

Readily available –COOH groups on the surface of PAA can be easily reacted with not just the DNA but also a wide range of drug molecules and other biomolecules containing $-NH_2$ or -OH functionalities. However, its hydrophobicity is a major drawback for their potential *in vivo* applications (48). But their use in combination with hydrophilic polyacrylamide (PAAm) overcomes this limitation and offers a great promise in developing bio-chemical sensors that are responsive in different temperatures, pH, light and concentrations of the target analytes (29,49-52).

PAAm are stimuli responsive polymer networks that form hydrogel nanoparticles. These polymers predominately exhibit temperature responsive reversible volume transition above their upper critical solution temperature (UCST), temperature beyond which the polymer becomes miscible for all compositions (53). This suggests that when PAA/ PAAm hydrogel NPs are kept at the temperatures above their UCST, the hydrogen bonds existing within their hydrophilic chains weaken and swells the NPs. Likewise, when their temperature is decreased below their UCST, the hydrogen bonds re-establish and keep the NPs in a shrunken state (54). Incorporation of DNA into thermo responsive PAA/PAAm hydrogels provides smart materials where DNA can be a functional monomer or cross-linker of the hydrogel formulation to provide a DNA capture-release switch or analyte recognition tools. Incorporation of DNA into polymers also protects it from enzymatic degradation by nuclease. Moreover, selective recognition provided by oligonucleotides means that they can also be used as solid phase immobilised recognition element in immunoassays as a direct replacement of the antibodies (55). Figure 5.6 presents the schematics for DNA incorporation into PAAm hydrogels.

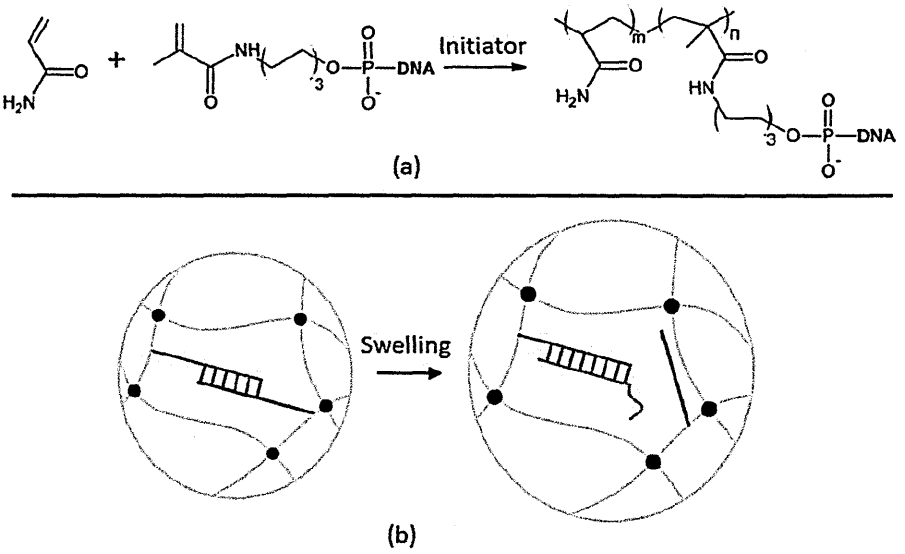

Figure 5.6: Incorporation of DNA into PAAm hydrogels; (a) Co-polymerisation of Acrydite™ modified DNA with acrylamide monomers to form DNA immobilised PAAm hydrogel and (b) Temperature responsive swelling of oligonucleotide immobilised PAAm hydrogel NPs producing a recognition signal; adapted from (56).

Figure 5.6a explains that the $-NH_2$ functionalised DNA can be covalently bound to the acrylamide monomers and co-polymerise to form PAAm based hydrogels. Since hydrogels are thermo responsive, an increase in the temperature above its UCST results into swelling of NPs by breaking hydrogen bonds between their chains. This allows binding of the target or the complimentary DNA to the immobilised DNA in the PAAm matrix of the NPs (as seen in Figure 5.6b).

Cross-linked nanogels not only provide protection to DNA against enzymatic degradation but also hold the DNA chain in its favourable conformation in a densely cross-linked matrix which ensures efficient target recognition. As discussed earlier in section 5.2.1, the most commonly used DNA modification are its 3' or 5'-phosphoramidite (Acrydite™) derivatives. However, very few of these modifications have introduced suitable polymerisable moieties that might transform the DNA into a more classical "monomer" capable of undergoing radical polymerisation processes without losing its primary recognition functions.

Recent studies conducted by our research group has found that chemical modifications obtained on the nitrogen bases in addition to the phosphoramidite modifications of an aptamer sequence can significantly improve their target recognition performance. The obtained results suggest that the chemical modifications from multiple sites of a nucleoside make them polymerisable and provide better integration into their polymer carriers. The study

has also found improved enzymatic stability of an aptamer chemically modified by the proposed strategy into polymer NPs than a non-modified aptamer (57). From this, it can be stated that the recognition performance of the DNA-polymer systems can be enhanced even further by imprinting the target analyte into the polymer matrix; this can be achieved by the technique of molecular imprinting. Section 5.2.3 discusses the usefulness of MIPs in preparing smart polymeric systems for improving DNA recognition.

5.2.3. MIPs for DNA recognition

MIPs represent an important class of recognition materials which provide much greater flexibility of design for small molecules to bio-macromolecules, such as, toxins, pollutants, drugs, explosives, proteins and even bacterial cells (58-62). MIPs exhibit considerably longer shelf-life, high resistance to different pH and temperatures and negligible cost of preparation as compared to their natural antibody counterparts (63).

Among all other MIP formats, MIP based NPs are regarded as the closest tailor-made materials to that of natural biomolecules such as proteins or nucleic acids due to their comparable size, dispersibility, selectivity for the target and spatial distribution of the binding sites together with improved robustness than that of biomolecules (64). Their miniaturised form also provides a large surface area to volume which enables improved template binding and removal kinetics (57).

Past decade has seen tremendous progress in the development of MIP NPs for different applications. These include the use of MIP NPs as enzyme analogs (65), drug delivery (66,67), antibody analogue in immunoassays (21) and even for *in vivo* diagnosis (61,68). In spite of being depicted as antibody analogs, MIP NPs have suffered from the lack of suitable methods of preparation for commercial or clinical applications.

Reported literature suggests that the MIP NPs have been prepared by several methods as those used for the preparation of MIP micro particles, which include, precipitation polymerisation, core-shell polymerisation, living radical polymerisations as well as mini and micro emulsion polymerisation. Most of these methods include elaborate optimisation steps using surfactants and other crucial experimental parameters such as the temperature, rotation speed and the volume of the pre-polymerisation mixture. These parameters highly influence the particle size distribution of the resulting polymer and limits automation of the polymerisation process (64). Additionally, formation of the template selective pores in a MIP matrix can be crucial as the soluble template usually undergoes conformational changes during the pore formation process. This may result into varied orientation of the template and

thereby form heterogeneous pores entrapping some of the template molecules within the MIP cross-links. These entrapped templates may also leach from the MIP matrix during analysis which leading to false interpretation of the template recognition performance of the MIPs (63).

The strategy of hierarchical templated MIP synthesis has helped in resolving the template leaching issue since the template is not removed in the post-polymerisation step but the entire imprinted polymer particle is detached from the stationary phase rendering the template to be reusable for subsequent batches of MIP preparation (69). One of the first attempts of MIP preparation with immobilised template has suggested that the recognition performance of the MIPs can be enhanced when the template was immobilised into polymer matrix as a polymerisable unit (70). This finding is particularly useful since immobilisation of the template also resulted into improvement of the template recognition even when the cross-linking degree of the polymer was quite low (less than 50 %). In another attempt, MIP preparation has been carried out in the presence of an immobilised template in the pores of silica microparticles. It has found that post polymerisation dissolution of silica microparticles in strong acids can destroy the template and silica microparticles forming MAA-EGDMA based MIPs NPs into its pores (71). However, this approach is not devoid of the lack of scalability issues, commonly faced in other MIP related studies.

To address these issues, another study has been presented more recently for the preparation of MIP NPs using immobilised protein template in an automated reactor. The study has combined the benefits of automated solid phase synthesis and the technique of molecular imprinting to produce polymer NPs with selective recognition of the target.

Figure 5.7 shows schematics of the mode of operation of the automated solid phase MIP NPs synthesiser.

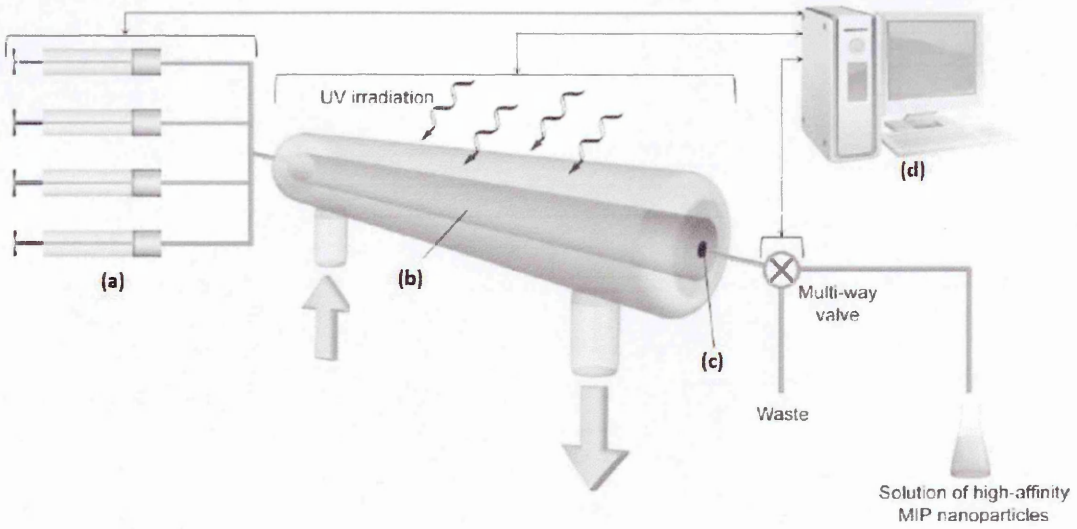

Figure 5.7: Schematics of the operational stages of automated MIP NPs synthesiser, (a) Syringe pumps for polymerisation mixture and elution solvents, (b) Packed solid phase with immobilised template with transparent water cooling jacket and transparent to UV irradiation, (c) Internal heating to maintain column temperature suitable for the polymerisation and (d) Computer platform for the precise control of flow rate, temperature, irradiation time, washing and product collection; adapted from (63).

This finding has grabbed much attention due to the ease, scalability and flexibility of MIP NPs preparation with improved protein recognition performance. Not to mention, unlike the earlier methods it also regenerates the template after each cycle of nanoparticle preparation which is more economic for imprinting biological molecules. This has marked the beginning of a new era in the development of molecular imprinting where prepared MIP NPs can be truly dubbed as antibody analogs since they are water-soluble, biodegradable and miniaturised; they can selectively bind the target molecules and can also be prepared on a large scale by automated reactors.

Based on a similar approach, protein imprinted MIP NPs have also been successfully used as a recognition element in an ELISA as a direct replacement of biological antibodies (21). As discussed earlier in Section 5.2, nucleosides and oligonucleotides also possess excellent molecular recognition but with slightly improved stability than that of natural antibodies. To this end, a study has reported the development of multilayer polymeric microparticles having incorporated thymine for the recognition of its complimentary nitrogen base, adenine. Here, incorporation of thymine into the polymer matrix has been achieved by its photodimerisation. This unique strategy of incorporating complimentary nitrogen base into the polymer matrix

has been found to enhance the template recognition in template rebinding analysis. However, the adsorption capability of the polymer towards different nitrogen bases is different which implies that the proposed strategy may not be universally applicable to other nitrogen bases. Besides, it does not support a strategy for the incorporation of actual nucleosides or oligonucleotides sequences with phosphate-sugar backbones. Although the results obtained in the study are far away from readily applicable, it has opened up a new strategy of exploiting Watson-Crick's classic base pair interactions by utilising nitrogen bases as photopolymerisable cross-linkers as well as template-pairing monomers in preparing imprinted polymers for nucleoside recognition (72). Later on, some more studies have reported preparation of MIP monoliths and MIP membranes for imprinting nucleosides. However, such monolithic and membrane polymers will obviously be exempted from any potential biological applications (64,73,74).

Another recent study has reported development of imprinted nanogel having incorporated aptamers for the detection of its target virus. In this study, the aptamers are immobilised onto PAAm based nanogel through its 5' phosphoramidite modifications which shows selective rebinding of previously imprinted viral protein or whole virus by its thermo selective shrinking or swelling property (75).

However, one of the studies recently reported by our research group has proposed that the 3' or 5' phosphoramidite modifications carried out on the terminals of oligonucleotides may not provide sufficient improvement in its recognition performance since such modifications render oligonucleotide chain more flexible and less integrated into the polymer matrix. Such flexibility may potentially reduce the selective interaction of aptamers with their target or may increase cross-reactivity with other compounds. Not to mention, more flexible nucleosides or oligonucleotides may be more prone to the enzymatic degradation too (as discussed earlier in Section 5.2). On the other hand, chemical modification of nucleosides or oligonucleotides from multiple sites may help improve their integration into the polymer matrix and thereby improve their target recognition performance. Reported literature suggests that the scope of MIP technology has been little explored for the development of nucleoside or oligonucleotide imprinted NPs which exhibit the true potential of being used for real biological applications. In this regard, Section 5.2.4 discusses the strategy proposed by our research group for the development of MIP NPs for DNA recognition.

5.2.4. Hybrid DNA- MIP system: The proposed approach

In a recent study reported by our research group, it has been reported for the first time that the strategy of solid phase oligonucleotide chemistry can be exploited for covalent immobilisation of the nucleoside template into cross-linked hydrogel MIP NPs. To do so, nucleoside imprinted MIP NPs have been generated by incorporating modified 2'-deoxyuridine (dU) into thermo responsive PAAm based MIP NPs. In addition to the modification of the nitrogen bases, the nucleoside has also been modified by phosphoramidite chemistry for its immobilisation onto the solid phase. This is then followed by the preparation of PAAm based thermoresponsive cross-linked hydrogel NPs in the presence of the immobilised template nucleoside (36).

Since the immobilised nucleoside template is chemically modified in this approach, it serves as a polymerisable monomer which is capable of being incorporated covalently into the resultant MIP NPs. Previous studies have reported imprinting of the biomolecules within cross-linked hydrogel NPs made up of traditional monomers (61); whereas our study has found that integration of an additional biological recognition monomer (such as, complimentary nucleoside to that of the template) seems to improve the template recognition even further than that achieved by the MIPs prepared just with the traditional monomers. Figure 5.8 shows the schematics of the preparation of nucleoside imprinted polymeric NPs used in our study.

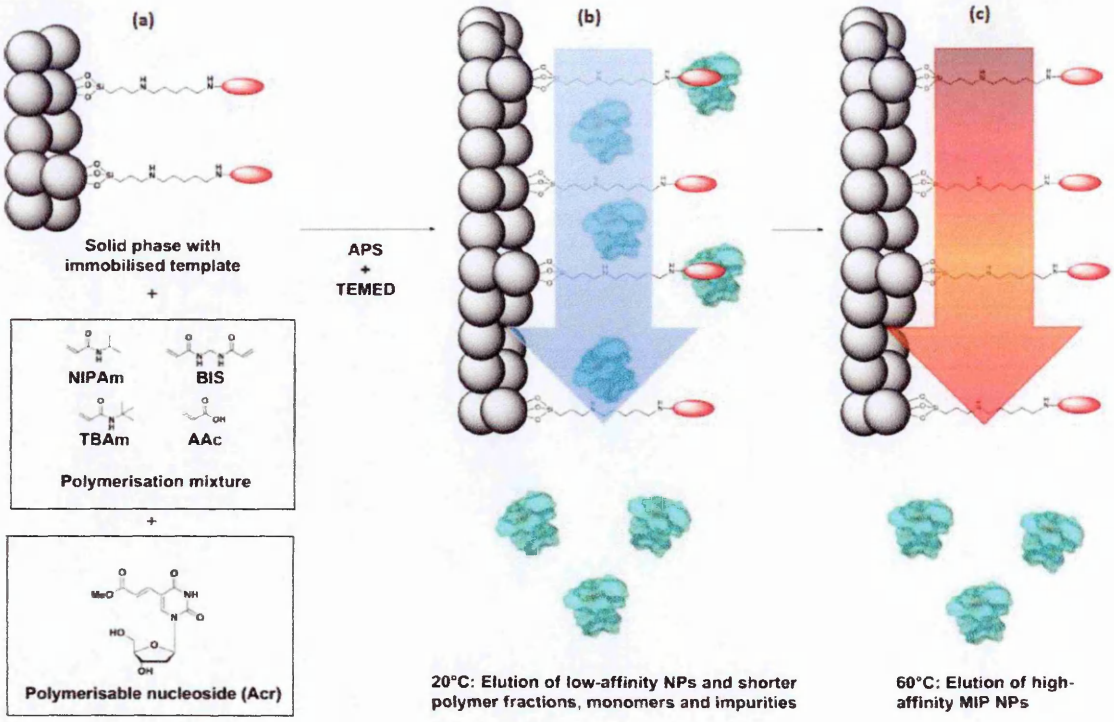

the pre-polymerisation mixture together with the polymerisable dU monomer (Acr), (b) Redox polymerisation carried out by addition of APS (ammonium persulfate) and TEMED (N,N,N',N'-tetramethylenediamine followed by elution of low affinity NPs and other impurities at 20 °C and (c) Elution of high affinity MIP NPs at 60 °C; adapted by (36).

Figure 5.8a shows the preparation of nucleoside imprinted polymeric NPs by the proposed approach where the template nucleosides are immobilised onto nonporous glass beads, used as stationary phase. Monomer mixture together with the polymerisable nucleoside monomer (complimentary to that of the immobilised template) is then added to the stationary phase. Following a polymerisation strategy reported earlier, polymerisation is carried out at room temperature by using redox initiators to allow the formation of polymeric NPs in mild aqueous conditions since biomolecules are used as templates (63). Once the polymerisation is complete, nucleoside tethered PAAm NPs are released from the stationary phase by exploiting thermo responsive nature of the PAAm based hydrogel NPs (as discussed earlier in Section 5.2.2). The UCST (Upper Critical Solution Temperature) of the PAAm based polymer hydrogels is about 53 °C. Therefore, at any temperature below their UCST (53 °C), nanogel particles would remain hydrated whilst maintaining the hydrogen bonds between the template nucleoside and its complimentary nucleoside tethered within the polymer. This means that

elution at such temperatures can remove other impurities, such as, unreacted monomers and low affinity polymer NPs (as shown in Figure 5.8b).

On the other hand, for the elutions above its UCST (60 °C, as used in the experiments), the hydrogel particles would shrink due to breaking of hydrogen bonds that once existed between the template nucleoside and the nucleoside tethered into polymeric NPs. This would release the polymer NPs without affecting covalently bound template nucleoside (as shown in Figure 5.8c). Cross-reactivity studies performed between different templates and dU tethered MIP NPs has suggested that the prepared MIP NPs can specifically recognise dA, whereas no imprinting has been observed when dG and dC are used as templates against dU tethered MIP NPs. Moreover, the study also demonstrates that introduction of a suitable polymerisable monomer (polymerisable dU) into MIP NPs can be achieved for up to 45 % (w/v) which improves their template recognition performance without altering their size, shape and dispersibility. Not to mention, the template is also regenerated at the end of each cycle of NPs preparation for up to 30 cycles which can be quite economical for expensive biological templates, such as proteins and nucleic acids (36).

In a more recently published study by our research group, a novel approach has been used for the development of MIP NPs selective towards an aptamer (single stranded oligonucleotide) target. Figure 5.9 shows the schematics of modification strategy used for the chemical modification of the aptamer sequence used in the study.

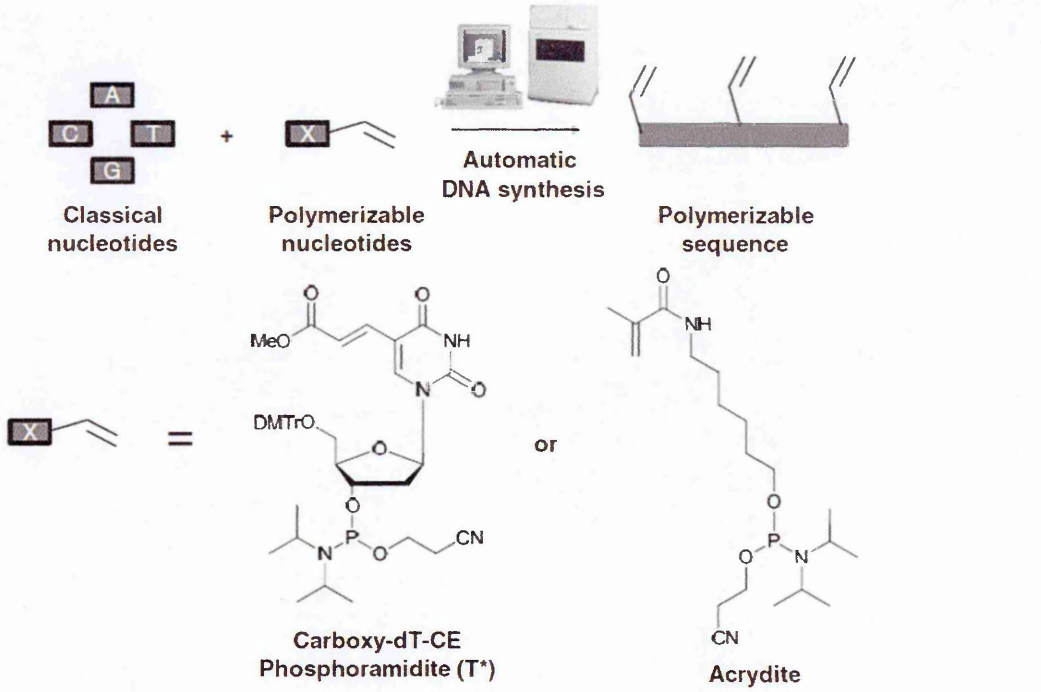

(a)

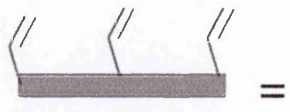

- **Cocaine aptamer (T*6):**
  5'-GAC AAG GAA AAT* CCT* T*CA AT*G AAG T*GG GT*C-3'
- **Cocaine aptamer (T*1):**
  5'-GAC AAG GAA AAT CCT TCA ATG AAG TGG GT*C-3'
- **Cocaine aptamer with commercial Acrydite™ (Acrydite):**
  5'-Acryd-GAC AAG GAA AAT CCT TCA ATG AAG TGG GTC-3'
- **Poly T 12mer (PolyT, control):**
  5'-T*TT TTT TTT TTT-3'

(b)

Figure 5.9: Schematics showing the synthesis of polymerisable aptamer sequences, (a) by using the modified Carboxy-dT-CE Phosphoramidite (T*) or the Acrydite and (b) List of polymerisable DNA sequences used in this: cocaine aptamer with one (T*1) or six (T*6) polymerisable nucleosides or with 5' phosphoramidite modification (commercial Acrydite™). Poly T 12mer is a 5' phosphoramidite derivative, synthesised as a control aptamer sequence; adapted from (57).

Classic nucleotides, particularly, dT have been immobilised on the stationary phase by using their 5' phosphoramidite derivatives (Acrydite™) and further oligonucleotide sequence have been prepared with the aid of an automatic DNA synthesiser (as seen in Figure 5.9a) (36).

Besides its phosphoramidite modification, aptamers are also modified by introducing C-5 alkene substituted 2'-deoxyuridine (T*) residues in its sequence to allow for its incorporation into the polymer from multiple points. Depending on the number of modified deoxythymidine (dT) residues present, the aptamer sequences are called T*1 and T*6 containing one and six polymerisable dT residues respectively (as seen in Figure 5.9a) (57). All the aptamer sequences are then allowed to equilibrate with immobilised cocaine (its target) to allow aptamers to acquire specific three dimensional shapes in the presence of its target (as discussed earlier in Section 5.2.1). This is followed by addition of the pre-polymerisation mixture to produce PAAm based NPs having covalently incorporated aptamer sequence in its matrix. The study has reported that incorporation of up to 75 % (w/v) of polymerisable aptamer can be achieved within the NPs matrix by using the proposed strategy. The resultant aptamer tethered NPs are then recovered by exploiting the thermo responsive property of the PAAm based hydrogels as obtained in earlier study (as explained in Figure 5.8). The obtained results strongly indicate that the enzymatic stability and thereby the target recognition performance of an aptamer sequence can be improved further when it is covalently integrated into the polymer from multiple points (by the virtue of both the phosphoramidite and base pair modifications from multiple points) than just the phosphoramidite modifications (36). The experimental data presented in this chapter consists of the latest study conducted for the development of a hybrid DNA-MIP system.

In the presented study, an oligonucleotide polymer NP system (OligoMIP NPs) is presented for imprinting oligonucleotide sequence into highly cross-linked polymer NPs. Molecular imprinting has been implemented together with the solid phase synthesis to obtain scalable and highly selective polymeric materials for the recognition of oligonucleotides. Following similar experimental protocol from earlier studies, the target oligonucleotide strand (12 base pairs) has been immobilised on the solid phase by the means of multiple chemical modifications including C-5 alkene substituted 2'-deoxyuridine (T*) as well as their 5' phosphoramidite (Acrydite™) derivatisation (36). The immobilised template oligonucleotide strand is then allowed to attain thermodynamic equilibrium with its complementary DNA strand and then locked into highly cross-linked polymeric NPs through the covalent integration. Figure 5.10 shows the schematics of the protocol used for the preparation of OligoMIP NPs in the study.

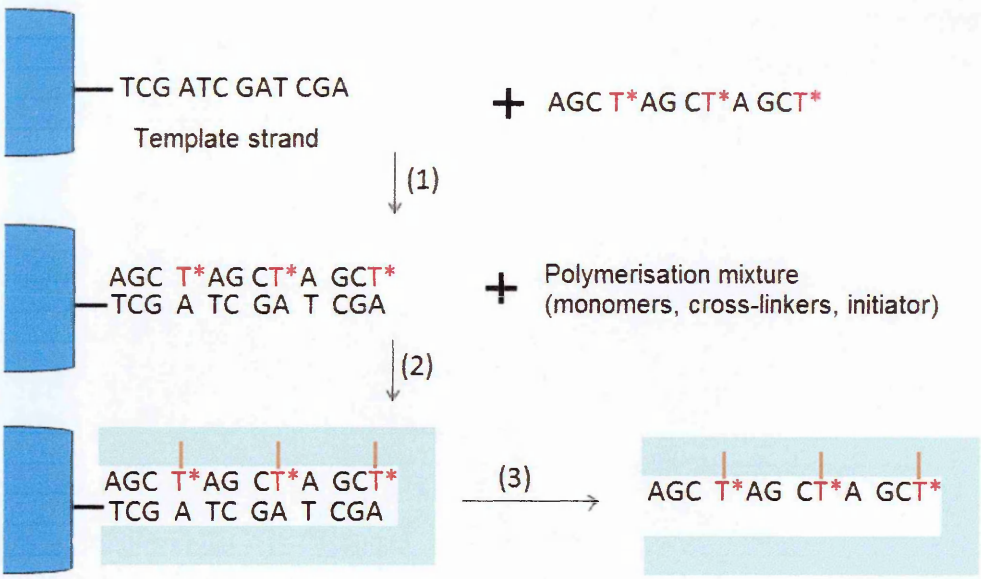

Figure 5.10: Schematic representation of the solid-phase synthesis and selection of OligoMIP NPs, (1) The polymerisable oligonucleotide sequence incubated with the solid phase bearing the oligonucleotide template strand, (2) Pre-polymerisation mixture is added to the solid phase to allow interaction between the complementary DNA strands, and the polymerisation is initiated, (3) High affinity OligoMIP NPs bearing the oligonucleotide sequence are obtained by eluting them at 60 °C; adapted from (63).

The physical analysis of the obtained OligoMIP NPs shows spherical particles with narrow particle size distributions, comparable to natural antibodies. QCM microgravimetric analysis of the synthesised OligoMIP NPs has also been performed which confirms that maximum specificity and selectivity are achieved only when the complementary DNA sequence is structurally supported and locked in into the MIP matrix by multiple anchoring points by the virtue of its polymerisable modified nucleotides.

The study presented here of an OligoMIP NPs system together with earlier studies seems to show consistent improvement of the recognition of not only nucleosides but also of aptamer and oligonucleotides by the strategies proposed by our research group. Such OligoMIP NPs systems can potentially be applied for the development of MIP NPs based assays such as ELISA, where the prepared MIP NPs can be used as a direct replacement of the natural antibodies. Such MIP NPs may also be useful for developing DNA based biosensors for medical diagnostics. The nanoparticulate formulation of such systems would not either rule out their possible applications for in *in vivo* diagnostics. The obtained OligoMIP NPs are currently being investigated for such potential applications.

The following sub sections (5.2.5 to 5.2.8) describe the principles of different analytical techniques used during the study for the analysis of OligoMIP NPs.

5.2.5. Transmission electron microscopy

TEM is a commonly used electron microscopy technique for the analysis of biological as well as non-biological samples for their morphology, shape, size and size distribution studies. Since TEM measures the particle size in the dry state, the obtained values are believed to be the closest to that of the particles original sizes. However, the particle size measurement is carried out semi-quantitatively or manually in this technique. Therefore, the results obtained from TEM are sometimes correlated with other particle sizing techniques, such as DLS (dynamic light scattering). Such correlation is particularly useful for the analysis of polymer colloidal systems in buffers, intended for their biological applications.

In a typical TEM analysis, a focused beam of electrons (80-120 kV) is transmitted through a thin specimen. The acceleration voltage of the electrons may vary depending on the TEM make up. Sometimes, TEM with acceleration voltage of up to 500 kV to 3 MV are also used to attain high transmission. The electrons transmitted through the specimen are collected which then create an image which can be resolved or magnified further through the built in camera. Scanning electron microscopy (SEM) differs from TEM in a way that the sample is scanned by a focused beam of electrons which produces signals that give information about the surface topography and composition of the sample material (78).

5.2.6. Dynamic light scattering (DLS)

DLS is a useful technique for measuring particle size distribution of colloidal micro and nanoparticle formulations. The technique measures the particle size and particle size distribution of the samples by measuring the amount of the scattered light due to the Brownian motion of the particles on a microsecond scale. When light strikes on a colloidal matter, the electric field of the light causes oscillation of its molecules and causes polarization of electrons in the molecules. As a result, the molecules generate a secondary source of light which subsequently scatters the incident light. The scattering patterns largely depend on the size and shape of the colloidal particles, the idea that a larger particle would show less random movement as compared to a small particle. The difference in this intensity of this light is converted to the Hydrodynamic Radius (R_h) of the solvated particle moving in that particular medium by using the Stokes-Einstein relationship with the aid of electrodynamics and theory of time dependent statistical mechanics (77). The hydrodynamic diameter or Stokes diameter is a sphere with same translational diffusion coefficient as that of the colloid on its own, with a

hydration layer surrounding it. Therefore, DLS can accurately measure particle size and its size distribution in the range between 0.5 nm to 100 nm (78). Figure 5.11 shows a typical particle size distribution curve obtained from DLS measurement.

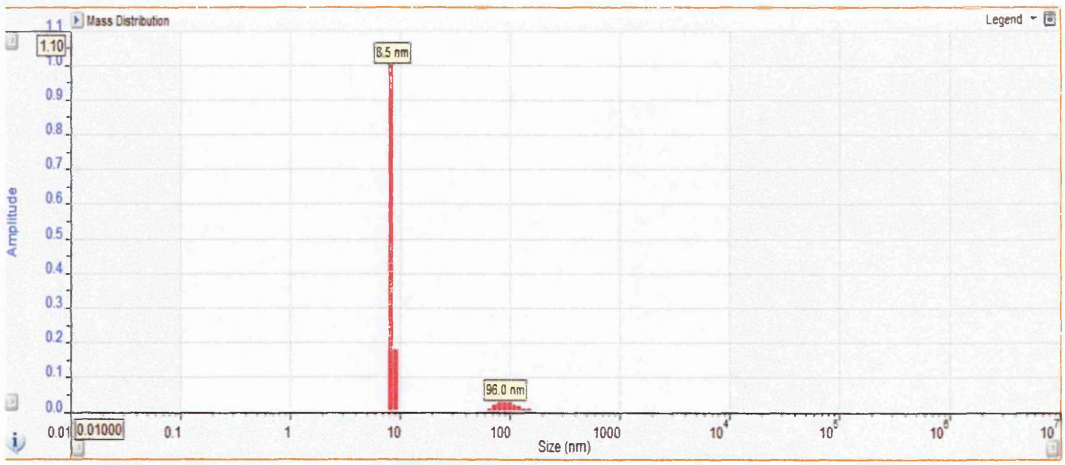

Figure 5.11: Particle size distribution of the OligoMIP NPs obtained from OMNISIZE platform by using DLS.

OMNISIZE software platform is designed to measure the particle size distribution of a colloidal formulation which gives plots of amplitude versus average hydrodynamic radii (R_h) obtained by scattering the light through the samples filled in the cuvette. Figure 5.11 shows a typical plot obtained from the DLS analysis in the reported study where the amplitude (on the Y axis) indicates relative proportion of the particle population of a specific average hydrodynamic radius. Triplicate measurements of each sample have been carried out in the study and mean as well as standard deviations obtained have been reported. Alongside the particle size, different OligoMIP NPs were also analysed for their particle charge or zeta potential as described in Section 5.2.7.

5.2.7. Zeta potential analysis

Zeta potential is a rheological parameter which is widely used to explain the magnitude of electrochemical property of a colloidal suspension. When charged particles are present in an aqueous solution, they give rise to electric double layer where the outermost layer of the charged species of the material is surrounded by counter ions (80). The principle of zeta potential is based on measuring the movement of these counter ions in the presence of external electrical field (81). Zeta potential is a fundamental parameter in determining the colloidal stability of particulate formulations in different conditions of temperature, pH and strength of the solvents (82,83). Figure 5.12 explains the zeta potential theory in colloidal dispersions.

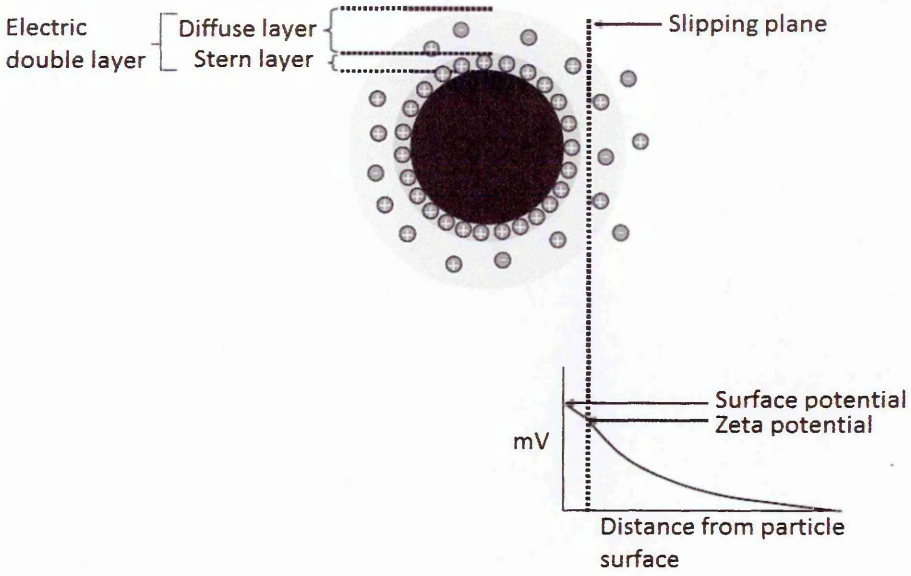

Figure 5.12: Schematics showing different counter ion layers surrounding a colloidal particle. Zeta potential is the electrical potential at the slipping plane; adapted from (84).

When colloids are present in aqueous dispersions, they are surrounded by the ions oppositely charged to their surface, also referred to as the counter ions. The arrangement of the counter ions is highly dense in the layer adjacent to the surface of the colloids; this layer is called the Stern layer (as seen in Figure 5.12). However, the arrangement of these counter ions get more diffused as the distance from the surface of the colloids increases. The decreasing charge density of the counter ions then results in the formation of diffused layer (as seen in the Figure 5.12). In this regard, the space beyond the diffused layer is even lightly populated with such ions. This space is referred to as the slipping plane and the electrical potential arising from the counter ions in this region is called the zeta potential. In general, sufficient amount of the counter ions on the surface of colloidal particle formulation is crucial in keeping it flocculated which further enhances its stability (84). Prepared OligoMIP NPs have been analysed for their DNA recognition performance by QCM which is described in Section 5.4.4.

5.2.8. QCM microgravimetric analysis of Plain and OligoMIP NPs

QCM is a widely used sensory technique to detect the signals brought upon by a change in the oscillation frequency of the crystal used in the instrument. It is usually used as an oscillator control of the circuit which is made up of anode and cathode electrodes. Figure 5.13 explains the components of a typical QCM device.

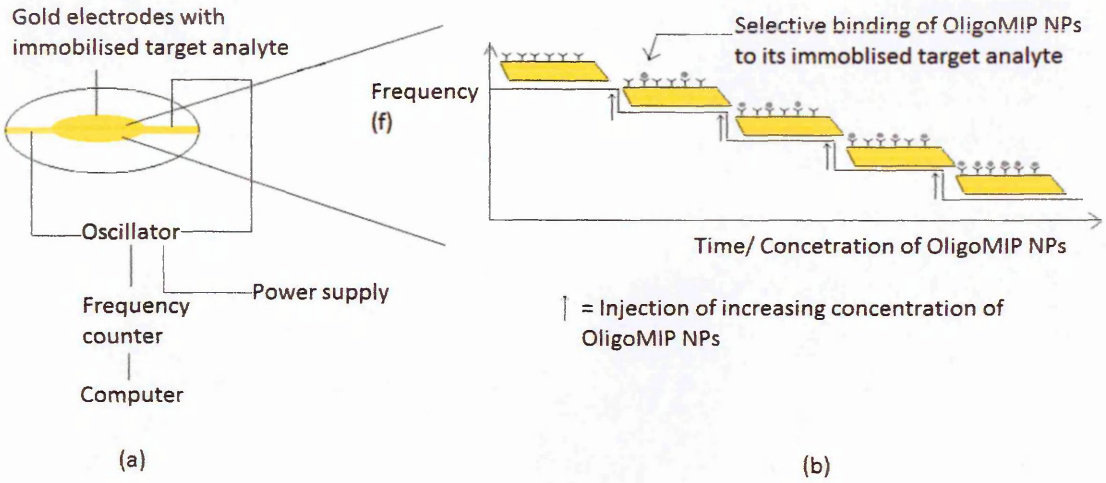

Figure 5.13: QCM analysis of the prepared OligoMIP NPs for their DNA recognition performance; (a) A typical QCM set up with its components and (b) A typical sensorgram obtained from the QCM analysis of OligoMIP NPs under study where increasing concentration of the prepared OligoMIP NPs consistently increases its selective interaction with the immobilised target which in turn consistently decreases the oscillation frequency of the gold crystal from its original base frequency.

The gold crystal used in the QCM circuit immobilises the analyte of interest, for example, an oligonucleotide sequence being used in this study (as seen in in Figure 5.13a). Usually, the crystal with an immobilised analyte (oligonucleotide sequence) oscillates with a certain base frequency. However, when another recognition element (such as, the OligoMIP NPs) is flown through this gold crystal, it selectively interacts with its complimentary oligonucleotide sequence immobilised on the crystal by forming hydrogen bonds through their complimentary nitrogen bases. Such interactions deposit OligoMIP NPs on the surface of the crystal and may continue to deposit even further upon repeated injections of the OligoMIP NPs. Deposition of an increasing amount of OligoMIP NPs mass on the crystal surface then continually decreases resonance frequency of the gold crystal from its base frequency (as seen in Figure 5.13b). This means that the higher the selectivity of synthesised OligoMIP NPs towards its target analyte, the higher its deposition on the gold crystal and the more the decrease in the resonance frequency of the gold crystal. This will be discussed further whilst analysing the results obtained from QCM analysis in the experiments. Section 5.4 discusses results obtained from the physical analysis as well as the DNA recognition performance of the OligoMIP NPs.

The following Section 5.3 includes detailed description on the materials and methods used for the preparation and physicochemical analysis of the OligoMIP NPs used in this study.

5.3. Materials and methods

This section is divided into materials and methods used for the preparation and analysis of the obtained MIP NPs.

5.3.1. Materials

N-isopropylacrylamide (NIPAm), *N,N,N',N'*-tetra-methylethylenediamine (TEMED), ammonium persulphate (APS), acrylic acid (AAc), *N,N'*-methylenebisacrylamide (BIS), *N-tert*-butyl acrylamide (TBAm), 3-aminopropyltriethyloxy-silane (APTES), cysteamine, glass beads, SPE cartridges with frits, toluene, methanol and acetone were purchased from Sigma-Aldrich (UK). Sodium hydroxide, sulfuric acid, 1-ethyl-3-(3-dimethylaminopropyl)carbodiimide (EDC), imidazole, ethylenediaminetetraacetic acid (EDTA) and phosphate buffered saline (PBS) were purchased from Fisher Scientific (UK). Ethanol and hydrogen peroxide were purchased from VWR (UK). DNA sequences bearing the Acrydite® and phosphate (Phos) modification were purchased from Integrated DNA Technologies, Inc (USA). Carboxy-dT-CE Phosphoramidite was purchased from Link (UK). Double-distilled water (Millipore) was used for analysis. All chemicals and solvents were analytical or HPLC grade and were used without further purification.

The following sections will describe the methodology used for the preparation and analysis of the OligoMIP NPs.

5.3.2. Synthesis of polymerisable oligonucleotide sequences (PolyT*12, Poly(AGCT*)$_3$, PolyT ACRYD and Poly(AGCT)$_3$ ACRYD)

Figure 5.11 explains the schematics of the chemical modification of the nucleosides and further synthesis of oligonucleotide sequence by using automatic DNA synthesizer.

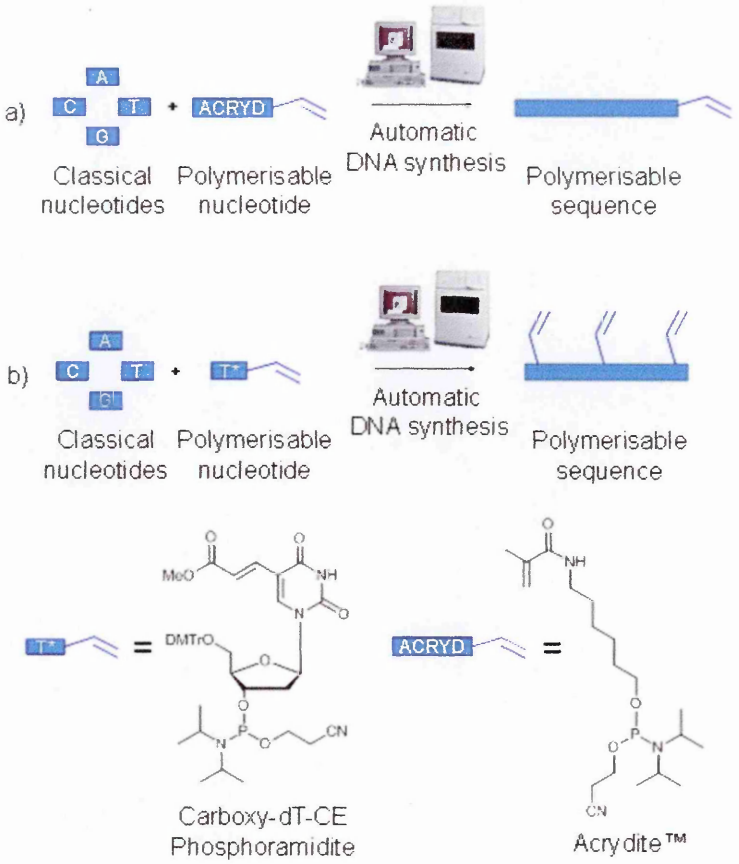

Figure 5.14: Schematics for the preparation of polymerisable oligonucleotide sequences by DNA synthesiser, (a) Nucleoside containing a single polymerisable moiety through Acrydite™ commercial modification or (b) Nucleoside containing several polymerisable moieties through C-5 alkene 2'-deoxyuridine modifications.

Different oligonucleotide strands were prepared by incorporating modified nitrogen bases (as seen in Figure 5.11) with the aid of an automated DNA synthesiser. Figure 5.12 shows the list of polymerisable oligonucleotide sequences used as recognition elements to be incorporated into the OligoMIP NPs in the study.

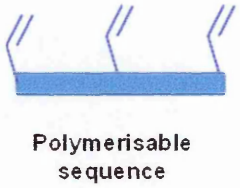

=

1) Poly(AGCT*)$_3$:
5'-AGC T*AG CT*A GCT*-3'

2) Poly(AGCT)$_3$ ACRYD:
5'-Acryd-AGC TAG CTA GCT-3'

3) PolyT*12:
5'-T*T*T* T*T*T* T*T*T* T*T*T*-3'

4) PolyT ACRYD:
5'-Acryd-TTT TTT TTT TTT-3'

Figure 5.15: List of oligonucleotides being used as recognition elements in the OligoMIP NPs composition; "ACRYD" represents the 5'-phosphoramidite oligonucleotides (Acrydite™); whereas T* represents the C-5 alkene-modified 2'-deoxyuridine residues.

The commercial Acrydite™ modification can only be performed at the 3' or 5'-terminal end of the oligonucleotide sequence, whilst the C-5 alkene-modified 2'-deoxyuridine residues can provide multiple anchoring points between the DNA strand and the polymer matrix which should allow for the oligonucleotide to be held firmly into the cross-linked polymer matrix, thus favouring the best possible recognition performance. Moreover, another advantage of this nucleotide modification strategy in comparison to the Acrydite™ method is that the frequency and the location of base modifications could be entirely tailor-made as needed.

5.3.3. Preparation of Poly(AGCT)$_3$-derivatised glass beads as affinity media

Glass beads (125 g, 75 µm diameter, Supelco) were activated by boiling in NaOH (1 M) for 10 min, then washed thoroughly with double-distilled water at 60 °C, acetone and finally dried at 80 °C. This step was performed to maximise the immobilisation of the -OH group on the glass beads. The beads were then silanised by incubating in a solution of APTES (2 %, v/v) in anhydrous toluene overnight at room temperature, then washed with acetone and dried under vacuum. The Phos-AGCT (12 mer) template sequence (425 nmol) was activated in 283 µL PBS (0.01 M, EDTA 0.01 M, pH 7.2) by adding 40 µL EDC and immediately transferring this solution into 22.5 g of APTES-derivatised glass beads suspended in 10 mL of imidazole buffer (0.1 M, pH 6.0). The glass beads were incubated with the DNA template for 2 h at 50 °C and then overnight at room temperature (0.67 mL solution g^{-1} of glass beads). The derivatised beads were washed thoroughly with double-distilled water and dried under vacuum. After this step the glass beads were used straight away for the synthesis of the MIP NPs without further storage. The amount of oligonucleotide could be quantified spectrophotometrically (at λ = 260 nm) by analysing the amount of DNA unbound to the glass beads and found in the washings collected from the immobilisation step. Previous study conducted by our group established

that immobilisation of about 0.5-1.5 μmol g^{-1} nucleotides could be achieved using this this strategy (36).

5.3.4. Solid-phase synthesis of Poly(AGCT)$_3$ OligoMIP NPs

A solution (2.5 mL) of each polymerisable DNA oligomer sequence in PBS (0.005 M, pH 7.4) was degassed by purging argon (Ar) for 10 min and then incubated for 1 h at room temperature in a 14 mL glass vial closed using a Teflon screw-cap and containing 5 g of AGCT-derivatised glass beads (0.67 mL solution g^{-1} glass beads), for a total of six polymerisation vials (Plain MIP NPs, Commercial Acrydite AGCT MIP NPs, PolyT T*12 MIP NPs, PolyT T*1 MIP NPs, AGCT T*3 MIP NPs). In the case of Plain MIP NPs, 2.5 mL of PBS were added to maintain the incubation conditions similar to the other samples. Prior to the addition of the oligomer solutions, the vials containing the solid phase were degassed under vacuum and the air inside the vials then replaced with Ar (3 times). In the meantime, the following monomers were dissolved in PBS (0.005 M, pH 7.4, 50 mL): NIPAm (39 mg, 0.35 mmol, 53 %), BIS (2 mg, 0.01 mmol, 2 %), TBAm (33 mg, 0.26 mmol, 40 %) and AAc (2.2 μL, 0.03 mmol, 5 %). TBAm was previously dissolved in EtOH (1 mL) and then added to the aqueous solution. The total monomer concentration was 13 mM at this stage. The solution was degassed under vacuum and sonication for 10 min, and then purged with Ar for 30 min.

After this time, aliquots of 2.5 mL of solution were transferred in the vials previously incubated with the polymerisable DNA, thus reaching a total volume of 5 mL and a final monomer concentration of 6.5 mM. The polymerisation was started by adding an APS aqueous solution (50 μL, 60 mg mL^{-1}) and TEMED (1.5 μL). The polymerisation was then carried out at 20 °C for 20 h. After the polymerisation, the contents of the vials were transferred into SPE cartridges fitted with a polyethylene frit (20 μm porosity) in order to perform the temperature-based affinity separation of MIP NPs. The temperature of PBS and the SPE cartridges was kept at 20 °C (same as the polymerisation step). Washing was performed with 3 × 5 mL of PBS (0.005 M, pH 7.4), applying manual pressure with a syringe if needed. This was done in order to remove non-polymerised monomers and low-affinity MIP NPs.

The effectiveness of the washing was verified by measuring the UV absorbance of washing aliquots, in order to ensure complete monomer removal as well as to quantify the incorporation of polymerisable DNA into the polymer matrix (by difference of the absorbance measured at λ = 260 nm). Afterwards the SPE cartridges containing the solid phase with high-affinity MIP NPs attached were heated up to 60 °C and eluted with 5 × 5 mL H_2O at 60 °C. The concentration of the nanoparticles fractions could be evaluated by evaporation of the eluted

fractions; previous studies found that the preparation of the MIP NPs by using solid phase synthesis could produce NPs with varying yields of NPs ranging from 15 % w/v to 60 % w/v depending on the amount of immobilised template on the glass beads (36,72,76). Plain MIP NPs were prepared by imprinting the same template [Poly(AGCT)$_3$ 12mer] into the polymeric NPs made up of traditional monomers without the incorporation of oligonucleotide sequence as an additional polymerisable element of the MIP NPs. Section 5.4 describes the principle and methods used for analysing prepared OligoMIP NPs.

5.4. Polymer analysis

This section will describe different analytical techniques used for physicochemical analysis of the prepared OligoMIP NPs.

5.4.1. Transmission electron microscopy

Transmission Electron Microscopy (TEM) images of MIP NPs were taken using a JEOL JEM 1400, 120kV high contrast TEM equipped with an AMT XR60 mid-mount digital camera (11 megapixels). Samples for the analysis have been prepared by depositing a drop of the MIP NPs solution, previously filtered through a 0.45 µm PTFE syringe filter, on a carbon-coated TEM copper grid (300 mesh, from Agar Scientific, UK), blotting away the excess and leaving them to dry overnight at room temperature.

5.4.2. Dynamic light scattering (DLS)

The MIP NPs samples for DLS were prepared in deionized H_2O, sonicated for 5 minutes, then filtered through 0.45 µm PTFE syringe filters and analysed in Quartz SUPRASIL (1.5 × 1.5 mm) cuvette at 25 °C by using Malvern Viscotek DLS (Malvern Instruments Ltd.) equipped with OMNISIZE 3.0 software.

5.4.3. Zeta potential measurements

The MIP NPs were prepared dispersed in PBS (10 mM, pH-7.4) and transferred to DTS1060C clear disposable 1 mL zeta flow-cells. The analysis was done on Malvern Zetasizer Nano Z (Malvern Instruments Ltd.) using the Smoluchowski model (79).

5.4.4. Quartz Crystal Microbalance (QCM) measurements

QCM crystals (5 MHz Cr/Au, polished, Testbourne Ltd., UK) were cleaned by immersion in Piranha solution (H_2SO_4: H_2O_2, 3: 1, v/v) for 5 min. Then they were thoroughly rinsed with double-distilled water and left in MeOH overnight. The immobilisation of the templates has

been performed by incubating the crystals in a solution of cysteamine (0.2 mg mL^{-1}) in EtOH at 4 °C for 24 hours, after which they have been washed with EtOH and incubated for at least 48 h at room temperature in a 10 mL of imidazole buffer (0.1 M, pH 6.0) solution of Phos-AGCT template sequence (425 nmol), previously activated in 283 µL PBS (0.01 M, EDTA 0.01 M, pH 7.2) by adding 40 µL EDC (same activation as for the immobilization onto the glass beads). Once the immobilisation was completed, the crystals were washed thoroughly with double-distilled water before being mounted in the QCM flowcell.

Plain and OligoMIP NPs adsorption to $Poly(AGCT)_3$ template was monitored using a QCM200 5 MHz quartz crystal microbalance (Stanford Research Systems, UK). The modified QCM chips were maintained hydrated during mounting in the QCM flowcell. MIP NPs solutions and running buffer were introduced using an Instech P720 peristaltic pump equipped with 0.020" ID tubing (Linton Instrumentation, UK) and flowing at 0.1 µL min^{-1}. The QCM chip bearing the template was first stabilised in running buffer (PBS 0.003 M, pH 7.4) at 20 °C until the system reached a stable baseline. Affinity analysis was carried out by sequentially by flowing each MIP NPs solution for 5 min (500 µL) and analysing the sensor response for 15 mins. This process was repeated over the concentration range of 0.125 to 2 µg mL^{-1}.

5.5. Results and discussion

This section includes the result obtained from the physical analysis of the OligoMIP NPs which include their particle size and size distribution, zeta potential and morphology characteristics. The physical analysis is then correlated to their template (DNA) recognition performance too. All the formulations of OligoMIP NPs [plain, PolyT ACRYD, PolyT*12, $Poly(AGCT)_3$ ACRYD and $Poly(AGCT^*)_3$] were analysed in identical manner to obtain comparable results. Section 5.5.1 begins with the electron microscopy analysis of the OligoMIP NPs.

5.5.1. Transmission electron microscopy

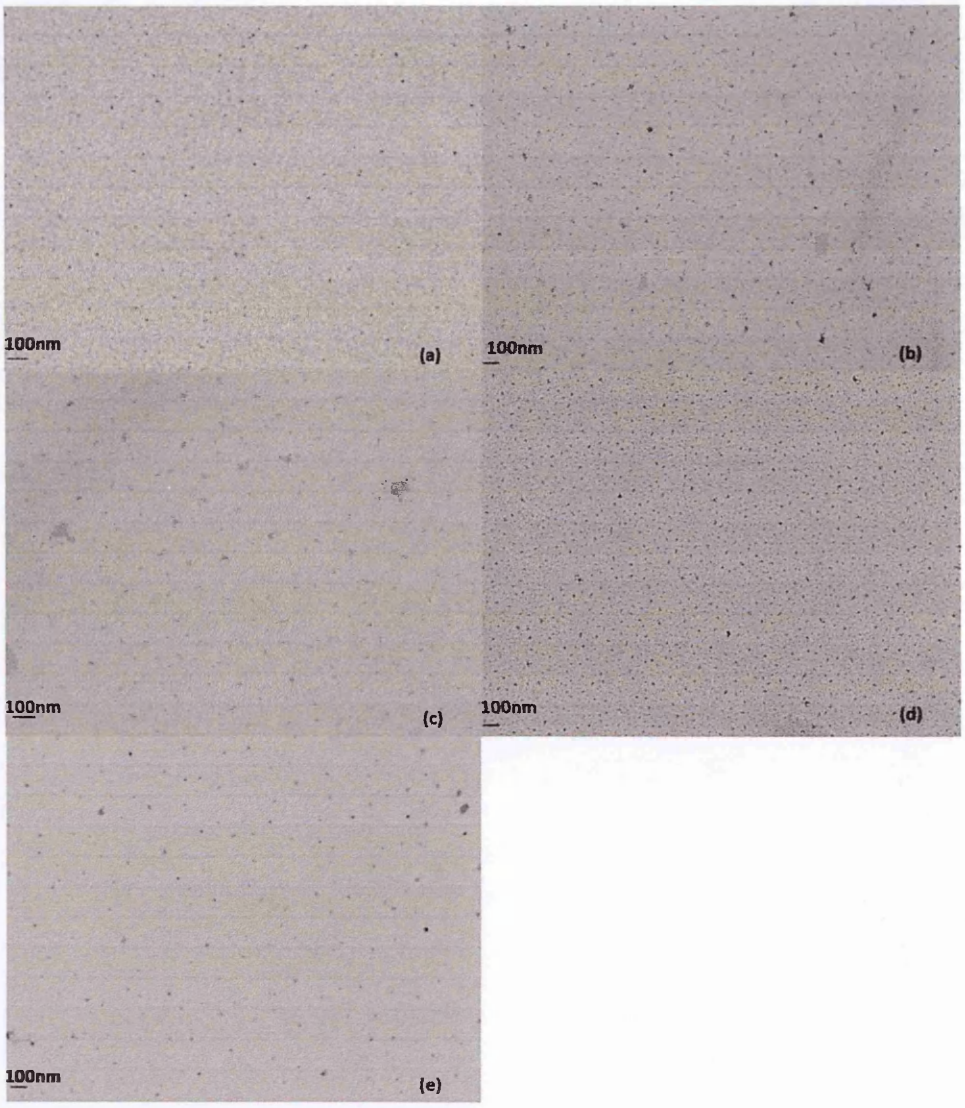

Figure 5.16: Transmission Electron Microscopy (TEM) image of different MIP NPs formulations at; (a) Plain MIP NPs (b) PolyT ACRYD MIP NPs (c) PolyT*12 MIP NPs (d) Poly $(AGCT)_3$ ACRYD MIP NPs (e) Poly$(AGCT^*)_3$ MIP NPs (30,000X magnification).

TEM analysis of different MIP NPs suggested that different formulations of OligoMIP NPs appeared spheroidal in shape with their mean size of about 10-30 nm (as seen in Figure 5.16). However, PolyT ACRYD and PolyT*12 formulations were found to show slightly aggregated NPs (as seen in Figures 5.16b and 5.16c). Not to forget, these OligoMIP NPs were prepared by imprinting PolyT (12 base pairs) as a template into polymer matrix having incorporated Poly$(AGCT)_3$; however incorporation of PolyA instead would have maximised the base pairing. In this regard, observed aggregation into these formulations (PolyT ACRYD and PolyT*12) suggested that lack of enough base pairing could change conformation of the oligonucleotide

strands which could disrupt the electrostatic balance between MIP NPs and might result into formation of aggregated MIP NPs.

On the other hand, PlainMIP NPs Poly(AGCT)$_3$ ACRYD MIP NPs and Poly(AGCT*)$_3$ MIP NPs showed more defined spheroid NPs (as seen in Figures 5.16a, 5.16d and 5.16e). These formulations were prepared by imprinting Poly(AGCT)$_3$ template into polymer matrix having incorporated its complimentary sequence Poly(AGCT)$_3$ within it. Defined morphology of these formulations suggested that when complimentary oligonucleotide sequences interacted, they would form maximum number of complimentary base pairing which might hold DNA into the favourable position obtaining favourable electrostatic balance which might not affect the perfect spheroid shapes of the MIP NPs.

It was observed that the PlainMIP NPs were imprinted with Poly(AGCT)$_3$ but without having incorporated any oligonucleotide sequence within their polymer matrix. Therefore, incorporation of any "special monomer" did not seem to affect shape and size of the resulting MIP NPs as the PlainMIP NPs were well defined spheroids within the particle size range of 10-30 nm, as observed with other formulations (as seen in Figure 5.16).

To study particle morphology even further, Poly(AGCT*)$_3$ MIP NPs formulations was viewed at higher magnification, as seen in Figure 5.17.

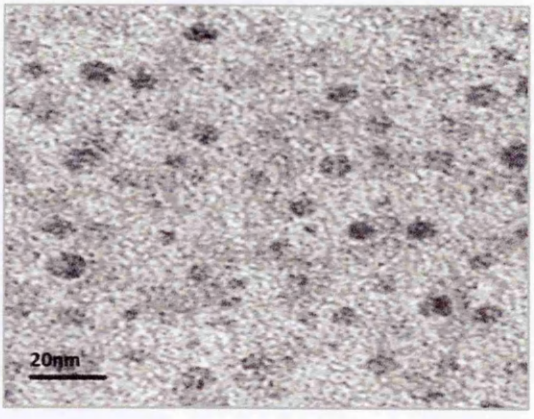

Figure 5.17: Transmission Electron Microscopy (TEM) image MIP NPs Poly(AGCT*)$_3$ MIP NPs (80,000X magnification).

Upon increasing the magnification up to 80Kx, the prepared OligoMIP NPs continued to appear as spheroids however the background noise increased at this higher magnification (as seen in Figure 5.17) which made it increasingly difficult to study the surface texture of the NPs. Overall, the mean particle size and its distribution obtained in this study was comparable to our previous studies where the nucleoside imprinted polymer NPs and MIP NPs synthesised for

the recognition of an aptamer target were found to be in the similar size range of 10-40 nm (36,57). Another study reported preparation of PAAm based MIP NPs for imprinting oligopeptide (melittin) with the comparable mean particle size of 50 nm as well (61).

An earlier study investigated the particle size of the MIP NPs by using TEM and suggested that the mean particle size was dependent on the length of the UV irradiation time when the polymerisation was carried out by UV irradiation. The obtained results in the study suggested that the mean particle size of protein imprinted NPs increased from 150 nm to 400 nm when the UV irradiation time of polymerisation was increased from 2.5 minutes to 4.5 minutes (63). In the presented study, the same length of polymerisation (20 hrs) was used for all the polymers which reflected in their comparable particle size distributions; however it would be interesting to study the effect of the polymerisation time on the particle size of resulting NPs since this has not been studied for a redox initiated polymerisation. Mean hydrodynamic radii (R_h) different OligoMIP NPs was then studied by Dynamic Light Scattering (DLS) as discussed in Section 5.5.2.

5.5.2. Dynamic light scattering

Dynamic Light Scattering (DLS) analysis of the prepared OligoMIP NPs would be vital in understanding the swelling capacity of the hydrogels as the particle size analysis would be performed on the NPs in their hydrated state. The mean hydrodynamic radii (R_h) obtained from the DLS analysis could be useful in understanding how a nanoparticulate formulation might behave in biological samples. DLS analysis particularly of different OligoMIP NPs under the study could help to understand whether the degree of swelling of the OligoMIP NPs could be driven by the type of chemical modification used on the oligonucleotide sequence for their incorporation into MIP NPs. The R_h values obtained from DLS analysis could thereby be used as the direct comparison to the results obtained from TEM to give a good understanding of the degree of swelling into the OligoMIP NPs. Prepared OligoMIP NPs were analysed for their mean particle radii (R_h) by DLS technique (as explained earlier in Section 5.4.2). The obtained values of R_h were then summarised, as seen in Table 5.2.

Table 5.2: Particle size distribution analysis of Plain and OligoMIP NPs in PBS 0.1 M at pH 7.4. Error bars represent ±1 SD (n = 3).

Type of OligoMIP NPs	Mean particle radii (nm)
Plain	11.6 ± 0.46
PolyT ACRYD	5.13 ± 0.32
PolyT*12	16.63 ± 0.57
Poly(AGCT)$_3$ ACRYD	9.57 ± 3.42
Poly(AGCT*)$_3$	16.23 ± 2.49

In general, the mean particle diameters of all OligoMIP NPs formulations obtained from DLS analysis were in the range of 10-30 nm. This was in agreement with the results obtained from the TEM analysis of the same formulations (as discussed earlier in Section 5.4.1).

Having studied the pattern of the obtained particle size, it was found that the incorporation of ACRYD modified oligonucleotides [PolyT ACRYD and Poly(AGCT)$_3$ ACRYD] resulted in slightly smaller MIP NPs as compared to the PlainMIP NPs. On the other hand, incorporation of the modified deoxyuridine containing oligonucleotide MIP NPs [PolyT*12 and Poly(AGCT*)$_3$] resulted into slightly larger OligoMIP NPs in comparison to the PlainMIP NPs (as seen in Table 5.2). From this, it could be hypothesised that the slight changes observed in the particle diameter could be derived from the type of chemical modification of the oligonucleotide sequences, particularly the fact that the Acrydite™ modification would possess more of a hydrophobic character due to the introduction of a C6 carbon chain at the end of the DNA sequence in comparison to the C-5 alkene deoxyuridine modification. Such hydrophobic modifications obtained by the Acrydite™ derivatisation might result into a more "compact" conformation and smaller size in buffer solution.

In this study, the mean particle diameter obtained by both the TEM and DLS were quite similar which also indicated negligible swelling of the MIP NPs in water (as discussed in Sections 5.4.1 and 5.4.2). This reaffirmed the earlier hypothesis that "compact" conformation of the polymer NPs caused by integrating oligonucleotide in its matrix from multiple points might restrict water intrusion. Therefore, OligoMIP NPs would show minimal swelling in their wet state. In an earlier study, MIP NPs imprinted with nucleosides showed slightly more swelling in water than

in their dry state (36). This behavior might be due to the fact that integration of a nucleoside from a single point in the NPs matrix could result into a comparatively loosely fitted polymer matrix allowing more water intrusion. This might be the reason why nucleoside imprinted NPs appeared slightly bigger in their wet state during DLS analysis than when in dry state. Overall, the mean particle size of the OligoMIP NPs obtained by DLS was found to be comparable to that of natural antibodies (85). In comparison to other dispersion polymerisation techniques, solid phase templated synthesis (as proposed in this study) produced smaller MIP NPs with narrow particle size distributions (86,87).

Some other studies also reported that the R_h obtained from the DLS analysis of PAAm based hydrogel MIP NPs could be affected by the pH and temperature conditions. One study found that MIP NPs formulations consisted of NPs in the range of 50-150 nm at 37 °C; however they showed considerable amount of swelling (upto 4 to 5 times) at 25 °C (76). This would be expected as the hydrogen bonds between the polymer chains would likely to be formed at lower temperatures and the NPs would swell in their hydrated state. On the other hand, higher temperatures could break hydrogen and even electrostatic bonding within the NPs matrix shrinking the NPs and thereby resulting into smaller R_h in DLS analysis. That said, the degree of swelling would be largely driven by the type and amount of other functional monomers and cross-linkers used for the preparation of hydrogel MIP NPs.

In a similar way, different pH conditions could also affect the R_h of the hydrogel MIP NPs. A study reported that extremely acidic and alkaline pH could lead to protonation or deprotonation of the functional groups of the monomers which might increase electrostatic repulsion between these functional groups and thereby result into bigger particle sizes. On the other hand, neutral pH could provide perfect balance between electrostatic repulsive and attractive forces and would result into comparatively smaller and compact hydrogel NPs. Such thermo and pH sensitive properties of hydrogels could be exploited in developing signaling sensors and drug or gene release-capture switches. DLS analysis experiments in this study were carried out at the neutral pH since the aim of developing OligoMIP NPs was to investigate their DNA recognition property and not the release efficiency. However, it would be useful to study whether different pH and temperature conditions could affect the recognition performance of the prepared OligoMIP NPs by attributing conformational changes to the incorporated oligonucleotide sequence in its polymer matrix.

Alongside the morphology and particle size distribution, the surface charge of the MIP NPs would also be crucial in defining the long term stability of the developed NPs. Therefore,

prepared OligoMIP NPs formulations were analysed for their zeta potentials as discussed in section 5.5.3.

5.5.3. Zeta potential measurements

Zeta potential measurements of the prepared MIP NPs were carried out to study their colloidal stability. The measurements were based on the fact that sufficient amount of charged species on the surface of colloidal particles would be crucial in maintaining their dispersibility at any given pH or temperature. Since the value of zeta potential would reflect into the amount of charged species at the interface, the higher the zeta potential the more stable a particulate formulation would be (as explained earlier in Section 5.4.3).

The objective to carry out zeta potential measurements of OligoMIP NPs was to study whether integration of oligonucleotide sequence within the polymer NPs could alter the zeta potential and thereby colloidal stability of the MIP NPs. Since the obtained NPs were mainly composed of acrylate derivatised acrylamide cross-linkers, they would be expected to show negative zeta potential values. Not to mention, negative zeta potential values could also be enhanced by the incorporation of negatively charged oligonucleotide chains which could be studied by comparative analysis of different OligoMIP NPs and PlainMIP NPs. To do so, obtained OligoMIP NPs were analysed by Zetasizer as described earlier in Section 5.4.3. All the experimental parameters were kept constant for different samples to obtain comparable results. The obtained results were then summarised as shown in Table 5.3.

Table 5.3: Particle size distribution and zeta potential analyses of Plain and OligoMIP NPs in PBS 0.1 M at pH 7.4. Error bars represent ±1 SD (n = 3).

Type of MIP NPs	Zeta potential (mV)
Plain	-10.53 ± 0.32
Poly T ACRYD	-5.81 ± 0.34
PolyT*12	-24.47 ±0.65
Poly(AGCT*)$_3$	-9.0 ± 0.34

AAm-AAc-TBAm based cross-linked nanogels would be usually expected to show negative zeta potentials due to dissociation of –COOH groups on their surface (88). This hypothesis was found to be supported by the obtained zeta potentials in the presented study where all the MIP NPs were found to show negative zeta potentials (as seen in Table 5.3). Comparative analysis also suggested that PolyT*12 and Poly(AGCT*)$_3$ OligoMIP NPs exhibited a more

negative zeta potential value than the PlainMIP NPs which indicated that incorporation of the polymerisable oligonucleotide monomers through multiple chemical modifications contributed towards the stabilisation of the MIP NPs dispersions. On the other hand, PolyT ACRYD and Poly(AGCT)$_3$ ACRYD OligoMIP NPs exhibited more similar Zeta potential values to PlainMIP NPs, which suggested that ACRYD modified oligonucleotide monomers either destabilised or did not exhibit any effect on the stability of MIP NPs dispersions.

Overall, obtained zeta potentials were comparable to those reported in other studies where PAAm based cross-linked nanogels were developed. It was interesting to notice here that the mean particle size of the NPs was much similar in all the studies which meant they would exhibit much similar surface area too. Since zeta potential would be a measure of the surface charge and charge density on the particles, it suggested that the similar particle size of these PAAm NPs might result into much similar zeta potentials too. In all the studies, zeta potentials of PlainMIP NPs were quite similar regardless of the relative proportions of their functional monomers (AAc) with different acrylamide based cross-linkers as well (86,88,89).

Plain MIP NPs were also developed in one of the earlier studies reported by our group with exactly similar monomer ratios. Zeta potential analysis of the PlainMIP NPs obtained both in the previous and the current study showed quite similar values. The same study also found that incorporation of chemically modified nucleosides into the MIP NPs increased the negative value of zeta potential considerably which was in agreement with the results obtained in this study (36).

This reaffirmed the earlier hypothesis that when incorporation of nucleosides or oligonucleotides into polymer NPs was achieved through their multiple chemical modifications (both the base and ACRYD modifications), they improved dispersibility of the resulting NPs. On the other hand, just the ACRYD modifications of nucleosides or oligonucleotides failed to improve dispersibility of the polymeric NPs. To understand this behaviour further, the results obtained from zeta potential analysis were correlated to that obtained from DLS analysis of the OligoMIP NPs under study. This suggested that the MIP NPs having incorporated oligonucleotides just with ACRYD modifications produced loosely packed and swollen NPs with lower dispersibility. However, chemical modifications of the bases alongside their ACRYD modifications improved incorporation of oligonucleotides into the polymeric NPs which produced tightly packed, small and highly dispersed OligoMIP NPs (as discussed earlier in Section 5.5.2). It would be important to mention here that zeta potential experiments in this study were performed in buffers at physiological conditions; however it might useful to study the effect of different temperatures and pH on the zeta potentials of different OligoMIP NPs

under study. After having studied the physical properties of MIP NPs, they were analysed for their template recognition performance which was conducted by QCM (Quartz Crystal Microbalance) microgravimetric analysis as discussed in Sections 5.5.4.

5.5.4. QCM microgravimetric analysis

QCM gravimetric analysis of the obtained OligoMIP NPs was carried out to test their oligonucleotide recognition performance. Clarification of the obtained results was based on the hypothesis that reduction in oscillation frequency of the gold crystal (having immobilised the template oligonucleotide) would indicate selective interaction between the template and the MIP NPs, the magnitude of which would indicate the strength of interactions. In other words, the lower the oscillation frequency of the QCM crystal (from its base frequency), the higher the template recognition performance of the MIP NPs (as discussed earlier in Section 5.4.5).

The objective for conducting QCM analysis was to understand relative strength of the recognition performance of different MIP NPs towards their template [poly(AGCT)$_3$] by studying;

a) Whether incorporation of a complimentary oligonucleotide [such as, Poly(AGCT)$_3$ and Poly(AGCT*)$_3$] in the NPs matrix could help improve recognition of their temple oligonucleotide (through base pair matching according to Watson-Crick DNA model);
b) Whether the template recognition performance of the OligoMIP NPs with immobilised oligonucleotide sequence surpassed to that exhibited by PlainMIP NPs (NPs made up of traditional monomers without the incorporation of a complimentary oligonucleotide in its matrix);
c) Whether the strategy used for incorporation of oligonucleotides within the NPs influenced their template recognition performance. This was carried out to understand whether incorporation of oligonucleotide through its multiple chemical modifications (modification of their nitrogen bases along with their ACRYD modification) could improve their template recognition performance even further as compared to single point chemical modification used for incorporating them into MIP NPs (ACRYD modification) and even PlainMIP NPs (with no incorporation of oligonucleotide).

The length of all the oligonucleotide chains used in this study was kept the same (12 base pairs) to facilitate selective recognition of the complimentary nitrogen bases.

From the understanding of the natural base-pairing in DNA, the OligoMIP NPs having incorporated poly(AGCT)$_3$ would be expected to show improved recognition of the template [poly(AGCT)$_3$] compared to polyT incorporated MIP NPs. The results obtained through the DLS and zeta potential analysis suggested that the OligoMIP NPs obtained by incorporating oligonucleotide through its chemical modification from multiple points (modification of their nitrogen bases along with their ACRYD modification) showed higher electrochemical stability possibly due to tighter integration of the oligonucleotide sequence.

From this, it could be hypothesised that such multiple chemical modifications could "lock" the polymerisable oligonucleotide in its favourable conformation within highly cross-linked polymer NPs and thereby exhibit improved template recognition performance. On the other hand, the OligoMIP NPs obtained by incorporating oligonucleotide through its chemical modification from a single point (chain end ACRYD modification) showed lower electrochemical stability and loose integrations of the polymerisable oligonucleotide sequence. Observed lower electrochemical stability might cause aggregation of the MIP NPs and loosely integrated oligonucleotide could constantly change their conformation resulting into compromised template recognition performance (as discussed earlier in Sections 5.5.2 and 5.5.3).

To test the hypothesis, template recognition analysis of the prepared MIP NPs was carried out using QCM. In the analysis, the template [poly(AGCT)$_3$] was immobilised on the QCM gold crystal by using the same immobilisation strategy as was used during solid phase synthesis of these OligoMIP NPs. This was done to ensure that the template was orientated in exactly the same direction as it was during the polymerisation and thereby would favour its recognition by the MIP NPs. Different OligoMIP NPs formulations were flown through the flowcell containing template immobilised on the crystal. PlainMIP NPs having immobilised no oligonucleotide within their matrix were also used for a comparative analysis with the OligoMIP NPs (oligonucleotide immobilised MIP NPs). Different concentrations of all the OligoMIP NPs and PlainMIP NPs were injected through the QCM flowcell under identical conditions to obtain comparable results and the obtained QCM sensorgrams were plotted as seen in Figure 5.18.

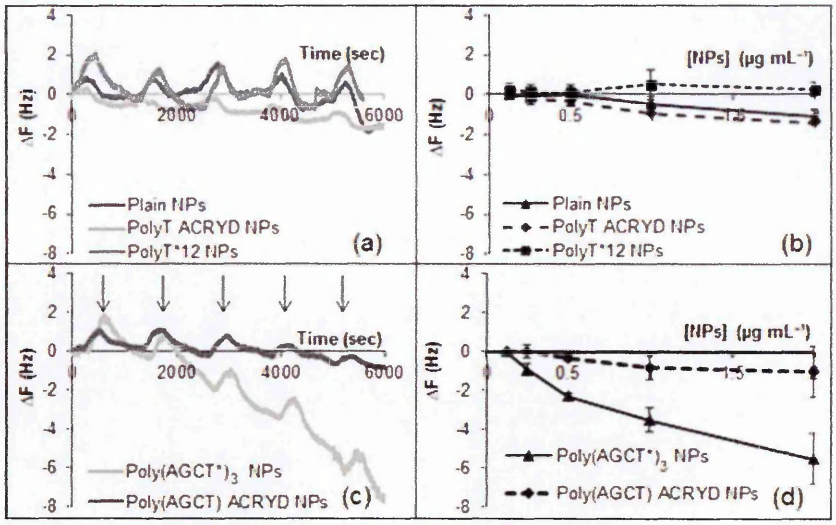

Figure 5.18: Template rebinding analysis by QCM; (a) A typical QCM sensorgram obtained by rebinding different control MIP NPs (Plain, PolyT ACRYD, and PolyT*12 MIP NPs) on a Poly(AGCT)$_3$ oligonucleotide derivatised gold surface; arrows indicate the points of injection; (b) Rebinding performance of control NPs (Plain, PolyT ACRYD, and PolyT*12 MIP NPs) to Poly(AGCT)$_3$ functionalised gold surface; (c) A typical QCM response obtained by rebinding Poly(AGCT)$_3$ ACRYD MIP NPs and Poly(AGCT*)$_3$ MIP NPs to the complementary template oligonucleotide Poly(AGCT)$_3$ derived gold surface; arrows indicate the points of injection; (d) Rebinding performance of Poly(AGCT)$_3$ ACRYD and Poly(AGCT*)$_3$ MIP NPs to the complementary Poly(AGCT)$_3$ derived gold surface. Drop in frequency (on the Y-axis) indicates the binding event of the MIP NPs to the surface-immobilised oligonucleotide sequence. QCM measurements were performed in PBS (0.03 M, pH 7.4) at 20 °C for the NPs concentrations from 0.125 to 2 μg mL^{-1}; error bars representing ±1 SD (n = 3).

The obtained QCM sensorgrams suggested that the Plain, PolyT ACRYD and PolyT*12 MIP NPs did not exhibit considerable binding when tested against the template [poly(AGCT)$_3$] as none of these MIP NPs showed drop in the oscillation frequency of QCM crystal by no more than 1.5 units (as seen in Figures 5.18a and 5.18b). This was an expected behavior because according to the principle of base pairing in oligonucleotides, the template [poly(AGCT)$_3$] would not selectively bind to any of the polymerisable nucleotides present within the mentioned MIP NPs Such poor and inconsistent base pairing (as seen in Figure 5.18a and 5.18b) between the template and polymerisable oligonucleotide during polymerisation might generate heterogeneous binding sites within the resulting MIP NPs matrix resulting into their poor template recognition, as observed.

To understand this hypothesis further, poly(AGCT)$_3$ bearing MIP NPs were also tested for their template poly(AGCT)$_3$ recognition performance in identical manner and QCM sensorgrams

were recorded. When flown through the immobilised template, Poly(AGCT)$_3$ ACRYD MIP NPs dropped the oscillation frequency of the gold crystal by about one unit; however Poly(AGCT*)$_3$ MIP NPs dropped it by more than 6 units (as seen in Figure 5.18c and 5.18d). This indicated that Poly(AGCT*)$_3$ MIP NPs exhibited considerably higher binding to the template [poly(AGCT)$_3$] than Poly(AGCT)$_3$ ACRYD MIP NPs. It was interesting to observe that although Poly(AGCT)$_3$ ACRYD MIP NPs contained the exact fitting base pair sequence to that of the template, they failed to improve template recognition any further than that achieved with the control MIP NPs (as seen in Figures 5.18a and 5.18b). This suggested that the only possible reason for the observed difference in the performances of Poly(AGCT)$_3$ MIP NPs and Poly(AGCT*)$_3$ MIP NPs must be due to the differences in the chemical modification strategies used to incorporate oligonucleotides within them.

This was in agreement with the hypothesis chemical modifications obtained on the nitrogen bases in addition to the ACRYD modification of oligonucleotides could provide multiple points for better integration into polymeric NPs. This in turn could help in holding oligonucleotide "locked" in its favourable conformation for improved template recognition. On the other hand, oligonucleotide incorporation into polymer backbones just through single point (by their ACRYD) modification might not be sufficient to improve their template recognition performance. Moreover, the results obtained from electron microscopy, DLS and zeta potential analysis of Poly(AGCT*)$_3$ MIP NPs suggested that their improved template recognition was achieved without affecting their size and dispersibility (as discussed in Sections 5.5.1, 5.5.2 and 5.5.3).

To investigate these findings further, these MIP NPs were also tested against polyA (12 base pairs) immobilised gold surface in identical manner. From the results obtained so far, it could be hypothesised that successfully imprinted poly(AGCT*)$_3$ MIP NPs [imprinted for the template poly(AGCT)$_3$] would not show recognition of polyA template due to lack of exact base pair fitting between them. The hypothesis was tested further by performing their QCM analysis and the obtained sensorgrams were plotted as shown in Figure 5.19.

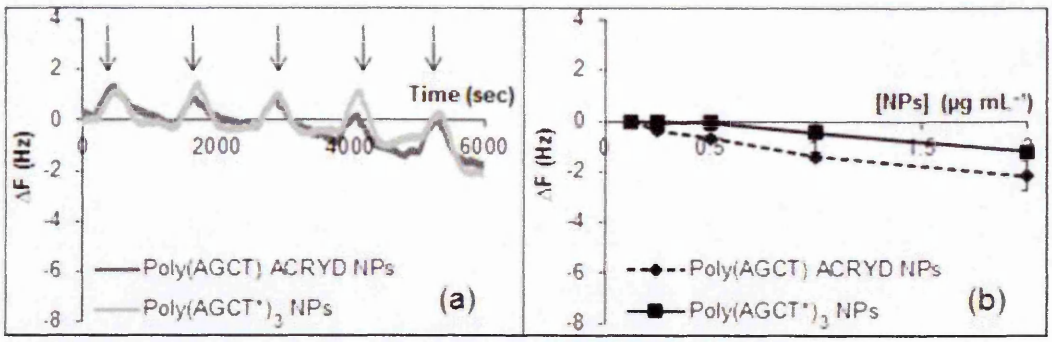

Figure 5.19: Cross-reactivity study of the OligoMIP NPs: (a) A typical QCM sensorgram obtained by injecting Poly(AGCT)$_3$ ACRYD and Poly(AGCT*)$_3$ MIP NPs onto a PolyA (12mer) functionalised gold crystal; arrows indicating the points of injection of OligoMIP NPs; (b) Rebinding performance of Poly(AGCT)$_3$ ACRYD and Poly(AGCT*)$_3$ MIP NPs to a polyA (12 base pairs) functionalised gold surface. Drop in frequency (on the Y-axis) indicates the binding event of the MIP NPs to the surface-immobilised oligonucleotide sequence. QCM measurements were performed in PBS (0.03 M, pH 7.4) at 20 °C for the NPs concentrations from 0.125 to 2 μg mL^{-1}.; error bars representing ±1 SD (n = 3).

The obtained sensorgrams suggested that Poly(AGCT)$_3$ MIP NPs showed very little binding to the template (polyA, 12 base pairs) since the oscillation frequency of the crystal did not drop by more than 2 units (as seen in Figures 5.19a and 5.19b). This was in agreement with the hypothesis that the OligoMIP NPs imprinted with poly(AGCT)$_3$ showed selective recognition of its template [poly(AGCT)$_3$] but showed little recognition of a closely related oligonucleotide (polyA) (as seen in Figures 5.19c and 5.19d). From this, it could be suggested that incorporating an oligonucleotide (complimentary to the template oligonucleotide) into polymeric NPs was the key to achieving successful imprinting and thereby selective template recognition.

Development of MIP based nanomaterials for DNA recognition had not been reported until some recent findings by our research group. However, one study recently obtained incorporation of ACRYD modified nucleosides into polymers to develop bio-sensing platforms. The study explored use of ACRYD modifications for integration of aptamer sequences into hydrogels for subsequent recognition of its viral target. ACRYD modifications used in the study were prepared in the form of grating followed by template recognition analysis performed by a laser diffraction bio-sensing platform based on the shrinkage and swelling behavior of hydrogels. Although the study reported a successful gel imprinting system, it did not explore any chemical modifications of the nucleic acid other than its phosphoramidite derivatives (widely regarded as Acrydite™). The study also used different polymer format than NPs and

even used a different sensing platform than QCM. Therefore, it could not be directly compared to the study reported here (75).

For a more direct comparison, the obtained results were correlated with other recent studies reported by our research group where chemically modified aptamer sequences were developed for the recognition of its target molecule. Chemical modifications achieved in the study were similar to those proposed in the present study wherein an aptamer sequence was modified from multiple points via C-5 substitutions of its nitrogen bases in addition to its chain end modification obtained by phosphoramidite strategy. These were then covalently incorporated into polymer NPs in the presence of its target to achieve suitable 3D folding of the aptamer. When aptamer tethered NPs were analysed for their target recognition performance, they exhibited improved recognition of the target as compared to the natural aptamer itself and even the commercially available phosphoramidite modified aptamer tethered NPs (57). This suggested that the proposed strategy of multiple chemical modifications of aptamers helped in improving the target recognition performance of aptamer tethered MIP NPs. The improvement in the template recognition performance observed in both the studies suggested that the proposed chemical modifications could be used for developing polymer based recognition materials with smaller aptamer targets as well as short oligonucleotide sequences (12 base pairs) (57). The reproducible results achieved so far strongly recommended that the proposed strategy could be analysed even further for developing polymeric materials for the recognition of entire DNA molecules of various biochemical interests.

In another study, MIP NPs were prepared in identical manner but for the recognition of nucleosides where deoxyuridine (dU) was incorporated into polymer NPs by its chemical modifications in the presence of different template nucleosides (dA, dC and dG). The template recognition studies were then performed by QCM analysis which suggested that the recognition of the template nucleoside was improved when the MIP NPs were prepared by the proposed strategy. In other words, chemical modifications of a nucleoside on the C-5 position in addition to its phosphoramidite (ACRYD) modifications not only improved its integration into the polymer backbone but also resulted in its improved template recognition performance in comparison to the PlainMIP NPs (prepared just with the traditional monomers without integration of any nucleoside) as well as ACRYD modified nucleoside tethered MIP NPs (36). This is exactly what was observed in the presented study for the recognition of oligonucleotide templates.

Such direct comparison of the obtained results with those obtained from previous studies helped in understanding reproducibility and transferability of the proposed strategy. One of the important findings was that the improvement in template recognition performance could be achieved for nucleoside as well as for short chain oligonucleotide (12 base pairs) templates by combining the virtues of molecular imprinting together with the solid phase oligonucleotide synthesis. This finding could be very encouraging especially when all the commercially available oligonucleotide sequences would only contain ACRYD modifications for developing different bio-sensing platforms; whereas the strategies proposed in the present study could attain improved recognition performance even further than the ACRYD modification strategies. This would not even rule out a possibility of exploiting multiple chemical modifications for simultaneous tagging of nucleic acids with dye or drug molecules for potential diagnostic and therapeutic applications together with improved electrochemical stability which could open up several other possibilities in developing even better recognition materials.

5.6. Summary

The aim of this study was to develop polymeric materials for the improvement of DNA recognition. To this end, the study combined renowned techniques of molecular imprinting and solid phase oligonucleotide synthesis to introduce selective recognition towards template oligonucleotide by incorporating oligonucleotide sequence as "additional monomer" into the matrix of polymer NPs. To ensure the best base pair fit between these oligonucleotides, they were allowed to attain equilibrium by forming hydrogen bonds through their nitrogen bases. The template was immobilised on a solid phase whilst its complimentary oligonucleotide was chemically modified to be covalently incorporated into the backbone of the resulting polymer nanogel. The OligoMIP NPs were successfully prepared having incorporated oligonucleotide as "additional monomer". Temperature sensitive nature of the polymer nanogel was exploited in releasing formed NPs from the solid phase whilst regenerating the immobilised template oligonucleotide for further rounds of synthesis.

To enhance the recognition of the template [poly(AGCT)$_3$], chemically modified oligonucleotides were covalently incorporated into different formulations, such as;

- PlainMIP NPs (NPs obtained without the integration of oligonucleotide sequence) used as a control,
- PolyT ACRYD and Poly(AGCT)$_3$ ACRYD MIP NPs (NPs obtained with the integration of ACRYD modified oligonucleotide sequence) and

- PolyT*12 and Poly(AGCT*)$_3$ MIP NPs (NPs obtained with the integration of ACRYD as well as base modified oligonucleotide sequence)

Physical analysis of the prepared MIP NPs by electron microscopy and dynamic light scattering suggested that the formulations contained spheroid shaped NPs with similar particle size distribution. In other words, incorporation of oligonucleotide did not alter either shape or size of the resulting MIP NPs. The mean particle diameter of the developed OligoMIP NPs was also comparable to that of natural antibodies. When analysed for their electrochemical stability by zeta potential analysis, it was found that the incorporation of oligonucleotides into the polymer backbone generally improved their stability in comparison to the PlainMIP NPs prepared without having incorporated any oligonucleotide in their matrix.

Furthermore, the improvement in the stability of the OligoMIP NPs was found to be dependent on the type of chemical modification used for the covalent integration of this oligonucleotide into MIP matrix. In this regard, the MIP NPs having incorporated modified oligonucleotides through multiple modifications (C-5 base modification in addition to the chain end ACRYD modification) exhibited higher stability than the MIP NPs containing oligonucleotides with single modification (ACRYD modification). When Poly(AGCT*)$_3$ MIP NPs were analysed for their template recognition performance by QCM analysis, they exhibited strong base pair matching by selectively recognising its template [poly(AGCT)$_3$]; however it did not show recognition of a different oligonucleotide (polyA). In a similar way, Poly(AGCT*)$_3$ MIP NPs showed improved recognition of the template [poly(AGCT)$_3$]; whereas PolyT MIP NPs could not recognise this template due to lack of base pairing.

Another interesting observation was made which suggested that improved template recognition was not achieved just with the incorporation of complimentary oligonucleotide [poly(AGCT)$_3$] in the MIP NPs. It was rather dependent on what chemical modification strategy was used to incorporate them into the NPs. Single point ACRYD modification of poly(AGCT)$_3$ clearly did not recognise the template [poly(AGCT)$_3$] any better than that achieved by PolyT MIP NPs or even PlainMIP NPs. On the other hand, MIP NPs having incorporated oligonucleotide through its chemical modification from multiple points (modification of their bases along with its ACRYD modification) exhibited significantly improved template recognition.

Correlation of physical analysis to template recognition performance of the OligoMIP NPs strongly recommended that the chemical modification of oligonucleotides from multiple points helped in holding it "locked" into template selective conformation within polymer NPs

which not only improved their dispersibility but also improved their template recognition performance. On the other hand, commercially used chain end modifications of oligonucleotides (single point modifications) resulted into its loose packing within the polymer NPs which resulted into poorly dispersed MIP NPs. Obtained MIP NPs in this way also showed poor template recognition performance which might be due to its constantly changing conformation imparted by single point attachments to the polymer.

From the results obtained during this study, it could be strongly recommended that exact base pair matching of the oligonucleotides alone might not be sufficient to improve the target recognition performance. Introduction of a chemically modified recognition element (such as an oligonucleotide sequence used in this study) into cross-linked polymeric backbone was the key factor in attaining highly selective binding sites for template recognition in comparison to traditional polymer NPs (PlainMIP NPs). The proposed strategy of incorporating uniquely modified oligonucleotides within NPs matrix could be further investigated for improving recognition of longer oligonucleotide sequences or even entire DNA molecules of bio-chemical importance.

5.7. Future work

During this study, some of the data were collected to investigate the amount of immobilised oligonucleotides, which would be investigated further in improving the protocol for future studies. This might be particularly useful since increasing the amount of the immobilised template could increase the yields of the resulting MIP NPs. Perhaps, this strategy could be explored further for the development of the MIP NPs with multiple binding sites for the template; particularly small molecule being used as templates could significantly enhance the available surface area even further and thereby improve the template recognition performance of the developed MIP NPs.

In this study the analysis of the MIP NPs was carried out in physiological conditions. However, it would be interesting to study the effect of different pH conditions on the particle size and zeta potential to investigate other potential applications in developing bio-sensing platforms. Although the length of the polymerisation was kept constant during this study, it might also be useful to study the effect of different polymerisation times on the particle size of resulting MIP NPs for a redox initiated polymerisation, as used in the study. The strategy of multiple chemical modifications used in this study could also be potentially exploited for labelling of the oligonucleotide entities with dyes or even metals (iron or copper) for improving recognition of faulty genetic biomarkers in biological samples.

It would be interesting to study if shorter polypeptides or even large proteins could be imprinted by incorporating mRNA sequences into MIP NPs by using the proposed technique. Since the mean particle size of these OligoMIP NPs was smaller than 100 nm, it would not either rule out potential use of the developed OligoMIP NPs for *in vivo* diagnostics. Temperature responsive PAAm based nanogels with the incorporation of uniquely modified oligonucleotides could also be used for labelling drugs and contrast agents to provide simultaneous therapeutic and diagnostic (theranostic) platforms upon detecting faulty genetic bio-markers.

5.8. Bibliography for Chapter 5

1. Zhao, M., Wu, T., Xiao, X., Liu, Y., and Su, X. (2013) New Advances in Molecular Recognition Based on Biomolecular Scaffolds. *Analytical and Bioanalytical chemistry* **405**, 5679-5685.
2. Sellergren, B. (1997) Noncovalent Molecular Imprinting: Antibody-like Molecular Recognition in Polymeric Network Materials. *Trends in Analytical Chemistry* **16**, 310-320.
3. Vincent, J., Mark, L., Michel, H., Hauke, S., and Van der Oost, J. (2011) Alternative Affinity Tools: More Attractive Than Antibodies? *Biochemical Journal* **436**, 1-13.
4. Poma, A., Brahmbhatt, H., Pendergraff, H. M., Watts, J. K., Turner, N. W. (2014) Generation of Novel Hybrid Aptamer- Molecularly Imprinted Polymeric Nanoparticles. *Advanced Materials* **27**, 750-758.
5. Famulok, M., Mayer, G., and Blind, M. (2000) Nucleic Acid Aptamers From Selection *in Vitro* to Applications *in Vivo*. *Accounts of Chemical Research* **33**, 591-599.
6. Brody, E. N., and Gold, L. (2000) Aptamers as Therapeutic and Diagnostic Agents. *Reviews in Molecular Biotechnology* **74**, 5-13.
7. Keefe, A. D., Pai, S., and Ellington, A. (2010) Aptamers as Therapeutics. *Nature Reviews Drug Discovery* **9**, 537-550.
8. Ruigrok, V. J. B. (2013) Selection and Characterization of DNA Aptamers.
9. Mairal, T., Özalp, V. C., Sánchez, P. L., Mir, M., Katakis, I., and O'Sullivan, C. K. (2008) Aptamers: Molecular Tools for Analytical Applications. *Analytical and Bioanalytical chemistry* **390**, 989-1007.
10. Giovannoli, C., Baggiani, C., Anfossi, L., and Giraudi, G. (2008) Aptamers and Molecularly Imprinted Polymers as Artificial Biomimetic Receptors in Affinity Capillary Electrophoresis and Electrochromatography. *Electrophoresis* **29**, 3349-3365.

11. Wojciechowski, F., and Leumann, C. J. (2011) Alternative DNA Base-pairs: From Efforts to Expand the Genetic Code to Potential Material Applications. *Chemical Society Reviews* **40**, 5669-5679.

12. Belinsky, S. A., Nikula, K. J., Palmisano, W. A., Michels, R., Saccomanno, G., Gabrielson, E., Baylin, S. B., and Herman, J. G. (1998) Aberrant Methylation of p16INK4a is an Early Event in Lung Cancer and a Potential Biomarker for Early Diagnosis. *Proceedings of the National Academy of Sciences* **95**, 11891-11896.

13. Lovell, M. A., Gabbita, S. P., and Markesbery, W. R. (1999) Increased DNA Oxidation and Decreased Levels of Repair Products in Alzheimer's Disease Ventricular CSF. *Journal of Neurochemistry* **72**, 771-776.

14. Lofton-Day, C., Model, F., DeVos, T., Tetzner, R., Distler, J., Schuster, M., Song, X., Lesche, R., Liebenberg, V., and Ebert, M. (2008) DNA Methylation Biomarkers for Blood-based Colorectal Cancer Screening. *Clinical Chemistry* **54**, 414-423.

15. Lefkimmiatis, K., and Zaccolo, M. (2014) cAMP Signaling in Subcellular Compartments. *Pharmacology & therapeutics* **143**, 295-304.

16. Rybalkin, S. D., Yan, C., Bornfeldt, K. E., and Beavo, J. A. (2003) Cyclic GMP Phosphodiesterases and Regulation of Smooth Muscle Function. *Circulation research* **93**, 280-291.

17. Sassolas, A., Leca-Bouvier, B. D., and Blum, L. J. (2008) DNA Biosensors and Microarrays. *Chemical Reviews* **108**, 109-139.

18. Yoo, S. M., Choi, J. H., Lee, S. Y., and Yoo, N. C. (2009) Applications of DNA Microarray in Disease Diagnostics. *Journal of Microbiololgy and Biotechnology* **19**, 635-646.

19. Baeissa, A., Dave, N., Smith, B. D., and Liu, J. (2010) DNA-functionalized Monolithic Hydrogels and Gold nanoparticles for Colorimetric DNA Detection. *ACS Applied Materials & Interfaces* **2**, 3594-3600.

20. Tierney, S., and Stokke, B. T. (2009) Development of an Oligonucleotide Functionalized Hydrogel Integrated on a High Resolution Interferometric Readout Platform as a Label-free Macromolecule Sensing Device. *Biomacromolecules* **10**, 1619-1626.

21. Chianella, I., Guerreiro, A., Moczko, E., Caygill, J. S., Piletska, E. V., De Vargas Sansalvador, I. M. P., Whitcombe, M. J., and Piletsky, S. A. (2013) Direct Replacement of Antibodies with Molecularly Imprinted Polymer Nanoparticles in ELISA Development of a Novel Assay for Vancomycin. *Analytical Chemistry* **85**, 8462-8468.

22. Fant, K., Esbjörner, E. K., Jenkins, A., Grossel, M. C., Lincoln, P., and Nordén, B. (2010) Effects of PEGylation and Acetylation of PAMAM Dendrimers on DNA Binding,

Cytotoxicity and *in vitro* Transfection Efficiency. *Molecular pharmaceutics* **7**, 1734-1746.

23. Mokhir, A. A., Tetzlaff, C. N., Herzberger, S., Mosbacher, A., and Richert, C. (2001) Monitored Selection of DNA-hybrids Forming Duplexes with Capped Terminal C: G Base Pairs. *Journal of Combinatorial Chemistry* **3**, 374-386.

24. Bandy, T. J., Brewer, A., Burns, J. R., Marth, G., Nguyen, T., and Stulz, E. (2011) DNA as Supramolecular Scaffold for Functional Molecules: Progress in DNA Nanotechnology. *Chemical Society Reviews* **40**, 138-148.

25. Dave, N., Chan, M. Y., Huang, P.-J. J., Smith, B. D., and Liu, J. (2010) Regenerable DNA-functionalized Hydrogels for Ultrasensitive, Instrument-free Mercury (II) Detection and Removal in Water. *Journal of the American Chemical Society* **132**, 12668-12673.

26. Chen, C., Geng, J., Pu, F., Yang, X., Ren, J., and Qu, X. (2011) Polyvalent Nucleic Acid/Mesoporous Silica Nanoparticle Conjugates: Dual Stimuli-Responsive Vehicles for Intracellular Drug Delivery. *Angewandte Chemie International Edition* **50**, 882-886.

27. Choi, Y., Thomas, T., Kotlyar, A., Islam, M. T., and Baker, J. R. (2005) Synthesis and Functional Evaluation of DNA-assembled Polyamidoamine Dendrimer Clusters for Cancer Cell-specific Targeting. *Chemistry &Biology* **12**, 35-43.

28. Cho, H., Alcantara, D., Yuan, H., Sheth, R. A., Chen, H. H., Huang, P., Andersson, S. B., Sosnovik, D. E., Mahmood, U., and Josephson, L. (2013) Fluorochrome-functionalized Nanoparticles for Imaging DNA in Biological Systems. *ACS Nano* **7**, 2032-2041.

29. Kang, H., Trondoli, A. C., Zhu, G., Chen, Y., Chang, Y.-J., Liu, H., Huang, Y.-F., Zhang, X., and Tan, W. (2011) Near-infrared Light-responsive Core–shell Nanogels for Targeted Drug Delivery. *Acs Nano* **5**, 5094-5099.

30. Baker, B. R., Lai, R. Y., Wood, M. S., Doctor, E. H., Heeger, A. J., and Plaxco, K. W. (2006) An Electronic, Aptamer-based Small-molecule Sensor for the Rapid, Label-free Detection of Cocaine in Adulterated Samples and Biological Fluids. *Journal of the American Chemical Society* **128**, 3138-3139.

31. Goodchild, J. (1990) Conjugates of Oligonucleotides and Modified Oligonucleotides: A Review of Their Synthesis and Properties. *Bioconjugate Chemistry* **1**, 165-187.

32. Prakash, T. P. (2011) An Overview of Sugar-modified Oligonucleotides for Antisense Therapeutics. *Chemistry & Biodiversity* **8**, 1616-1641.

33. Deleavey, G. F., and Damha, M. J. (2012) Designing Chemically Modified Oligonucleotides for Targeted Gene Silencing. *Chemistry & Biology* **19**, 937-954.

34. Geary, R. S., Norris, D., Yu, R., and Bennett, C. F. (2015) Pharmacokinetics, Biodistribution and Cell Uptake of Antisense Oligonucleotides. *Advanced Drug Delivery Reviews*.

35. Mukae, M., Ihara, T., Tabara, M., and Jyo, A. (2009) Anthracene-DNA Conjugates as Building Blocks of Designed DNA Structures Constructed by Photochemical Reactions. *Organic & Biomolecular Chemistry* **7**, 1349-1354.

36. Poma, A., Brahmbhatt, H., Watts, J. K., and Turner, N. W. (2014) Nucleoside-Tailored Molecularly Imprinted Polymeric Nanoparticles (MIP NPs). *Macromolecules* **47**, 6322-6330.

37. Brotschi, C., Mathis, G., and Leumann, C. J. (2005) Bipyridyl- and Biphenyl-DNA: A Recognition Motif Based on Interstrand Aromatic Stacking. *Chemistry – A European Journal* **11**, 1911-1923.

38. Amblard, F., Cho, J. H., and Schinazi, R. F. (2009) Cu(I)-Catalyzed Huisgen Azide–Alkyne 1,3-Dipolar Cycloaddition Reaction in Nucleoside, Nucleotide, and Oligonucleotide Chemistry. *Chemical Reviews* **109**, 4207-4220.

39. Wenge, U., Ehrenschwender, T., and Wagenknecht, H.-A. (2013) Synthesis of 2'-O-Propargyl Nucleoside Triphosphates for Enzymatic Oligonucleotide Preparation and "Click" Modification of DNA with Nile Red as Fluorescent Probe. *Bioconjugate chemistry* **24**, 301-304.

40. El-Sagheer, A. H., and Brown, T. (2010) Click Chemistry with DNA. *Chemical Society Reviews* **39**, 1388-1405.

41. Burgula, L. N., Radhakrishnan, K., and Kundu, L. M. (2012) Synthesis of Modified Uracil and Cytosine Nucleobases Using a Microwave-assisted Method. *Tetrahedron Letters* **53**, 2639-2642.

42. Peng, L., Wu, C. S., You, M., Han, D., Chen, Y., Fu, T., Ye, M., and Tan, W. (2013) Engineering and Applications of DNA-grafted Polymer Materials. *Chemical Science* **4**, 1928-1938.

43. Dudley, E., and Bond, L. (2014) Mass Spectrometry Analysis of Nucleosides and Nucleotides. *Mass Spectrometry Reviews* **33**, 302-331.

44. Nguyen, D. N., Green, J. J., Chan, J. M., Langer, R., and Anderson, D. G. (2009) Polymeric Materials for Gene Delivery and DNA Vaccination. *Advanced Materials* **21**, 847-867.

45. Lee, C. C., MacKay, J. A., Fréchet, J. M., and Szoka, F. C. (2005) Designing Dendrimers for Biological Applications. *Nature biotechnology* **23**, 1517-1526.

46. Lynn, D. M., and Langer, R. (2000) Degradable Poly(β-amino esters): Synthesis, Characterization, and Self-Assembly with Plasmid DNA. *Journal of the American Chemical Society* **122**, 10761-10768.

47. Taira, S., and Yokoyama, K. (2004) Self-assembly DNA-conjugated Polymer for Detection of Single Nucleotide Polymorphism. *Biotechnology and Bioengineering* **88**, 35-41.

48. Rutnakornpituk, M., Puangsin, N., Theamdee, P., Rutnakornpituk, B., and Wichai, U. (2011) Poly(acrylic acid)-grafted Magnetic Nanoparticle for Conjugation with Folic Acid. *Polymer* **52**, 987-995.

49. Hamner, K. L., Alexander, C. M., Coopersmith, K., Reishofer, D., Provenza, C., and Maye, M. M. (2013) Using Temperature-sensitive Smart Polymers to Regulate DNA-mediated Nanoassembly and Encoded Nanocarrier Drug Release. *ACS Nano* **7**, 7011-7020.

50. Wei, B., Cheng, I., Luo, K. Q., and Mi, Y. (2008) Capture and Release of Protein by a Reversible DNA-Induced Sol–Gel Transition System. *Angewandte Chemie International Edition* **47**, 331-333.

51. Kang, H., Liu, H., Zhang, X., Yan, J., Zhu, Z., Peng, L., Yang, H., Kim, Y., and Tan, W. (2011) Photoresponsive DNA-Cross-Linked Hydrogels for Controllable Release and Cancer Therapy. *Langmuir* **27**, 399-408.

52. Cheng, E., Xing, Y., Chen, P., Yang, Y., Sun, Y., Zhou, D., Xu, L., Fan, Q., and Liu, D. (2009) A pH-Triggered, Fast-Responding DNA Hydrogel. *Angewandte Chemie* **121**, 7796-7799.

53. Peppas, N. A., Khare, A. R. (1993) Preparation, Structure and Diffusional Behaviour of Hydrogels in Controlled Release. *Advanced Drug Delivery Reviews* **11**, 1-35.

54. Owens, D. E., Jian, Y., Fang, J. E., Slaughter, B. V., Chen, Y.-H., and Peppas, N. A. (2007) Thermally Responsive Swelling Properties of Polyacrylamide/Poly(acrylic acid) Interpenetrating Polymer Network Nanoparticles. *Macromolecules* **40**, 7306-7310.

55. Butler, J. E. (2000) Solid Supports in Enzyme-linked Immunosorbent Assay and Other Solid-phase Immunoassays. *Methods* **22**, 4-23.

56. Liu, J., and Lu, Y. (2007) Non-Base Pairing DNA Provides a New Dimension for Controlling Aptamer-Linked Nanoparticles and Sensors. *Journal of the American Chemical Society* **129**, 8634-8643.

57. Poma, A., Brahmbhatt, H., Pendergraff, H. M., Watts, J. K., and Turner, N. W. (2014) Generation of Novel Hybrid Aptamer–Molecularly Imprinted Polymeric Nanoparticles. *Advanced Materials* 1-9.

58. Ye, L., and Mosbach, K. (2008) Molecular Imprinting: Synthetic Materials as Substitutes for Biological Antibodies and Receptors. *Chemistry of Materials* **20**, 859-868.

59. Alexander, C., Andersson, H. S., Andersson, L. I., Ansell, R. J., Kirsch, N., Nicholls, I. A., O'Mahony, J., and Whitcombe, M. J. (2006) Molecular Imprinting Science and Technology: A Survey of the Literature for the Years up to and Including 2003. *Journal of Molecular Recognition* **19**, 106-180.

60. Bacskay, I., Takátsy, A., Végvári, Á., Elfwing, A., Ballagi-Pordány, A., Kilar, F., and Hjertén, S. (2006) Universal Method for Synthesis of Artificial Gel Antibodies by the Imprinting Approach Combined with a Unique Electrophoresis Technique for Detection of Minute Structural Differences of Proteins, Viruses, and Cells (Bacteria). III: Gel Antibodies Against Cells (bacteria). *Electrophoresis* **27**, 4682-4687.

61. Hoshino, Y., Koide, H., Furuya, K., Haberaecker, W. W., Lee, S.-H., Kodama, T., Kanazawa, H., Oku, N., and Shea, K. J. (2012) The Rational Design of a Synthetic Polymer Nanoparticle that Neutralizes a Toxic Peptide *in vivo*. *Proceedings of the National Academy of Sciences* **109**, 33-38.

62. Turner, N. W., Holdsworth, C. I., Donne, S. W., McCluskey, A., and Bowyer, M. C. (2010) Microwave Induced MIP synthesis: Comparative Analysis of Thermal and Microwave Induced Polymerisation of Caffeine Imprinted Polymers. *New Journal of Chemistry* **34**, 686-692.

63. Poma, A., Guerreiro, A., Whitcombe, M. J., Piletska, E. V., Turner, A. P. F., and Piletsky, S. A. (2013) Solid-Phase Synthesis of Molecularly Imprinted Polymer Nanoparticles with a Reusable Template–"Plastic Antibodies". *Advanced Functional Materials* **23**, 2821-2827.

64. Poma, A., Turner, A. P. F., and Piletsky, S. A. (2010) Advances in the Manufacture of MIP Nanoparticles. *Trends in Biotechnology* **28**, 629-637.

65. Wulff, G., Chong, B. O., and Kolb, U. (2006) Soluble Single-Molecule Nanogels of Controlled Structure as a Matrix for Efficient Artificial Enzymes. *Angewandte Chemie International Edition* **45**, 2955-2958.

66. Cunliffe, D., Kirby, A., and Alexander, C. (2005) Molecularly imprinted drug delivery systems. *Advanced Drug Delivery Reviews* **57**, 1836-1853.

67. Cirillo, G., Iemma, F., Puoci, F., Parisi, O., Curcio, M., Spizzirri, U., and Picci, N. (2009) Imprinted Hydrophilic Nanospheres as Drug Delivery Systems for 5-fluorouracil Sustained Release. *Journal of Drug Targeting* **17**, 72-77.

68. Hoshino, Y., Koide, H., Urakami, T., Kanazawa, H., Kodama, T., Oku, N., and Shea, K. J. (2010) Recognition, Neutralization, and Clearance of Target Peptides in the

Bloodstream of Living Mice by Molecularly Imprinted Polymer Nanoparticles: A Plastic Antibody. *Journal of the American Chemical Society* **132**, 6644-6645.

69. Titirici, M. M., Hall, A. J., and Sellergren, B. (2002) Hierarchically Imprinted Stationary Phases: Mesoporous Polymer Beads Containing Surface-confined Binding Sites for Adenine. *Chemistry of Materials* **14**, 21-23.

70. Garcinuno, R. M., Chianella, I., Guerreiro, A., Mijangos, I., Piletska, E. V., Whitcombe, M. J., and Piletsky, S. A. (2009) The Stabilisation of Receptor Structure in Low Cross-linked MIPs by an Immobilised Template. *Soft Matter* **5**, 311-317.

71. Shen, X., and Ye, L. (2011) Molecular Imprinting in Pickering Emulsions: A New Insight Into Molecular Recognition in Water. *Chemical Communications* **47**, 10359-10361.

72. Plewa, A., Yusa, S.-I., Szuwarzyński, M., Szczubiałka, K., Morishima, Y., and Nowakowska, M. (2012) Molecularly Imprinted Hybrid Adsorbents for Adenine and Adenosine-5'-triphosphate. *Journal of Medicinal Chemistry* **55**, 8712-8720.

73. Aouled, N. O., Hallil, H., Plano, B., Rebiere, D., Dejous, C., Delepee, R., and Agrofoglio, L. (2013) Love Wave Sensor Based on Thin Film Molecularly Imprinted Polymer: MIP Layer Morphology and Nucleosides Analogs Detection. in *SENSORS, 2013 IEEE*, 1-4.

74. Krstulja, A., Lettieri, S., Hall, A. J., Delépée, R., Favetta, P., and Agrofoglio, L. A. (2014) Evaluation of Molecularly Imprinted Polymers Using 2', 3', 5'-tri-O-acyluridines as Templates for Pyrimidine Nucleoside Recognition. *Analytical and bioanalytical chemistry* **406**, 6275-6284.

75. Bai, W., and Spivak, D. A. (2014) A Double-Imprinted Diffraction-Grating Sensor Based on a Virus-Responsive Super-Aptamer Hydrogel Derived from an Impure Extract. *Angewandte Chemie* **126**, 2127-2130.

76. Pan, G., Guo, Q., Cao, C., Yang, H., and Li, B. (2013) Thermo-responsive Molecularly Imprinted Nanogels for Specific Recognition and Controlled Release of Proteins. *Soft Matter* **9**, 3840-3850.

77. Nobbmann, U., Connah, M., Fish, B., Varley, P., Gee, C., Mulot, S., Chen, J., Zhou, L., Lu, Y., Sheng, F., Yi, J., and Harding, S. E. (2007) Dynamic Light Scattering as a Relative Tool for Assessing the Molecular Integrity and Stability of Monoclonal Antibodies. *Biotechnology and Genetic Engineering Reviews* **24**, 117-128.

78. (a) Berne, B. J. Pecora, R. (2000) *Dynamic Light Scattering: With Applications to Chemistry, Biology and Physics*, Dover Publications, New York. (b) Asua, J. M. (1997) *Polymeric Dispersions: Principles and Applications.* NATO ASI Series. Springer Science. Kluwer Academic Publishers, 1st edition, 446-450.

79. Shaw, D. J. Everett, D. H., Ross, S., Morrison, I. D., Lyklema, J. Technical Note: Zeta Potential An Introduction in 30 Minutes. Malvern Instruments Ltd.

80. Nel, A. E., Madler, L., Velegol, D., Xia, T., Hoek, E. M. V., Somasundaran, P., Klaessig, F., Castranova, V., and Thompson, M. (2009) Understanding Biophysicochemical Interactions at the Nano-bio Interface. *Nature Materials* **8**, 543-557.

81. Kirby, B. J., and Hasselbrink, E. F. (2004) Zeta Potential of Microfluidic Substrates: 1. Theory, Experimental Techniques, and Effects on Separations. *Electrophoresis* **25**, 187-202.

82. He, C., Hu, Y., Yin, L., Tang, C., and Yin, C. (2010) Effects of Particle Size and Surface Charge on Cellular Uptake and Biodistribution of Polymeric Nanoparticles. *Biomaterials* **31**, 3657-3666.

83. Lundqvist, M., Stigler, J., Elia, G., Lynch, I., Cedervall, T., and Dawson, K. A. (2008) Nanoparticle Size and Surface Properties Determine the Protein Corona with Possible Implications for Biological Impacts. *Proceedings of the National Academy of Sciences* **105**, 14265-14270.

84. Kaszuba, M. C., J. Watson, F. M. Jones, A. (2010) High-concentration Zeta Potential Measurements Using Light-scattering Techniques. *Philosophical Transactions of the Royal Society A* **368**, 4439-4451.

85. Hawe, A., Kasper, J. C., Friess, W., and Jiskoot, W. (2009) Structural Properties of Monoclonal Antibody Aggregates Induced by Freeze–thawing and Thermal Stress. *European Journal of Pharmaceutical Sciences* **38**, 79-87.

86. Zeng, Z., Hoshino, Y., Rodriguez, A., Yoo, H., and Shea, K. J. (2010) Synthetic Polymer Nanoparticles with Antibody-like Affinity for a Hydrophilic Peptide. *ACS Nano* **4**, 199-204.

87. Yang, K., Berg, M. M., Zhao, C., and Ye, L. (2009) One-Pot Synthesis of Hydrophilic Molecularly Imprinted Nanoparticles. *Macromolecules* **42**, 8739-8746.

88. Zhang, Q., Zha, L., Ma, J., and Liang, B. (2009) A Novel Route to Prepare pH- and Temperature-sensitive Nanogels via a Semibatch Process. *Journal of Colloid and Interface Science* **330**, 330-336.

89. Banquy, X., Suarez, F., Argaw, A., Rabanel, J.-M., Grutter, P., Bouchard, J.-F., Hildgen, P., and Giasson, S. (2009) Effect of Mechanical Properties of Hydrogel Nanoparticles on Macrophage Cell Uptake. *Soft Matter* **5**, 3984-3991.

Chapter 6

General Discussion and Future Work

This chapter will summarise the findings discussed in the previous chapters and will also discuss potential future implications of the obtained findings later in this chapter. Section 6.1 summarises the results and discusses them briefly here.

6.1. General Discussion

In brief review, the introductory **Chapter 1** laid out the foundation and structure of the presented thesis by describing its aim and objectives.

Chapter 2 presented a review of the literature to lead into the experimental case studies that were to be presented in the following Chapters. To begin with, it discussed the principle and types of molecular imprinting commonly used for developing selective recognition polymers. It emphasised the importance of the experimental parameters involved with a typical polymerisation protocol since they would largely reflect on both the physical properties and the recognition performance of the resulting polymers. The discussion also outlined the characteristics and the effects of different polymer formats and their preparation methods on the physicochemical properties of the prepared polymers. With the aid of literature, this highlighted the need and the motivation behind conducting the experiments presented in this report.

In **Chapter 3**, polymerisation by microwave energy was investigated as a possible alternative method for the development of MIPs in comparison to traditional methods (such as, oven and UV polymerisation). The obtained results demonstrated:

- MW polymerisations were extremely fast and produced MIP monoliths with comparable recognition performance to that produced by oven and UV polymerisations.
- Controlled rates of heating obtained in a MW polymerisation could produce polymers with considerable differences in their cross-linking degree, surface area, thermal stability and even porosity.

Another objective of this study was to understand the effect of different experimental parameters (such as polymerisation rate, time and temperature) on the physical properties as well as recognition performance of the MW MIPs. The obtained results indicated:

- Slower polymerisations produced MIPs with higher cross-linking degree and lower thermal stability. The MIPs showed higher surface area, improved recognition performance and improved imprinting efficiency too.

- Different lengths of polymerisation slightly affected physical properties of the MIPs. Shorter polymerisation times, such as 5 minutes of MW polymerisation and 4-8 hours of oven and UV polymerisations were sufficient to produce MIPs with optimum cross-linking degree, surface area, recognition performance and even imprinting efficiencies. Extended polymerisations either maintained or deteriorated mentioned characteristics of MIPs.
- Improved surface area did not necessarily result into improvement in the template recognition performance of the MIPs. Formation of template selective binding sites within the MIPs was influenced by their polymerisation temperature and cross-linking degree too.
- Polymerisation kinetics was crucial in producing stable monomer-template cavities which produced highly template selective binding cavities. On the other hand, sufficient degree of cross-linking was essential in maintaining the integrity of the created template selective binding cavities.

These findings suggest that further investigations of MW as a suitable alternative polymerisation technique to develop imprinted polymers are warranted.

The aim of the study presented in **Chapter 4** was to develop cross-linked polymers as alternative recognition materials to be used in ToxiQuant technology for selective mycotoxin recognition. To this end, polymers of the same component mixture were prepared in different formats by using different methods. Following from Chapter 3, the primary method of preparation was MW polymerisation to generate polymers with faster and automated preparation protocols for industrial applications. The experimental parameters were chosen such that the analysis of both the caffeine MIPs and ToxiQuant MW polymers were comparable. The trends observed in the mentioned properties were in strong agreement with the results obtained earlier from the study of caffeine MW MIPs which suggested:

- Physical properties and mycotoxin recognition performance of the ToxiQuant MW polymers (such as, cross-linking degree, thermal stability, surface area, pore volumes, pore size and morphology) were affected considerably by the polymerisation rates (MW powers) used for their preparation.
- The composition of pre-polymerisation mixture was less influential on the physicochemical properties of the resulting polymers than the experimental parameters used for their preparation.
- Both the studies (caffeine MW MIPs and ToxiQuant MW polymers) collectively found that the change in the composition of the monomer mixture did not affect the size of

the pores created in the resulting polymers; the pore sizes were mainly affected by the polymerisation rates (MW powers) used for their preparation.

- Different monomer compositions led to considerable differences in the AFT clean-up and AFT recovery performances of the resulting polymers.
- The developed polymers could obtain comparable AFT clean-up efficiency; however the recoveries of immobilised AFT in the subsequent steps were considerably low when compared to that of existing recognition materials used in ToxiQuant.

The results obtained were in agreement with the study presented in Chapter 3 and strongly recommended that MW polymerisation could be investigated further as a suitable alternative polymerisation technique to develop non-imprinted or molecularly imprinted polymers.

The study also reported preparation of polymer microparticles by suspension and core-shell polymerisations. Preparation of the suspension microparticles involved the study and optimisation of multiple experimental parameters and reaction components involved in its preparation. The obtained results suggested:

- Electron microscopy studies indicated that the obtained suspension polymers were spherical, porous and within the desired particle size distribution.
- Precipitation polymerisation produced homogenous formulations of polymer microspheres with average particle size of less than 10 µm and were further used as cores in developing core-shell microparticles.
- Core-shell microparticles were prepared by an earlier protocol reported and the resulting particles were analysed by electron microscopy. This suggested that the preparation of core-shell polymer microparticles needed further investigation by using other protocols since the resulting microparticles did not contain desired physical properties.

These methods remain effective in the development of recognition polymers but proved not suitable for the requirements of mycotoxin absorption in this required setting.

The aim of the study presented in **Chapter 5** was to develop polymeric materials capable of targeted DNA recognition. To enhance the recognition of the template [poly(AGCT)$_3$], chemically modified oligonucleotides were covalently incorporated as additional monomers into the backbone of resulting OligoMIP NPs. The developed MIP NPs were then analysed for their physical properties and oligonucleotide recognition performance. The obtained results indicated:

- Electron microscopic and light scattering analysis of the OligoMIP NPs suggested that the formulations contained spheroid shaped NPs with much similar particle size distribution.
- Incorporation of oligonucleotide did not alter either shape or size of the MIP NPs. The mean particle diameter of the developed OligoMIP NPs was also comparable to that of natural Abs.
- Zeta potential analysis suggested that the incorporation of oligonucleotides (as additional monomers) into the backbone of OligoMIP NPs generally improved their stability in comparison to the PlainMIP NPs which was prepared without having incorporated any oligonucleotide in their matrix.
- MIP NPs having incorporated modified oligonucleotides through multiple modifications (C-5 base modification in addition to the chain end ACRYD modification) exhibited higher electrochemical stability than the MIP NPs containing oligonucleotides with single modification (commercially used ACRYD modification).
- QCM analysis suggested that Poly(AGCT*)$_3$ MIP NPs exhibited strong base pair matching ability by selectively recognising its template [poly(AGCT)$_3$]; however it did not show recognition of a different oligonucleotide (polyA). Likewise, Poly(AGCT*)$_3$ MIP NPs showed improved recognition of the template [poly(AGCT)$_3$]; whereas PolyT MIP NPs could not recognise this template due to lack of base pairing.
- Chemical modification of oligonucleotides from multiple points helped in holding it "locked" into template selective conformation within polymer NPs which not only improved their dispersibility but also improved their template recognition performance.

This strongly recommended that the proposed strategy of incorporating uniquely modified oligonucleotides within NPs matrix could be further investigated for improving recognition of longer oligonucleotide sequences or even entire DNA molecules of bio-chemical importance.

6.2. Future work

The aim of the presented thesis was to develop polymeric materials for selective recognition of different chemical and biological analytes. To this end, different polymeric materials have been developed (as presented in Chapters 3, 4 and 5).

The study presented in Chapter 3 offers insight into the flexibility of the MW as a tool for generating MIPs.

Further studies in this area should include:

- Further comparative studies between MW generated and other formats using a wide range of physical techniques, including porosity characters (such as, surface area, pore volume and pore radii).
- An expansion of the study to other templates to demonstrate the capabilities of the MW reactor. These should include templates with ranging polarity, size and stability.
- The heating profiles and reactivity of compounds within a MW reactor often depend on the polarity and dielectric constants of the components. A study into different monomers, cross-linking monomer and solvents should be undertaken.
- Different initiators may allow for the rate of polymerisation to be affected, hence affect the properties of the polymers. Likewise differing temperatures could be used.
- With additional attachments to the instrument, MW reactors could also be further investigated for the development of polymer microparticles by different dispersion polymerisation methods.

Since the physical make up of a polymer holds the key to its recognition performance, this study can help in generating different MW polymerisation protocols to prepare polymers with predictable physical properties and thereby analyte recognition performance.

In Chapter 4, non-imprinted polymers have been developed for mycotoxin recognition. The polymers have been prepared in different formats by using different methods. Prepared microparticles by suspension polymerisation will be studied further for their mycotoxin recognition performance. Alongside, newer core-shell polymerisation strategies will be developed to prepare microparticles and study them for their mycotoxin clean-up and recovery performances. This will help developing a coherent study to understand the mycotoxin recognition performance of different polymer formats prepared by MW, oven, suspension and core-shell polymerisations. This in turn will help in selecting the best polymeric material for the future ToxiQuant technology and develop research strategies accordingly. Besides HPLC analysis, the future studies will also be performed on the ToxiQuant prototype to

generate a direct comparison between the two methods and to implement the use of polymers from the lab to the end user mycotoxin detection kits.

In Chapter 5, oligonucleotide imprinted NPs (OligoMIP NPs) have been developed for recognition of oligonucleotide. In this study, the analysis of the MIP NPs has been carried out in physiological conditions. However, more experiments will be carried out to study the effect of different pH conditions on both the particle size and zeta potential of the resulting MIP NPs to investigate their other potential applications in developing bio-sensing platforms.

Study of the effect of different polymerisation times will also be performed to investigate its effect on the particle size of resulting MIP NPs. The developed NPs are also currently being investigated as recognition elements in ELISA style assays for the recognition of nucleosides and oligonucleotides. This exciting study can open up an entire new domain for the use of MIP NPs for the detection of cancer biomarkers from clinical samples as well. Since the prepared MIP NPs are smaller than 100 nm and are developed in physiological conditions, they may potentially be studied for *in vivo* diagnostics too.

Further work that is specific to this study would be:

- A study to see if the affinity observed by the OligoMIP NPs towards their corresponding sequences is affected by single base pair alteration/mutation/deletions; and hence in turn observe whether oligo-MIPs can be potentially used for diagnostic tools.
- To explore if DNA bound to a polymer via a multi-point binding can maintain its sequence specificity and high affinity beyond the 12 base pairs limit demonstrated in proof-of-concept work.
- To analyse further potential binding chemistries between DNA and polymer, beyond those demonstrated in the prior work, which will allow: (a) the formation of Oligo-MIP NPs in other formats; and (b) improve the affinities observed in the prior work.

Appendix

1. Calibration curve for monomer conversion studies

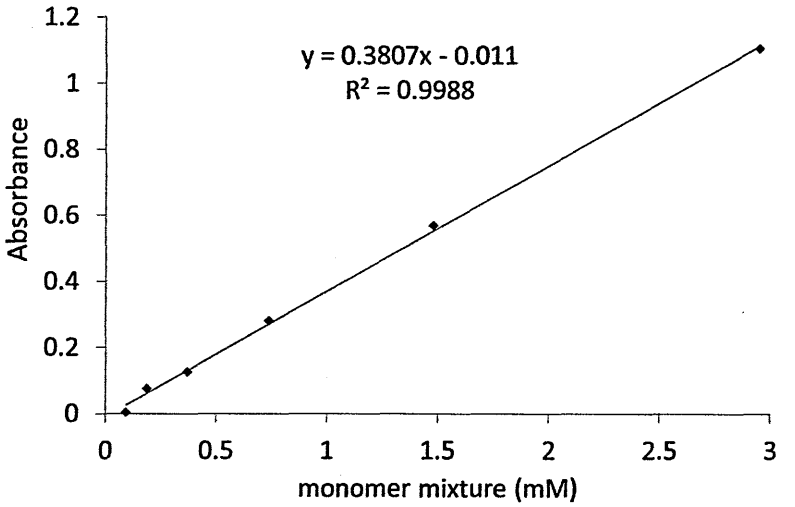

2. Caffeine rebinding studies – HPLC calibration curve